DISSERTATION

LANDSLIDE RISKSCAPES IN THE COLORADO FRONT RANGE: A QUANTITATIVE GEOSPATIAL APPROACH FOR MODELING HUMAN-ENVIRONMENT INTERACTIONS

Submitted by

Heather Brainerd Hicks

Department of Ecosystem Science and Sustainability

In partial fulfillment of the requirements

For the Degree of Doctor of Philosophy

Colorado State University

Fort Collins, Colorado

Spring 2021

Doctoral Committee:

Advisor: Melinda Laituri

Steven Fassnacht
Neil Grigg
Sara Rathburn

ABSTRACT

LANDSLIDE RISKSCAPES IN THE COLORADO FRONT RANGE: A QUANTITATIVE GEOSPATIAL APPROACH FOR MODELING HUMAN-ENVIRONMENT INTERACTIONS

This research investigated the application of riskscapes to landslides in the context of geospatial inquiry. Riskscapes are framed as a landscape of risk to represent risk spatially. Geospatial models for landslide riskscapes were developed to improve our understanding of the spatial context for landslides and their risks as part of the system of human-environment interactions. Spatial analysis using Geographic Information Systems (GIS) leveraged modeling methods and the distributed properties of riskscapes to identify and preserve these spatial relationships.

This dissertation is comprised of four separate manuscripts. These projects defined riskscapes in the context of landslides, applied geospatial analyses to create a novel riskscape model to introduce spatial autocorrelation methods to the riskscape framework, compared geostatistical analysis methods in these landslide riskscape assessments, and described limitations of spatial science identified in the riskscape development process.

The first project addressed the current literature for riskscapes and introduced landslides as a measurable feature for riskscapes. Riskscapes are founded in social constructivist theory and landslide studies are frequently based on quantitative risk assessment practices. The uniqueness of a riskscape is the inclusion of human geography and environmental factors, which are not consistently incorporated in geologic or natural hazard studies. I proposed the addition of spatial theory constructs and methods to create spatially measurable products. I developed a conceptual

framework for a landslide riskscape by describing the current riskscape applications as compared to existing landslide and GIS risk model processes. A spatial modeling formula to create a weighted sum landslide riskscape was presented as a modification to a natural hazard risk equation to incorporate the spatial dimension of risk factors.

The second project created a novel method for three geospatial riskscapes as an approach to model landslide susceptibility areas in Boulder and Larimer Counties, Colorado. This study synthesized physical and human geography to create multiple landslide riskscape models using GIS methods. These analysis methods used a process model interface in GIS. Binary, ranked, and human factor weighted sum riskscapes were created, using frequency ratio as the basis for developing a weighting scheme. Further, spatial autocorrelation was introduced as a recommended practice to quantify the spatial relationships in landslide riskscape development. Results demonstrated that riskscapes, particularly those for ranked and human factor riskscapes, were highly autocorrelated, non-random, and exhibited clustering. These findings indicated that a riskscape model can support improvements to response modeling, based on the identification of spatially significant clustering of hazardous areas.

The third project extended landslide riskscapes to measurable geostatistical comparisons using geostatistical tools within a GIS platform. Logistic regression, weights of evidence, and probabilistic neural networks methods were used to analyze the weighted sum landslide riskscape models using ArcGIS and Spatial Data Modeler (ArcSDM). Results showed weights of evidence models performed better than both logistic regression and neural networks methods. Receiver Operator Characteristic (ROC) curves and Area Under the Curve validation tests were performed and found the weights of evidence model performed best in both posterior probability prediction and AUC validation.

A fourth project was developed based on the limitations discovered during the analytical process evaluations from the riskscape model development and geostatistical analysis. This project reviewed the issues with data quality, the variations in results predicated on the input parameters within the analytical toolsets, and the issues surrounding open-source application tools. These limitations stress the importance of parameter selection in a geospatial analytical environment.

These projects collectively determined methods for riskscape development related to landslide features. The models presented demonstrate the importance and influence of spatial distributions on landslide riskscapes. Based on the proposed conceptual framework of a spatial riskscape for landslides, weighted sum riskscapes can provide a basis for prioritization of resources for landslides. Ranked and human factor riskscapes indicate the need to provide planning and protection for areas at increased risk for landslides. These studies provide a context for riskscapes to further our understanding of the benefits and limitations of a quantitative riskscape approach. The development of a methodological framework for quantitative riskscape models provides an approach that can be applied to other hazards or study areas to identify areas of increased human-environment interaction. Riskscape models can then be evaluated to inform mitigation and land-use planning activities to reduce impacts of natural hazards in the anthropogenic environment.

ACKNOWLEDGEMENTS

There are a great number of people to acknowledge and thank, who, whether they knew it or not, helped me along this path. I cannot possibly thank enough my advisor, Dr. Melinda Laituri. I first met her when I applied to the Colorado State University Ph.D. program while still enrolled in my master's degree program at the University of Denver. I knew I wanted to continue my education, and I knew I wanted to go to CSU. Dr. Laituri met with me amid a chaotic end to my master's degree and agreed to take me on as a Ph.D. student. Her faith in me awes me to this day. She provides inspiration to me personally, and I thank her for her time investment in supporting my journey into scholarship.

I would also like to thank my committee members, Dr. Sara Rathburn, Dr. Neil Grigg, and Dr. Steven Fassnacht. It was a privilege to work with such talented scholars who supported my project and challenged me to think about the work in new ways and how it fit into this interdisciplinary realm. And I appreciate them stepping in to support and review this work relatively late in my process. The addition of pandemic-related restrictions further complicated matters. I truly appreciate the time and effort everyone has committed to supporting this project.

Certainly, any work in this field is indebted to those that preceded us. Riskscapes are an interdisciplinary topic, related to multiple theoretical constructs and ideations. Leaders and scholars in varied fields of geography, disaster vulnerability, landslide studies, geospatial analysis, and natural hazard risk assessments influenced my thinking for these manuscripts and allowed me to form new ideas on the process development of riskscapes related to landslides. Acknowledgement in the form of citations does not seem to adequately express my gratitude for the knowledge imparted through their thought-provoking publications. While there was a lot of

reading, it was rewarding to delve into these studies and see the contributions the authors made to their communities of practice.

This work would not be possible without the support of family and friends. My parents and sister have always encouraged me to pursue my interests and always provided a platform to do so. And my husband has spent decades supporting me through this and many other journeys as well. And everything I do, I do for my sons.

DEDICATION

To Erik and Logan

TABLE OF CONTENTS

ABSTRACT ii
ACKNOWLEDGEMENTS v
DEDICATION vii
LIST OF TABLES xii
LIST OF FIGURES xv
LIST OF KEYWORDS xxi
CHAPTER 1: INTRODUCTION TO THE DISSERTATION 1
1.1 Introduction 1
1.2 Research objectives and overview 2
1.3 Background 5
1.4 Summary 8
References 10
CHAPTER 2: RISKSCAPES AS A GEOSPATIAL CONSTRUCT: A CONCEPTUALIZATION OF LANDSLIDE RISKSCAPES IN HUMAN-ENVIRONMENT SYSTEMS 12
2.1 Summary of the manuscript 12
2.2 Introduction 12
2.3 Natural hazards and riskscapes 14
2.4 Risk equations and riskscapes 17
2.5 Riskscapes in the literature, evolving definitions 20
2.5.1 Riskscapes: environmental and natural hazard risk-management frameworks 20
2.5.2 Riskscapes: social theory and actor-network theory frameworks 25
2.6 Relating riskscapes, spatial processes and landslide studies 27
2.7 Spatial risk characteristics 29
2.7.1 Multiplicity of riskscapes 29
2.7.2 Spatial scales in riskscapes 30
2.8 Vulnerability in riskscapes 32
2.9 Applied riskscapes, multi-hazards, and interdisciplinary approaches 33
2.10 Technology approaches 35
2.10.1 The RiskScape Project: A GIS-based loss-modeling framework 35
2.10.2 United Nations Economic and Social Commission for Asia and the Pacific (UNESCAP) project 37
2.10.3 Geospatial riskscapes for landslides in Colorado 38
2.11 Conceptualizing a landslide riskscape 38
2.12 Conclusions 41
References 44
CHAPTER 3: GEOSPATIAL APPLICATIONS TO LANDSLIDE RISKSCAPE DEVELOPMENT: A MODELING APPROACH TO QUANTIFY LANDSLIDE RISKSCAPES IN THE COLORADO FRONT RANGE 49
3.1 Summary of the manuscript 49
3.2 Introduction 50
3.2.1 Objective of study 52

3.3 Study area 53
3.4 Data and methods 55
3.4.1 Data 56
3.4.2 Data preparation 56
3.4.3 Landslide riskscape class development methods 58
3.4.4 Spatial autocorrelation factors and clustering method 60
3.5 Riskscape results 62
3.5.1 Binary riskscape results 62
3.5.2 Ranked riskscape results 64
3.5.3 Human riskscape results 66
3.6 Spatial autocorrelation results 68
3.6.1 Binary landslide riskscape spatial autocorrelation results 68
3.6.2 Ranked landslide riskscape spatial autocorrelation results 69
3.6.3 Human factor landslide riskscape spatial autocorrelation results 69
3.7 Discussion 70
3.8 Conclusions 77
References 79
CHAPTER 4: GEOSTATISTICAL ASSESSMENTS OF LANDSLIDE RISKSCAPES: A COMPARISON OF LOGISTIC REGRESSION, WEIGHTS OF EVIDENCE, AND PROBABILITISTIC NEURAL NETWORKS 82
4.1 Summary of the manuscript 82
4.2 Introduction 83
4.2.1 Literature background: landslide geostatistical approaches 83
4.3 Study area 86
4.4 Geostatistical background 88
4.4.1 Weights of evidence 88
4.4.2 Logistic regression 90
4.4.3 Artificial neural networks 90
4.5 Materials and methods 91
4.5.1 Data processing 92
4.5.2 Data preparation 94
4.5.3 Training sites in ArcSDM 95
4.5.4 Weighting the tables 95
4.5.5 Neural network data preparation 97
4.6 Results 98
4.6.1 Weighting results 98
4.6.2 Prior probability 99
4.6.3 Weights of evidence, calculate response results 99
4.6.4 Logistic regression results 103
4.6.5 Probabilistic neural network results 107
4.6.6 Validation tests 112
4.7 Discussion 118
4.8 Conclusions 120
References 122
CHAPTER 5: LIMITATIONS OF GEOSPATIAL SCIENCE IN LANDSLIDE RISKSCAPES: PROJECTS, PRECISION, AND PARAMETERS 128

5.1 Summary of the manuscript 128
5.2 Introduction to riskscape datasets and challenges 129
5.3 Data quality limitations 131
5.4 Data quality factors 131
5.4.1 Data quality 133
5.4.2 Challenges with data acquisition 133
5.4.3 Completeness 134
5.4.4 Data currency 136
5.4.5 Metadata 136
5.4.6 Validity (appropriateness) 137
5.5 Classifications issues and the challenge of subjectivity 138
5.6 Resolution and scale issues 144
5.7 Temporal scales 146
5.8 Influences of parameter settings in a tool structure 147
5.9 Software and coding 150
5.10 Conclusions 151
References 153
CHAPTER 6: CONCLUSIONS 155
6.1 Summary of contributions and implications for landslide riskscape methodologies 155
6.2 Riskscape frameworks 156
6.3 Riskscape spatial modeling 158
6.4. Geostatistical riskscapes 160
6.5 Spatial data limitations in riskscapes 161
6.6 Summary of riskscape modeling 163
6.7 Recommendations and future work 165
6.7.1 Data types and features 165
6.7.2 Methods and approaches 166
6.7.3 Expanding geographies of riskscapes 167
6.8 Conclusions 168
References 170
CHAPTER 7: RECOMMENDATIONS AND REFLECTION 172
7.1 Riskscape processes and geospatial science, what is next? 172
7.1.1 Data 172
7.1.2 Geostatistical methods 173
7.1.3 Geographic engagement through technology 174
7.1.4 Spatial representation in spatial structures 174
7.1.5 Riskscapes and the Internet of Things (IoT) 175
7.1.6 Summary of thoughts on riskscapes 176
7.2 Potential for a riskscape role in natural hazards educational content 176
7.3 Personal reflections 181
References 187
APPENDICES 188
APPENDIX A: DATA SOURCES 189
APPENDIX B: APPENDIX TO CHAPTER 3 MANUSCRIPT 191
B.1 Data sources 192
B.2 Methods specifications 193

APPENDIX C: RESULTS TABLES 195
APPENDIX D: MODELBUILDER DATA PROCESSING MODELS 209
APPENDIX E: MAPS 221
APPENDIX F: RESULTS CHARTS 238
APPENDIX G: GEOSTATISTICAL MAPS 254
APPENDIX H: CALCULATE WEIGHTS TABLES 267

LIST OF TABLES

Page
Table 2.1. Terms and definitions for riskscapes and geospatial applications to landslides. 14
Table 2.2. Risk equation summary from selected riskscape and natural hazard literature. 18
Table 2.3. Risk literature for landslides, proto-riskscapes, and riskscapes..... 33

Table 3.1. Weighting scheme for landslide riskscape types. 57
Table 3.2. Classification of spatial autocorrelation methods and measurements. Global methods apply all features in the dataset; local methods apply neighboring features to the analysis. 60
Table 3.3. Classified binary weighted sum riskscape for Boulder and Larimer Counties. Bold text indicates a probabilistic frequency ratio greater than 1, demonstrating the relative weight of landslide susceptibility cells. 63
Table 3.4. Ranked weighted sum riskscape, showing class value, start and end ranges for number of factors, areal extent percentages and landslide riskscape percentages. Probabilistic frequency ratios (PFR) are the calculation relating the percent landslide riskscape to the areal extent coverage. Bold text indicates a PFR greater than 1, demonstrating the relative weight of landslide susceptibility cells. 65
Table 3.5. Human factor weighted sum riskscape, showing class value, start and end ranges for number of factors, areal extent percentages and landslide riskscape percentages. Probabilistic frequency ratios (PFR) are the calculation relating the percent landslide riskscape to the areal extent coverage. Bold text indicates a PFR greater than 1, demonstrating the relative weight of landslide susceptibility cells. 67
Table 3.6. Comparison of ranked and human factor riskscapes with urban area classification. Bold text indicates a probabilistic frequency ratio greater than 1, demonstrating the relative weight of landslide susceptibility cells. 73

Table 4.1. Data types and sources. 93
Table 4.2. Datasets without relevant weight classes, removed from weights of evidence and logistic regression analyses. 99
Table 4.3. Prior probability values from training datasets. 99
Table 4.4. Receiver Operating Characteristic Area Under the Curve (ROC-AUC) values for Boulder County riskscapes. Values shown in red range from 0.4 – 0.6, within 0.1 of the random guess threshold of 0.5. 114
Table 4.5. Receiver Operating Characteristic Area Under the Curve (ROC-AUC) values for Larimer County riskscapes. Values shown in red range from 0.4 – 0.6, within 0.1 of the random guess threshold of 0.5. 117
Table 4.6. Riskscape Area Under the Curve model averages (all training datasets). 118

Table 5.1. Definitions of data quality measurements. 132
Table 5.2. Comparison of spatial autocorrelation results for human factor riskscape models. .. 149

Table 6.1. Research questions and key findings. 155

Table B.1. List of data sources (* denotes data derived from DEM source) 192

Table C.1. Landslide percentage for Boulder and Larimer Counties, Colorado. Data source: Colorado Geological Survey. CGS Open File Report datasets 14-02 (Boulder County) and 15-13 (Larimer County). (Morgan, White et al. 2014, Wait, Morgan et al. 2015) 196
Table C.2. Aspect classes for Boulder and Larimer Counties, showing slope face direction. Data derived from U.S. Geological Survey Digital Elevation Model data. 196
Table C.3. Slope classes in degrees for Boulder and Larimer Counties. Data derived from U.S. Geological Survey Digital Elevation Model data. 197
Table C.4. Elevation classes in meters for Boulder and Larimer Counties. Data derived from U.S. Geological Survey Digital Elevation Model data. 197
Table C.5. Combined curvature classes for Boulder County. Data derived from U.S. Geological Survey Digital Elevation Model data. 198
Table C.6. Combined curvature classes for Larimer County. Data derived from U.S. Geological Survey Digital Elevation Model data. 198
Table C.7. Boulder County hydrology flowlines (50-meter buffer) and landslides percentages. 198
Table C.8. Boulder County waterbodies (50-meter buffer) and landslides percentages. 199
Table C.9. Larimer County hydrology flowlines (50-meter buffer) and landslides percentages. 199
Table C.10. Larimer County waterbodies (50-meter buffer) and landslides percentages. 199
Table C.11. Boulder County lithologic types and landslide percentages. 199
Table C.12. Boulder County faults (50-meter buffer) and landslides percentages. 200
Table C.13. Larimer County lithologic types and landslide percentages. 200
Table C.14. Larimer County faults (50-meter buffer) and landslides percentages. 200
Table C.15. Boulder County soil classification and landslide percentages. 200
Table C.16. Larimer County soil classification and landslide percentages. 201
Table C.17. Boulder County land cover and landslide percentages. 201
Table C.18. Larimer County land cover and landslide percentages. 203
Table C.19. Boulder County urban area classifications and landslide percentages. 206
Table C.20. Larimer County urban area classifications and landslide percentages. 206
Table C.21. Boulder County building buffer (100-meter) and landslide percentages. 206
Table C.22. Larimer County building buffer (100-meter) and landslide percentages. 207
Table C.23. Boulder County population values within Census blocks and landslide percentages. 207
Table C.24. Larimer County population values within Census blocks and landslide percentages. 207
Table C.25. Boulder County transportation and landslide percentages. 207
Table C.26. Larimer County transportation and landslide percentages. 208

Table H.1. Boulder County, binary riskscapes, all classes, calculate weights tables (classes with no points were removed, 6 from 500 training points, 5 from 1000 training points, and 6 from 20% training points). 268
Table H.2. Boulder County, ranked riskscapes, all classes, calculate weights tables (classes with no points were removed, 37 from 500 training points, 27 from 1000 training points, and 31 from 20% training points). 269

Table H.3. Boulder County, human factor riskscapes, all classes, calculate weights tables (classes with no points were removed, 45 from 500 training points, 40 from 1000 training points, and 30 from 20% training points). 276
Table H.4. Larimer County, binary riskscapes, all classes, calculate weights tables (classes with no points were removed, 7 from 500 training points, 7 from 1000 training points, and 6 from 20% training points). 284
Table H.5. Larimer County, ranked riskscapes, all classes, calculate weights tables (classes with no points were removed, 41 from 500 training points, 38 from 1000 training points, and 34 from 20% training points). 285
Table H.6. Larimer County, human factor riskscapes, all classes, calculate weights tables (classes with no points were removed, 46 from 500 training points, 44 from 1000 training points, and 37 from 20% training points). 291

LIST OF FIGURES

Page

Figure 1.1. Location of study areas and landslide susceptibility areas, Boulder and Larimer Counties, Colorado. Data Sources: Morgan et al. (2014); T. C. Wait et al. (2015)..... 5

Figure 2.1. Risk equations and relationships adapted from van Westen (2013) based on the interactions of risk components and variable characteristics of risk inputs. Source: van Westen (2013). 19
Figure 2.2. Riskscape conceptual model showing theoretical frameworks, data sources, and methodological approach. 25
Figure 2.3. Timeline depicting milestones in riskscape development, GIS, and landslide studies. 28
Figure 2.4. Example of multiple riskscapes in response to a landslide. Based on riskscape perspectives model from Müller-Mahn and Everts (2013, p. 34)..... 30
Figure 2.5. Workflow diagram adapted from the RiskScape Project, “Conceptual diagram of the RiskScape model framework” Source: RiskScape (2016)..... 36
Figure 2.6. Landslide Riskscape conceptual diagram. This model outlines the elements of a spatialized landslide riskscape, derived from modifications to the risk equation (R=HCE) from Bell and Glade (2004). 39

Figure 3.1. Boulder and Larimer Counties with urban areas and clusters. Landslide susceptibility data shown from Colorado Geological Survey Open File Report data (OF14-02 and OF15-13). Data credit: (Morgan et al., 2014; T. C. Wait et al., 2015)..... 55
Figure 3.2. Geospatial workflow for riskscape development for data processing, analysis, and spatial autocorrelation tasks. Datasets processed are listed in Appendix B..... 58
Figure 3.3. Anselin Local Moran's *i* equations. Source: Esri (2019)..... 62
Figure 3.4. Binary weighted-sum riskscape inset maps, showing five classes for landslide riskscapes, Red Feather Lakes, Larimer County (a), Estes Park and Allenspark, Larimer and Boulder Counties (b) Nederland and Boulder Canyon, Boulder County (c), and urban corridor (d). 64
Figure 3.5. Ranked weighted-sum riskscape inset maps, showing five classes for landslide riskscapes, Red Feather Lakes, Larimer County (a), Estes Park and Allenspark, Larimer and Boulder Counties (b) Nederland and Boulder Canyon, Boulder County (c), and urban corridor (d). 66
Figure 3.6. Human factor weighted-sum riskscape inset maps, showing five classes for landslide riskscapes, Red Feather Lakes, Larimer County (a), Estes Park and Allenspark, Larimer and Boulder Counties (b) Nederland and Boulder Canyon, Boulder County (c), and urban corridor (d). 68
Figure 3.7. Ranked (a) and human factor (b) multipart raster riskscape Anselin Local Moran's *i* cluster outlier map in urban corridors for Boulder and Larimer Counties, Colorado..... 70
Figure 3.8. Ranked (a) and human factor (b) riskscapes for the Boulder and Larimer County urban corridor..... 72

Figure 3.9. Ranked and human factor riskscape urban area comparison. Ranked probabilistic frequency ratio (PFR) peaks at the moderate class, human factor probabilistic frequency ratio peaks at the high class..... 74
Figure 3.10. Human factor riskscape coincident with high and medium Wildland Urban Interface (WUI) area. Example from Estes Park, Allenspark, and Lyons Colorado. Urban classifications, elevation, and roadways in the area lead to increased riskscape values..... 75

Figure 4.1. Boulder and Larimer counties in Colorado, urban areas, and landslide susceptibility areas. Data sources: Colorado Geological Survey, U.S. Census Bureau, U.S. Geological Survey. 88
Figure 4.2. Workflow for data preparation steps. 94
Figure 4.3. Workflows for logistic regression and weights of evidence analysis models in ArcSDM. 97
Figure 4.4. Neural network workflow in ArcSDM. 98
Figure 4.5. Boulder County weights of evidence posterior probability, all riskscape classes.... 100
Figure 4.6. Allenspark region, Boulder County. Weights of evidence posterior probability shown with wildland urban interface areas (1000 point training dataset). 101
Figure 4.7. Larimer County weights of evidence posterior probability, all riskscape classes.... 102
Figure 4.8. Red Feather Lakes, Larimer County. Weights of evidence posterior probability shown with wildland urban interface areas (20% point training dataset). 103
Figure 4.9. Map A: Boulder County logistic regression maps for all classes. Map B: Inset of Allenspark region (1000 point training dataset). 105
Figure 4.10. Map A: Larimer County logistic regression maps for all classes. Map B: Inset of Red Feather Lakes region (1000 point training dataset). 107
Figure 4.11. Boulder County probabilistic neural networks for all training classes. Higher values (red) indicate higher probabilities. Map B shows the Allenspark region with WUI medium and high area classifications (1000 point training dataset). 109
Figure 4.12. Larimer County probabilistic neural networks for all training classes. Higher values (red) indicate higher probabilities. Map B shows the Red Feather Lakes region with WUI medium and high area classifications (1000 point training dataset). 111
Figure 4.13. Boulder County PNN showing the coincidence of lower PNN values with lake and urban features highlighted (1000 point dataset example). 111
Figure 4.14. Larimer County PNN showing the coincidence of lower PNN values with lake and urban features highlighted (1000 point dataset example). 112
Figure 4.15. Boulder County AUC values. Red is binary riskscape, blue is human factor riskscape, and green is ranked riskscape values. 113
Figure 4.16. Larimer County AUC values. Red is binary riskscape, blue is human factor riskscape, and green is ranked riskscape values. 116

Figure 5.1. Data quality factor relationship model. 132
Figure 5.2. Soil data from USDS NRCS for Boulder County, Colorado. 2.29% of the study area was classified as Data Not Available. 135
Figure 5.3. Larimer county building address points (Source: Larimer County GIS 2020) and building footprint outlines (Source: Microsoft open building, 2018). Image shows offset and areal extent differences between address points and building footprint locations. Buffer

zones of 100 meters converted to raster grids for analysis show the difference between point locations, footprints, and areal extents. 138
Figure 5.4. Human factor riskscapes showing differences in classification schemes. The top map shows the full urban area with areas of difference highlighted. The lower map shows an inset area in Boulder County. Map A shows human factor riskscape classes by equal interval, Map B by basing the classes on the ranked riskscape model classes and Map C by natural breaks (Jenks) method. Blocks show areas to highlight differences in rankings. Source: Hicks and Laituri (2020) 142
Figure 5.5. Boulder County human factor riskscape comparison. Equal interval (blue) shows the highest peak. Ranked classes (orange) show the cell counts are more heavily weighted in the upper classes, due to the higher weighting of human factor datasets. Natural Breaks (grey) shows a normal curve distribution. Data source: Hicks and Laituri (2020). 143
Figure 5.6. Larimer County human factor riskscape comparison. Equal interval (blue) shows the highest peak. Ranked classes (orange) show the cell counts are more heavily weighted in the upper classes, due to the higher weighting of human factor datasets. Natural Breaks (grey) shows a normal curve distribution. Data source: Hicks and Laituri (2020). 143
Figure 5.7. Raster data showing the mixed pixel problem. Larimer County, Colorado. Data source: USDA NRCS soils data. 146

Figure 6.1. Landslide riskscapes in Boulder and Larimer Counties, Colorado. Map A shows binary riskscape values for all classes. Map B is the classified ranked riskscape. Map C is the classified human factor riskscape. 164

Figure D.1. Landslide preprocessing model. 210
Figure D.2. Landslide processing model. 210
Figure D.3. DEM processing model. 211
Figure D.4. Elevation reclassification model. 211
Figure D.5. DEM to aspect model. 212
Figure D.6. Aspect processing model. 212
Figure D.7. Slope preprocessing model. 213
Figure D.8. Slope processing model. 213
Figure D.9. Hydrology preprocessing model. 214
Figure D.10. Hydrology processing model. 214
Figure D.11. Geology preprocessing model. 215
Figure D.12. Geology processing model. 215
Figure D.13. Soil preprocessing model. 216
Figure D.14. Soil processing model. 217
Figure D.15. Land cover preprocessing model. 217
Figure D.16. Urban areas processing model. 217
Figure D.17. Building preprocessing model. 218
Figure D.18. Building processing model. 218
Figure D.19. Population processing model. 219
Figure D.20. Transportation preprocessing model. 219
Figure D.21. Transportation processing model 220

Figure E.1. Landslide susceptibility areas for Boulder and Larimer Counties, Colorado. Data source: Colorado Geological Survey. CGS Open File Report datasets 14-02 (Boulder County) and 15-13 (Larimer County). (Morgan et al., 2014; T. Wait et al., 2015)..... 222
Figure E.2. Colorado Digital Elevation Model (DEM) for Boulder and Larimer Counties, Colorado. Data source: U.S. Geological Survey Digital Elevation Model data. 223
Figure E.3. Slope classifications in degrees for Boulder and Larimer Counties, Colorado. Data derived from U.S. Geological Survey Digital Elevation Model data. 224
Figure E.4. Slope aspect showing direction of slope face (orientation) for Boulder and Larimer Counties, Colorado. Data derived from U.S. Geological Survey Digital Elevation Model data. 225
Figure E.5. Hydrology network showing areas within 50 meters of waterbodies (lakes and reservoirs) and flowlines (rivers and streams) for Boulder and Larimer Counties, Colorado. Data source: U.S. Geological Survey National Hydrology Dataset (NHD). 226
Figure E.6. Geology including lithology classes and proximity to faults (50-meter buffer), Boulder and Larimer Counties, Colorado. Data source: Colorado Geological Survey. 227
Figure E.7. Soil order classes, Boulder and Larimer Counties, Colorado. Data source: U.S. Department of Agriculture Natural Resources Conservation Service (NRCS). 228
Figure E.8. Land cover vegetation classes, Boulder and Larimer Counties, Colorado. Data source: U.S. Geological Survey, GAP Analysis Project. 229
Figure E.9. GAP land cover symbology. 230
Figure E.10. Urban area classes for Boulder and Larimer Counties, Colorado. Data source: U.S. Census Bureau. 231
Figure E.11. Buildings with 100-meter buffer for Boulder and Larimer Counties, Colorado. Data source: Microsoft building footprint data 2018. 232
Figure E.12. Population by census block for Boulder and Larimer Counties, Colorado. Data source: U.S. Census Bureau. 233
Figure E.13. Transportation classes for Boulder and Larimer Counties, Colorado including 50-meter buffer for railroads and roadways, and 500-meter buffer for airports. Data sources: Colorado Department of Transportation, Boulder County, and Larimer County. 234
Figure E.14. Binary weighted-sum riskscape for Boulder and Larimer Counties, Colorado indicating number of factors present in 10-meter grid locations. 235
Figure E.15. Ranked weighted-sum riskscape for Boulder and Larimer Counties, Colorado indicating number of factors present in 10-meter grid locations. 236
Figure E.16. Human factor weighted-sum riskscape for Boulder and Larimer Counties, Colorado indicating number of factors present in 10-meter grid locations. 237

Figure F.1. Landslide percentage for Boulder and Larimer Counties, Colorado. Data source: Colorado Geological Survey. CGS Open File Report datasets 14-02 (Boulder County) and 15-13 (Larimer County). (Morgan et al., 2014; T. Wait et al., 2015)..... 239
Figure F.2. Aspect classes for Boulder County, showing slope face direction. Data derived from U.S. Geological Survey Digital Elevation Model data. 240
Figure F.3. Aspect classes for Larimer County, showing slope face direction. Data derived from U.S. Geological Survey Digital Elevation Model data. 240
Figure F.4. Slope classes in degrees for Boulder County. Data derived from U.S. Geological Survey Digital Elevation Model data. 241

Figure F.5. Slope classes in degrees for Larimer County. Data derived from U.S. Geological Survey Digital Elevation Model data. 241
Figure F.6. Elevation classes in meters for Boulder County. Data derived from U.S. Geological Survey Digital Elevation Model data. 242
Figure F.7. Elevation classes in meters for Larimer County. Data derived from U.S. Geological Survey Digital Elevation Model data. 242
Figure F.8. Combined curvature (planimetric and profile) classes for Boulder County. Data derived from U.S. Geological Survey Digital Elevation Model data. 243
Figure F.9. Combined curvature (planimetric and profile) classes for Larimer County. Data derived from U.S. Geological Survey Digital Elevation Model data. 243
Figure F.10. Hydrology classes for Boulder County, showing areas within 50 meters of waterbodies (lakes and reservoirs) and flowlines (rivers and streams). Data source: U.S. Geological Survey National Hydrology Dataset (NHD) data. 244
Figure F.11. Hydrology classes for Larimer County, showing areas within 50 meters of waterbodies (lakes and reservoirs) and flowlines (rivers and streams). Data source: U.S. Geological Survey National Hydrology Dataset (NHD) data. 244
Figure F.12. Fault classes (presence or absence), Boulder and Larimer Counties, showing areas within 50 meters of fault lines. Data source: Colorado Geological Survey. 245
Figure F.13. Lithology classes, Larimer County (classes with less than 0.5% areal extent and water classes were removed from chart). Data source: Colorado Geological Survey. 245
Figure F.14. Soil order classes, Boulder County. Data source: U.S. Department of Agriculture Natural Resources Conservation Service (NRCS). 246
Figure F.15. Soil order classes, Larimer County. Data source: U.S. Department of Agriculture Natural Resources Conservation Service (NRCS). 246
Figure F.16. Land cover classes, Boulder County (with classes for water and pasture removed). Data source: U.S. Geological Survey, GAP Analysis Project. 247
Figure F.17. Land cover classes, Larimer County (with classes for water and pasture removed). Data source: U.S. Geological Survey, GAP Analysis Project. 247
Figure F.18. Urban area classes for Boulder and Larimer Counties. Data source: U.S. Census Bureau. 248
Figure F.19. Building classes for Boulder and Larimer Counties, with 100-meter buffer. Data source: Microsoft building footprints (2018). 248
Figure F.20. Transportation classes for Boulder County, with 50-meter buffer for railroads and roadways, and 500-meter buffer for airports. Data source: Colorado Department of Transportation and Boulder County. 249
Figure F.21. Transportation classes for Larimer County, with 50-meter buffer for railroads and roadways, and 500-meter buffer for airports. Data source: Colorado Department of Transportation and Larimer County. 249
Figure F.22. Population classes for Boulder County. Data source: U.S. Census Bureau. 250
Figure F.23. Population classes for Larimer County. Data source: U.S. Census Bureau. 250
Figure F.24. Boulder County binary riskscape weighted factors and landslide percentages. 251
Figure F.25. Larimer County binary riskscape weighted factors and landslide percentages. 251
Figure F.26. Boulder County ranked riskscape weighted factors and landslide percentages. 252
Figure F.27. Larimer County ranked riskscape weighted factors and landslide percentages. 252
Figure F.28. Boulder County human factor riskscape weighted factors and landslide percentages. 253

Figure F.29. Larimer County human factor riskscape weighted factors and landslide percentages. 253

Figure G.1. Boulder County weights of evidence posterior probability maps using 20% training point dataset. 255
Figure G.2. Boulder County weights of evidence posterior probability maps using 500 point training point dataset. 256
Figure G.3. Boulder County weights of evidence posterior probability maps using 1000 point training point dataset. 257
Figure G.4. Boulder County logistic regression posterior probability maps using 20% training point dataset. 258
Figure G.5. Boulder County logistic regression posterior probability maps using 500 point training point dataset. 259
Figure G.6. Boulder County logistic regression posterior probability maps using 1000 point training point dataset. 260
Figure G.7. Larimer County weights of evidence posterior probability maps using 20% training point dataset. 261
Figure G.8. Larimer County weights of evidence posterior probability maps using 500 point training point dataset. 262
Figure G.9. Larimer County weights of evidence posterior probability maps using 1000 point training point dataset. 263
Figure G.10. Larimer County logistic regression posterior probability maps using 20% training point dataset. 264
Figure G.11. Larimer County logistic regression posterior probability maps using 500 point training point dataset. 265
Figure G.12. Larimer County logistic regression posterior probability maps using 1000 point training point dataset. 266

LIST OF KEYWORDS

Chapter 3: Riskscape, Geographic Information Systems, Landslide susceptibility hazards, Spatial autocorrelation, Weighted sum analysis.

Chapter 4: GIS, ArcSDM, Landslide susceptibility, Riskscape, Logistic regression, Weights of evidence, Probabilistic neural networks.

Chapter 5: GIS, Scale, Classification, Data errors, Spatial autocorrelation, Riskscapes.

CHAPTER 1: INTRODUCTION TO THE DISSERTATION

1.1 Introduction

Riskscapes represent the spatial distribution of risks across a landscape. These dynamic features can change based on events, transitions in population (population growth or movement), or changes in local conditions. Riskscapes form the basis for introducing human dimensions into natural hazard risk equations.

Landslide studies frequently use risk equations to model areas that are susceptible or vulnerable to landslides (van Westen, 2013). Risk equations presented in these studies, like those of Bell and Glade (2004), relate risk to the characteristics of the area: elements that are proximal, the valuation or quantification of those assets, and the probability of a hazard occurrence in the area (Bell & Glade, 2004; Guzzetti, 2006; Schmidt et al., 2011; van Westen, 2013). Mathematical assessments of these risk equations and factors do not determine the relationships spatially. Developing a constructed riskscape approach to these quantitative landslide assessments by applying spatial modeling techniques will create a spatial approach to the risk equations, allowing us to place risk in a spatial context to improve our understanding of the distributions of risk across a landscape. Riskscapes then become an interdisciplinary application, providing measurable accountability to the social construction of risk, and adding spatial construction to the landslide risk equations.

This dissertation is presented in seven chapters. This first chapter includes an introduction to riskscapes and overview of the research objectives. The following four chapters are based on manuscripts submitted to four peer-reviewed journals. The final sections of the

dissertation include the conclusions and reflections chapters. Maps, tables, and graphs that were developed but not included in the publication submissions are included in the appendices.

1.2 Research objectives and overview

This dissertation approaches landslide susceptibility, urban environments, and geospatial techniques through the lens of riskscapes. Given the intrinsic independent (individual) character of risk, which is based on an individual's own view of their physical and social spaces, riskscapes are composed of multiple facets to incorporate different risk characteristics and perceptions (Müller-Mahn & Everts, 2013). This project is focused on the physicality of landslides and how technology applications support risk identification and susceptibility mapping including urban and human factors as features with measurable spatial distributions. The implications of landslides in urban areas necessitate a model to understand how riskscapes are related to events and space. The development of a riskscape process for landslide hazards introduces quantification methods to the social construction aspects of riskscapes. In riskscape models, space matters, and the determination of the spatial aspects of landslide riskscapes will provide a framework for prioritization of planning and response for hazard events.

Understanding this human-environmental interaction through a landslide riskscape perspective will improve the understanding we have of the space in which these risks occur. Developing an applied, measurable, and quantifiable riskscape model will help to inform planning and reduce the potential for damage. In Chapter Two, I review and assess the riskscapes of landslides and define riskscapes within the context of landslides, a definition which has been lacking. The primary objective of Chapter Two is to address the definitional gap in riskscape literature and account for riskscapes as a spatial feature as applied to landslide hazards. Through a quantitative landslide modeling framework, landslide riskscapes will be defined to account for

their spatial aspects. Additionally, I develop a conceptual framework to address these questions and provide a spatial riskscape weighted sum model equation derived from natural hazard risk equations found in landslide susceptibility studies.

Riskscapes as spatial features should incorporate the spatiality of the human-environment system. However, as based in social-constructivist theories, this spatiality is not measurable. The lack of spatial modeling through applied spatial autocorrelation methods creates a gap in our understanding of how spatially relevant the riskscape and landslide susceptibility modeling are in terms of the strength of the spatial relationships of the input factors. In Chapter Three, an operationalized geographic information systems (GIS) model is created to quantitatively define landslide riskscapes based on geospatial analytical methods. The creation of a riskscape analysis for Boulder and Larimer Counties in Colorado will demonstrate the practicality of this assessment (see Figure 1 for study area locations). The objective of Chapter Three is to develop a method for quantitative weighted sum landslide riskscapes to further the understanding of landslide riskscapes as a geospatial model-driven tool. Further, spatial autocorrelation and clustering models are developed using Global Moran's *i* and Anselin Local Moran's *i* algorithms to introduce the spatial relationship measurement to the landslide riskscape model to address this quantitative modeling gap.

Geostatistical models are used in quantitative landslide susceptibility modeling to explore the relationships between correlated factors and hazard events. In Chapter Four, a geostatistical comparison of the landslide riskscapes is developed using the Spatial Data Modeler (ArcSDM) extension to the ArcGIS platform to evaluate logistic regression, probabilistic neural networks, and weights of evidence approaches to landslide riskscapes. Applied riskscape models as developed in Chapter Three are used to determine the relative efficacy of three geostatistical

models for predicting landslide riskscapes within the study areas. The goal of this comparison is to determine both the effectiveness of the ArcSDM toolsets and the effectiveness of the different geostatistical methods for developing a geostatistical landslide riskscape analysis for the study areas. This manuscript will contribute to our understanding of the relative efficacy of three statistical models commonly used in landslide susceptibility studies — logistic regression, neural networks, and weights of evidence — and how these models perform in a spatialized riskscape analysis. Comparing the results of geostatistical models for landslide riskscapes will help us understand appropriate methodologies and determine appropriate usage for the geostatistical tools.

Finally, a discussion on limiting factors for the riskscape approach is explored as the fourth manuscript in this dissertation, through the examples discovered during the analytical processes in the previous chapters. In Chapter Five, limitations of spatial science and data as applied to landslide riskscapes are reviewed. This assessment will contribute to our overall understanding of the limitations of the operational riskscape model, the requirements for datasets and data quality issues, and the spatial dimensions of applied landslide riskscapes. This manuscript will address the following questions: What is the influence of spatial data on riskscape development? What are the limitations of applied riskscapes and how can we address these challenges? Answering these questions will improve our understanding of the appropriate use and limitations of riskscape models and the influence of parameter selection on spatial analyses.

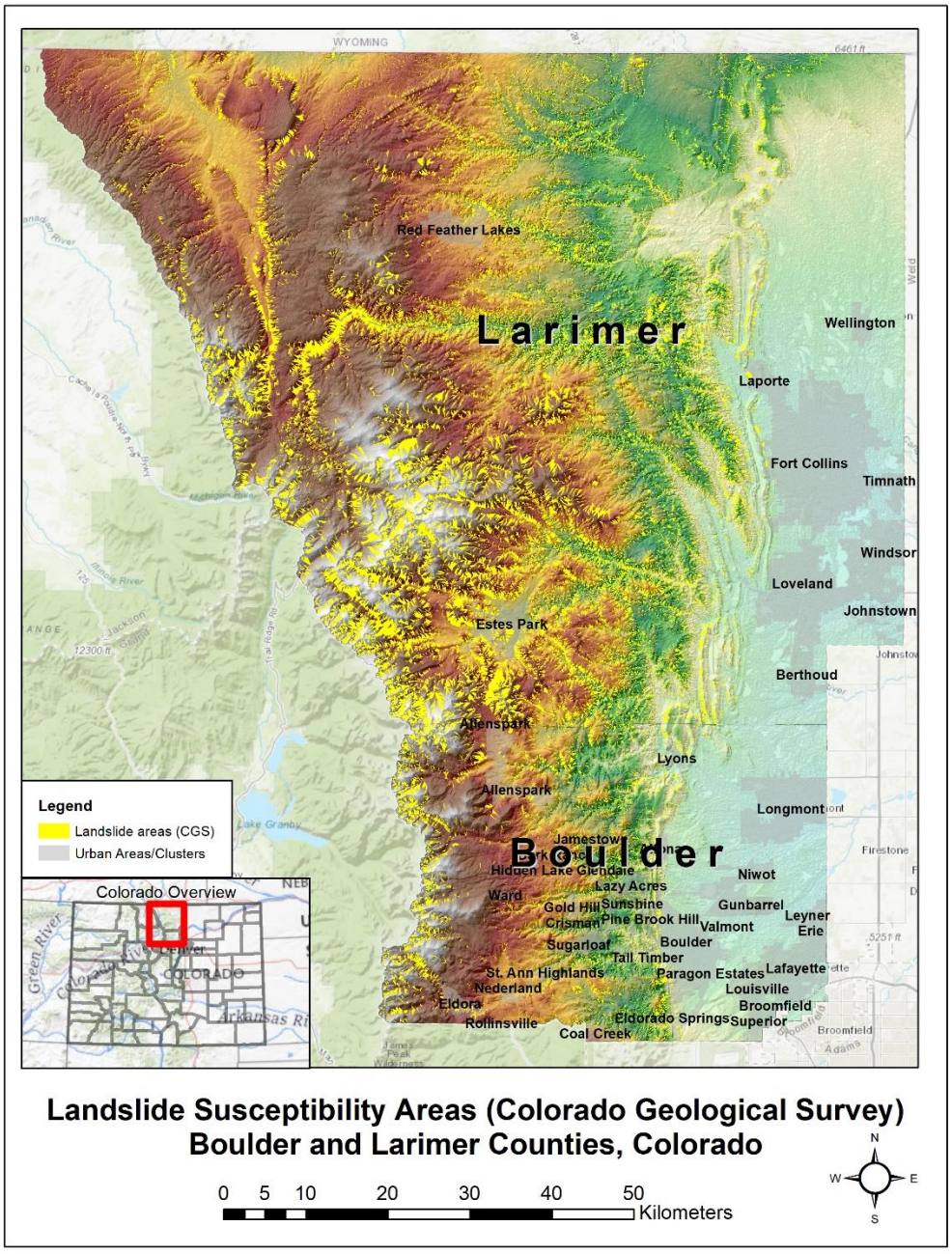

Figure 1.1. Location of study areas and landslide susceptibility areas, Boulder and Larimer Counties, Colorado. Data Sources: Morgan et al. (2014); T. C. Wait et al. (2015)

1.3 Background

Landslides are a global issue, costing billions of dollars and damaging human settlements and urbanized locations as well as remote, rural regions globally. As urbanization expands, landslides can increasingly occur in urban environments (He & Beighley, 2008), including

existing population centers, areas planned for future development (exurban, future growth) and other human-built environments such as roads and transportation networks. Any landslide occurrence in urban environments is especially concerning as significant loss of life and economic damage may occur (Chau & Chan, 2005; Dai & Lee, 2001, 2002, 2003; Dai et al., 2002; Lee, 2005; Lee & Pradhan, 2007; Oh et al., 2009; Varnes, 1978).

Advances in geospatial technology allow for the development of analytical methods designed to predict where landslides are more likely to occur, the risks of their occurrence, and the associated potential damage. Knowing these locations of higher landslide probability, especially those within the urban landscape and built environment, provides opportunity for better planning of roads and development; improved land-use decisions; and protection of humans, property, and sensitive environmental factors. Multiple statistical methods are used in landslide susceptibility modeling; therefore, one challenge is to determine which models apply most appropriately to regional landslide susceptibility modeling. Given the variety of methods used, the challenge becomes determining if any of these methods are more accurate or effective at modeling sites and are these models inclusive of relevant factors. These GIS landslide studies utilize a variety of geospatial techniques, and to date, no conclusive, single method of modeling landslide susceptibility within the geoprocessing tool environment has been identified as preferential. Bednarik et al. (2012, p. 548) state "there is still no common methodology for landslide risk assessment in medium to large scale (1:10,000 and larger) in particular." A recent publication by Reichenbach et al. (2018) details statistical assessment literature for landslide susceptibility.

In landslide-prone regions, the geographic scheme of landslide studies and related urbanization factors that may either influence the occurrence of landslides or be directly or

indirectly impacted by the events need to be considered. This leads to the emergence of riskscapes. Current technology applications in machine learning and more comparative literature are being developed, but no clear trends have emerged in terms of which methods are the most effective in determining areas of increased landslide risk. Further, these works focus on geomorphic aspects or environmental factors, and do not include human factors to a significant degree over a regional geographic scale.

Riskscapes developed as a named concept in the early 1990s based on work by Susan Cutter (Cutter, 1993, 1994, 2001) who described environmental and technological riskscapes as places where hazard events intersect social structures. Concurrently, Arjun Appadurai (1990) designated "scapes" as a term for spatial distribution of social and economic applications. Appadurai (1990) conceptualized the diverse themes of ethnography, media, finance, technology and ideology as features similar to landscapes, albeit with changing boundaries (Appadurai, 1990). Further development of the riskscape idea is defined in more recent works by Müller-Mahn and Everts (2013); Müller-Mahn et al. (2018), who describe riskscapes as the spatial dimension of risks and characterize riskscapes as socially-constructed features. The RiskScape Project (RiskScape, 2016) is a risk management platform used in Schmidt et al. (2011), who apply risk equations and create a framework for analyzing multiple natural hazards. A detailed method is developed in Hicks and Laituri (2020), presented in Chapter Three of this dissertation to propose a geospatial and spatial autocorrelation approach to modeling landslide riskscapes.

Riskscapes allow for inclusion of these human factors into a susceptibility model over a larger geographic region than other risk modeling approaches, such as quantitative risk assessment (QRA). Bilderback (2017) investigated a rockfall event that damaged the Zion Lodge in Zion National Park, Utah, and conducted a risk assessment of rockfall hazard. The author uses

a probabilistic risk equation that includes human factors (risk to person, risk to property), and thus presents a social risk vulnerability measurement. This is a similar measurement and premise to a riskscape approach but is spatially restricted in scope and does not measure risk spatially (presented as a mapped output) as a regional classification. Riskscape models can expand these quantitative landslide risk assessment studies in geographic scale and as a spatially-weighted riskscape surface.

Increases in conflict between expanding human environments and urbanized areas and landslide (and other natural) hazards lead to the need to develop riskscapes. Riskscapes are inherently linked to the impacted population, such as the homeowner/landowner, urban planning department, and scientific researcher, but multiple riskscapes can exist and be related by occupying the same space (Müller-Mahn & Everts, 2013). These riskscapes can work together to form a more complete picture of complex, interrelated, and spatially distributed phenomena. Technology applications are used to model and interpret these at-risk areas and to create maps and analyses that form the foundation of riskscapes. GIS is used to manage and manipulate the data to create these information surfaces. Discussions on the literature background for riskscapes are found in Chapter Two.

1.4 Summary

This dissertation presents four publication submissions to address four areas within riskscape approaches as applied to landslides. First, defining riskscapes within the literature to create a framework for quantitative riskscape modeling is developed, submitted to Earth Interactions Journal. Second, an operational riskscape is constructed for landslides in a regional area in Colorado, submitted to Natural Hazards Journal. Third, a comparison of geostatistical approaches will further the development of our understanding of riskscape processes, submitted

to Computers & Geosciences journal. Finally, the limitations of the riskscape modeling process, especially as pertains to the data development and analysis cycles is discussed in a manuscript, submitted to Geo-Spatial Information Science Journal. The intent of these studies is to develop the background of riskscapes and spatial implications of landslides, create a riskscape procedure to utilize geospatial analysis, and review geostatistical methods applied to landslide riskscapes. Instead of combining environmental and social risk frameworks independently, my contribution to riskscapes adds a spatial theory framework to create measurable surface features of risk for landslides focusing on the urban and wildland urban interface sections in two study areas of the Colorado Front Range. These riskscape models demonstrate the strength of the spatial relationships of these human-environment surface features to support more advanced planning, preparedness activities, and mitigation for these regions of increased risk.

References

Appadurai, A. (1990). Disjuncture and Difference in the Global Cultural Economy. *Public Culture*, *2*(2), 1–24. https://doi.org/10.1215/08992363-2-2-1

Bednarik, M., Yilmaz, I., & Marschalko, M. (2012). Landslide hazard and risk assessment; a case study from the Hlohovec-Sered' landslide area in south-west Slovakia. *Natural Hazards*, *64*(1), 547-575. https://doi.org/10.1007/s11069-012-0257-7

Bell, R., & Glade, T. (2004). Quantitative risk analysis for landslides - Examples from Bildudalur, NW-Iceland. *Natural Hazards and Earth Science Systems*, *4*, 14.

Bilderback, E. (2017). *Zion Lodge Rockfall Risk Assessment, Winter 2016-2017 Events* National Resource Stewardship and Science, Issue. U. S. D. o. t. Interior.

Chau, K. T., & Chan, J. E. (2005). Regional bias of landslide data in generating susceptibility maps using logistic regression; case of Hong Kong Island. *Landslides*, *2*(4), 280-290. https://doi.org/10.1007/s10346-005-0024-x

Cutter, S. L. (1993). *Living with risk : the geography of technological hazards*. London ; New York : E. Arnold ; New York : Routledge, Chapman and Hall distributor.

Cutter, S. L. (1994). *Environmental risks and hazards* (S. Cutter, Ed.). Prentice Hall.

Cutter, S. L. (2001). *American hazardscapes: the regionalization of hazards and disasters*. Washington, D.C. : Joseph Henry Press.

Dai, F. C., & Lee, C. F. (2001). Terrain-based mapping of landslide susceptibility using a geographical information system; a case study. *Canadian Geotechnical Journal = Revue Canadienne de Geotechnique*, *38*(5), 911-923.

Dai, F. C., & Lee, C. F. (2002). Landslide characteristics and slope instability modeling using GIS, Lantau Island, Hong Kong. *Geomorphology*, *42*(3), 213-228.

Dai, F. C., & Lee, C. F. (2003). A spatiotemporal probabilistic modelling of storm-induced shallow landsliding using aerial photographs and logistic regression. *Earth Surface Processes and Landforms*, *28*(5), 527-545. https://doi.org/10.1002/esp.456

Dai, F. C., Lee, C. F., & Ngai, Y. Y. (2002). Landslide risk assessment and management; an overview. *Engineering Geology*, *64*(1), 65-87.

Guzzetti, F. (2006). *Landslide hazard and risk assessment: concepts, methods, and tools for the detection and mapping of landslides, for landslide susceptibility zonation and hazard assessment, and for landslide risk evaluation* [Dissertation, University of Bonn]. Bonn, Germany. http://geomorphology.irpi.cnr.it/Members/fausto/PhD-dissertation/Landslide_Hazard_and_Risk_Assessment.pdf

He, Y., & Beighley, R. E. (2008). GIS-based regional landslide susceptibility mapping; a case study in Southern California. *Earth Surface Processes and Landforms*, *33*(3), 380-393. https://doi.org/10.1002/esp.1562

Hicks, H., & Laituri, M. (2020). *Geospatial applications to landslide riskscape development: a modeling approach to quantify landslide riskscapes in the Colorado Front Range [Manuscript submitted for publication]* [Manuscript]. Colorado State University.

Lee, S. (2005). Application of logistic regression model and its validation for landslide susceptibility mapping using GIS and remote sensing data. *International Journal of Remote Sensing*, *26*, 1477-1491.

Lee, S., & Pradhan, B. (2007). Landslide hazard mapping at Selangor, Malaysia using frequency ratio and logistic regression models. *Landslides*, *4*(1), 33-41. https://doi.org/10.1007/s10346-006-0047-y

Morgan, M. L., White, J. L., Fitzgerald, F. S., & Berry, K. A. (2014). *Foothill and mountainous regions in Boulder County, Colorado that may be susceptible to earth and debris/mud flows during extreme precipitation events* Colorado Geological Survey. https://coloradogeologicalsurvey.org/publications/landslide-susceptibility-extreme-precipitation-boulder-colorado

Müller-Mahn, D., & Everts, J. (2013). Riskscapes: the spatial dimension of risk. In H.-D. Müller-Mahn & C. Ebooks (Eds.), *The spatial dimension of risk: How geography shapes the emergence of riskscapes*. Routledge.

Müller-Mahn, D., Everts, J., & Stephan, C. (2018). RISKSCAPES REVISITED - EXPLORING THE RELATIONSHIP BETWEEN RISK, SPACE AND PRACTICE. *Erdkunde*, *72*(3), 197-213. https://doi.org/10.3112/erdkunde.2018.02.09

Oh, H.-J., Lee, S., Chotikasathien, W., Kim, C. H., & Kwon, J. H. (2009). Predictive landslide susceptibility mapping using spatial information in the Pechabun area of Thailand. *Environmental Geology [Berlin]*, *57*(3), 641-651. https://doi.org/10.1007/s00254-008-1342-9

Reichenbach, P., Rossi, M., Malamud, B. D., Mihir, M., & Guzzetti, F. (2018). A review of statistically-based landslide susceptibility models. *Earth-Science Reviews*, *180*, 60-91. https://doi.org/10.1016/j.earscirev.2018.03.001

RiskScape, P. (2016). *The RiskScape Project: About the Project*. New Zealand Foundation for Reseaerch, Science, and Technology. Retrieved October 1, 2016 from https://riskscape.niwa.co.nz/about-the-project/funding

Schmidt, J., Matcham, I., Reese, S., King, A., Bell, R., Henderson, R., Smart, G., Cousins, J., Smith, W., & Heron, D. (2011). Quantitative multi-risk analysis for natural hazards: a framework for multi-risk modeling. *Natural Hazards*, *58*, 1169-1192.

van Westen, C. J. (2013). 3.10 Remote Sensing and GIS for Natural Hazards Assessment and Disaster Risk Management. In J. F. Shroder (Ed.), *Treatise on Geomorphology* (pp. 259-298). Academic Press. https://doi.org/https://doi.org/10.1016/B978-0-12-374739-6.00051-8

Varnes, D. J. (1978). *Slope movement types and processes* (0360859X). Special Report: Landslides analysis and control Issue.

Wait, T. C., Morgan, M. L., Fitzgerald, F. S., Morgan, K. S., Berry, K. A., & White, J. L. (2015). *OF-15-13 Debris Flow Susceptibility Map of Larimer County, Colorado*. Golden, Colorado: State of Colorado Retrieved from https://coloradogeologicalsurvey.org/publications/debris-flow-susceptibility-map-larimer-colorado

CHAPTER 2: RISKSCAPES AS A GEOSPATIAL CONSTRUCT: A CONCEPTUALIZATION OF LANDSLIDE RISKSCAPES IN HUMAN-ENVIRONMENT SYSTEMS[1]

2.1 Summary of the manuscript

Riskscapes have been applied to technological and natural hazards to describe social implications of risk across a region. Multiple types of riskscapes based on natural hazards (floods, tsunamis), environmental topics (pollution, noise), conflicts (war, terrorism), and social issues (diseases, access to food) are described in the literature, though no unified definition exists. This paper summarizes riskscape literature, identifies the riskscape theoretical frameworks over time, and introduces spatial theory, the concept of measurable space as a methodological approach to these existing frameworks. A conceptualization of a landslide riskscape model is proposed to introduce a quantitative method to the social constructivist riskscape model through the addition of spatial components. The synthesis of these frameworks with the contribution of spatial theory will provide a framework to operationalize spatial riskscapes to inform the human-environment interactions based on landslide risk.

2.2 Introduction

A riskscape is a conceptual framework for integrating the complexity of risk across a landscape. Using this framework to assess landscapes enables researchers to link social and physical processes to better understand this complexity and enable mitigation and planning strategies by communities and decision makers. This paper includes the following: a short

[1] This chapter is a manuscript co-authored with Melinda Laituri, submitted to a peer-reviewed journal for review.

description of the origins of riskscape in the natural hazard literature; an overview of the riskscape framework that spans multiple disciplines; the role of geospatial approaches in enhancing riskscape applications using landslides as an example hazard; and concludes with a discussion of the riskscape as a conceptual model for hazard mitigation.

Riskscapes are based on a social constructivist theory for risk assessments across a landscape, revealing interactions between humans and their environment (Müller-Mahn, 2013). Social construction theories are based on meanings, understanding, and perceptions being constructed by people based on their interactions with their environment, society, and the world (Creswell, 2009). However, riskscapes do not include measurable spatial formulae and frequently lack quantification. Risk analyses tools are used in landslide modeling to determine areas of increased risk, but do not measure the spatial components of that risk. Developing a conceptual framework for applied spatial landslide riskscapes for allows for the application of spatial tools to measure the potential landslide risks. The riskscape of landslides presents an approach to further understanding of human-environment interactions.

This paper develops an inclusive definition of riskscapes to incorporate the existing literature to inform the riskscape framework but highlights the spatial components of what makes a riskscape a "scape". This approach expands riskscapes to a quantifiable model by applying spatial theory to the social characterizations and frameworks of risk. A meta-analysis of riskscape literature, landslide susceptibility risk literature, and GIS methods in landslide literature is conducted to approach landslide riskscapes through the spatial theory lens, and to develop a conceptual diagram to classify the data types required to create a measurable landslide riskscape.

The current landslide risk studies apply GIS in their geomorphic analyses and use statistical tools to determine probabilities. However, these geomorphic or environmentally based approaches do not include the social/human-environment interactions that take place on the surface of the Earth. Human features included in spatial datasets need to be addressed outside of the scope of vulnerability, as they are features that occupy space and interact with the geomorphic and surficial environment in which the landslides occur, making them part of the landscape of risk. Social constructivist theory riskscape literature does not provide a quantifiable platform but provides the theoretical framework for human-environment interaction within a spatial context. The addition of the spatial theory to these methods will create a methodological approach to improve our ability to incorporate human features as part of the risk landscape.

2.3 Natural hazards and riskscapes

Natural hazards and natural hazard risk related terms specify different aspects of hazards that are complex, overlapping, and often derived from geologic and geomorphic control parameters (Chuang & Shiu, 2018; van Westen, 2013). Riskscape terminology is similarly complicated due to the interdisciplinary nature of risk. Riskscapes interrelate multiple aspects of risk, hazard, and spatial terminology. The United Nations created a terminology guideline as part of the International Strategy for Disaster Reduction (UNISDR, 2009). van Westen (2013) used these definitions in a review of geospatial applications for natural hazard risk and disaster management which provides a thorough glossary of terms related to natural hazards, risks, and disaster management (van Westen, 2013).

Table 2.1 includes commonly used terms in natural hazard assessments to establish a baseline of natural hazard language used throughout this paper.

Table 2.1. Terms and definitions for riskscapes and geospatial applications to landslides.

Term	Definition	References
1. Disaster	"A serious disruption of the functioning of a community or a society involving widespread human, material, economic or environmental losses and impacts, which exceeds the ability of the affected community or society to cope using its own resources."	UNISDR (2009)
2. Risk	"Likelihood of the occurrence of the hazard."	Cutter (1993)
3. Hazard	"A dangerous phenomenon, substance, human activity or condition that may cause loss of life, injury, or other health impacts, property damage, loss of livelihoods and services, social and economic disruption, or environmental damage."	UNISDR (2009)
4. Consequence	"The expected losses in a given area as a result of a given hazard scenario."	van Westen (2013)
5. Elements at risk (or Exposure, or Assets)	"Population, properties, economic activities, including public services, or any other defined values exposed to hazards in a given area. Also referred to as "assets." The amount of elements-at-risk can be quantified either in numbers (of buildings, people, etc.), in monetary value (replacement costs, market costs, etc.), area, or perception (importance of elements-at-risk)."	van Westen (2013)
6. Vulnerability	"The conditions determined by physical, social, economic, and environmental factors or processes, which increase the susceptibility of a community to the impact of hazards. Can be subdivided in physical, social, economical, and environmental vulnerability."	van Westen (2013)
7. Riskscape	The spatial dimension of risk, the landscape of risk, landscape of potential damage.	Müller-Mahn (2013); Khan (2012)
8. Hazardscape	"The landscape of hazards", existing and potential source of threats.	Cutter (2001); Khan (2012)
9. Landslide	"Downward and outward movement of slope-forming materials composed of natural rock, soils, artificial fills, -or combinations of these materials."	Varnes (1958)
10. Quantitative risk assessment	Site-specific assessment of risk, "values of consequences are combined with probabilities of occurrence."	Cutter (1993); Lee (2009)
11. Qualitative risk assessment	A heuristic risk assessment approach using classifications, an inductive method of disaster research.	Castellanos Abella and van Westen (2008); Phillips (2014)
12. Geographic Information Systems (GIS)	"A computer-based system to aid in the collection, maintenance, storage, analysis, output, and distribution of spatial data and information."	Bolstad (2019)
13. RiskScape Project	A risk modeling program developed in New Zealand to create natural hazard loss maps and asset loss calculations.	RiskScape (2016)
14. Natural hazard	"Natural process or phenomenon that may cause loss of life, injury or other health impacts, property damage, loss of livelihoods and services, social and economic disruption, or environmental damage."	UNISDR (2009)

15. Disaster risk	"The potential disaster losses, in lives, health status, livelihoods, assets and services, which could occur to a particular community or a society over some specified future time period."	UNISDR (2009)
16. Landslide hazard	"Probability of a danger or threat arising from a landslide event."	Lee (2009)
17. Probability	"A measure of the degree of certainty. This measure has a value between zero (impossibility) and 1.0 (certainty). It is an estimate of the likelihood of the magnitude of the uncertain quantity, or the likelihood of the occurrence of the uncertain future event."	van Westen (2013)
18. Loss	Can be environmental, human, or cost losses, amount of damage.	van Westen (2013)
19. Areal Impact	"Measuring the extent of the geographical area that potentially will be affected by a hazard event."	Kappes et al. (2012)
20. Intensity	"Measuring the intensity level of a hazard", how strong or damaging the event is.	Kappes et al. (2012)

Several discrepancies exist within the definitions of these terms. For example, element-at-risk, exposure, and asset (5) are used interchangeably in the risk formulae as seen in Bell and Glade (2004); Fuchs et al. (2012); Lee (2009); Schmidt et al. (2011); van Westen (2013) to mean the elements or areas that are exposed to the hazard. Cutter (2001, p. 2) explicitly states "within the broad community of hazards researchers and practitioners, hazard, risk, and disaster are terms that are used interchangeably, although they do have different meanings (Cutter 1993, 1994, Kunreuther and Slovic 1996, Quarantelli 1998, Mileti 1999)."

Natural hazards, specifically landslides, are defined as the event or events that may take place. Cutter (1993) describes hazards as inclusive of frequency and magnitude along with the probability of occurrence, while other authors such as van Westen (2013) and Chen et al. (2016) are not as specific regarding recurrence when describing a hazard. Multi-hazards include more than one hazard event type, such as flooding, tsunamis, earthquakes, landslides, or volcanic eruptions.

Risk is associated with two primary approaches: social/qualitative and physical/quantitative. Risk is an emergent property based on a social construct that changes due to fluctuating environmental factors (Müller-Mahn & Everts, 2013). The fluctuations of surfaces from social features such as population movement, changes in urbanization and development as well as the environmental changes due to geomorphic processes and land cover or vegetation lead to changing risk throughout the region. Measurable, probability, and quantitative risk assessment (QRA) based risk evaluations are based on the calculations of risk, often related to losses and counts related to buildings or lives, or economic factors. Risks change with time, space, feature evolution (e.g., changes in land use/land cover, population movement), and can be measured across multiple scales (e.g., human, individual, ecosystem, political region).

2.4 Risk equations and riskscapes

Risk equations are presented in natural hazard literature to demonstrate the ability to mathematically calculate specific risk in an area. Multiple studies apply versions of the risk equation to assess potential landslide risk in a quantitative approach (Fuchs et al., 2013; Remondo et al., 2005; Schmidt et al., 2011; Smith, 2013).

Bell and Glade (2004) define the risk equation as R = H x C x E in their work on landslide risk analysis in Iceland.

Equation 1. Risk equation from Bell and Glade (2004)

$$R = H \times C \times E$$

Where R is risk, H is hazard (or the probability of a natural hazard event occurring), C is consequences (or the outcome of the event occurring, also defined as vulnerability and impacts),

and E is the elements susceptible to risk (including the human and built environment factors) (Bell & Glade, 2004).

Other studies express natural hazard risk similarly and provide risk equations based on vulnerability (Chen et al., 2016; Smith, 2013; van Westen, 2013), temporal aspects (Chen et al., 2016; Kappes et al., 2012; van Westen, 2013), and intensity (Kappes et al., 2012; van Westen, 2013). Smith (2013) used risk = hazard probability x elements at risk x vulnerability as the risk equation, opting to use vulnerability instead of consequences. The factors from the risk equations shown categorically in Table 2.2 indicate the usage of both physical and social datasets. Each study bases the risk equations on the presence or potential for the hazard event, and evaluates that risk in the context of the social aspects of elements at risk, consequences, or vulnerability. Kappes et al. (2012) approaches the risk equation based on a Hazard Score (HS) index, incorporating event frequency (probability) and intensity with the areal extent or distribution of the event (Kappes et al., 2012) without including the elements at risk, vulnerability, or consequences found in the other works. Collectively, these equations do not fully incorporate both the spatial and the social aspects with the hazard potential. Riskscape features — the combination of risk, space, and social elements — are not fully included in these approaches to modeling risk.

Table 2.2. Risk equation summary from selected riskscape and natural hazard literature.

Reference	Hazard (3)	Consequence (4)	Elements at risk (5)	Vulnerability (6)	Temporal or spatio-temporal probability (17)	Loss (amount) (18)	Areal impact (19)	Intensity (20)
Bell and Glade (2004)	X	X	X					
Chen et al. (2016)	X		X	X	X			
Kappes et al. (2012)	X				X		X	X
Smith	X		X	X				

(2013)								
van Westen (2013)	X	X	X	X	X	X		

(#) indicates definition element from Table 2.1.

van Westen (2013, p. 271) developed multiple formulae shown in Figure 2.1 to express risk for natural hazards derived from the characteristics of the inputs (hazard duration, type, intensity, and extents; vulnerability intensity, damage, type, and exposure of elements at risk; and elements at risk including type, number, value, and location).

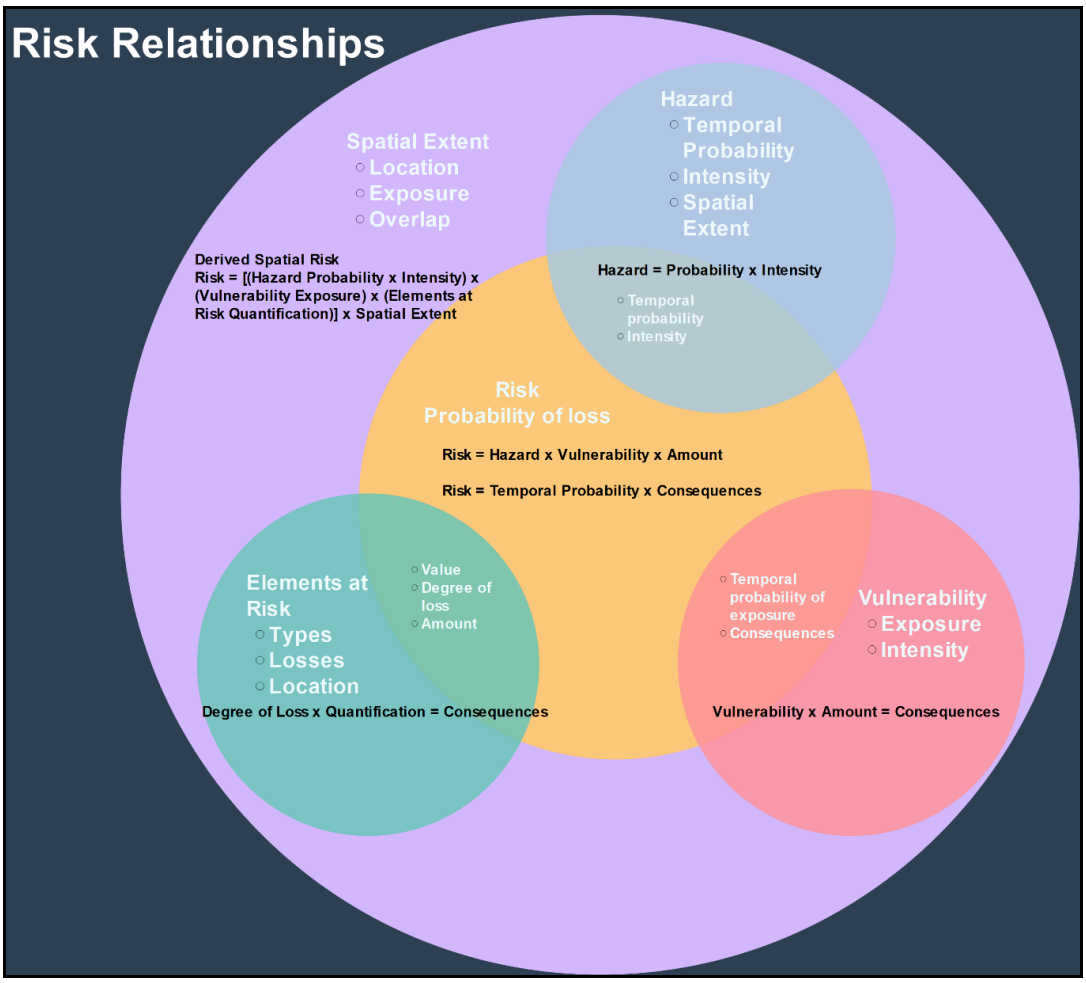

Figure 2.1. Risk equations and relationships adapted from van Westen (2013) based on the interactions of risk components and variable characteristics of risk inputs. Source: van Westen (2013).

Risk is an emergent property based on the components of the setting in which it occurs. As human and environmental systems interact, risk develops based on the nature of the events (hazard) and the human factors (elements at risk). These approaches to defining risk incorporate various elements related to the hazard, the frequency probability, and impacted features (elements, consequences, or vulnerability). But the value of the spatial component is not measured consistently and does not use the geographic distribution as a measurable feature in these equations. The risk equations presented focus on these event and human factor components of risk quantitatively but non-spatially.

We propose that riskscapes are the spatial representation of the risk equation. Applying the spatialization to the risk equation will contribute to the understanding of human-environment interactions and provide a platform for improved safety, planning, and decision making.

2.5 Riskscapes in the literature, evolving definitions

2.5.1 Riskscapes: environmental and natural hazard risk-management frameworks

"Riskscape" refers to places of risk (Hewitt & Burton, 1971)[2], the landscape of risk (Cutter, 1993, 1994), and the spatial dimension of risk (Müller-Mahn & Everts, 2013). Riskscapes are emergent spaces where risks are multiple, present and interact. 'Scaping' is described in Appadurai (1990) with reference to multiple themes including ethoscapes, ideoscapes, mediascapes, technoscapes, and financescapes. Müller-Mahn and Everts (2013) present riskscapes as a social constructivist theory structure based on these earlier works by Appadurai (1990) with the identification of multiple 'scapes' that apply outside of a traditional landscape. 'Scaping' functions, such as riskscapes, hazardscapes, landscapes, and soundscapes,

[2] The authors do not use the term riskscape but establish places of risk as a topic incorporating locational elements into the risk discussion.

are geographic concepts denoting the relationship between spatial features and spatial extent of the area. Riskscapes demonstrate the risk present in an area, emphasizing the spatial construction of the risk features, inclusive of the social constructivist theory structure mentioned earlier.

Riskscapes are a formative concept, often used as a representative ideal and not specifically as a measurable feature with distinct numerical values as seen in the multiple works of Cutter (1984); Cutter (1993, 1994, 1996, 2001), noted in Laituri (1993) in the context of environmental justice, and explored in other works (Jenerette et al., 2011; Konisky & Reenock, 2018; Morello-Frosch et al., 2001; Müller-Mahn & Everts, 2013). Riskscapes may be considered as a geographic construction that relates the risks present in an area to the spatial features and sensitive receptors or community present in that area.

Susan Cutter contributes extensively to places of risk and hazard literature, through publications in risk practices and vulnerability assessments (Cutter, 1984; Cutter, 1993, 1994, 1996, 2001). Cutter explores multiple aspects of risk, hazard, and vulnerability (Cutter, 1993, 2001). In *Living with Risk*, Cutter (1993, p. 103) introduces 'scape' terminology as a geographic pattern of hazards or accidents and grounds the natural-hazard works in previous human geography studies from Barrows (1923), developed by others including White, Burton, and Kates (Cutter, 1993, p. 178). In *Environmental Risks and Hazards*, Cutter (1994) explores natural hazards as spatial phenomena. The author situates hazards as multifaceted events that interact within their spaces and further claims, "hazards in context claims that the nature-society interaction entails a dialogue between the physical setting, the political-economic context, and the role of individuals and agents in effecting change" (Cutter, 1994, p. 76). As defined in Cutter (1993) risks are "the measure of likelihood of occurrence of the hazard" while hazards are more broadly-based (Cutter, 1993, p. 2), as the author states,

> *'hazard' is a much broader concept that incorporates the probability of the event happening, but also includes the impact or magnitude of the event on society and the environment, as well as the sociopolitical contexts within which these take place.*
>
> *Cutter (1993)*

Cutter (1994, p. xiv) summarizes by stating,

> *Also, hazards are no longer viewed as singular events, but as complex interactions between natural, social, and technological systems… Hazards are embedded in larger political, social, economic, and technological structures, and it is often impossible to separate these influences from the impacts of the event.*
>
> *Cutter (1994)*

Further work from Cutter outlines 'scapes' as a term, in *American Hazardscapes: The Regionalization of Hazards and Disasters* (Cutter, 2001). This work sets the definition of hazardscape to "the landscape of hazards" (Cutter, 2001, p. iii). Cutter (2001, p. 16) defines risk assessment for natural hazards as a "systematic process of defining the probability of an adverse event (e.g., flood) and where that event is most likely to occur."

These initial works are focused on the environmental context, relating detrimental inputs (e.g., air pollution or water contamination) to locations of increased risk of exposure. This advent of 'scaping' is a spatial approach to the documentation and integration of multiple datasets inclusive of the geophysical and environmental setting, land use/land cover, urbanization, and social population factors.

Morello-Frosch et al. (2001) use riskscapes in their work on southern California air quality. The authors introduce the term 'riskscape' and define it as a phenomenon where risks can both "accumulate" and "overlap" (Morello-Frosch et al., 2001, p. 572). The authors

introduce analytical terms found in standard GIS geoprocessing toolsets, such as the Overlay, Intersect and Merge tools, which can form the basis of a quantifiable riskscape procedure. These analyses develop the landscape of risk, revealing areas where physical and social data features intersect spatially, to prepare for hazard events and inform policy makers and the public. The authors generate a riskscape for air quality for urban environments and interpret the results to assess the overall theme of environmental justice in the region. Environmental justice is the inequitable distribution of pollution and other environmental degradation more proximal to communities with lower incomes or communities of color (Konisky & Reenock, 2018; Morello-Frosch et al., 2001). The extent and magnitude of environmental justice is spatially measurable through riskscape techniques, using demographic information with environmental risk data to determine inequality in exposure risks (Konisky & Reenock, 2018; Morello-Frosch et al., 2001). Morello-Frosch et al. (2001, p. 555) also focus on integrating data and methods into a new "comparative risk assessment framework" process. The authors conclude with their description of an applied riskscape, and it provides important context to this discussion.

> *In our view, social, economic, and political forces inevitably create myriad "riskscapes" in which overlapping air pollution plumes emitted by point, area, or mobile sources lead to cumulative exposures that pose health risks to diverse communities. Future research should elucidate how institutional discrimination, uneven regional development, and a spatialized political economy shape distributions of environmental hazards, which in turn determine variations in community exposures and susceptibility to environmental hazards.*

Morello-Frosch et al. (2001, p. 572)

Riskscapes as interactive spaces between the physical risk and the exposed population is highlighted in research by Jenerette et al. (2011). Their definition of riskscape combines both the spatial factors and the notion of vulnerability, stating that a riskscape was "defined as the spatial

variation in risk exposure and potential human vulnerability" (Jenerette et al., 2011, p. 2637). The authors' methods are designed to detect patterns, and are based on secondary sourced data from existing agencies (Landsat imagery, USGS datasets, US Census Bureau, NOAA) (Jenerette et al., 2011).

Several authors provide an overview of the risk process and this is well documented in the risk management framework developed in van Westen (2013), including aspects of risk management (the overall process of responding to risk), risk assessment (the process including the risk estimation, risk analysis, and risk evalution), risk analysis (the identification of hazard and vulnerability, commonly the risk equation), and risk evaluation (the determination of specific risks) (Chen et al., 2016; Kappes et al., 2012; Schmidt et al., 2011; van Westen, 2013). These aspects of risk management practices can be applied to a riskscape approach, which incorporates the systems theory and social theory backgrounds with the risk theory structures and in this interpretation of a riskscape developed in this chapter, the introduction of spatial theory. Figure 2.2 presents a conceptual framework for a landslide riskscape, relating theoretical backgrounds, data sources, and methods.

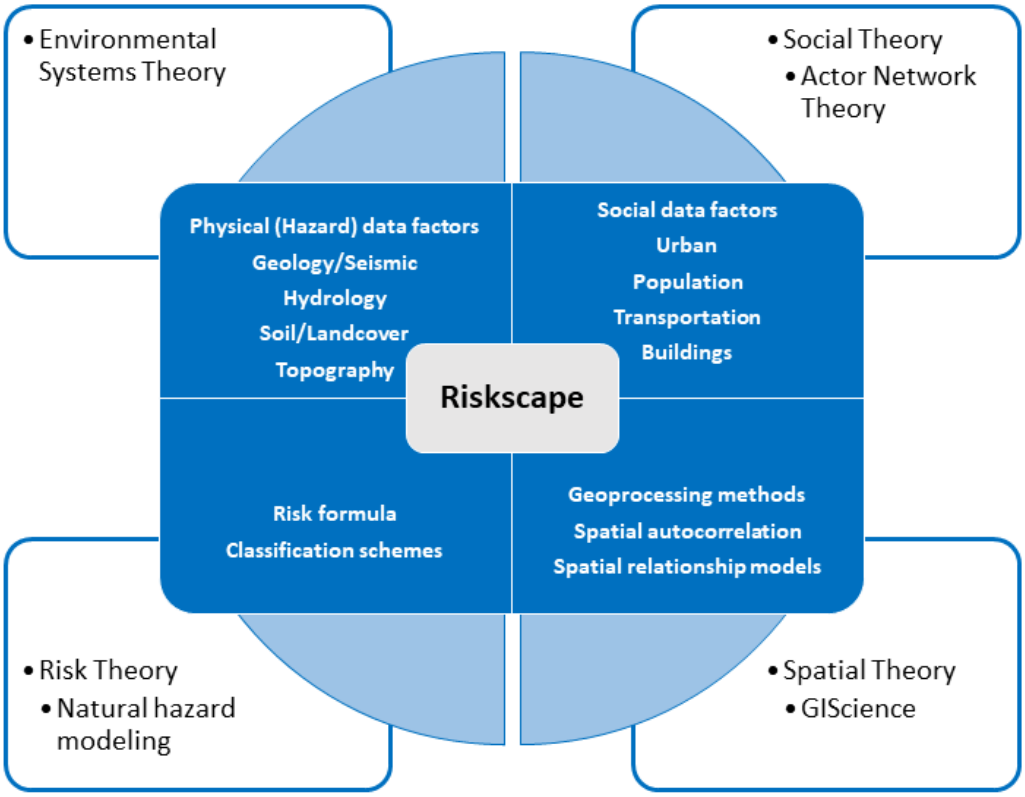

Figure 2.2. Riskscape conceptual model showing theoretical frameworks, data sources, and methodological approach.

2.5.2 Riskscapes: social theory and actor-network theory frameworks

Müller-Mahn and Everts (2013) expand these earlier works in riskscapes to create a riskscape definition based on the social aspects of risk, regardless of the hazard type (physical/natural, social, technological). Müller-Mahn and Everts (2013) contextualize riskscapes as landscapes of multiple and interacting risks, including human perceptions and actual risks that change due to human activity.

Riskscapes were further defined in a special edition of *Erdkunde* (volume 72 number 3), covering an array of topics, including social aspects of flood risk management (Stephan, 2018), climate change (Gebreyes & Theodory, 2018), food supply (Everts et al., 2018), and technology hazard incidents related to critical infrastructure (Krings, 2018). These riskscape studies focused

on the social and vulnerability aspects of riskscapes as applied to different hazards. Common among them is the focus on riskscapes as a social theory, with risk perception as a key indicator of the scale of the risk.

Updating their previous research (2013), Müller-Mahn et al. (2018, p. 199) add "power relations and temporalities" to their model. In this updated definition, Müller-Mahn et al. (2018, p. 197) incorporate spatial attributes, stating "more specifically, we define riskscape as landscapes of risk that exist in relation to practice, or as socially produced 'temporalspatial phenomena (Schatzki 2010)."

Neisser (2014) develops riskscapes in the context of actor-network theory (ANT). The author approaches ANT as an analytical framework and applies this framework to managing disaster risk through the separate mechanisms that involve the interactions of the actor and the network. Neisser (2014, p. 94) defines the term actor as "'any element which bends space around itself, makes other elements depend upon itself and translates their will into a language of its own' (Callon and Latour, 1981, p. 286)." Networks are defined as "a heterogeneous chain of its links" (Neisser, 2014, p. 94), referring to the multiple facets of connectedness in technological, political, and social aspects. Based on the connectedness of risk, its property as an emergent feature, ANT fits a riskscape model (Neisser, 2014). Inkpen (2016) applied the ANT model to develop a riskscape tool for a volcanic risk study in Iceland to interrelate volcanic riskscapes, enhancing the riskscape and ANT discussion through the inclusion of the power function, or the relationships of risks to distance and proximity. Inkpen (2016, p. 51) describes ANT as a "relational landscape" which can alter and deform the topography of the area. The distance decay expressed within the power function aligns this ANT riskscape approach with Tobler's First Law

of Geography, commonly given as “everything is related to everything else, but near things are more related than distant things” (Tobler, 1970, p. 236)

November (2008) provides a Commentary titled *Spatiality of risk* that further aligns with risk as part of an ANT and social structure. This work describes the importance of space in determining risk, based on the interactions of risk that can occur in the same areal extent. A key concept introduced is that risks modify the spaces they occupy (November, 2008). In several examples, the author indicates that risk behaves as an actor, shaping responses to it (November, 2008).

November et al. (2010) present an argument for using spatial mapping to bridge the barrier between physical and human geography. This work discusses spatial mapping applications (GIS) and how they can portray images of space, arguing that risk can be mapped as any other spatial feature.

The common practice for these perspectives is they describe the spatial importance of risks to various hazards. While space is considered differently between the approaches, the spatial component is the basis of the differentiator between them. Understanding these spatial components forms the foundation of a quantifiable riskscape practice, and this is demonstrated in a landslide riskscape approach developed in Hicks and Laituri (2020).

2.6 Relating riskscapes, spatial processes and landslide studies

Based in risk geography, hazardous places, and spatial dimensions, riskscapes evolved based on multiple theoretical frameworks. To develop riskscapes into a measurable spatial tool for landslides, other significant milestones are recognized. GIS as applied to landslide susceptibility modeling also informs the landslide riskscape model. As GIScience developed based on improved computing capabilities, landslide models using GIS tools evolved with early

contributions by Earl Brabb (Brabb, 1977; Brabb, 1984; Brabb et al., 1972) and Alberto Carrara (Carrara, 1983a, 1983b, 1988; Carrara et al., 1991; Carrara et al., 1977; Carrara et al., 1982) and refined further by Carrara et al. (1999); Guzzetti (2006); Guzzetti et al. (1999). Figure 2.3 outlines the emergence of riskscapes over time as related to GIScience developments and applications of GIS to landslide studies.

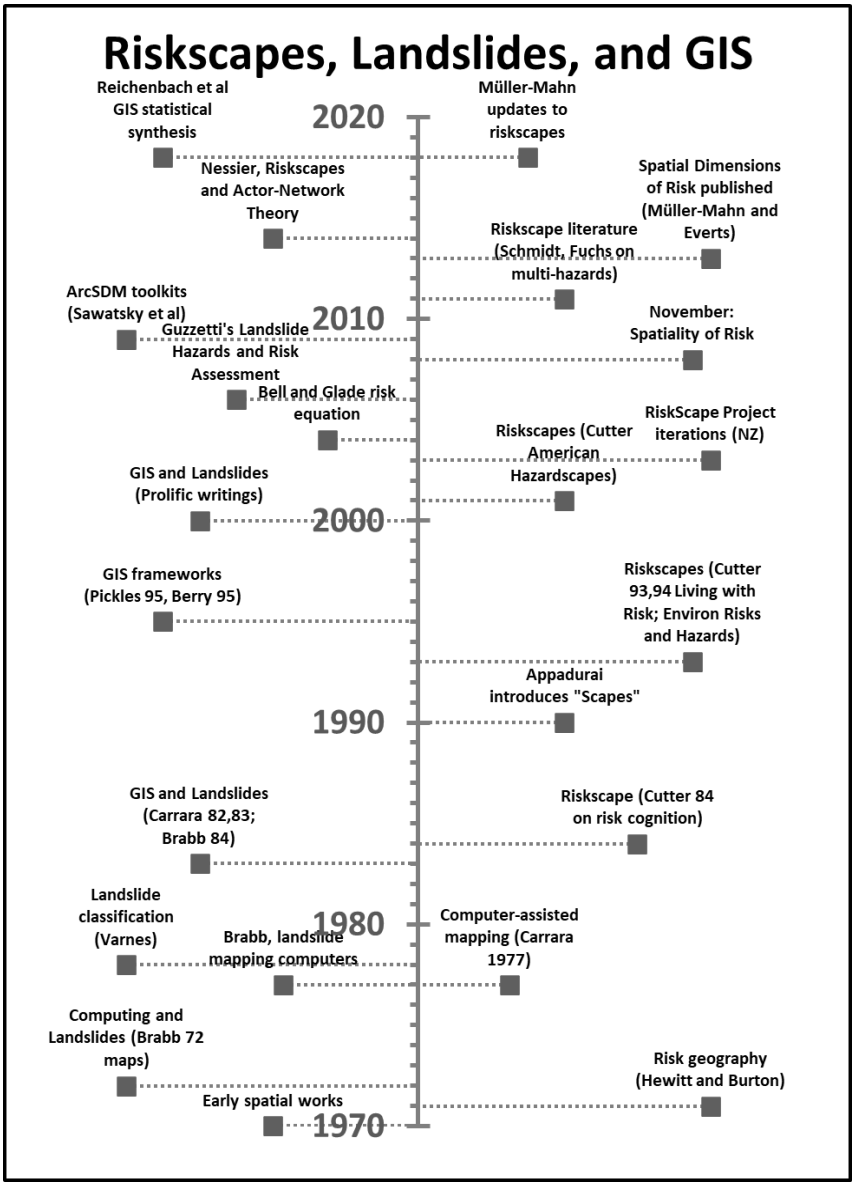

Figure 2.3. Timeline depicting milestones in riskscape development, GIS, and landslide studies.

2.7 Spatial risk characteristics

The spatial context of risk – where risks occur – is fundamental to understanding riskscapes. Risk assessment and management are broad fields that include both qualitative (i.e., ranked suitability, classes of risk) and quantitative approaches (i.e., probability, frequency, and magnitude classifications). Riskscapes are a discrete application focusing on the "where" component of risk and hazards, and depending on the framework (social, environmental, or technological approaches), focus on the qualitative aspects of risk related to perceptions and social dimensions of hazards.

2.7.1 Multiplicity of riskscapes

A key attribute of riskscapes is their multiplicity. Multiple risks can exist in a location, and perceptions of these risks are dependent on the individuals occupying those spaces (Cutter, 1994; Phillips, 2014). Müller-Mahn and Everts (2013) describe riskscapes as the emergence of multiple risks through practice, meaning that their riskscapes are based on social practices rather than strictly landscape-based. The authors align multiple riskscapes with the multiple facets of risk – multiple types of risk in an area as well as multiple perceptions of that risk. Figure 2.4 presents a multi-perspective diagram to demonstrate the multiplicity of riskscapes in place, based on a landslide example.

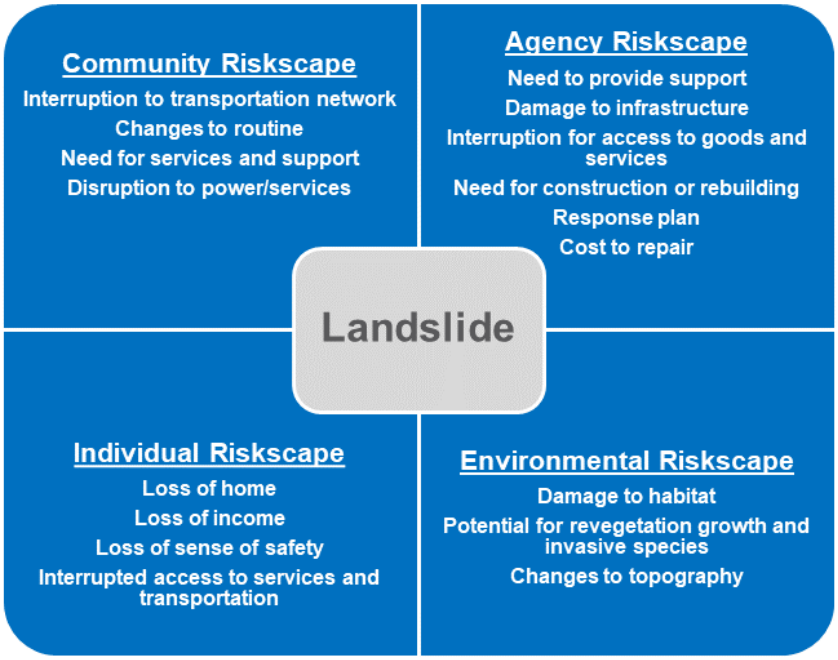

Figure 2.4. Example of multiple riskscapes in response to a landslide. Based on riskscape perspectives model from Müller-Mahn and Everts (2013, p. 34)

2.7.2 Spatial scales in riskscapes

Riskscapes are subject to the modifiable area unit problem (MAUP). The MAUP refers to a spatial analysis issue where the size and scale of the analysis can influence the results due to the limitations of the scope of the analysis (Fuchs et al., 2012). These are scale-dependent features and fill the space between traditional geomorphic hazard evaluations and the anthropologic surficial features that define disaster criteria. Disasters are defined as the impact of a hazard on life and property, damage to things considered of value as defined by humans. Geomorphic scales of studies use defined areas of geologic and topologic features to determine regions. Humans and anthropogenic features are organized by human-defined political units. The riskscape revises the scale from the geologic and geomorphic scales of landslide studies into the impacted population scale of human development. This transition is necessary to create a riskscape by incorporating the human factors in the human scale. Size of scales are also relevant

to the riskscape methods and studies. National level (small-scale) creates too generalized an output; local small scales ignore external boundary areas that may be useful for mitigation or have policy implications. A regional scale is appropriate to reflect the human dimensions of natural hazards and develop policies that may support response by the regional agencies.

Temporal aspects are critical to risk assessment studies where riskscapes are bounded by both time and space. The multidimensional aspects of riskscapes form a dependency on time and space scales, or *riskscale* (Cutter, 1994, 1996) – how are you measuring the riskscape? What limitations are placed upon the riskscape by the inherent spatial extent of the risks and communities or by the time lapsed between the events? A riskscape is a dynamic feature, dependent on time. When no events of record have occurred within a community during human memory or generational experience, it may be that the knowledge and experience, the appreciation, understanding, or valuation of the event has been lost (Cutter, 1993; Hewitt & Burton, 1971). Areas with high risk, constant events, or where a significant event takes place may see a continuation or increase in support for preparedness measures (Cutter, 1993). Risk models require a time-series component to address the amount or effect of time gaps in events of a region. These time factors influence the *perception* of a risk as being relevant to a community (Cutter, 2001; Ley-García et al., 2015). These perceptions will not affect the actual risk at all, as risk defined here is the mathematical probability of an event occurring, not how people feel about it. Ley-García et al. (2015, p. 494) found that both "amplification" (perceiving more risk than is proximal) and "attenuation" (also called "invisibility," not perceiving risk that is present) existed in perceptions of regional hazards in a study in Mexicali, Mexico, and that both perceptions can increase risk and losses.

Aubrecht et al. (2013) emphasize this temporal element in their assessments of risk processes. The authors determine that scale is inclusive of spatial and temporal aspects and that these timescales are dynamic, specifying that multiple time scales of risks (short and long term) are critical to inform decision-making (Aubrecht et al., 2013).

2.8 Vulnerability in riskscapes

Vulnerability is defined by Cutter (1993, 2001) as the potential for loss varying by time and location, or the likelihood of an entity being affected by a hazard (Cutter, 1993). By providing measurable quantitative spatial data for vulnerable assets, vulnerability is a critical difference in landslide risk assessments versus landslide riskscapes. Vulnerability is looking through the lens of natural hazards to view what may be affected, what is in the path of the hazard. The data factors that support spatial and vulnerability analyses extend the risk component for hazards to include not only the natural physical attributes (in the case of landslides, the geologic setting, topographic setting, ecologic setting, and triggering events) that may influence the occurrence of the event but also the social setting data (roads, buildings, human population, diurnal/nocturnal populations). These vulnerable elements include humans and the built environment in which they reside along with other factors less tangible such as economic impacts and flow of goods, services, and the ability to communicate information (Cutter, 2001).

These studies note the emergence of the population criteria as part of the datasets to be analyzed, not just the rationale for the project. While human factors, societal impacts and vulnerable communities (human or natural systems such as sensitive environmental factors) remain a driving factor in the significance of these studies, their inclusion as part of the dataset for the creation of riskscapes supports pattern identification (Jenerette et al., 2011). The riskscape

is inclusive of the physical parameters of the natural hazard (landslide) and the landslide-affected or vulnerable elements.

2.9 Applied riskscapes, multi-hazards, and interdisciplinary approaches

Interdisciplinary riskscapes and those related to multiple hazards are creating a platform for riskscape modeling. Aubrecht et al. (2013, p. 1208) emphasize the building structures needed to determine risks using interdisciplinary approaches, "to assess risk, various inputs (data, concepts, models, calculations, assumptions, simplifications, etc.) from different disciplines can be applied (Neuhold 2011)." Fuchs et al. (2012) discuss the relevance of risk processes used and include the human-built environment, noting susceptibility evaluations could result in the reduction of losses, indicating that policies including these multi-factor risk-mitigation strategies can make a difference in protecting communities.

These initial studies in riskscapes as applied to environmental features can be classified by topic and spatial approaches. Table 2.3 shows early works as applied to landslides, based on risk equations and thematic areas of riskscape studies.

Table 2.3. Risk literature for landslides, proto-riskscapes, and riskscapes.

Study: Author, Date	**GIS**	**Landslide**	**Topic**	**Area**	**Formula**
Risk Equation Studies					
Aubrecht et al. (2013)	Yes	No	Risk Management	NA (review)	R=HCE
Fuchs et al. (2012)	Yes	Yes	Vulnerability	Austria	R=HEV
Bell and Glade (2004)	Yes	Yes	Quantitative Risk	Iceland	R=HCE
Remondo et al. (2005)	Yes	Yes	Quantitative Risk	Spain	R=HVE

Fuchs et al. (2013)	No	Multi-hazard	Mountain Hazards	Alps	R=HpC
Lee (2009)	No	Yes	Probability	Hong Kong	R=HpC
Riskscape Studies					
Jenerette et al. (2011)	No/RS	No	Urban Heat	Phoenix AZ	NA (energy balance and NDVI)
Schmidt et al. (2011)	Yes	Multi-hazard	Flooding	New Zealand	R=HAC
Lane et al. (2015)	Yes	Yes	Tsunami	New Zealand	NA (tsunami inundation volume)
Macey (2010)	Yes	No	Respiratory Riskscape	Texas	NA (emissions)
Morello-Frosch et al. (2001)	Yes	No	Air Quality	California	Cancer risk equation (individual risk estimate compared to census block population
Khan (2012)	Yes	No	Hazardscape perception	New Zealand	NA (hazardscape and response practices)
Cutter (1993)	No	Multi-hazard	Risk	Book (Not regional)	NA
Cutter (2001)	Yes	Multi-hazard	Hazardscape	Book (Not regional)	NA
Ley-García et al. (2015)	Yes (spatial)	Multi-hazard	Perception	Mexico	NA (spatial autocorrelation for perception)

R equals risk, H equals hazard, Hp is the probability of the hazard occurring, E is elements at risk, C is consequences, A is assets, and V is vulnerability. NA is not applicable, meaning the publication did not include a specific risk-based equation for natural hazards risk. RS is remote sensing.

Early work in the interactive space of hazards highlighted the duality of the relationship between people and their environments where both positive and negative aspects of the interaction occurred, determined as positive factors (such as resources) and negative factors (such as hazards) (Hewitt & Burton, 1971). The authors described this interaction as a 'hazard system' that forms the basis for a riskscape framework that integrates humans and environmental

factors. The authors express the connectedness of the hazard events to the socioeconomic conditions and implications for policy makers. Hewitt and Burton (1971) set natural and technological hazards within the social context, establishing the link between the risk of people in their spatial environment, not just specific to the risk to people from a specific hazard event. They establish the phrase "hazards of place" (Hewitt & Burton, 1971, p. 146) to include spatial risk-based assessments that focus on the integration of human and environmental factors.

2.10 Technology approaches

2.10.1 The RiskScape Project: A GIS-based loss-modeling framework

An advancement in riskscape research is the development of the applied RiskScape Project tool, a GIS-based software product developed in New Zealand by a research team founded by The Foundation for Research, Science, and Technology in 2004 (RiskScape, 2016). The RiskScape Project created a technology approach to develop an operational riskscape tool, based on a GIS platform to spatially analyze the outputs of risk-prone areas (RiskScape, 2016). The tool has supported natural hazard projects and assessments in New Zealand, and was designed to support multiple types of risks using a single platform and process for analyses (Schmidt et al., 2011). The application contains several modules and is capable of modeling multiple hazard types, including earthquakes, landslides, volcanic hazards, tsunamis, and flooding. The RiskScape Project uses a modelling approach, and uses GIS and spatial data modules for hazards, vulnerability, and assets to create a riskscape output consisting of maps for affected assets, damage to building units, and the loss or costs associated with those damages (Reese et al., 2007).

Figure 2.5 depicts the conceptual workflow for the RiskScape Project model (RiskScape, 2016). While the same elements are included in this model as in risk equations, namely hazards,

assets, and vulnerability, the application output is focused on loss calculations and the financial impacts of the disaster.

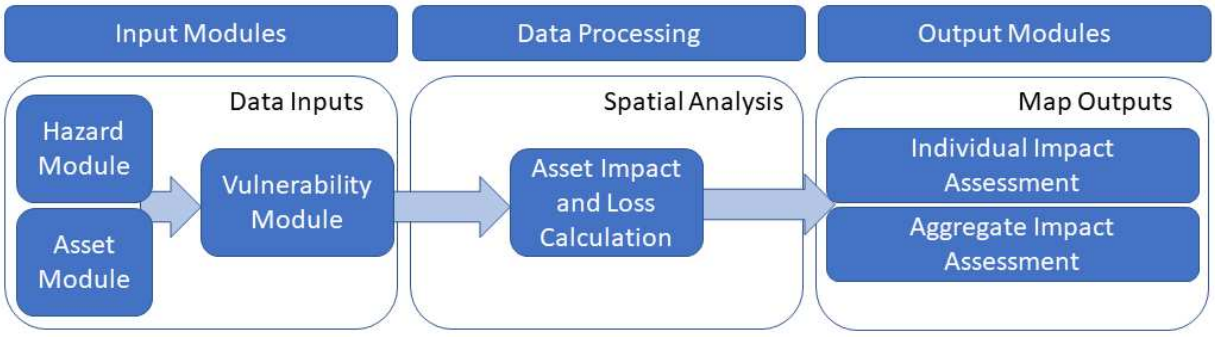

Figure 2.5. Workflow diagram adapted from the RiskScape Project, "Conceptual diagram of the RiskScape model framework" Source: RiskScape (2016)

Several studies have used this application to develop riskscapes to identify areas of higher risk of exposure to hazards and to guide policy makers in the resource-allocation process. Reese et al. (2007) applied the RiskScape Project to model the costs associated with hazards in the region of Hawkes Bay, New Zealand. Lane et al. (2015) used the RiskScape Project to determine tsunami inundation zones triggered by submarine landslides in Wellington, New Zealand, to calculate the potential damage to buildings.

Schmidt et al. (2011), in their applied multi-hazard study using the RiskScape Project software, highlight the interactive space between human factors and physical risks. The authors define the multi-hazard approach as:

> *Quantitative estimation of the spatial distribution of potential losses for an area (a confined spatial domain), multiple (ideally all) natural hazards, multiple (ideally a continuum of) event probabilities (return periods), multiple (ideally all) human assets, and multiple potential loss components (for each of the assets, e.g., buildings, streets, people, etc.). (page 1170)*

From this definition, the inclusion of assets and components is not based on valuation but on quantity. Value is found in the "fragility" component of risk calculations or as part of the asset-loss function (Schmidt et al., 2011, pp. 1174-1175) and is part of the attribution of the features, but not the only outcome, or a major input feature.

The authors describe the concept for this software program as the consolidation of multiple types of natural hazards into a single processing tool and perceive this as a challenge or at least a dependency, stating "multi-risk analysis involves different hazards, disciplines, and terminologies. Finding a common framework requires a translation of different science methodologies and terminologies in one system." (Schmidt et al., 2011, p. 1170). In the authors' example of historic events in a region prone to multiple natural hazard types, the riskscape models were displayed in building assets lost or replacement costs (Figure 2.7, pages 1185 - 1187). These elements of fragility, consequence, and vulnerability form the human component of the riskscape model.

2.10.2 United Nations Economic and Social Commission for Asia and the Pacific (UNESCAP) project

Further technology development work was done within the context of the UN's Economic and Social Commission for Asia and the Pacific (UNESCAP), with the publication of the *Disaster Riskscape Across Asia-Pacific* in 2019 (Alisjahbana et al., 2019). This UN publication approaches riskscapes for multi-hazards (tsunami, earthquakes, climate conditions including drought and cyclones, and flooding) through a probabilistic risk model (Alisjahbana et al., 2019).

2.10.3 Geospatial riskscapes for landslides in Colorado

Another example of applied riskscapes is documented in Chapter Three, a manuscript in review for publication (Hicks & Laituri, 2020) for a geospatial approach to develop landslide riskscapes in Colorado. This manuscript, in review, applies the risk equation formula to spatial datasets, using a GIS-based weighted-sum approach and riskscape factors [geology, distance to faults, hydrology (lakes, rivers and streams), elevation, slope, aspect, curvature, soil type, land cover, proximity to buildings, urban area classifications, population, transportation (buffered roads, railroads, and airports)].

2.11 Conceptualizing a landslide riskscape

To conceptualize this riskscape for landslides, the different components of riskscapes must be identified and classified. For all riskscapes, these components include the risk elements of the hazard, elements at risk, the probability of the event, and the vulnerability factor for the impacted elements but more critically, these elements must be spatially defined. The human aspect or vulnerability is generally missing from both geospatial mapping analysis processes and landslide studies.

Given the shift towards labeling our current timeframe as the "Anthropocene" to indicate the human impacts on the physical environment (James et al., 2013), we propose using riskscapes to shift the focus from the geologic and geomorphic perspectives of the hazards to the anthropological dimensions of landslide hazards. Human factors are not only the recipients of the damage from natural disasters, but rather part of the surficial environment, and using the multiplicity of a riskscape approach can enhance the understanding of risk in place. This complexity of the human-environment interaction can be understood better through developing a more spatially comprehensive framework.

To analyze landslide riskscapes, the physical environmental setting must be considered in context of the surrounding spatial aspects. Using the basic risk equation and combining it with the geospatial analysis functionality, a landslide riskscape can be conceptualized, as in Figure 2.6.

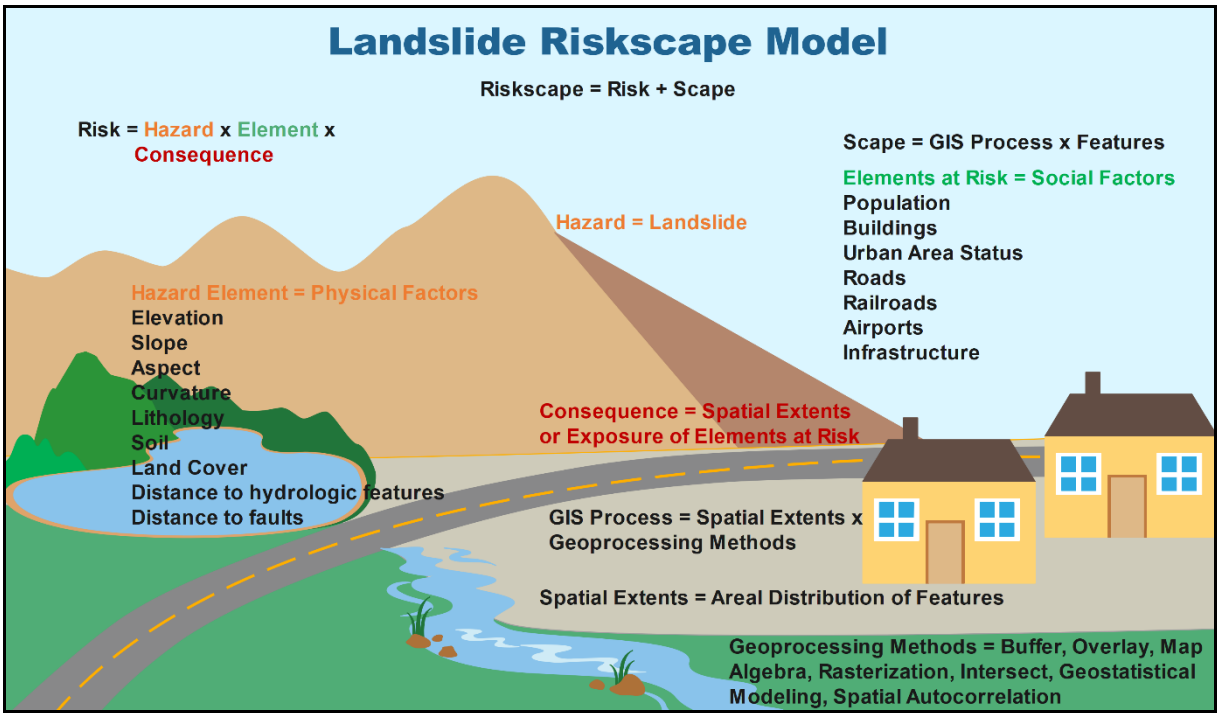

Figure 2.6. Landslide Riskscape conceptual diagram. This model outlines the elements of a spatialized landslide riskscape, derived from modifications to the risk equation (R=HCE) from Bell and Glade (2004).

Conceptualization of a riskscape based on a landscape visualization can be approached through a diagrammatic representation of a landslide model. This figure (2.6) depicts the spatial relationships between factors of a landslide riskscape and forms the basis of a framework for establishing a methodology for approaching landslide riskscapes analytically. Physical factors, the foundation of geomorphic analysis of landslide susceptibility and risk modeling are part of

the physical environment in which the landslide occurs and relate to the presence and absence of landslide factors. Also present are the consequential factors of human and built environment, including buildings, roadways and transportation networks, and human population centers. To produce the riskscape, the spatial analysis process incorporates these datasets through spatial modeling processes and creates a riskscape based on the weighting of the factors. Riskscapes actively measure the weights of the factors present and do not differentiate between the type of factors included.

An equation can be developed to reflect the operational spatial elements of a landslide riskscape. The spatial, or areal, extent for each riskscape factor is given by,

Equation 2.2.

$$\text{AF} = \left(\frac{f_{CC_n}}{A_{CC_h}}\right) \times 100$$

Where AF is the areal percentage for each factor, f_{ccn} is the factor cell count for each factor class, A_{cch} is the areal extent cell count of the hazard. The AF formula generates a percentage of the areal extent for each hazard class. The weighting scheme for the riskscape can be developed based on the percentage of occurrence of the hazard within each factor class. An example from Hicks and Laituri (2020) uses multiple weighting schemes based on the presence or absence of the hazard features (binary), a scheme accounting for higher percentages receiving higher weights (ranked), and a scheme with all human factors weighted at the highest value (human factor). From the developed weighting scheme, a weighted sum riskscape can be developed, using the formula,

Equation 2.3.

$$\text{WsRS} = \sum_{C=1}^{n} w_{fcc_1} + w_{fcc_2} + \cdots + w_{fcc_n}$$

Where WsRS is the weighted sum riskscape, and Wfcc is the weighted factor cell count classification scheme. This model as applied to landslides is further developed in Hicks and Laituri (2020).

2.12 Conclusions

Riskscapes as interdisciplinary terms derive from multiple streams of literature and theoretical frameworks. The notion of a riskscape is found sporadically in literature for natural hazards but not specifically for landslides. Risk has been studied in relation to urban landslide and other natural hazard events, through multiple assessment methods and from various perspectives or stages of landslide studies, including: determinations of susceptibility zones (Guzzetti, 2006); classifications of landslide types (Cruden & Varnes, 1996; Hungr et al., 2014; Varnes, 1958; Varnes, 1978); mapping existing occurrences (historic or ancient events, and new events) (Guzzetti, 2006); and, calculating the mathematical risk or probability of a landslide occurrence in a particular area (Ayalew & Yamagishi, 2005; Ayalew et al., 2005; Lee, 2009; Lee et al., 2007; Tien Bui et al., 2013; van Westen et al., 1997). These methods lead to vulnerability assessments of impacted regions to determine what sensitive receptors, naturally occurring or anthropogenic (urban areas), are in the region of potential damage (Ebert et al., 2009; van Westen et al., 2002).

Riskscapes are a geographic progression through a hazard analysis, emerging within the framework of modeling physical elements of the hazard (hazard analysis), and progressing to incorporate environmental and social aspects (vulnerability). Riskscapes can be used to develop a risk assessment based on these combined factors. Risk assessment allows for probability calculations based on the regional geographic differences. This geographic expression is unique

to spatial methods. Therefore, riskscapes create a geospatially operationalized risk profile for landslides.

Riskscapes may present a new tool to develop frameworks for supporting communities in their response to landslides by providing a better understanding of features and attributes that are present in the areas exposed to risk, particularly the vulnerability and social factors. The integration of multiple factors for both the geologic (lithology and fault structures) and environmental aspects (hydrology, soils, land cover) along with the urbanization classifications (urban area types, parcels and building locations) will support response and mitigation/preparedness processes. Increased knowledge of both the regions at risk and the derivative factors contributing to risk may be combined to improve the efficiency of response practices and the timeliness and tactical deployment for support.

Riskscapes present an opportunity to further develop geospatial methodologies to integrate landslide event modeling and risk processes with spatial elements and the interaction between them. Future work to operationalize the riskscape for landslides, especially in urban and developing areas will fill this gap. This formulation of a riskscape as a geospatial tool is a spatial extension of the risk equation, creating it as an operational tool methodology within a geospatial operating environment.

Riskscapes further the social construct of risk approach by shifting the focus from the hazard occurrences of landslides to the outcomes and interactions of the spatial hazard and the social risk. Riskscapes as methods and trends are a novel technical approach to modeling hazards, and landslides should be included in these assessments. GIS applications are well-suited to create operationalized riskscapes through their data management and analytical capabilities.

The challenge is to assess the state of the riskscape literature to account for the significant technological and methodological advancements in geospatial computing and mapping applications. As Fuchs et al. (2013, p. 1224) wonders, “Why has there been so little progress in our ability to mitigate and adapt to natural hazards?” The development of a riskscape framework will allow this model to be applied to hazards based on processes that are measurable and quantifiable in the geospatial application methodology, to inform improved planning, mitigation, response, and decision-support functions.

References

Alisjahbana, A. S., Zahedi, K., & Bonapace, T. (2019). *The Disaster Riskscape Across Asia-Pacific: Pathways for Resilience, Inclusion and Empowerment* [Asia-Pacific Disaster Report 2019]. U. N. publications. https://www.unescap.org/sites/default/files/publications/Asia-Pacific%20Disaster%20Report%202019_full%20version.pdf

Appadurai, A. (1990). Disjuncture and Difference in the Global Cultural Economy. *Public Culture*, *2*(2), 1–24. https://doi.org/10.1215/08992363-2-2-1

Aubrecht, C., Fuchs, S., & Neuhold, C. (2013). Spatio-temporal aspects and dimensions in integrated disaster risk management. *Natural Hazards*, *68*(3), 1205-1216. https://doi.org/10.1007/s11069-013-0619-9

Ayalew, L., & Yamagishi, H. (2005). The application of GIS-based logistic regression for landslide susceptibility mapping in the Kakuda-Yahiko Mountains, central Japan. *Geomorphology*, *65*(1-2), 15-31. https://doi.org/10.1016/j.geomorph.2004.06.010

Ayalew, L., Yamagishi, H., Marui, H., & Kanno, T. (2005). Landslides in Sado Island of Japan; Part II, GIS-based susceptibility mapping with comparisons of results from two methods and verifications. *Engineering Geology*, *81*(4), 432-445. https://doi.org/10.1016/j.enggeo.2005.08.004

Barrows, H. H. (1923). GEOGRAPHY AS HUMAN ECOLOGY. *Annals of the Association of American Geographers*, *13*(1), 1-14. https://doi.org/10.1080/00045602309356882

Bell, R., & Glade, T. (2004). Quantitative risk analysis for landslides - Examples from Bildudalur, NW-Iceland. *Natural Hazards and Earth Science Systems*, *4*, 14.

Bolstad, P. (2019). *GIS Fundamentals: A First Text on Geographic Information Systems* (6th ed.). XanEdu.

Brabb, E. (1977). The landslide hazard in the San Francisco Bay region. *Water, Air, and Soil Pollution*, *7*(2), 237-238. https://doi.org/10.1007/BF00280865

Brabb, E. E. (1984). *Innovative approaches to landslide hazard and risk mapping = Innovation dans la preparation des cartes de glissements*. s.n.

Brabb, E. E., Pampeyan, E. H., & Bonilla, M. G. (1972). *Landslide Susceptibility in San Mateo County, California* [MF-360].

Carrara, A. (1983a). Geomathematical assessment of regional landslide hazard. In (pp. 3-27). Pitagora Ed. : Bologna, Italy.

Carrara, A. (1983b). Multivariate models for landslide hazard evaluation. *Journal of the International Association for Mathematical Geology*, *15*(3), 403-426.

Carrara, A. (1988). Landslide hazard mapping by statistical methods; a 'black-box' model approach. In (pp. 205-224). U. S. National Science Foundtion, United States.

Carrara, A., Cardinali, M., Detti, R., Guzzetti, F., Pasqui, V., & Reichenbach, P. (1991). GIS techniques and statistical models in evaluating landslide hazard. *Earth Surface Processes and Landforms*, *16*(5), 427-445.

Carrara, A., Carratelli, E. P., & Merenda, L. (1977). Computer-based data bank and statistical analysis of slope instability phenomena. *Zeitschrift fuer Geomorphologie*, *21*(2), 187-222.

Carrara, A., Catalano, E., Reali, C., & Sorriso-Valvo, M. (1982). Computer-assisted techniques for regional landslide evaluation. *Studia Geomorphologica Carpatho-Balcanica*, *15*, 99-113.

Carrara, A., Guzzetti, F., Cardinali, M., & Reichenbach, P. (1999). Use of GIS technology in the prediction and monitoring of landslide hazard. *Natural Hazards*, *20*(2-3), 117-135. http://www.springerlink.com/(j0cav1mkaqwmj255qh105vjp)/app/home/journal.asp?referrer=parent&backto=linkingpublicationresults,1:102967,1

Castellanos Abella, E. A., & van Westen, C. J. (2008). Qualitative landslide susceptibility assessment by multicriteria analysis; a case study from San Antonio del Sur, Guantanamo, Cuba. *Geomorphology*, *94*(3-4), 453-466. https://doi.org/10.1016/j.geomorph.2006.10.038

Chen, L., van Westen, C. J., Hussin, H., Ciurean, R. L., Turkington, T., Chavarro-Rincon, D., & Shrestha, D. P. (2016). Integrating expert opinion with modelling for quantitative multi-hazard risk assessment in the Eastern Italian Alps. *Geomorphology*, *273*, 150-167. https://doi.org/10.1016/j.geomorph.2016.07.041

Chuang, Y.-C., & Shiu, Y.-S. (2018). Relationship between landslides and mountain development—Integrating geospatial statistics and a new long-term database. *Science of the Total Environment*, *622-623*, 1265-1276. https://doi.org/10.1016/j.scitotenv.2017.12.039

Creswell, J. W. (2009). *Research design : qualitative, quantitative, and mixed methods approaches / John W. Creswell* (Third edition. ed.). Los Angeles : Sage.

Cruden, D. M., & Varnes, D. J. (1996). *Landslide Types and Processes* (Special Report: Transportation Research Board, Issue.

Cutter, S. (1984). Risk cognition and the public: The case of Three Mile Island. *Environmental Management*, *8*(1), 15-20. https://doi.org/10.1007/BF01867869

Cutter, S. L. (1993). *Living with risk : the geography of technological hazards*. London ; New York : E. Arnold ; New York : Routledge, Chapman and Hall distributor.

Cutter, S. L. (1994). *Environmental risks and hazards* (S. Cutter, Ed.). Prentice Hall.

Cutter, S. L. (1996). Vulnerability to environmental hazards. *Progress in human geography*, *20*(4), 529-539. https://doi.org/10.1177/030913259602000407

Cutter, S. L. (2001). *American hazardscapes : the regionalization of hazards and disasters*. Washington, D.C. : Joseph Henry Press.

Ebert, A., Kerle, N., & Stein, A. (2009). Urban social vulnerability assessment with physical proxies and spatial metrics derived from air- and spaceborne imagery and GIS data. *Natural Hazards*, *48*(2), 275-294. https://doi.org/10.1007/s11069-008-9264-0

Everts, J., Jackson, P., Meah, A., & Viehoff, V. (2018). NEGOTIATING THE RISKSCAPES OF CONVENIENCE FOOD. *Erdkunde*, *72*(3), 171-184. https://doi.org/10.3112/erdkunde.2018.02.08

Fuchs, S., Keiler, M., Sokratov, S., & Shnyparkov, A. (2013). Spatiotemporal dynamics: the need for an innovative approach in mountain hazard risk management. *Natural Hazards*, *68*(3), 1217-1241. https://doi.org/10.1007/s11069-012-0508-7

Fuchs, S., Ornetsmuller, C., & Totschnig, R. (2012). Spatial scan statistics in vulnerability assessment: an application to mountain hazards. *Natural Hazards*, *64*, 2129-2151.

Gebreyes, M., & Theodory, T. (2018). UNDERSTANDING SOCIAL VULNERABILITY TO CLIMATE CHANGE USING A 'RISKSCAPES' LENS: CASE STUDIES FROM

ETHIOPIA AND TANZANIA. *Erdkunde*, *72*(2), 135-150. https://doi.org/10.3112/erdkunde.2018.02.05

Guzzetti, F. (2006). *Landslide hazard and risk assessment: concepts, methods, and tools for the detection and mapping of landslides, for landslide susceptibility zonation and hazard assessment, and for landslide risk evaluation* [Dissertation, University of Bonn]. Bonn, Germany. http://geomorphology.irpi.cnr.it/Members/fausto/PhD-dissertation/Landslide_Hazard_and_Risk_Assessment.pdf

Guzzetti, F., Carrara, A., Cardinali, M., & Reichenbach, P. (1999). Landslide hazard evaluation; a review of current techniques and their application in a multi-scale study, central Italy. *Geomorphology*, *31*(1-4), 181-216. http://www.sciencedirect.com/science/journal/0169555X

Hewitt, K., & Burton, I. (1971). *The hazardousness of a place : a regional ecology of damaging events*. University of Toronto Press.

Hicks, H., & Laituri, M. (2020). *Geospatial applications to landslide riskscape development: a modeling approach to quantify landslide riskscapes in the Colorado Front Range [Manuscript submitted for publication]* [Manuscript]. Colorado State University.

Hungr, O., Leroueil, S., & Picarelli, L. (2014). The Varnes classification of landslide types, an update. *Landslides*, *11*(2), 167-194. https://doi.org/10.1007/s10346-013-0436-y

Inkpen, R. (2016). 'Riskscapes' as a heuristic tool for understanding environmental risks: The Eyjafjallajokull volcanic ash cloud of April 2010. *Risk Management*, *18*(1), 47 - 63. https://doi.org/10.1057/rm.2016.1

James, L. A., Harden, C. P., & Clague, J. J. (2013). 13.1 Geomorphology of Human Disturbances, Climate Change, and Hazards. In J. F. Shroder (Ed.), *Treatise on Geomorphology* (pp. 1-13). Academic Press. https://doi.org/https://doi.org/10.1016/B978-0-12-374739-6.00339-0

Jenerette, G. D., Harlan, S. L., Stefanov, W. L., & Martin, C. A. (2011). Ecosystem services and urban heat riskscape moderation: water, green spaces, and social inequality in Phoenix, USA. *Ecological Applications*, *21*(7), 2637-2651. https://doi.org/10.1890/10-1493.1

Kappes, M., Keiler, M., Elverfeldt, K., & Glade, T. (2012). Challenges of analyzing multi-hazard risk: a review. *Natural Hazards*, *64*(2), 1925-1958. https://doi.org/10.1007/s11069-012-0294-2

Khan, S. (2012). Disasters: contributions of hazardscape and gaps in response practices. *Natural Hazards and Earth System Sciences*, *12*(12), 3775. https://doi.org/10.5194/nhess-12-3775-2012

Konisky, D. M., & Reenock, C. (2018). Regulatory Enforcement, Riskscapes, and Environmental Justice. *Policy studies journal*, *46*(1), 7-36. https://doi.org/10.1111/psj.12203

Krings, S. (2018). "DEAR NEIGHBOURS..." A COMPARATIVE EXPLORATION OF APPROACHES TO MANAGING RISKS RELATED TO HAZARDOUS INCIDENTS AND CRITICAL INFRASTRUCTURE OUTAGES. *Erdkunde*, *72*(2), 103-123. https://doi.org/10.3112/erdkunde.2018.02.03

Laituri, M. (1993). Risk, equity and environment: A methodology for conducting an Environmental Equity Assessment. In A. M. Kirby (Ed.): ProQuest Dissertations Publishing.

Lane, E. M., Mountjoy, J., Power, W. L., Mueller, C., Paulik, R., & Crowley, K. (2015, 15 - 18 September 201). *The hazard and risk of tsunami inundation due to submarinelandslide-*

generated tsunamis in Cook Strait Canyon Coasts & Ports Conference 2015, Pullman Hotel, Auckland New Zealand.
Lee, E. (2009). Landslide risk assessment: The challenge of estimating the probability of landsliding. *Quarterly Journal of Engineering Geology and Hydrogeology*, *42*, 445-458. https://doi.org/10.1144/1470-9236/08-007
Lee, S., Ryu, J.-H., & Kim, I.-S. (2007). Landslide susceptibility analysis and its verification using likelihood ratio, logistic regression, and artificial neural network models: case study of Youngin, Korea. *Landslides*, *4*(4), 327-338. https://doi.org/10.1007/s10346-007-0088-x
Ley-García, J., Denegri de Dios, F. M., & Ortega Villa, L. M. (2015). Spatial dimension of urban hazardscape perception: The case of Mexicali, Mexico. *International Journal of Disaster Risk Reduction*, *14*, 487-495. https://doi.org/10.1016/j.ijdrr.2015.09.012
Macey, S. M. (2010). A Respiratory Riskscape for Texas Cities: A Spatial Analysis of Air Pollution, Demographic Attributes and Deaths from 2000 Through 2004. In P. S. Showalter & Y. Lu (Eds.), *Geospatial Techniques in Urban Hazard and Disaster Analysis* (Vol. 2). Springer. https://doi.org/10.1007/978-90-481-2238-7
Morello-Frosch, R., Pastor, M., & Sadd, J. (2001). Environmental justice and Southern California's "riskscape": The distribution of air toxics exposures and health risks among diverse communities. *Urban Affairs Review*, *36*(4), 551-578.
Müller-Mahn, D., & Everts, J. (2013). Riskscapes: the spatial dimension of risk. In H.-D. Müller-Mahn & C. Ebooks (Eds.), *The spatial dimension of risk: How geography shapes the emergence of riskscapes*. Routledge.
Müller-Mahn, D., Everts, J., & Stephan, C. (2018). RISKSCAPES REVISITED - EXPLORING THE RELATIONSHIP BETWEEN RISK, SPACE AND PRACTICE. *Erdkunde*, *72*(3), 197-213. https://doi.org/10.3112/erdkunde.2018.02.09
Müller-Mahn, H.-D. (2013). *The spatial dimension of risk: how geography shapes the emergence of riskscapes*. Routledge.
Neisser, F. M. (2014). 'Riskscapes' and risk management – Review and synthesis of an actor-network theory approach. *Risk Management*, *16*(2), 88. https://doi.org/10.1057/rm.2014.5
November, V. (2008). Spatiality of Risk. *Environment and Planning A: Economy and Space*, *40*(7), 1523-1527. https://doi.org/10.1068/a4194
November, V., Camacho-Hübner, E., & Latour, B. (2010). Entering a Risky Territory: Space in the Age of Digital Navigation. *Environment and Planning D: Society and Space*, *28*(4), 581-599. https://doi.org/10.1068/d10409
Phillips, B. D. (2014). *Qualitative disaster research*. Oxford University Press.
Reese, S., King, A., Bell, R., Schmidt, J., Pringle, R., & Henderson, R. (2007). Regional RiskScape: A Multi-Hazard Loss Modelling Tool.
Remondo, J., Bonachea, J., & Cendrero, A. (2005). A statistical approach to landslide risk modelling at basin scale: from landslide susceptibility to quantitative risk assessment. *Landslides*, *2*(4), 321-328. https://doi.org/10.1007/s10346-005-0016-x
RiskScape, P. (2016). *The RiskScape Project: About the Project*. New Zealand Foundation for Reseaerch, Science, and Technology. Retrieved October 1, 2016 from https://riskscape.niwa.co.nz/about-the-project/funding
Schmidt, J., Matcham, I., Reese, S., King, A., Bell, R., Henderson, R., Smart, G., Cousins, J., Smith, W., & Heron, D. (2011). Quantitative multi-risk analysis for natural hazards: a framework for multi-risk modeling. *Natural Hazards*, *58*, 1169-1192.

Smith, K. (2013). *Environmental hazards: assessing risk and reducing disaster* (6th ed.). Routledge.
Stephan, C. (2018). SOCIAL PRACTICES OF FLOOD (RISK) MANAGEMENT - A VISUAL GEOGRAPHIC APPROACH TO THE ANALYSIS OF SOCIAL PRACTICES IN AN EMPIRICAL CASE IN CHIAPAS, MEXICO. *Erdkunde*, *72*(2), 151-168. https://doi.org/10.3112/erdkunde.2018.02.06
Tien Bui, D. P., Biswajeet; Lofman, Owe; Revhaug, Inge; Dick, Oystein B. (2013). Regional predicition of landslide hazard using probability analysis of intense rainfall in the Hoa Binh province, Vietnam. *Natural Hazards*, *66*, 23.
Tobler, W. R. (1970). A Computer Movie Simulating Urban Growth in the Detroit Region. *Economic Geography*, *46*, 234-240. https://doi.org/10.2307/143141
UNISDR. (2009). *2009 UNISDR Terminology on Disaster Risk Reduction*. U. Nations.
van Westen, C. J. (2013). 3.10 Remote Sensing and GIS for Natural Hazards Assessment and Disaster Risk Management. In J. F. Shroder (Ed.), *Treatise on Geomorphology* (pp. 259-298). Academic Press. https://doi.org/https://doi.org/10.1016/B978-0-12-374739-6.00051-8
van Westen, C. J., Montoya, L., Boerboom, L., & Badilla Coto, E. (2002, 24-26 September 2002). *MULTI-HAZARD RISK ASSESSMENT USING GIS IN URBAN AREAS: A CASE STUDY FOR THE CITY OF TURRIALBA, COSTA RICA* Regional Workshop on Best Practices in Disaster Mitigation, Bali, Indonesia.
van Westen, C. J., Rengers, N., Terlien, M. T. J., & Soeters, R. (1997). Prediction of the occurrence of slope instability phenomena through GIS-based hazard zonation. *Geologische Rundschau*, *86*, 404-414.
Varnes, D. J. (1958). *Landslide types and processes* (Landslides and engineering practice Issue. N. R. Council.
Varnes, D. J. (1978). *Slope movement types and processes* (0360859X). (Special Report: Landslides analysis and control Issue.

CHAPTER 3: GEOSPATIAL APPLICATIONS TO LANDSLIDE RISKSCAPE DEVELOPMENT: A MODELING APPROACH TO QUANTIFY LANDSLIDE RISKSCAPES IN THE COLORADO FRONT RANGE[3]

3.1 Summary of the manuscript

Riskscapes are interdisciplinary concepts that integrate multiple facets of physical, environmental, and social components in a spatial and temporal context. While the notion of risk is well documented for landslides, riskscapes are a novel approach in the natural hazard and spatial assessment studies. This term, 'riskscape', is described in terms of parameters required and quantification methodological approaches. Geographic Information Systems (GIS) or geospatial methods are an appropriate tool to define the development of these riskscape quantification methods. A weighted sum overlay model for a riskscape is developed with three weighted approaches using GIS to measure the strength of spatial relationships across a regional landscape in Colorado, focused on landslide susceptibility modeling in the riskscape context. Binary riskscapes resulted in a limited understanding of the impact of features related to landslide riskscapes, but both ranked and human factor weighted riskscape models provided more details to inform land-use policy and plan for response to landslides. Clustering measures using spatial autocorrelation tools revealed that riskscape outputs are clustered and can further be used to identify areas of increased risk due to landslides in emerging population-growth areas. In conclusion, ranked and human factor riskscape models are developed and can support decision-making and prioritization for response deployment based on landslide susceptibility criteria to focus resources on areas of interaction between landslide risk and social factors. Identification of

[3] This chapter is a manuscript co-authored with Melinda Laituri, submitted to a peer-reviewed journal for review.

high classification riskscape regions and determination of clustering characteristics furthers the understanding of human-environment interactions in hazardous areas.

3.2 Introduction

Riskscapes for natural hazards are conceptual models that integrate the physical attributes and vulnerability dimensions of risk (Müller-Mahn & Everts, 2013) within a spatial context. Landslides, commonly defined as mass movements of earthen material down a slope (Varnes, 1958; Varnes, 1978) present hazards for many regions and increasingly interact with human-built environmental factors, becoming more threatening, damaging, and costly (Guzzetti, 2006). Development of riskscape methods and applications to landslides contributes to a regional framework to address gaps in human/hazard interaction studies. A riskscape approach supports mitigation of hazard conditions by identifying areas of increased susceptibility to landslides and includes consideration of urban and human impact factors, allowing for better planning decisions and response prioritization.

Riskscapes as the intersection of natural hazard features in their environment can be assessed more fully by applying spatial autocorrelation measurements to geospatial methods. GIS methods for creating a landslide riskscape are based on GIS methods applied to natural-hazard-assessment and landslide-susceptibility-modeling literature. Many authors have demonstrated the efficacy of various geostatistical and geospatial methods for creating landslide risk zones depending on a variety of environmental factors such as slope, aspect, curvature, geology, proximity to hydrologic and seismic features, soil characteristics, and land cover/vegetation (Carrara et al., 1991; Carrara et al., 1999; Dai & Lee, 2002; Guzzetti, 2006; Huabin et al., 2005; Huang et al., 2017; Lee & Choi, 2004; Legorreta Paulin et al., 2014; Magliulo et al., 2008; Zêzere et al., 2017). Reichenbach et al. (2018) provides a review of these

landslide models and statistical methodological approaches highlighting key contributors to the field, including Carrara (1977 – 2008) and Guzzetti (1999 – 2006).

From a GIS historical perspective, Curry (1995, p. 1007) in Pickles (1995) reflected on the placement of GIS and its capabilities in the geographic ethical realm, stating "the necessity of seeing a 'realm'", like GIS, as constituted of sets of interlocking and overlapping patterns of actions." This statement, though regarding the placement of GIS in the literature, applies the notion of overlapping elements in space and how GIS has a role in determining these "patterns of actions" (Curry, 1995). These patterns can lead to the discussion of riskscapes. The addition of riskscapes and focus on affected regions, in other words, the locations where the results matter, augments these GIS models with additional parameters and analytical processes. The goal of this study is to develop a model for GIS methods for developing landslide riskscapes in a regional-scale study area of Boulder and Larimer Counties, Colorado.

Riskscapes are composite models and represent the intersection of theoretical perspectives. Places of risk (Hewitt & Burton, 1971) and risk as similar to landscapes (Cutter, 1993) developed risk as a locational and pattern-driven feature. Müller-Mahn and Everts (2013) approached riskscapes as a social-theory structure, relating risk to the interaction of humans and environment, focusing on perspectives of riskscape participants, those who occupy the space where riskscapes occur. Applied riskscapes have explored multiple hazards assessments, using risk equations to calculate risk of natural hazard events and damages (Jenerette et al., 2011; Morello-Frosch et al., 2001; Schmidt et al., 2011; Schmidt et al., 2007). The RiskScape Project, a GIS application developed in New Zealand, is a module-based platform that creates cost loss estimates for modeled hazard events (RiskScape, 2016). This program applies GIS processing to a riskscape platform, but focuses on the economic factors, not on the spatial relationships.

Landslide risk assessment and susceptibility models lack regionally based spatial analyses that incorporate urban factors at a broad regional scale. Tobler's First Law of Geography states, "everything is related to everything else, but near things are more related than distant things" (Tobler, 1970, p. 236). Applying this law as an analytical and modeling platform, GIS can be used to develop a riskscape framework for evaluating regional distributions of landslide probability and susceptibility with measurements for spatial autocorrelation and clustering, an applied extension of this First Law of Geography. Geospatial analysis tools operationalize the riskscape through integration of data from diverse sources and across sectors (i.e., urban areas, geology, infrastructure, population) and should factor in proximity as well.

Riskscape parameters extend natural hazard studies to shift the focus from the physical attributes of events to the affected or impacted communities. The region and occupants of the region (community) or stakeholders (externally located but interested parties responsible for supporting response or policy making) are included and the physical attributes are evaluated from a human dimension perspective. For example, a resident whose home is damaged by a landslide is part of the riskscape and needs to be included when evaluating regional support by agencies responsible for safety, transportation, funding response, first responders, scientific researchers, and other agencies. Riskscape factors include an additional classification step for modeling by using human geography and urban classifications. These factors include urban classification (urban area or non-urban area), road presence, buildings, and potentially, response agencies, municipalities, population statistics, jurisdictions, or regions.

3.2.1 Objective of study

This study developed a riskscape method for landslides using GIS models to evaluate the applicability of spatially weighted models to landslide riskscapes. Using frequency ratios and

GIS weighted overlays, a landslide riskscape model was created for two study areas in Colorado. Spatial autocorrelation was calculated using Global Moran's *i* and Anselin Local Moran's *i* to test the strength of the spatial relationships.

Riskscapes can be developed based on these frameworks, applying analytical models while incorporating human factors and anthropogenic definitions lacking in traditional landslide susceptibility models. Landslide models in Colorado need to include spatial and human elements in addition to landslide susceptibility factors to better determine areas of potential impact. Areas identified as having potential higher impact can be used to develop policy and mitigation/preparedness strategies. The challenge is to create a framework for landslide riskscapes, and a methodological approach that can cohesively describe and quantify riskscapes and their relationship with spatially co-located features.

3.3 Study area

Boulder and Larimer Counties, located in the Front Range region of Colorado, are mixed urban and non-urban counties with a history of landslide activity. Landslides are prevalent due to the mountainous terrain and periodic intense precipitation events, as well as interactions with wildland fire burn-scar exposures (Coe et al., 2014; Patton et al., 2018) Boulder and Larimer Counties (Figure 3.1) have recent histories of landslides and populations present in urban, intermix, and rural spaces. These counties have been identified by the Colorado Geological Survey as the highest priority for mapping debris flows at the county scale based on their post-2013 Front Range flood evaluation (McCoy, 2016). Each county region has urban and non-urban areas, elevation changes, differing geologic lithology, hydrologic networks, human and urban factors, and a recent history of landslides.

Boulder County ranges in elevation from 1490 meters to over 4300 meters above sea level and has an area of approximately 1916 square kilometers (BoulderCounty.org, 2019). Larimer county has a similar elevation profile, from around 1450 meters to over 4100 meters above sea level and extends 6837 square kilometers (Larimer.org, 2019). Geologically, the counties range from shale deposits in the Plains to the metamorphic units of the Rocky Mountains. Land-use/land-cover classifications are primarily forested types in the mountains to developed and agricultural classes on the plains.

Boulder County population is estimated at 322,854 and Larimer County population is estimated at 343,853 (Affairs, 2017). The population has grown significantly in recent years, with approximately 30,000 additional residents in Boulder County between 2010 and 2018 (Review, 2020) and approximately 50,000 additional residents in Larimer County in the same timeframe (Review, 2020). These increases in population in the riskscape area can lead to increased risk to humans and property. Population growth in the wildland urban interface (WUI) needs to be considered as a contributing factor to riskscapes. WUI areas, the intersection between urban areas and wildland vegetation areas, are important spatial features indicating the relationship between human and natural features (Radeloff et al., 2018). Populations present in these areas are more at risk to wildland hazard events (Radeloff et al., 2018).

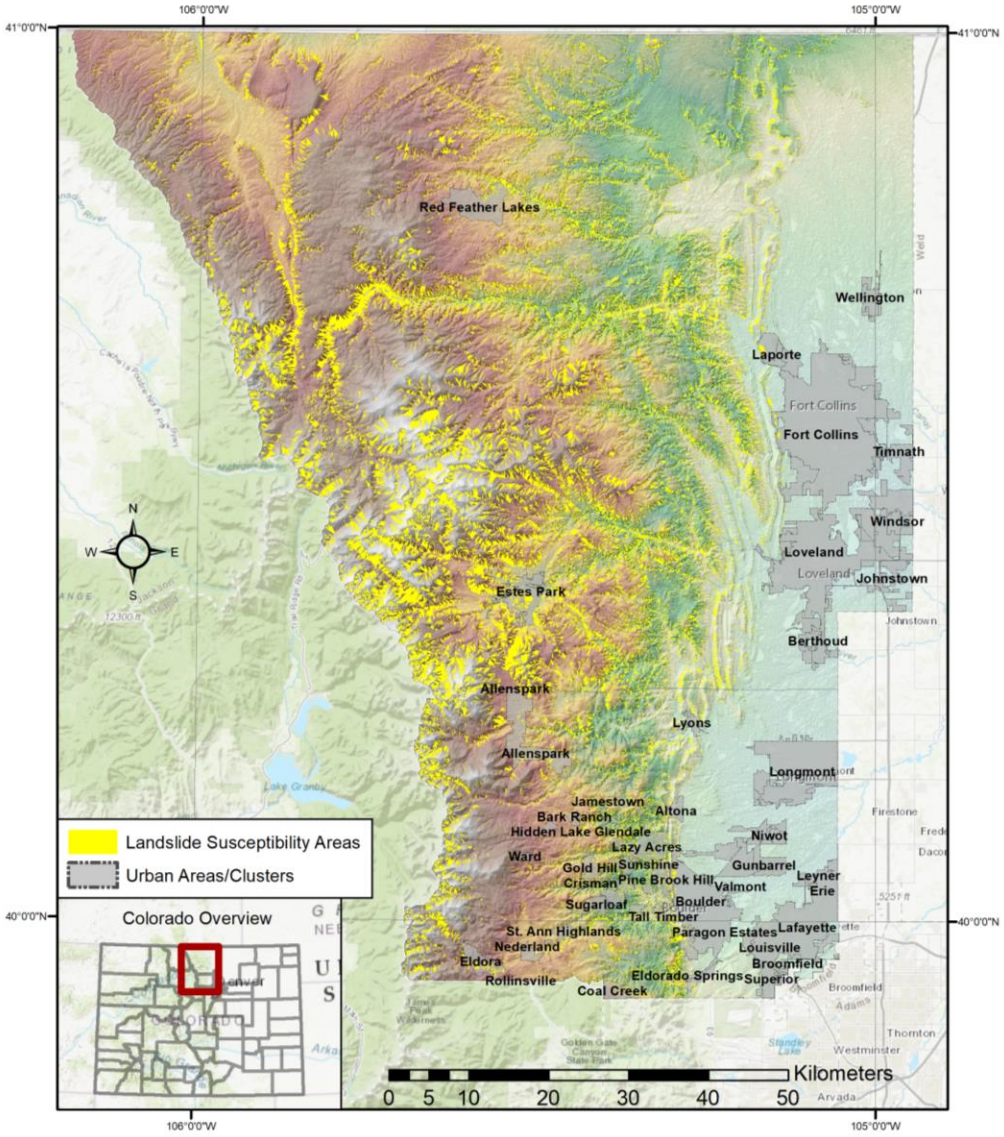

Figure 3.1. Boulder and Larimer Counties with urban areas and clusters. Landslide susceptibility data shown from Colorado Geological Survey Open File Report data (OF14-02 and OF15-13). Data credit: (Morgan et al., 2014; T. C. Wait et al., 2015)

3.4 Data and methods

Quantifiable approaches to risk incorporate various elements related to the hazard, the frequency probability, and impacted features (elements, consequences, or vulnerability). Multiple studies outline examples of risk equations for landslides or natural hazards, including Bell and Glade (2004); Kappes et al. (2012); Schmidt et al. (2011); van Westen (2013). These

interpretations of risk equations [often given as risk = hazard x element x consequence, from Bell and Glade (2004)] are based on the hazard event, though they approach risk differently through the emphasis on different criteria. For example, vulnerability to a hazard is a component of several approaches, but not included in all approaches. Areal impact, or the region of the impact is only specified in one study, Kappes et al. (2012). Loss as a function of vulnerability, expressed as direct or indirect economic costs was also only found in one approach, van Westen (2013). But the value of the spatial component is not measured consistently and does not use the geographic distribution as a measurable feature to assess the potential correlation of causative factors. To operationalize these elements in this research, a geospatial process was developed to integrate spatial aspects into the risk equation and create a riskscape for landslides based on the influential factors (e.g., physical features including slope, elevation, aspect, land cover, lithology, soil type, proximity to faults and hydrologic features and social elements-at-risk or consequence factors including transportation networks, urban area classification, population, and buildings).

3.4.1 Data

Data for the riskscape analysis are available from public sources (including U.S. Geological Survey, Colorado Geological Survey, U.S. Department of Agriculture, Colorado Department of Transportation, Colorado Department of Local Affairs, U.S. Census Bureau, Boulder County, and Larimer County). Data are divided into classifications of physical hazard factors, infrastructure elements, and human factors. A table of sources is included in the appendix for the manuscript (Appendix B).

3.4.2 Data preparation

Datasets were preprocessed before analysis to create compatible layers of information. A common framework for projection, scale, and area were applied, and a frequency ratio

calculation was performed to create a weighting scale (Table 3.1). A data preparation workflow is shown in Figure 3.2. Probabilistic frequency ratios were calculated from the percentages of landslides compared to the percentage of each class of the datasets present within the study area, using the formula from Pourghasemi et al. (2014) and methods from Islam (2013):

Equation 3.1. Probabilistic Frequency Ratio (PFR) formula

Percent landslide cells/percent total cells, or

(Landslide cells per class/total landslide cells) / (Class cells/total cells)

Table 3.1. Weighting scheme for landslide riskscape types.

Riskscape type	**Binary**	**Ranked**	**Human Factor**
Feature Presence			
Feature Present	1	x	x
Feature Absent	0	x	x
Feature Abundance			
Feature Absent	0	0	0
Feature Present (Non-human factor)			
Less than 1% of landslide cells	1	0.5	0.5
1 - <10%	1	1	1
10 - <30%	1	3	3
30% or greater	1	5	5
Feature Present (Human factor)			
Less than 1% of landslide cells	1	0.5	5
1 - <10%	1	1	5
10 - <30%	1	3	5
30% or greater	1	5	5

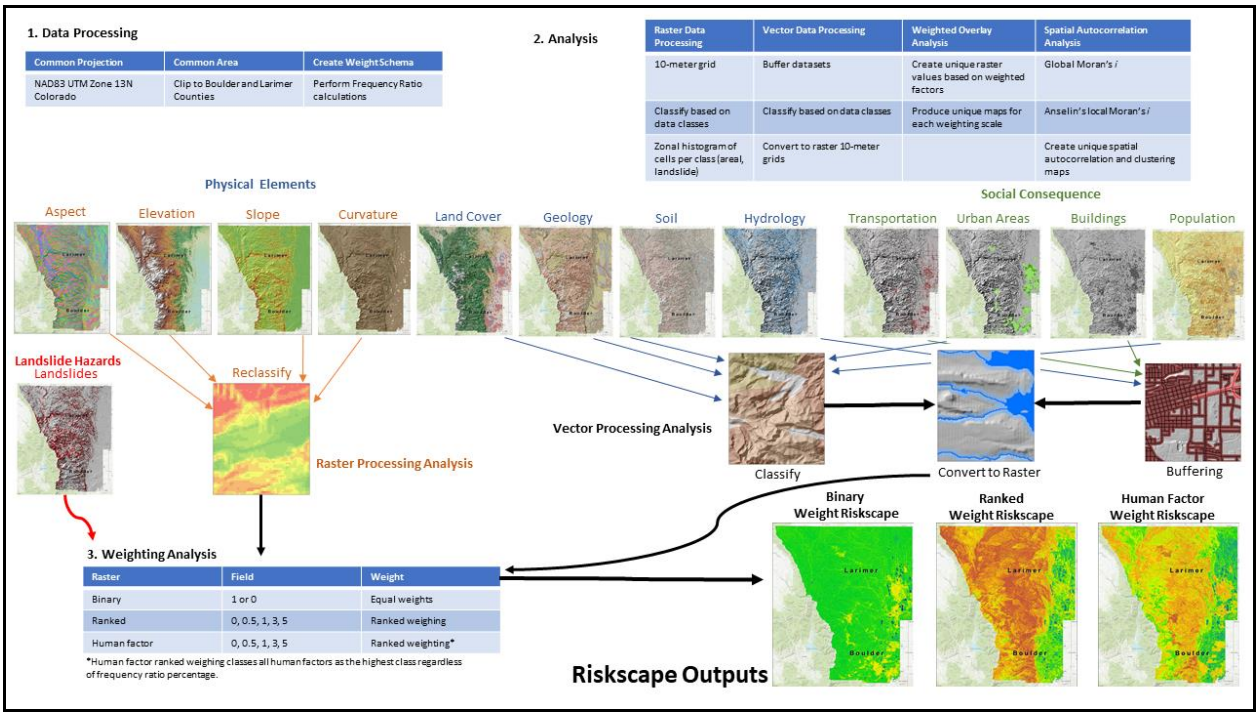

Figure 3.2. Geospatial workflow for riskscape development for data processing, analysis, and spatial autocorrelation tasks. Datasets processed are listed in Appendix B.

3.4.3 Landslide riskscape class development methods

To develop the riskscapes for landslides in Boulder and Larimer Counties, 16 factors (geologic lithology, distance to faults, soil type, land cover type, elevation in meters, slope in degrees, aspect or direction of slope, slope curvature, areas near flowlines [rivers and streams], areas near waterbodies, urban area classification, census population by block, distance to rail lines, distance to airports, distance to roads, and building footprints) were mapped and classified as related to landslide areas using a Zonal Histogram tool in ArcGIS Spatial Analyst. Factors were classified based on the presence or absence of landslide susceptibility cells within each dataset. The riskscape was created using three models: the binary weighting (landslide present/landslide absent); the ranked weighted model based on frequency calculations ranging from 0 to 5 weight; and, a human factor weighted model, where buildings, urban classes, and

population were all weighted 5 with other factors weighted based on their frequency. Three riskscapes were developed based on geospatial modeling techniques. Dorshow (2012) described a GIS predictive modeling process for archaeology that was applied in this study to riskscapes and natural hazards. The weighting scheme introduced by Dorshow (2012) included equal weights for all of the models for one iteration of the analysis, and raw data inputs using map algebra, a geospatial raster-cell-value based calculation that creates additive layers based on input criteria scales (e.g. 1 for low risk, 5 for high risk), for the comparative model.

Riskscape models for this study normalized the nominal data (geology, soil, and landcover type) and data were converted to a weighted scale based on the frequencies of the features as they occurred with the number of landslide susceptibility cells. Data classes were removed from the binary weighting, such as water bodies from soil and geology types, and flat curvature classes. Binary riskscape models use the presence/absence of a feature to generate the weighting percentages for an assessment of the features. This model includes only the location of a landslide susceptibility cell in the 10-meter grid as a weighted factor. The ranked model used a scaled presence, with weights emphasizing the relative importance of a type of class based on the probabilistic frequency ratio, or frequency of occurrence. The human factor model applied the highest ranking to all human (census population) and built environment features (urban class and buildings) regardless of the historic landslide presence or susceptibility ranking.

For this study, the input weight criteria were based on a binary presence/absence model (1/0) and a ranked weighting based on frequency calculations. Esri's ArcGIS version 10.6.1 and ArcGIS Pro version 2.3 were used to perform the spatial data analysis and to build spatial processing models (shown in Appendix D).

3.4.4 Spatial autocorrelation factors and clustering method

Two methods of spatial autocorrelation measurements were used, Global Moran's *i* and Anselin Local Moran's *i*, to assess the strength of the spatial relationships and clustering within the riskscapes, The Moran index from the Global Moran's *i* tool ranges from -1 which indicates a complete dispersion of features, to 0, a complete randomness of features, to +1, a complete clustering of features. This index can be used to determine the amount of spatial distribution within each feature. Anselin Local Moran's *i*, creates a mapping output of clustered areas based on a local neighborhood mathematical function, showing surrounding cells' relationships. Both clustering and cluster-outlier autocorrelation tools were performed on multipart (classed) rasters from the binary, ranked, and human factor input riskscape models. The functions of the spatial autocorrelation tools are described in Table 3.2.

Table 3.2. Classification of spatial autocorrelation methods and measurements. Global methods apply all features in the dataset; local methods apply neighboring features to the analysis.

Method	**Values**	**Tool**	**Type**	**Indicates**
Clustering/Dispersion		Moran's *i*	Global	Spatial autocorrelation on the global data scale
	Strong positive	Moran's *i*	Global	Clustering
	Strong negative	Moran's *i*	Global	Dispersion
	Neutral/0 value	Moran's *i*	Global	Random, lack of spatial autocorrelation
Cluster and Outlier analysis		Anselin Local Moran's *i*	Local	Clustering and outliers on the local data scale
	High-high (hot spot)	Anselin Local Moran's *i*	Local	Cluster of high values
	High-low (high outlier)	Anselin Local Moran's *i*	Local	High value surrounded by low values
	Low-high (low outlier)	Anselin Local Moran's *i*	Local	Low value surrounded by high values

	Low-low (cold spot)	Anselin Local Moran's *i*	Local	Cluster of low values

Global Moran's *i* spatial autocorrelation was calculated using three approaches, inverse distance, inverse distance squared, and zone of indifference. These methods differ in how the neighborhood weighting scheme in calculated but all are based on the fundamental rule of Tobler's law (Tobler, 1970), namely that proximity directly influences clustering and values within features. Inverse distance without fixed band zones (as used here) generates a local neighborhood based on creating a zone large enough that each feature has a minimum of one neighbor. Using the row standardization function can reduce bias introduced by aggregating polygonal data by summing the neighboring feature weights from each row (Esri, 2020). The inverse-distance-squared tool is based on the same concept but by squaring the distance function, it creates a steeper distance decay outside of the neighbor zone. Zone of indifference weights the cells within the distance-boundary setting equally and reduces those outside of the boundary based on the distance decay function (Esri, 2020).

The Local Moran's *i* spatial autocorrelation (Anselin Local Moran's *i* cluster outlier) was used to test for the spatial distribution of clusters within a dataset and generated z-scores, p-values, and output maps of clustered and outlier data. The tool created results for high and low value clusters or outliers. The map output indicates zones of clustering of high and low values where the cells are similar in rankings (hot and cold spots), and zones where outliers occur, or high or low values are surrounded by the other type of value (high and low outliers). Figure 3.3 exhibits the calculations performed with the autocorrelation tool for Anselin Local Moran's *i*.

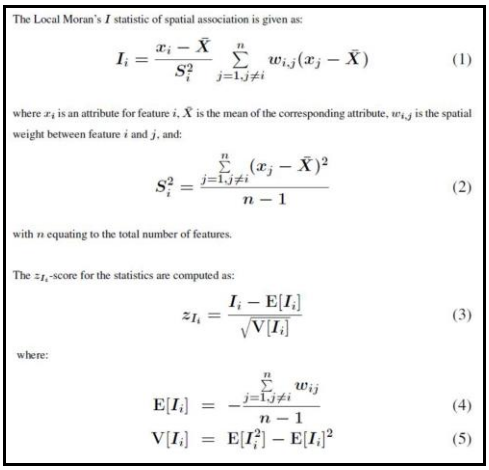

The Local Moran's I statistic of spatial association is given as:

$$I_i = \frac{x_i - \bar{X}}{S_i^2} \sum_{j=1, j \neq i}^{n} w_{i,j}(x_j - \bar{X}) \quad (1)$$

where x_i is an attribute for feature i, $\bar{X}$ is the mean of the corresponding attribute, $w_{i,j}$ is the spatial weight between feature i and j, and:

$$S_i^2 = \frac{\sum_{j=1, j \neq i}^{n} (x_j - \bar{X})^2}{n - 1} \quad (2)$$

with n equating to the total number of features.

The z_{I_i}-score for the statistics are computed as:

$$z_{I_i} = \frac{I_i - \mathrm{E}[I_i]}{\sqrt{\mathrm{V}[I_i]}} \quad (3)$$

where:

$$\mathrm{E}[I_i] = -\frac{\sum_{j=1, j \neq i}^{n} w_{ij}}{n - 1} \quad (4)$$

$$\mathrm{V}[I_i] = \mathrm{E}[I_i^2] - \mathrm{E}[I_i]^2 \quad (5)$$

Figure 3.3. Anselin Local Moran's *i* equations. Source: Esri (2019)

3.5 Riskscape results

3.5.1 Binary riskscape results

The binary riskscape ranged from three to thirteen factors. In Boulder County's binary weighted-sum riskscape based on five classes, the medium class (7 – 9 factors) accounted for 77% of the areal extent but over 88% of the landslide susceptibility cells. For individual classes of factors, the class with eight total binary riskscape factors accounted for the highest probabilistic frequency ratio at 1.58, with over 41% of the landslide susceptibility cells and 26% of the surface area. Larimer County had a similar concentration for the binary riskscape, with almost 90% of the area and over 94% of the landslide susceptibility cells occurring in the medium class (7 – 9 factors), shown in Figure 3.4. The highest individual class for landslide probabilistic frequency ratio was class 8 (with eight factors), at 1.39, with over 37% of the landslide susceptibility cells and 27% of the surface area. Table 3.3 shows the binary riskscape occurrences.

Table 3.3. Classified binary weighted sum riskscape for Boulder and Larimer Counties. Bold text indicates a probabilistic frequency ratio greater than 1, demonstrating the relative weight of landslide susceptibility cells.

Binary riskscape class value	**Areal extent (%)**	**Landslide susceptibility by riskscape class (%)**	**Probabilistic Frequency Ratio (PFR)**
Boulder County			
Low (3 – 5 factors)	0.75	0.01	0.01
Moderate (5 – 7 factors)	1.94	0.19	0.10
Medium (7 – 9 factors)	**77.72**	**88.86**	**1.14**
Elevated (9 – 11 factors)	18.37	10.32	0.56
High (11 – 13 factors)	1.21	0.62	0.51
Larimer County			
Low (3 – 5 factors)	0.65	0.01	0.01
Moderate (5 – 7 factors)	1.32	0.11	0.08
Medium (7 – 9 factors)	**89.75**	**94.43**	**1.05**
Elevated (9 – 11 factors)	7.95	5.35	0.67
High (11 – 13 factors)	0.29	0.10	0.33

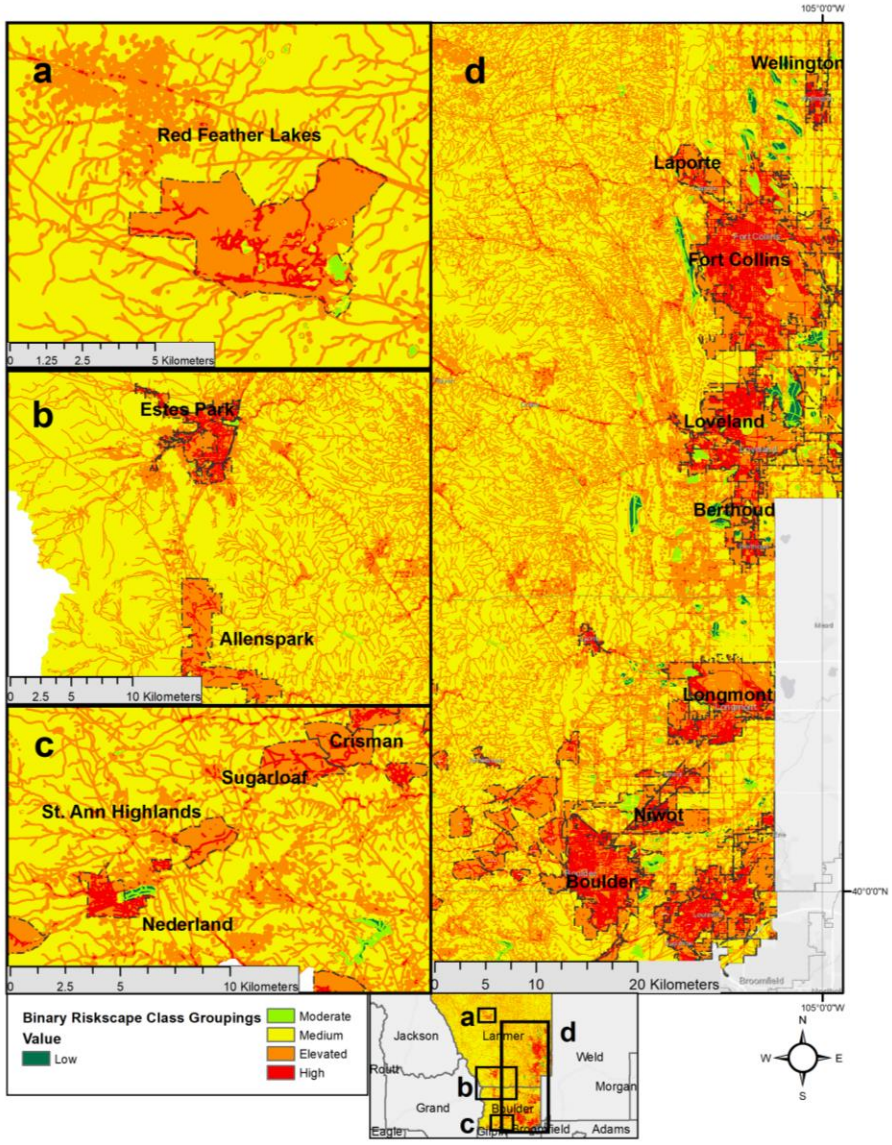

Figure 3.4. Binary weighted-sum riskscape inset maps, showing five classes for landslide riskscapes, Red Feather Lakes, Larimer County (a), Estes Park and Allenspark, Larimer and Boulder Counties (b) Nederland and Boulder Canyon, Boulder County (c), and urban corridor (d).

3.5.2 Ranked riskscape results

The ranked weighted-sum riskscape generated a larger distribution due to the increased number of factor classes. The ranked weighted sum riskscape was classified into nine classes using manual classification based on rounded Natural Breaks (Jenks), shown in Table 3.4.

Both counties showed that the higher factor classes had more prevelent landslide cells and higher probabilistic frequency ratios. Larimer County had high ratios in the highest classes, but these classes had few landslide susceptibility cells. The results shown in Table 3.4 demonstrated that while areas of the highest risk represent a smaller areal extent of each study area, their probabilistic frequency ratio was higher, indicating that the likelihood of the risk exceeds the base percentage of the areal coverage.

Table 3.4. Ranked weighted sum riskscape, showing class value, start and end ranges for number of factors, areal extent percentages and landslide riskscape percentages. Probabilistic frequency ratios (PFR) are the calculation relating the percent landslide riskscape to the areal extent coverage. Bold text indicates a PFR greater than 1, demonstrating the relative weight of landslide susceptibility cells.

Ranked value class	Ranked value range start	Ranked value range end	Boulder County areal extent (%)	Boulder County landslide susceptibility by riskscape class (%)	Boulder County PFR	Larimer County areal extent (%)	Larimer County landslide susceptibility by riskscape class (%)	Larimer County PFR
1	1	10	0.83	0.00	0.00	0.69	0.00	0.00
2	10	14.5	2.17	0.20	0.09	1.61	0.01	0.01
3	14.5	17	7.34	0.80	0.11	3.68	0.03	0.01
4	17	19.5	15.23	2.09	0.14	5.26	0.35	0.07
5	19.5	22.5	15.57	8.41	0.54	9.67	4.93	0.51
6	22.5	25.5	15.15	13.87	0.92	12.01	9.27	0.77
7	**25.5**	**28**	**18.93**	**25.33**	**1.34**	23.26	22.97	0.99
8	**28**	**31**	**12.41**	**20.32**	**1.64**	**23.16**	**26.85**	**1.16**
9	**31**	**40**	**12.36**	**28.96**	**2.34**	**20.65**	**35.59**	**1.72**
0	No Data	No Data	0.01	0.00	0.57	0.02	0.00	0.14

Using an equal-interval method for classification shows a different approach to viewing the data. This classification used integers grouped by fives to display data in an easier to read format, shown in Figure 3.5. The ranked riskscape using equal intervals showed in Larimer County that the two classes accounting for most of the landslides are class 25-30 factors with 44% of the areal extent and 45% of the landslide susceptibility cells, and class 30-35 factors with 21% of the surface areal extent and over 34% of the landslide susceptibility cells. For Boulder

County, classes with 25-30, 30-35, and 35-40 also had the highest probabilistic frequency ratios, 1.32, 2.22, and 3.23, respectively.

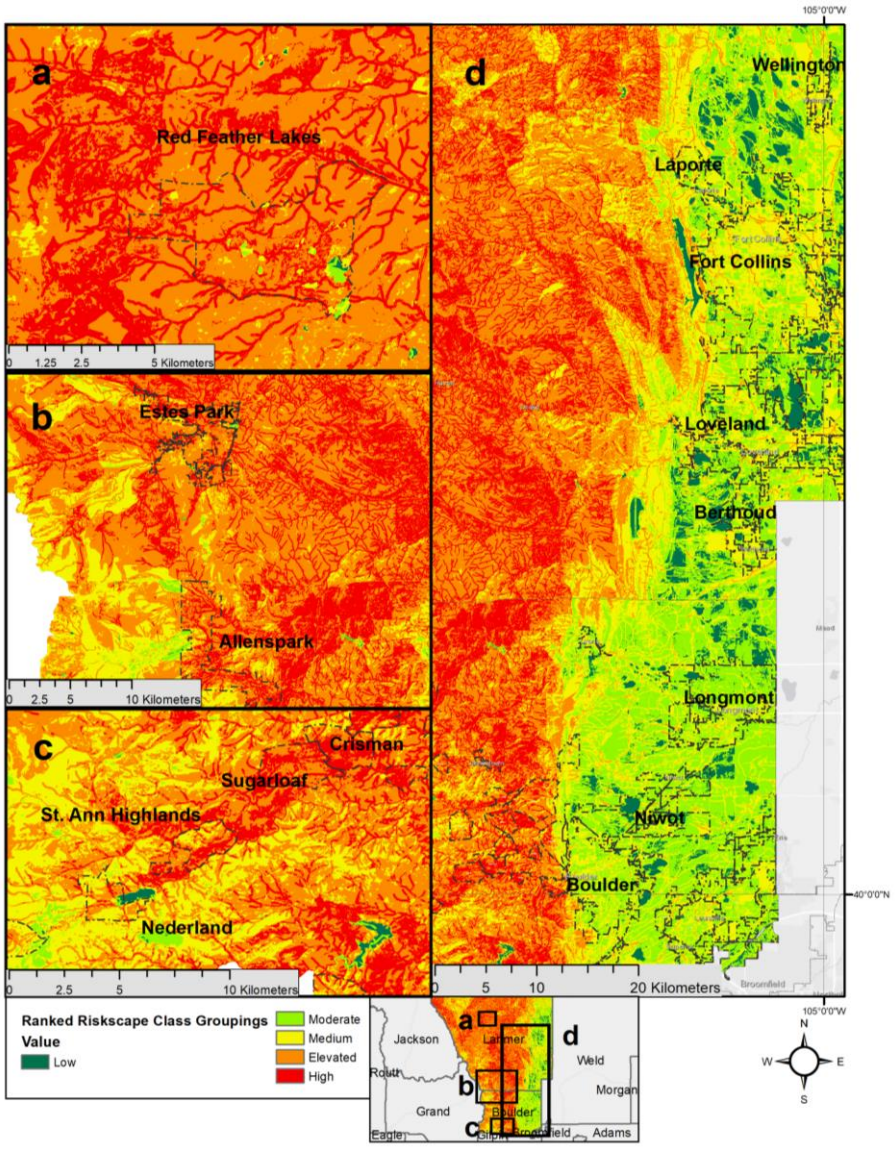

Figure 3.5. Ranked weighted-sum riskscape inset maps, showing five classes for landslide riskscapes, Red Feather Lakes, Larimer County (a), Estes Park and Allenspark, Larimer and Boulder Counties (b) Nederland and Boulder Canyon, Boulder County (c), and urban corridor (d).

3.5.3 Human riskscape results

The human factor weighted-sum riskscape values ranged from 7 to 51 total weighted factors for Boulder County and from 6.5 to 49 total weighted factors for Larimer County,

classified into nine classes (shown in Table 3.5) using manual classification based on rounded Natural Breaks (Jenks). Both counties show the highest probabilistic frequency ratio in the higher classes, though fewer landslide cells and less areal extent occur in these classes. Human factor landslide riskscapes are concentrated in classes 5, 7, 8, and 9 for Boulder County and classes 6, 7, 8, and 9 for Larimer County, showing the middle and upper ranges of factors contribute to the highest riskscape occurrence (Figure 3.6).

Table 3.5. Human factor weighted sum riskscape, showing class value, start and end ranges for number of factors, areal extent percentages and landslide riskscape percentages. Probabilistic frequency ratios (PFR) are the calculation relating the percent landslide riskscape to the areal extent coverage. Bold text indicates a PFR greater than 1, demonstrating the relative weight of landslide susceptibility cells.

Human factor value class	**Human factor range start**	**Human factor range end**	**Boulder County areal extent (%)**	**Boulder County landslide susceptibility by riskscape class (%)**	**Boulder County PFR**	**Larimer County areal extent (%)**	**Larimer County landslide susceptibility by riskscape class (%)**	**Larimer County PFR**
1	1	12.5	0.61	0.00	0.01	0.71	0.01	0.01
2	12.5	18	5.09	0.31	0.06	3.04	0.06	0.02
3	18	21.5	10.00	1.74	0.17	7.14	1.41	0.20
4	21.5	25	16.56	8.92	0.54	10.70	7.90	0.74
5	25	28	**22.83**	**26.72**	**1.17**	24.67	21.06	0.85
6	28	31	20.37	20.14	0.99	**25.45**	**25.54**	**1.00**
7	31	34.5	**13.79**	**19.87**	**1.44**	**16.54**	**20.47**	**1.24**
8	34.5	39	**8.46**	**18.76**	**2.22**	**10.84**	**21.89**	**2.02**
9	39	48	**2.28**	**3.52**	**1.54**	**0.90**	**1.66**	**1.85**
0	No Data	No Data	0.01	0.00	0.57	0.02	0.00	0.14

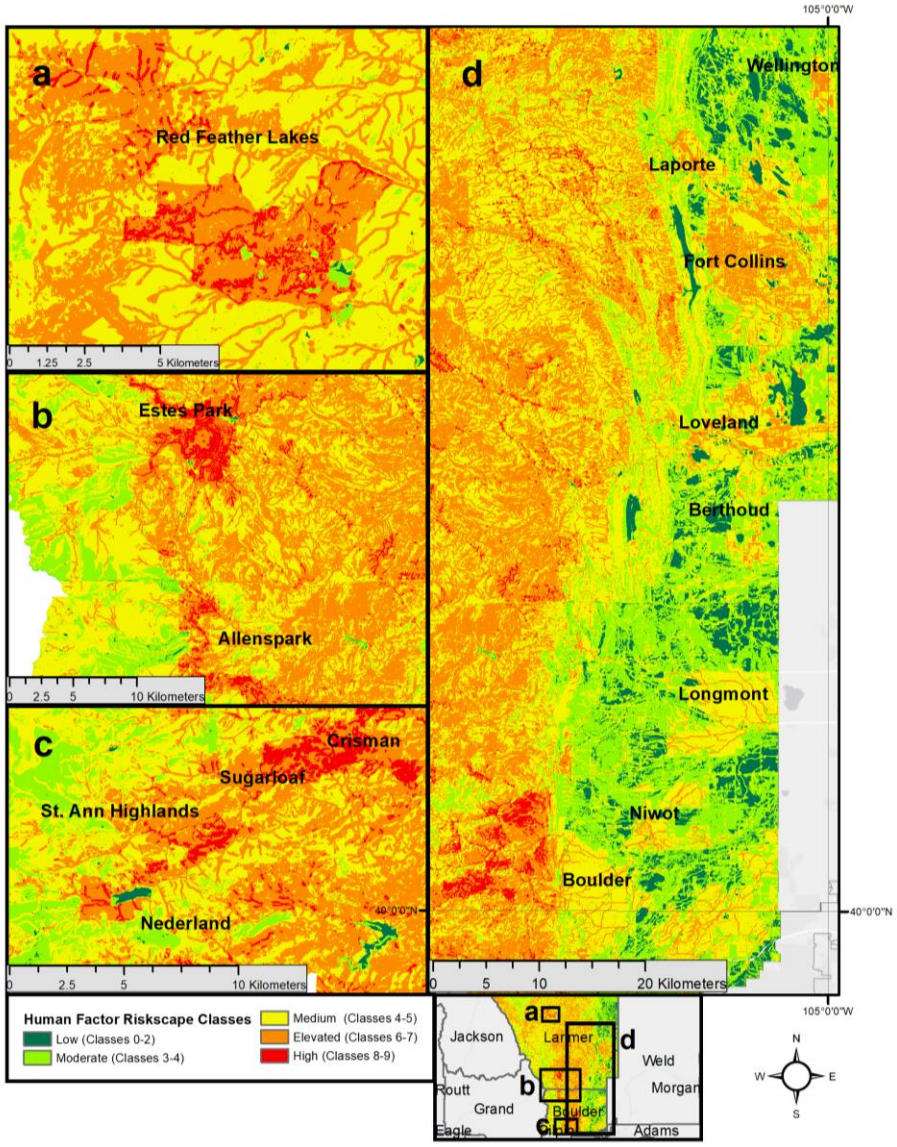

Figure 3.6. Human factor weighted-sum riskscape inset maps, showing five classes for landslide riskscapes, Red Feather Lakes, Larimer County (a), Estes Park and Allenspark, Larimer and Boulder Counties (b) Nederland and Boulder Canyon, Boulder County (c), and urban corridor (d).

3.6 Spatial autocorrelation results

3.6.1 Binary landslide riskscape spatial autocorrelation results

For Boulder County's binary weighted-sum riskscape using all classes Inverse Distance, row standardization and default threshold distances, the p-value was 0.00, and the z-score was 682.01. These show that the data are clustered, and that there is a statistically significant low

(less than 10%) chance of this being random. The Moran's index value of 0.52 indicated a clustering of values. The Larimer County binary riskscape showed a p-value of 0.00 and a z-score of 835.08. The Moran's index value of 0.47 indicated a clustering of values. These values indicate that the binary riskscape for Larimer County is also clustered. However, these results are not reliable as the binary riskscape only contained 14 total classes, less than the recommended 30 sample minimum. Therefore, it is recommended that the other ranked and human factor riskscape results be used to determine significance. These results demonstrated that this type of classification shows clustering but is not the most appropriate scale to measure autocorrelation.

3.6.2 Ranked landslide riskscape spatial autocorrelation results

For ranked riskscapes using all classes Inverse Distance, row standardization and default threshold distances, both counties indicated clustering for riskscape surface. Boulder County's ranked riskscape z-score was 2.06 and the p-value was 0.04, indicating the distributions were significant. The Moran index value of 0.08 indicates there is measurable clustering in the features. For Larimer County, the ranked riskscape z-score was 11.65 and the p-value was 0.00, showing that the results were significant and had a low chance of being randomly clustered. The Moran index value of 0.62 shows that there is clustering in the features.

3.6.3 Human factor landslide riskscape spatial autocorrelation results

Boulder County's human-factor riskscape z-score was 15.22 and the p-value was 0.00, indicating a low probability of the distributions being random. The Moran index value of 0.67 indicated there is clustering in the features. For Larimer County, the human-factor riskscape z-score was 18.47 and the p-value was 0.00, showing that the results were significant and had a low chance of being randomly clustered. The Moran index value of 0.57 shows that there is

clustering in the features. Figure 3.7 shows the ranked and human factor riskscape Anselin Local Moran's *i* clustering.

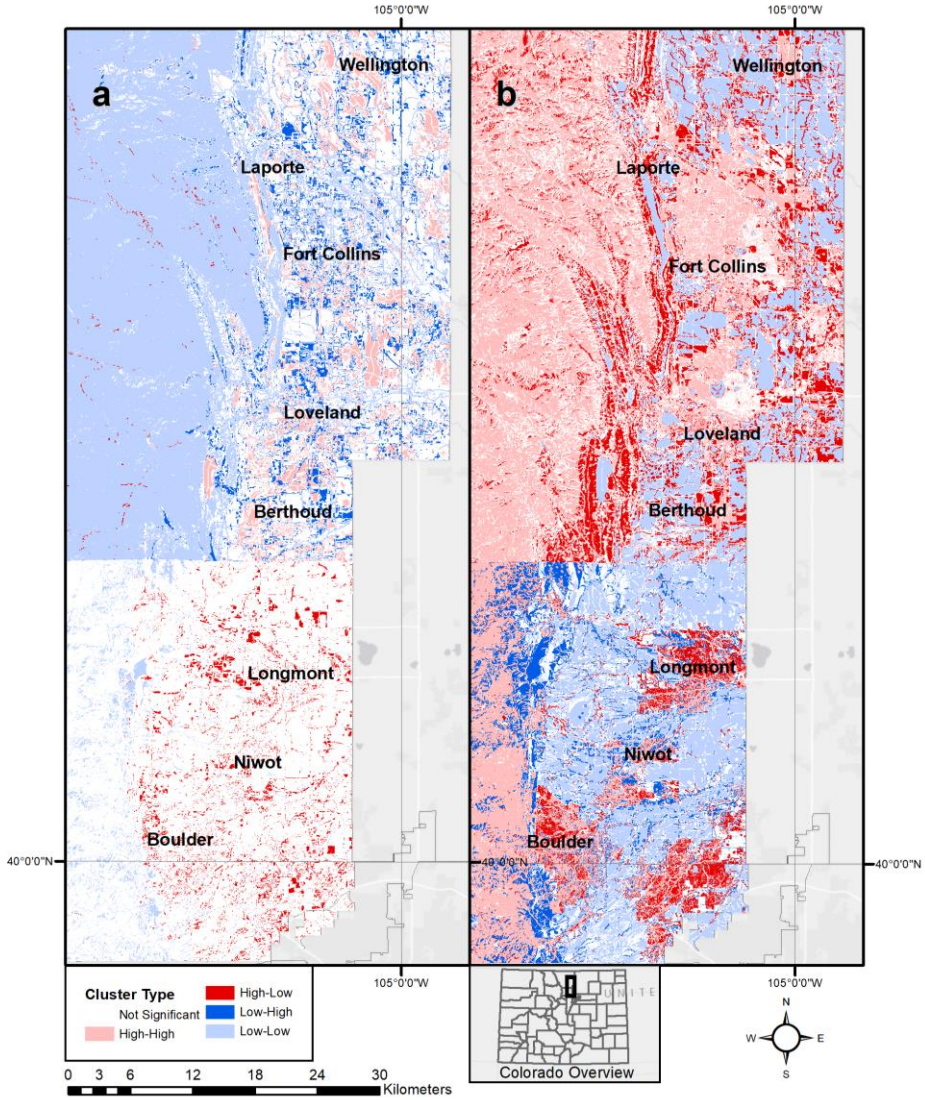

Figure 3.7. Ranked (a) and human factor (b) multipart raster riskscape Anselin Local Moran's *i* cluster outlier map in urban corridors for Boulder and Larimer Counties, Colorado.

3.7 Discussion

These riskscape and spatial autocorrelation results demonstrate the applicability of a riskscape approach to addressing risk in a regional environment. The different approaches in riskscape modeling show that the classified binary approach, while the most basic, does not yield

sufficient accuracy over the region to be used extensively in mitigation strategies. While a suitability ranking forms an intuitive scale for reading the output, using only five classes did not contribute enough information and distinction amongst the data classes to be applicable to modeling response. Ranked and human factor weighted sum riskscapes show more detail in the data and are more appropriate for use in response planning. Urban areas are highly weighted in the human-factor model, and the mapping output demonstrates the clustering of these urban areas. The ranked distribution in Figure 3.8, map A shows the influence of physical and environmental factors more strongly with redder colors representing higher classes and numbers of factors. The human factor map (Figure 3.8, map B) shows the urban areas emphasized.

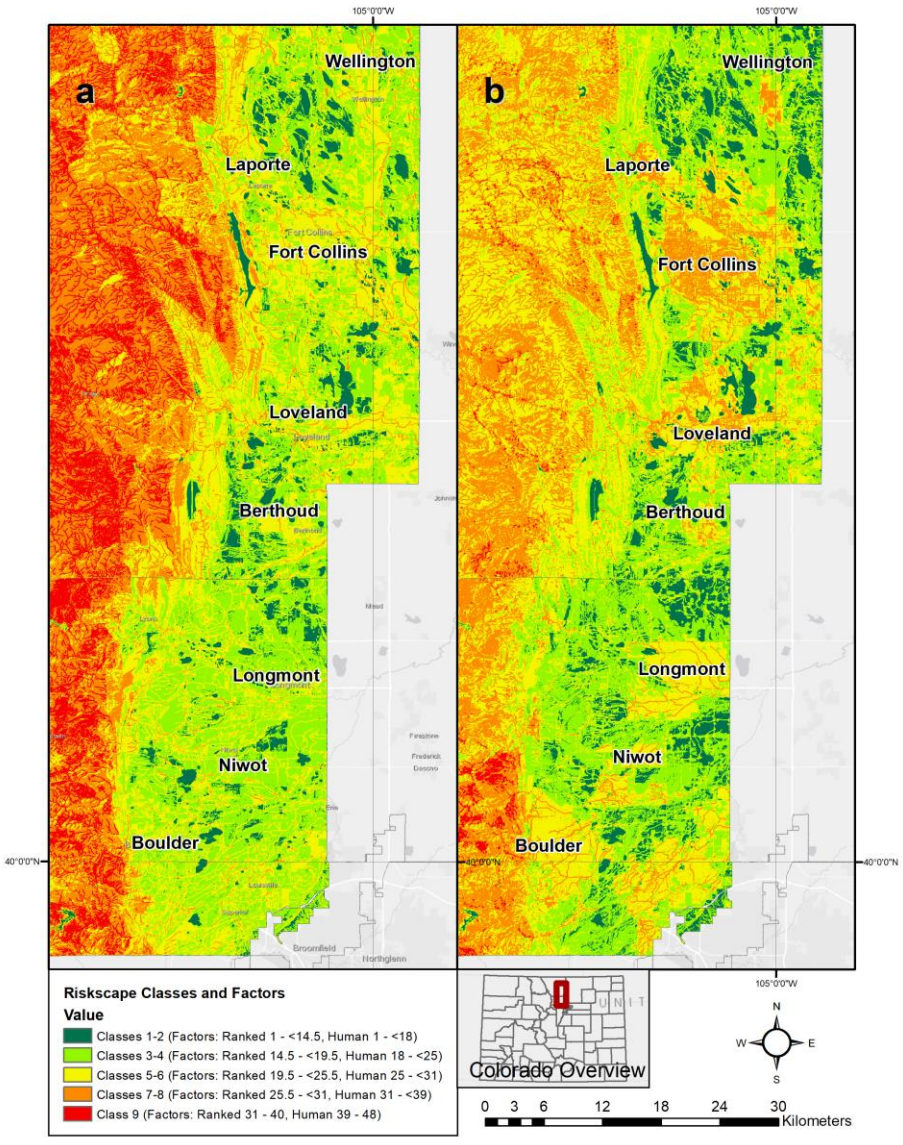

Figure 3.8. Ranked (a) and human factor (b) riskscapes for the Boulder and Larimer County urban corridor.

To compare the performance of human factor and ranked riskscapes for human-environment interactions, a zonal histogram process was run. This analysis calculated cell counts per riskscape class and urban area status to quantify the relative performance of riskscapes related to urban environments. Human factor riskscapes indicate the urban areas more significantly than the ranked classification. Table 3.6 shows the distribution of urban areas with

the ranked and human factor riskscapes. Higher probabilistic frequency ratios are associated with lower riskscape values for ranked riskscapes in both Boulder and Larimer Counties; human factor riskscapes show higher probabilistic frequency ratios for the higher classification categories. These results demonstrate the higher occurrence of urban classifications in the human factor riskscape classes. Figure 3.9 presents the riskscape classes and probabilistic frequency ratio values.

Table 3.6. Comparison of ranked and human factor riskscapes with urban area classification. Bold text indicates a probabilistic frequency ratio greater than 1, demonstrating the relative weight of landslide susceptibility cells.

Boulder County						
Riskscape Class	Ranked Riskscape Areal Percent	Ranked/Urban Areal Percent	Ranked PFR	Human Riskscape Areal Percent	Human/Urban Areal Percent	Human PFR
Low	**3.00**	**3.26**	**1.09**	5.70	0.90	0.16
Moderate	**22.58**	**37.25**	**1.65**	26.56	12.42	0.47
Medium	**30.72**	**35.23**	**1.15**	**43.19**	**51.58**	**1.19**
Elevated	31.34	15.35	0.49	**22.25**	**26.51**	**1.19**
High	12.36	8.90	0.72	**2.28**	**8.59**	**3.76**
Larimer County						
Low	**2.30**	**4.97**	**2.16**	3.75	2.46	0.66
Moderate	**8.94**	**30.23**	**3.38**	17.84	13.81	0.77
Medium	**21.68**	**48.66**	**2.25**	50.12	47.34	0.94
Elevated	46.41	12.23	0.26	**27.37**	**31.45**	**1.15**
High	20.65	3.88	0.19	**0.90**	**4.92**	**5.49**

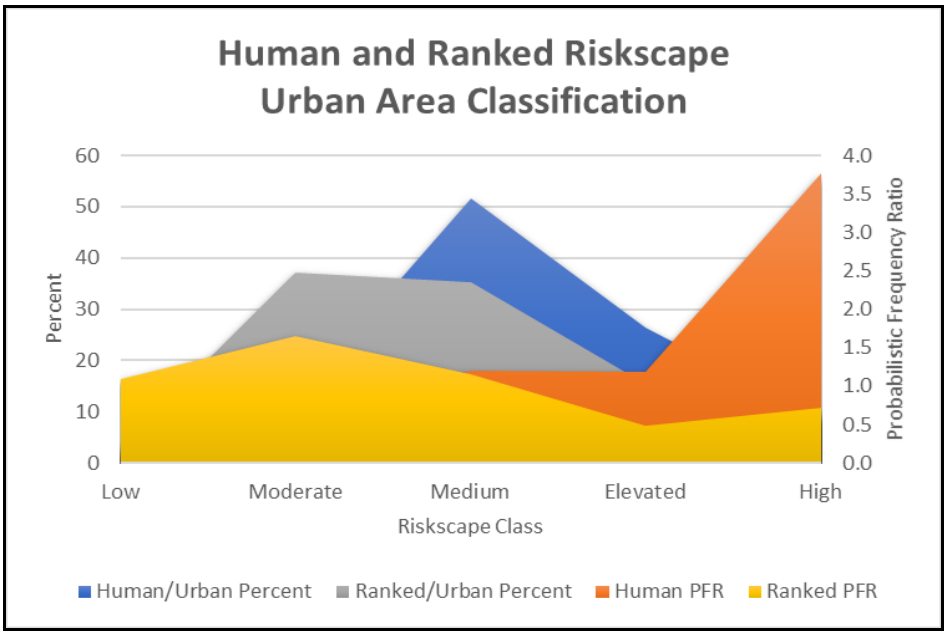

Figure 3.9. Ranked and human factor riskscape urban area comparison. Ranked probabilistic frequency ratio (PFR) peaks at the moderate class, human factor probabilistic frequency ratio peaks at the high class.

By including the urbanization factors, accounting for populations that may exist in the wildland urban interface (WUI) and more rural areas, more detailed models can be developed to protect exurban populations from landslide damage and define areas that must be included in land-use planning decisions or emergency response. Extending future planning and mitigation efforts to incorporate riskscape models supports decision-making and prioritization for response to landslides. Figure 3.10 shows human factor riskscapes coincident with WUI medium and high rankings.

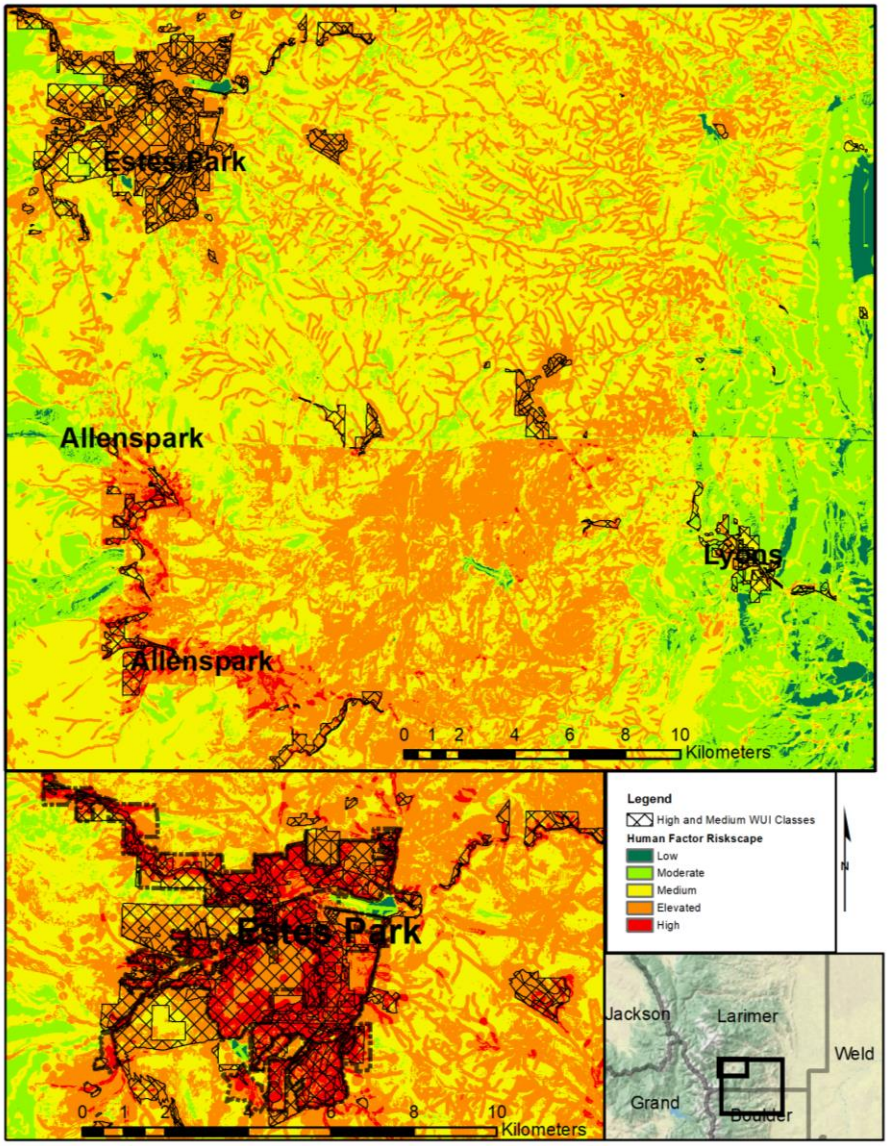

Figure 3.10. Human factor riskscape coincident with high and medium Wildland Urban Interface (WUI) area. Example from Estes Park, Allenspark, and Lyons Colorado. Urban classifications, elevation, and roadways in the area lead to increased riskscape values.

Clustering analysis for the landslide riskscapes also emphasizes the need to develop mitigation strategies based on built-environment and human factors. When evaluating spatial features, the strength of distributions can be measured using spatial autocorrelation and clustering measurements. Further, these relationships can be measured spatially for their strength and correlations by using spatial autocorrelation and clustering tools. Spatial autocorrelation

measures the amount of clustering within a dataset, and generates p-values, and z-scores to measure if these results are statistically significant. Spatial autocorrelation is not frequently expressed in landslide susceptibility studies. In traditional landslide susceptibility studies, these spatial relationships are often ignored (Erener & Düzgün, 2010), and Catani et al. (2016, p. 362) state "more quantitative information on the spatial variability of the MFDs [magnitude frequency distribution] of landslides in the geographical space is needed, a topic almost totally lacking in the relevant literature." Providing a quantitative modeling approach to determine the strength of the spatial relationships between features and the variability of landslide susceptibility across geographic scales seeks to address this lack. Global and local spatial autocorrelation tools were used to assess an urban hazard environment (termed a hazardscape) for Mexicali, Mexico, using multiple types of hazards (Ley-García et al., 2015). Catani et al. (2016) applied spatial autocorrelation to landslide hazards to determine volume and dimensional relationships. Due to the spatial nature of riskscapes, and the value of evaluating spatial distribution of risks, spatial autocorrelation is a tool that can support the assessment of the data for independence or relative clustering. Clustering demonstrates the spatial relationships amongst the riskscape classes, quantifying the strength of the riskscape distribution.

Limiting factors are noted in the data. The clustered nature of urban settlements may influence the amount of clustering seen in the spatial autocorrelation Global and Local clustering measurements. This effect is mitigated in part by the other features used to measure the riskscape such as the physical environmental features. However, human and built-environment features exhibit clustering which should be accounted for in the analysis. Classification of riskscape factors is also an area for improvement. Several classification methods exist, including natural breaks (Jenks), used here, as well as equal-interval and standard deviation classifications.

Depending on the content of the data, datasets applied, and number of factors, other classifications methods may be appropriate.

Despite results from the spatial autocorrelation Global Moran's *i* method showing significant clustering, the binary riskscape values were not effectively mapped given the lower number of classes (14 factor values including a NoData class). The ranked riskscape shows the emergence of patterns, with urban areas showing more high-low clustering in Larimer County in particular. The human factor riskscape provides more detailed clustering, with more urban and high elevation low-high and low-low clustering.

3.8 Conclusions

Riskscapes are transactions within space-time events, integrating quantitative and probabilistic approaches but expanding across a regional landscape. Riskscapes incorporate elements of physical and human geography with natural hazard events and risks. This interface between disciplines strengthens planning capabilities and measures capacity to respond by identifying priority areas for preparedness and mitigation strategy implementations.

Riskscape analyses differ from traditional landslide analyses by including the risk consequence and element data as part of the analysis; traditional landslide analyses are based on the evaluation of the factors influencing the physical hazard of the landslides. The riskscape incorporates the human factors and infrastructure data into the spatial model to evaluate the spatial relationships with the sensitive factors. Humans and the built environment are part of the landscape and influence the surficial changes. Spatially, these factors can be measured to determine the strength of the spatial relationships using the principles of Tobler's First Law of Geography. The clustering in riskscapes indicate the relevance of this law, given as "near things are more related than far things" (Tobler, 1970, p. 236). This geographic pronouncement

describes the relationship between features across spatial extents. Riskscapes can be measured by quantifying this notion spatially.

Spatial autocorrelation, the measure of the strength of these relationships between data, can be measured. For a riskscape, the spatial relationships are measured between all the factors in the region, including the hazard factors as well as the vulnerable elements and consequence data (human factors and built environment infrastructure).

The results show that riskscapes can be created across a regional study area using geospatial analysis to combine the elements of the risk equation, using hazard factors as well as consequence and elements. Human-factor based and ranked riskscape models outperformed the binary weighted-sum models in the classification and development of riskscape zones. Spatial autocorrelation determined that the level of clustering was significant in both human-factor and ranked riskscapes and provide a basis for resource allocation in response to landslides.

This riskscape approach is based on using a spatial integration method that expands on the use of risk equations for natural hazards in the context of landslides. Additional studies with different datasets or changes to scale (state-wide, municipality level) may yield results that place this regional approach in context.

Given the spatial nature of the riskscape, the focus of a landslide riskscape is on the spatial integration of risk impacts, in this case human and built-environment factors, to the susceptibility context of spatial locational assessments and relationships. Riskscapes for landslides indicate that the spatial distribution of landslide riskscapes are relevant, and effectively extend a landslide susceptibility study to incorporate the locational risk factors, creating a more inclusive evaluation of the landslide risk at a given location at the regional scale.

References

Affairs, C. D. o. L. (2017). *Colorado Department of Local Affairs GIS data* [GIS data].

Bell, R., & Glade, T. (2004). Quantitative risk analysis for landslides - Examples from Bildudalur, NW-Iceland. *Natural Hazards and Earth Science Systems*, *4*, 14.

BoulderCounty.org. (2019). *About Boulder County*. Boulder County, Colorado.

Carrara, A., Cardinali, M., Detti, R., Guzzetti, F., Pasqui, V., & Reichenbach, P. (1991). GIS techniques and statistical models in evaluating landslide hazard. *Earth Surface Processes and Landforms*, *16*(5), 427-445.

Carrara, A., Guzzetti, F., Cardinali, M., & Reichenbach, P. (1999). Use of GIS Technology in the Prediction and Monitoring of Landslide Hazard. *Natural Hazards*, *20*, 117-135.

Catani, F., Tofani, V., & Lagomarsino, D. (2016). Spatial patterns of landslide dimension: A tool for magnitude mapping. *Geomorphology*, *273*, 361-373. https://doi.org/10.1016/j.geomorph.2016.08.032

Coe, J. A., Kean, J. W., Godt, J. W., Baum, R. L., Jones, E. S., Gochis, D. J., & Anderson, G. S. (2014). New insights into debris-flow hazards from an extraordinary event in the Colorado Front Range. *GSA today*, *24*(10), 4-10. https://doi.org/10.1130/GSATG214A.1

Curry, M. R. (1995). GIS and the Inevitability of Ethical Inconsistency. In J. Pickles (Ed.), *Ground Truth: The Social Implications of Geographic Information Systems*. The Guilford Press.

Cutter, S. L. (1993). *Living with risk : the geography of technological hazards*. London ; New York : E. Arnold ; New York : Routledge, Chapman and Hall distributor.

Dai, F. C., & Lee, C. F. (2002). Landslide characteristics and slope instability modeling using GIS, Lantau Island, Hong Kong. *Geomorphology*, *42*(3), 213-228.

Dorshow, W. (2012). Predictive geospatial modeling for archaeological research and conservation: Case studies from the Galisteo Basin, Vermont and Chaco Canyon. In W. H. Wills, P. Crown, K. Prufer, & T. Wawrzyniec (Eds.): ProQuest Dissertations Publishing.

Erener, A., & Düzgün, H. (2010). Improvement of statistical landslide susceptibility mapping by using spatial and global regression methods in the case of More and Romsdal (Norway). *Landslides*, *7*(1), 55-68. https://doi.org/10.1007/s10346-009-0188-x

Esri. (2019). *How Cluster and Outlier Analysis (Anselin Local Moran's I) works*. https://pro.arcgis.com/en/pro-app/tool-reference/spatial-statistics/h-how-cluster-and-outlier-analysis-anselin-local-m.htm

Esri. (2020). *Modeling spatial relationships*. Environmental Systems Research Institute. Retrieved June 16, 2020 from https://pro.arcgis.com/en/pro-app/tool-reference/spatial-statistics/modeling-spatial-relationships.htm#GUID-729B3B01-6911-41E9-AA99-8A4CF74EEE27

Guzzetti, F. (2006). *Landslide hazard and risk assessment: concepts, methods, and tools for the detection and mapping of landslides, for landslide susceptibility zonation and hazard assessment, and for landslide risk evaluation* [Dissertation, University of Bonn]. Bonn, Germany. http://geomorphology.irpi.cnr.it/Members/fausto/PhD-dissertation/Landslide_Hazard_and_Risk_Assessment.pdf

Hewitt, K., & Burton, I. (1971). *The hazardousness of a place : a regional ecology of damaging events*. University of Toronto Press.

Huabin, W., Gangjun, L., Weiya, X., & Gonghui, W. (2005). GIS-based landslide hazard assessment: an overview. *Progress in Physical Geography*, *29*(4), 548-567. https://doi.org/10.1191/0309133305pp462ra

Huang, F., Yin, K., Huang, J., Gui, L., & Wang, P. (2017). Landslide susceptibility mapping based on self-organizing-map network and extreme learning machine. *Engineering Geology*, *223*, 11-22. https://doi.org/10.1016/j.enggeo.2017.04.013

Jenerette, G., Darrel, H., L., S., Stefanov, W. L., & Martin, C. A. (2011). Ecosystem services and urban heat riskscape moderation: water, green spaces, and social inequality in Phoenix, USA. *Ecological Applications*, *21*(7), 2637-2651.

Kappes, M., Keiler, M., Elverfeldt, K., & Glade, T. (2012). Challenges of analyzing multi-hazard risk: a review. *Natural Hazards*, *64*(2), 1925-1958. https://doi.org/10.1007/s11069-012-0294-2

Larimer.org. (2019). *About Larimer County*. Larimer County Colorado.

Lee, S., & Choi, J. (2004). Landslide susceptibility mapping using GIS and the weight-of-evidence model. *International Journal of Geographical Information Science*, *18*(8), 789-814. https://doi.org/10.1080/13658810410001702003

Legorreta Paulin, G., Bursik, M., Hubp, J. L., Mejia, L. M. P., & Aceves Quesada, F. (2014). A GIS method for landslide inventory and susceptibility mapping in the Rio El Estado watershed, Pico de Orizaba Volcano, Mexico. *Natural Hazards*, *71*(1), 229-241. https://doi.org/10.1007/s11069-013-0911-8

Ley-García, J., Denegri de Dios, F. M., & Ortega Villa, L. M. (2015). Spatial dimension of urban hazardscape perception: The case of Mexicali, Mexico. *International Journal of Disaster Risk Reduction*, *14*, 487-495. https://doi.org/10.1016/j.ijdrr.2015.09.012

Magliulo, P., Di Lisio, A., & Russo, F. (2008). Comparison of GIS-based methodologies for the landslide susceptibility assessment. *Geoinfomatica*, *13*(3), 12.

McCoy, K. (2016). *County-Scale Debris-/Mud-Flow Susceptibility Mapping*. Golden, Colorado: Colorado Geological Survey Retrieved from http://coloradohazardmapping.com/hazardMapping/debrisFlowMapping/Documents

Morello-Frosch, R., Pastor, M., & Sadd, J. (2001). Environmental justice and Southern California's "riskscape": The distribution of air toxics exposures and health risks among diverse communities. *Urban Affairs Review*, *36*(4), 551-578.

Morgan, M. L., White, J. L., Fitzgerald, F. S., & Berry, K. A. (2014). *Foothill and mountainous regions in Boulder County, Colorado that may be susceptible to earth and debris/mud flows during extreme precipitation events* Colorado Geological Survey. https://coloradogeologicalsurvey.org/publications/landslide-susceptibility-extreme-precipitation-boulder-colorado

Müller-Mahn, D., & Everts, J. (2013). Riskscapes: the spatial dimension of risk. In H.-D. Müller-Mahn & C. Ebooks (Eds.), *The spatial dimension of risk: How geography shapes the emergence of riskscapes*. Routledge.

Patton, A. I., Rathburn, S. L., Bilderback, E. L., & Lukens, C. E. (2018). Patterns of debris flow initiation and periglacial sediment sourcing in the Colorado Front Range. *Earth Surface Processes and Landforms*, *43*(15), 2998-3008. https://doi.org/10.1002/esp.4463

Pickles, J. (1995). *Ground truth: the social implications of geographic information systems*. New York: Guilford Press.

Radeloff, V. C., Helmers, D. P., Kramer, H. A., Mockrin, M. H., Alexandre, P. M., Bar-Massada, A., Butsic, V., Hawbaker, T. J., Martinuzzi, S., Syphard, A. D., & Stewart, S. I. (2018).

Rapid growth of the US wildland-urban interface raises wildfire risk. *Proceedings of the National Academy of Sciences of the United States of America*, *115*(13), 3314. https://doi.org/10.1073/pnas.1718850115

Reichenbach, P., Rossi, M., Malamud, B. D., Mihir, M., & Guzzetti, F. (2018). A review of statistically-based landslide susceptibility models. *Earth-Science Reviews*, *180*, 60-91. https://doi.org/10.1016/j.earscirev.2018.03.001

Review, W. P. (2020). *World Population Review*. Retrieved January 6, 2020 from www.worldpopulationreview.com

RiskScape, P. (2016). *The RiskScape Project: About the Project*. New Zealand Foundation for Reseaerch, Science, and Technology. Retrieved October 1, 2016 from https://riskscape.niwa.co.nz/about-the-project/funding

Schmidt, J., Matcham, I., Reese, S., King, A., Bell, R., Henderson, R., Smart, G., Cousins, J., Smith, W., & Heron, D. (2011). Quantitative multi-risk analysis for natural hazards: a framework for multi-risk modeling. *Natural Hazards*, *58*, 1169-1192.

Schmidt, J., Turek, G., Matcham, I., Reese, S., Bell, R., & King, A. (2007). RiskScape - an innovative tool for multi-hazard risk modelling. In J. Schmidt (Ed.).

Tobler, W. R. (1970). A Computer Movie Simulating Urban Growth in the Detroit Region. *Economic Geography*, *46*, 234-240. https://doi.org/10.2307/143141

van Westen, C. J. (2013). 3.10 Remote Sensing and GIS for Natural Hazards Assessment and Disaster Risk Management. In J. F. Shroder (Ed.), *Treatise on Geomorphology* (pp. 259-298). Academic Press. https://doi.org/https://doi.org/10.1016/B978-0-12-374739-6.00051-8

Varnes, D. J. (1958). *Landslide types and processes* (Landslides and engineering practice Issue. N. R. Council.

Varnes, D. J. (1978). *Slope movement types and processes* (0360859X). (Special Report: Landslides analysis and control Issue.

Wait, T. C., Morgan, M. L., Fitzgerald, F. S., Morgan, K. S., Berry, K. A., & White, J. L. (2015). *OF-15-13 Debris Flow Susceptibility Map of Larimer County, Colorado*. Golden, Colorado: State of Colorado Retrieved from https://coloradogeologicalsurvey.org/publications/debris-flow-susceptibility-map-larimer-colorado

Zêzere, J. L., Pereira, S., Melo, R., Oliveira, S. C., & Garcia, R. A. C. (2017). Mapping landslide susceptibility using data-driven methods. *Science of the Total Environment*, *589*(C), 250-267. https://doi.org/10.1016/j.scitotenv.2017.02.188

CHAPTER 4: GEOSTATISTICAL ASSESSMENTS OF LANDSLIDE RISKSCAPES: A COMPARISON OF LOGISTIC REGRESSION, WEIGHTS OF EVIDENCE, AND PROBABILITISTIC NEURAL NETWORKS[4]

4.1 Summary of the manuscript

Due to the spatial nature of risk, geospatial analysis in GIS (Geographic Information Systems) can be used to model and analyze risk spatially across a landscape. I applied a spatial approach to analyze riskscapes that consider the location and spatial relationships between landslide susceptibility and human-environment factors as a spatial distribution model. Using a study area in Colorado, logistic regression, weights of evidence and probabilistic neural network approaches were developed to determine the probabilistic relationship between landslide riskscapes modeled using binary, ranked, and human factor weighted sum overlays. Spatial Data Modeler (ArcSDM) and ArcGIS platforms were used to develop geostatistical models to determine the spatial distribution of riskscape relationships. Weights of evidence (WOE) demonstrated significant probability of predicting landslide riskscapes with strong AUC validation, while logistic regression results did not have a strong association with prediction. Probabilistic neural networks performed well in probability determinations, but AUC values approximated randomness. Overall, ArcSDM provides a platform for geostatistical analysis of landslide riskscapes to further analyze the spatial relationships and distributions of significance.

[4] This chapter is based on a manuscript co-authored with Melinda Laituri, submitted to a peer-reviewed journal for review.

4.2 Introduction

Landslides are natural hazards that become disasters when they occur in developed areas (Guzzetti, 2006; van Westen, 2013). Risks of landslides vary across the landscape, and riskscapes as applied in this study present a technology approach to assess landslide risk spatially. Landslide riskscapes create informational surfaces using the intersection of spatial factors based on landslide susceptibility inventory models. Geographic Information Systems (GIS) provide data-driven spatial analysis tools to incorporate the datasets required for quantitative riskscape development (Hicks & Laituri, 2020). Geostatistical tools in the Spatial Data Modeler extension (ArcSDM) are used to measure the spatial probabilities of landslide risk based on these riskscape models.

The purpose of this study is to examine the performance of three geostatistical models applied to landslide riskscapes and evaluate the relative applicability of these methods to broader riskscape models. This study uses landslide susceptibility inventory data for Boulder and Larimer Counties, Colorado as the basis to assess three different geostatistical methods — a logistic regression model, a weights of evidence (WOE) model, and a probabilistic neural network (PNN) model — to predict areas of vulnerability to landslide potential. A GIS tool in the Esri ArcGIS environment, ArcSDM, is used to run these geostatistical analyses. The goal of this study is to compare the outcome of these three geospatial models currently used in landslide susceptibility assessment within the geostatistical GIS environment to evaluate riskscapes of landslides.

4.2.1 Literature background: landslide geostatistical approaches

Landslide research using geospatial and data-driven geostatistical applications includes multiple methods and approaches to modeling landslide susceptibility using non-spatial

statistical tools. Three commonly used methods include logistic regression (Aditian et al., 2018; Akgun, 2012; Althuwaynee et al., 2014; Ayalew & Yamagishi, 2005; Bai et al., 2011; Dai & Lee, 2003; Duman et al., 2006; Falaschi et al., 2009; Lee, 2005; Lee et al., 2015; Ohlmacher & Davis, 2003; Regmi et al., 2014; Yilmaz, 2009), weights of evidence (R. K. Dahal et al., 2008; R.K. Dahal et al., 2008; Kouli et al., 2014; Poli & Sterlacchini, 2007; Prasannakumar & Vijith, 2012; Song et al., 2008), and neural networks (Aditian et al., 2018; Borgogno Mondino et al., 2009; Choi et al., 2012; Ercanoglu, 2005; Ermini et al., 2005; Falaschi et al., 2009; Kanungo et al., 2006; Lee, 2007; Lee & Evangelista, 2006; Lee et al., 2007; Lee et al., 2006; Lee et al., 2003; Pradhan & Lee, 2010; Tien Bui et al., 2012; Yesilnacar & Topal, 2005; Yilmaz, 2009).

Lee et al. (2000) provided a workflow and method for using geostatistical tools such as artificial neural networks, probability (probabilistic frequency ratio), and logistic regression as part of landslide susceptibility modeling. Lee et al. (2018) provided a method evaluating different approaches in GIS including weights of evidence and regression in GIS. Zêzere et al. (2017) applied regression and discriminant analysis statistical methods in GIS, and used ArcSDM to create terrain units. Ozdemir (2011) provided an overview of geostatistical methods used in landslide susceptibility modeling literature, including,

> *Logistic regression technique, weighting factors, weighted linear combination of instability factors, multivariate regression, information value, weights of evidence, frequency ratio approach, landside nominal risk factor, genetic algorithm, likelihood ratio, certainty factors and fuzzy sets to landslide susceptibility zonation*
>
> *Ozdemir, 2011, p. 1591*

Other geostatistical methods applied to landslide susceptibility include event trees (Lee, 2009) and random forests (Catani et al., 2013). Many of these methods are reviewed in Reichenbach et al. (2018), which provides a thorough assessment of current landslide susceptibility statistical modeling methods.

This literature is representative of the diversity of approaches available to assess riskscapes. Riskscape development procedures apply these modeling and geostatistical approaches to operationalize the models. Expanding both the risk- and landslide- focus of geostatistical models to include spatial extent and variability provides a more complete picture of the regional representation of landslide risk. Non-spatial statistical approaches evaluate the factors without consideration of the power function of spatial distribution, namely the distance decay function represented in Tobler's First Law of Geography, proposed by Waldo Tobler in 1970, which states that near things are more related than distant things (Tobler, 1970, p. 236). This distance weighting model was influenced by previous works by Borchert according to Tobler (1970, p. 235) and bear similarities to formative work by Zipf based on inverse-distance law (Cresswell, 2013, p. 96). Multiple methods for determining aspects of landslide risk (susceptibility, hazard inventory, risk assessments) defined in Guzzetti (2006) are based on non-spatial statistical methods. However, spatial data are unique in that there are relationships between the datasets based on proximity or distance between features (Tobler, 1970). Geostatistical models include the distribution of spatial probabilities, create mappable surfaces, and account for the influence of space in natural features, which are non-normal, non-independently distributed (Aditian et al., 2018; Nourani et al., 2014). The incorporation of geostatistical approaches reveals the statistical probabilities in the context of their locations. This

locational representation improves the understanding of the distribution of landslide risk through a riskscape process.

Spatial statistics apply the unique characteristics of spatial data to non-spatial statistical measurements (Oyana & Margai, 2016). These characteristics include proximity, size, shapes of boundaries, and relationships to neighboring features. Incorporating spatial characteristics in geostatistical analyses provides a model for furthering our understanding of how space influences riskscapes.

Riskscapes are defined as the "spatial dimension of risk" (Müller-Mahn & Everts, 2013) derived from social constructivist theories. Risk equations are presented in quantitative risk assessment studies as derivations of the relationship between risk and the hazard and social factors in the region. Bell and Glade (2004) present this risk equation as R = H x C x E where risk is the combination of the hazard (H) occurrence, the elements at risk (E) and the consequences of the event occurrence (C). Riskscapes as the spatial model of a risk equation are presented in Hicks and Laituri (2021) to include the spatial distribution of factors as a measurable feature of a landslide riskscape.

4.3 Study area

Boulder and Larimer Counties in Colorado have a history of landslide activity and a mix of urban, suburban, exurban, and remote areas. Geologically, the region includes the border between two geologic provinces, the Plains, and the Rocky Mountains. Geologic units include metamorphic and igneous lithologies forming the basis of the Rocky Mountains and sedimentary facies on the Plains. Landslides predominantly occur in mountainous regions granite and biotitic gneiss lithologies (Hicks & Laituri, 2020; Morgan et al., 2014; Tweto, 1979; Wait et al., 2015).

Elevations range from 1430 meters above mean sea level (AMSL) on the eastern border of the counties to mountain peaks 4300 meters AMSL.

Populations for both counites are similarly sized, with approximately 326,196 residents in Boulder County and 356,899 residents in Larimer County (Bureau, 2019). Land cover and urbanization includes a mix of urban and non-urban areas, with populations distributed in urban centers and in mountain communities. Boulder County has a higher percentage of urban areas, with 21.15% of the county classified as urban clusters or areas. Larimer County is predominantly non-urban, with 6.72% of the county classified as urban clusters or areas. Land cover consists primarily of developed and agricultural croplands on the plans with scrub/herb classes in the foothills and forest/woodland classes in the mountains (Survey, 2011).

Landslide susceptibility locations in Boulder and Larimer Counties were mapped by the Colorado Geological Survey and published in two open file reports, OFR15-13, and OFR-14-2 (Morgan et al., 2014; Wait et al., 2015). Landslide susceptibility locations and urban areas are shown in Figure 4.1. These datasets include 14,032 landslide susceptibility zone features (818 sq km) for Larimer County which covers 6,818 sq kms in areal extent, and 3,237 landslide susceptibility features (121 sq km) for Boulder County which covers 1,916 sq km in areal extent. Larimer County represents an area approximately 3.5 times as large as Boulder County, though other characteristics such as population, geology, and elevation profiles are similar. Population growth in the wildland urban interface (WUI) areas, where development and human populations encroach on wildland vegetation systems can be concerning due to the increased exposure to natural hazards (Radeloff et al., 2018). Population growth from 2010 within the counties is estimated at 30,000 for Boulder County and 50,000 in Larimer County (Review, 2020) and increases the potential for exposure in the sensitive WUI areas (Hicks & Laituri, 2020). These

population distributions and areas of wildland urban interface lead to increased risk of landslide impacts on the built environment. Riskscapes based on these distributions support determination of planning zones, areas of increased risk, and prioritized areas for mitigation and treatment.

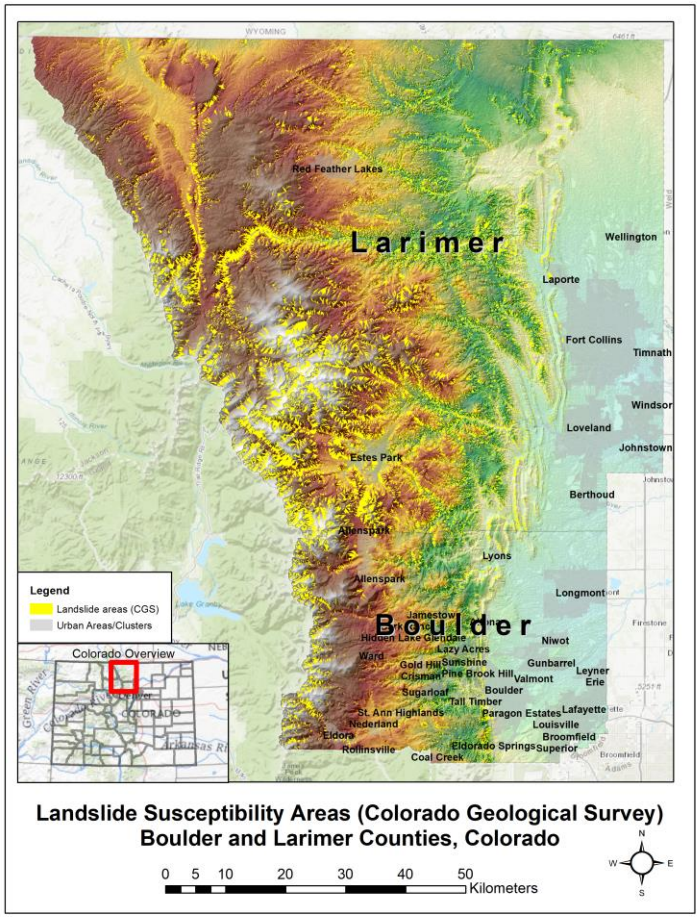

Figure 4.1. Boulder and Larimer counties in Colorado, urban areas, and landslide susceptibility areas. Data sources: Colorado Geological Survey, U.S. Census Bureau, U.S. Geological Survey.

4.4 Geostatistical background

4.4.1 Weights of evidence

Weights of evidence (WOE) methods are used in landslide susceptibility studies to determine weights for the landslide predictive factors. WOE models are predictive models based on Bayesian probability that characterize the landslide susceptibility. These processes in GIS

analyze factors for occurrence of an event based on the weights of the factors. The equations presented in Kouli et al. (2014) detail the natural log relationship between the presence and absence of event occurrence with the presence or absence of the factors.

$$W+ = \ln \frac{P(F|L)}{P(F|\bar{L})}$$

$$W- = \ln \frac{P(\bar{F}|L)}{P(\bar{F}|\bar{L})}$$

> *Where, W+ and W- are the weights for the presence or absence of landslides (L) within a certain class F of a conditioning factor map (F), P(F|L) is the conditional probability of F occurring given the presence of L, L signifies the presence of a landslide, F is a class of a causative factor, and the bar above a symbol signifies the absence (Kayastha et al. 2013a)*
>
> *Kouli et al. (2014, p. 5207)*

These weighting factors are calculated within the software environments based on the number of samples and number of factors. The spatial presence or absence of the phenomena, landslides in this case, are indicated by positive or negative values (Kouli et al., 2014).

ArcSDM weights of evidence methods for mineral exploration were applied in separate works by Harris (2002); Hartley (2014) to predict locations of mineral deposits in Ontario and Minnesota, respectively. ArcSDM models generates raster data outputs for posterior probability, standard deviation, and confidence intervals. Additionally, the weight tables include W+, W-, and the contrast measurements, which indicate the degree of correlation (Agterberg et al., 1990) between the factors and the event.

4.4.2 Logistic regression

Logistic regression is a data-driven inferential method that allows for prediction of occurrence of a factor or forecasting relationships between variables. GIS tools and geostatistical tools such as geographically weighted regression, ordinary least squares, or exploratory regression analysis tools in the modeling spatial relationships toolset can automate the process of regressions based on various input datasets for dependent and independent variables. Multiple landslide studies use logistic regression in a GIS platform. Dai and Lee (2002) indicate the appropriateness of applying logistic regression to model slope stability, applying binary (presence/absence) models for prediction of spatial probabilities. Saro Lee presented multiple logistic regression studies of landslides in Korea, and described the background for the application of logistic regression, highlighting the importance of logistic regression to analyze variables with non-normal distributions (Lee, 2005), a relevant aspect for natural features which may show non-normal distributions (Catani et al., 2016). Ohlmacher and Davis (2003) applied logistic regression and GIS to assess landslide hazards in Kansas, finding the spatial data procedure using logistic regression capable of predicting zones of landslide potential. Manzo et al. (2013) applied logistic regression using ArcSDM tools to a landslide susceptibility study in Italy, finding the logistic regression outperformed frequency ratio methods despite challenges in the data quality of landslide inventory, and the dependency on the input factors.

4.4.3 Artificial neural networks

Artificial neural networks (also referred to as neural networks or ANN) are applied to landslide modeling methods in multiple landslide studies (Aditian et al., 2018; Choi et al., 2012; Lee, 2007; Lee & Evangelista, 2006; Lee et al., 2007; Lee et al., 2004; Pradhan & Lee, 2007, 2010). The foundation for applying neural network methods to landslide susceptibility studies is

that landslides can be predicted using models based on networks similar to brain patterns. Neural networks are used specifically as a pattern recognition tool and attempt to recognize patterns within the datasets. Neural networks use a subset of dataset values to predict other, unknown values. They are made up of multiple layers and follow the process flow of input/process/output based on hidden layers in the learning process. Data are divided into training and classifying datasets. Training datasets (true positives and true negatives) are used to teach the ANN to identify areas that are correctly classified. The remaining dataset (classifying) is then analyzed by the ANN to predict the values. The adjustments occur within the "hidden layers" of the ANN, where the machine learning algorithm "learns" from the input training dataset and adjusts weights to optimize the output layers (Heaton, 2017; Hjort & Luoto, 2013). Probabilistic neural networks are a type of forward feed neural network that estimate the probability of class memberships from the input data (Ermini et al., 2005; Singer & Kouda, 1999).

ANN modeling processes within GIS are based on the system's ability to train itself from iterations of data modeling outcomes (Kanungo et al., 2006). Kanungo et al. (2006, p. 349) used ANN as part of a comparative study on landslide zonation evaluating the performance of ANN and fuzzy processes (the degree to which a factor is a member of a set) within a GIS environment. The authors found that ANN can be applied with various data scales including categorical data, which is important for riskscape modeling. Lee (2007) describes the weighting process for factors in the GIS environment using ANN methods. For riskscapes, these factors extend beyond the landslide factors to include the social factors from the spatial risk equation.

4.5 Materials and methods

GIS methods were used to calculate the geostatistical probabilities for logistic regression, weights of evidence, and neural networks, using the Spatial Data Modeler (ArcSDM) extension

and Spatial Analyst tools in Esri's ArcGIS platform (ArcGIS Desktop version 10.7.1 and ArcGIS Pro version 2.4).

ArcSDM is a modelling tool developed to support advanced geostatistical processing methods within Esri's ArcGIS platform. The toolset was originally developed with scientists from the U.S. Geological Survey and the Geological Survey of Canada (Sawatzky et al., 2009). ArcSDM code is currently maintained by the Geological Survey of Finland via a GitHub community (https://github.com/gtkfi/ArcSDM). Workflows within ArcSDM are python-based scripts that support analysis for calculating class and factor weights, modeling posterior probability based on training dataset input for weights of evidence and logistic regression models, and a neural network module to create probabilistic neural network (supervised) outputs.

4.5.1 Data processing

Multiple processing steps were used to calculate the geostatistical outputs for three types of riskscapes based on weighted sum landslide riskscape models developed in Hicks and Laituri (2020). The riskscape models are based on a probabilistic frequency ratio analysis of landslide susceptibility cells coincident with 16 factors, listed in Table 4.1. The factors used in the initial development of the landslide riskscape models include elevation, aspect, slope degrees, combined curvature, lithology, proximity to faults (50 meters), soil type, land cover classification, distance to hydrology features (lakes and streams set to 50-meter buffers), and human factors including building footprint buffers (100 meters), roads and railroads (50-meter buffers), airports (500-meter buffers), population data, and urban classification. Data for the geostatistical analyses were accessed from public sources in the study area. The derived riskscape input data were developed based on a method in Hicks and Laituri (2020).

Table 4.1. Data types and sources.

Type	Source	Date Publication	Purpose
Landslide susceptibility areas	Colorado Geological Survey Open File Reports	2014 and 2015	Dependent variable
Digital Elevation model	USGS National Map	2018	Input factor (physical)
Aspect*	USGS National Map	2018	Input factor (physical)
Slope degrees*	USGS National Map	2018	Input factor (physical)
Curvature*	USGS National Map	2018	Input factor (physical)
Lithology	Colorado Geological Survey	2013	Input factor (physical)
Faults	USGS/Mineral Resources	2005	Input factor (physical)
Flowlines (rivers and streams)	USGS National Hydrography Dataset (NHD)	2018	Input factor (physical)
Waterbodies (lakes and reservoirs)	USGS National Hydrography Dataset (NHD)	2018	Input factor (physical)
GAP Land cover	USGS GAP	2018	Input factor (physical)
Soil	USDA NRCS	2018	Input factor (physical)
Building footprints	Microsoft Open Buildings	2018	Input factor (social)
Roads	Colorado Department of Transportation	2018	Input factor (social)
Railways	Colorado Department of Transportation	2018	Input factor (social)
Airports	Colorado Department of Transportation	2018	Input factor (social)
Urban areas	US Census Bureau	2018	Input factor (social)
Census population	US Census Bureau	2018	Input factor (social)
Binary riskscape	Hicks and Laituri	2020 (in review)	Compiled model
Ranked riskscape	Hicks and Laituri	2020 (in review)	Compiled model
Human Factor riskscape	Hicks and Laituri	2020 (in review)	Compiled model

The derived weighting factors were based on either the presence/absence of the factor with landslide susceptibility cells (binary), or applied factor weights based on the percentage of landslide susceptibility cells present in the factor classes. Three weighed sum riskscapes used percentages based on the presence or absence of the feature to assign weights. These riskscapes used binary ranking, based on the presence or absence of the feature (0 = no feature, 1 = feature); weighted sum ranked, based on the proportion (frequency ratio) of the landslide cells within the features' classes (0 = 0 weight, greater than 0 to less than 1 = 0.5 weight, greater than 1 to less than 10 = 1 weight, greater than 10 to less than 30 = 3 weight, greater than 30 = 5 weight); and, weighted sum ranked with human factors, which included maximum weights (5) for building, population and urban classes regardless of landslide susceptibility frequency ratio zonation.

4.5.2 Data preparation

To utilize the toolsets in ArcSDM, certain parameters must be configured due to input setting requirements of the application. Tools required a common data projection, unit of scale, and study area boundary file. Data were projected to NAD83_UTM_Zone13_North (meters) for Colorado. Environmental settings were configured to include the processing extent of each county study area as a vector polygon boundary and a raster mask, and raster grid cell size for analysis (10 meters). The three modeled riskscapes were used as the evidence rasters for the analyses. Figure 4.2 shows the workflow for initial data preparation and training site creation, described in section 4.5.3.

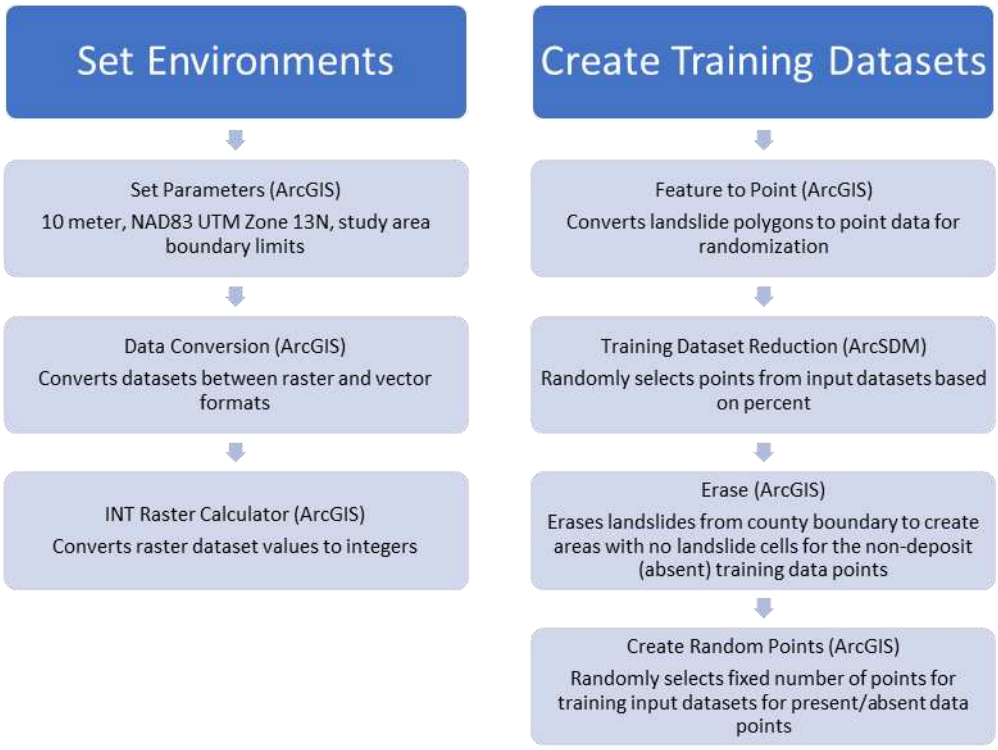

Figure 4.2. Workflow for data preparation steps.

4.5.3 Training sites in ArcSDM

Training sites were developed using the Training Site Reduction tool in ArcSDM. Landslide vector sites were used as the input layer, and the environmental mask (area where the calculations were performed) was set to each county. The random selection option was used and set to be 20%, resulting in 641 training points in Boulder County and 2789 for Larimer County. Due to a limitation in processing in ArcSDM, two additional random datasets of 500 and 1000 points were also created for analysis using the Create Random Point tool in ArcGIS for comparison for both the training datasets (presence of landslide susceptibility cells) and the non-deposit training datasets (absence of landslide susceptibility cells).

Training datasets for landslide susceptibility (20%, 500 points, and 1000 points) were used as the training data inputs. A non-deposit (ND) training dataset, points representing features not included in the landslide susceptibility point training dataset was required to show true negative locations (no landslide susceptibility cells). To generate the ND training set, points outside of the landslides were needed. To obtain these points, the landslide susceptibility polygons were erased from the county boundary using the ArcGIS Erase tool. The Create Random Points tool was used to create training datasets of 500 and 1000 points from the non-landslide susceptibility cells. The Training Site Reduction tool in ArcSDM was used to create 20% training dataset within the county extent for non-deposit training data (641 for Boulder County and 2789 for Larimer County).

4.5.4 Weighting the tables

The logistical regression and weights of evidence geostatistical analyses tools require weight tables based on the input raster datasets. These weights determine how the classes within each raster relate to the input training dataset and create outputs for W+, W-, the studentized

contrast and general classification weights to be used in further analyses. W^+ (or W plus) is the measure of a positive correlation in the weighting table, while W^- (or W minus) is the measure of a negative correlation, and the Contrast (W^+ - W^-) is "a measure of the strength of correlation" (Agterberg et al., 1993, p. 14). Hosseinali and Alesheikh (2008) specify the weighting factors are indicative of spatial influence related to probability with positive weights having a high significance and negative as a low significance.

The Calculate Weights tool requires integer rasters as inputs, which requires any raster inputs with non-integer values to be pre-processed using the Int() function in the Esri Spatial Analyst extension for ArcGIS. The Int() tool modifies the raster cell values by removing any decimal places in the raster. Riskscapes were calculated from ranked factors, with a double input (allowing for decimal values in ArcGIS) based on methods presented in Hicks and Laituri (2020). Therefore, the riskscape input rasters required conversion to a new integer type before processing to remove the decimal placeholder. This can cause issues for rasters with decimal values, but for the riskscape data, all the factors had been classified based on integer values, so no data quality was lost.

The Calculate Weights tool compares the training datasets to the input datasets to create weight tables with class weights, W+/-, and contrast values.

Parameter settings for the Calculate Weight tools include:

- Input integer raster
- Input type (Categorical for classified raster data)
- Input training datasets (20%, 500 points, 1000 points)
- Output raster name
- Confidence interval (set to 1.96, which corresponds to a 95% CI)

Logistic regression and weights of evidence workflows are based on the weight tables created in this process. ArcSDM uses the weight tables to run a spatial logistic regression or a weights of evidence model and outputs posterior probability, confidence interval, and standard deviation raster datasets for both types of analysis. Workflows are shown in Figure 4.3.

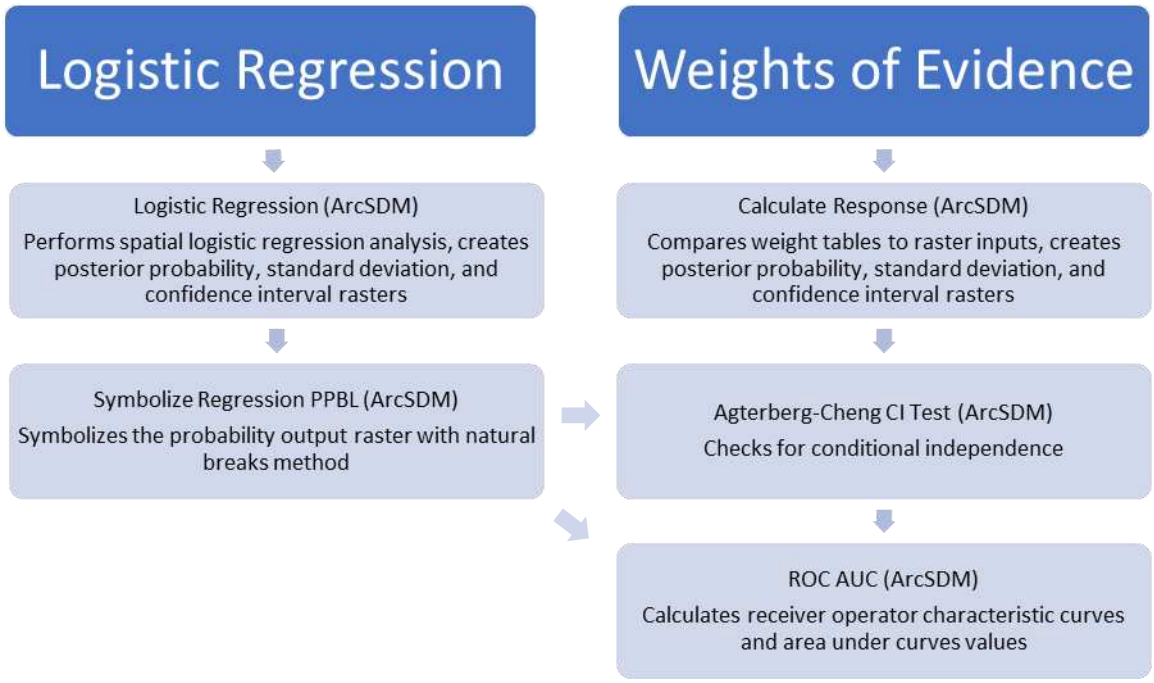

Figure 4.3. Workflows for logistic regression and weights of evidence analysis models in ArcSDM.

4.5.5 Neural network data preparation

Multiple steps were required to create input files for the probabilistic neural network (PNN) analysis. Unique condition unit raster datasets were created using the Combine tool in ArcGIS Spatial Analyst extension. Only one input raster was used for each Combine file, as the riskscape data contain the combined landslide riskscape factors. The Band Collection Statistics tool which determines the raster band statistics and includes the covariance (the measure of the

variance between the raster datasets) and a correlation matrix (the correlation between the raster band values) was run to create a table for input (Esri, 2020). The ArcSDM interface requires the Combine file as the input unique conditions raster, which is based on the riskscape raster. Input matrices were calculated using the Neural Network Input tool in ArcSDM. Data needed to be input into GeoXplore. GeoXplore, a Visual C++ module written by Looney et al. (2005), runs neural network training and classification on datasets developed in ArcSDM and these datasets are then fed back into ArcSDM to complete the neural network mapping. The neural network workflow is presented in Figure 4.4.

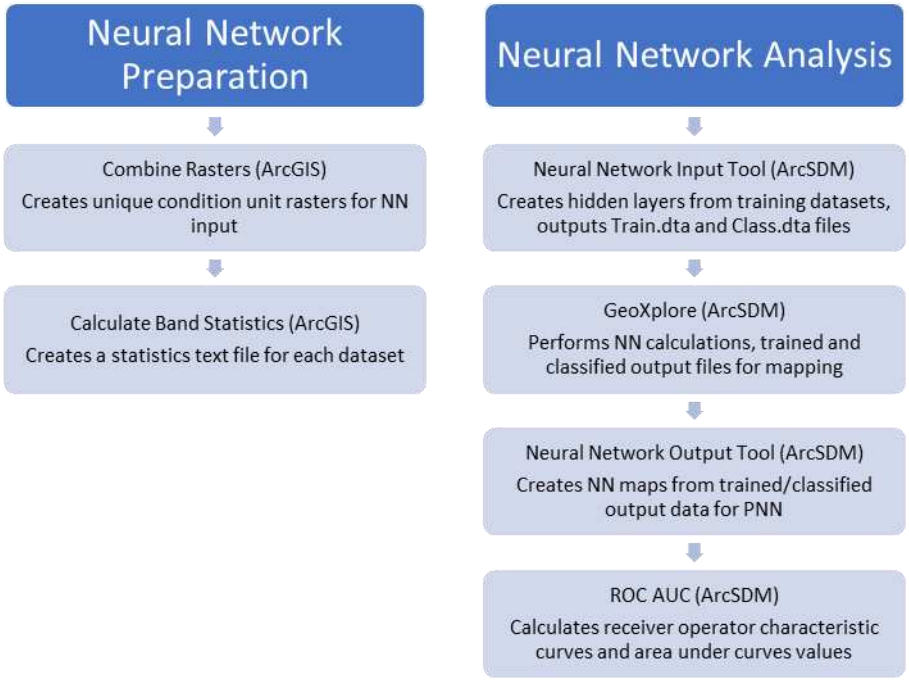

Figure 4.4. Neural network workflow in ArcSDM.

4.6 Results

4.6.1 Weighting results

Weighting calculations were completed for the 16 factor inputs to establish relative influence of the factors on the riskscapes. Most weights were coincident with landslide features. Several features were not coincident or influential with landslides and had classifications that did

not coincide with the training data, resulting in a classification of "99" or not weighted (Table 4.2). Weight tables for the riskscape models are included in Appendix H.

Table 4.2. Datasets without relevant weight classes, removed from weights of evidence and logistic regression analyses.

County	**20% training dataset**	**500 random point training dataset**	**1000 random point training dataset**
Boulder	Airports Lakes Railways Roads	Airports Faults Roads	Airport
Larimer	Airports	Airports Railways Roads	Airports Railways

4.6.2 Prior probability

The prior probability is based on the training datasets and indicates the correlation between the landslide susceptibility point training data and the factor data (factors and riskscapes). This prior probability is the probability of the occurrence within the training data, or number of training data cells/number of area cells (Hartley, 2014). Table 4.3 shows the prior probability for the landslide training datasets for the three training models.

Table 4.3. Prior probability values from training datasets.

County	20% training dataset (thinned) number of points	20% training dataset (thinned) prior probability	500 random point training dataset prior probability	1000 random point training dataset prior probability
Boulder	641	0.335	0.261	0.522
Larimer	2789	0.409	0.073	0.147

4.6.3 Weights of evidence, calculate response results

Weights of evidence (WOE) models used a Calculate Weights and Calculate Response method in ArcSDM. Calculate Response requires input rasters to weight, the weight tables, and the training dataset, and creates output maps of standard deviation, posterior probability, and confidence, or the ratio between posterior probability and the standard deviation (maps included

in Appendix G). WOE for Boulder County shows the best response with the 20% point training dataset for both ranked and human factor riskscapes with a range from 0.032 to 0.989 (ranked) and 0.015 to 0.987 (human factor). Distributions of these high probability areas reflect the geomorphic riskscape features in the ranked riskscape and the human factors riskscape urban areas (Figure 4.5).

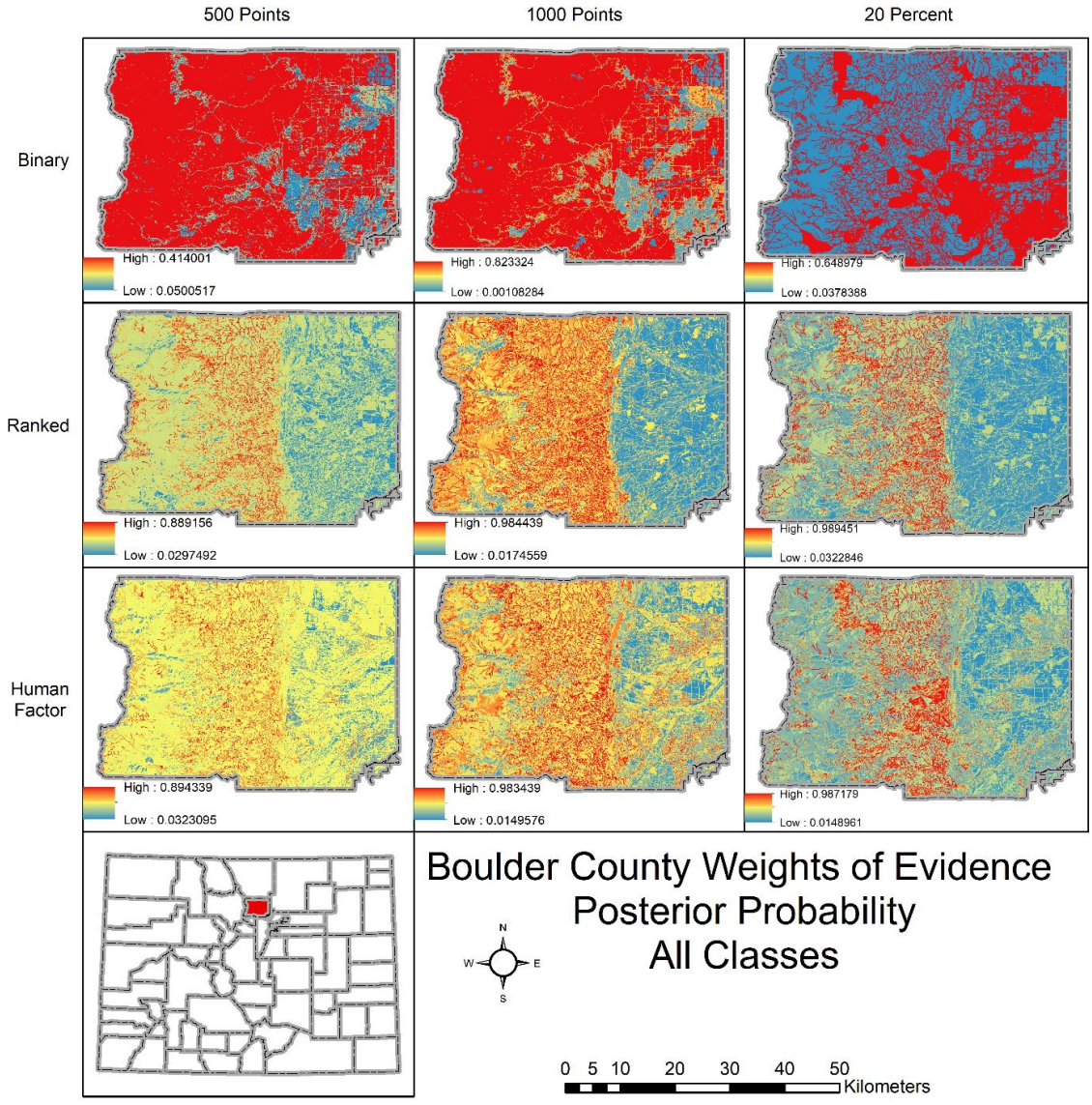

Figure 4.5. Boulder County weights of evidence posterior probability, all riskscape classes.

A subset view of the Allenspark region in Boulder County shows the intersection of the WOE posterior probability rasters (1000 training point dataset) with the WUI areas identified (Figure 4.6). WUI areas are primarily within and adjacent to the higher probability regions. The ranked riskscape shows more areas of higher probability outside of the town borders, reflecting the preferential weighting of the riskscape factors for physical features.

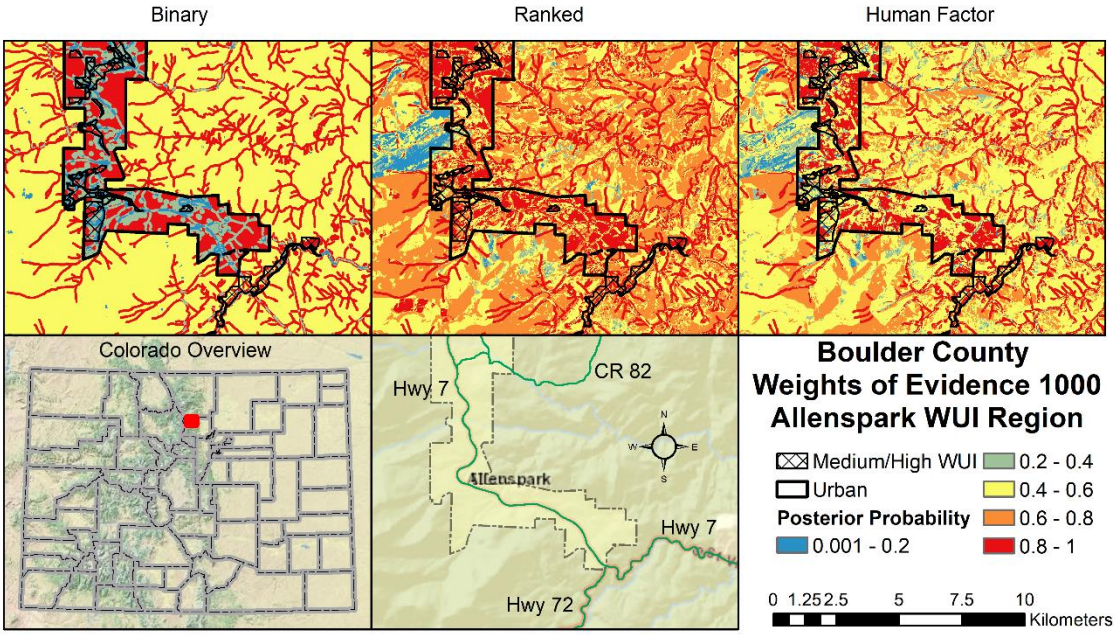

Figure 4.6. Allenspark region, Boulder County. Weights of evidence posterior probability shown with wildland urban interface areas (1000 point training dataset).

Larimer County's best performance was for the 20% training dataset, which significantly outperformed the other training datasets, and all Boulder county values. Ranked (range 0.018 to 0.997) and human factor (range 0.024 to 0.998) demonstrate values close to one, considered a very high probability for the central areas of the county, the foothills area. In the human factor maps, the urban areas are more distinctive than in the ranked models (Figure 4.7).

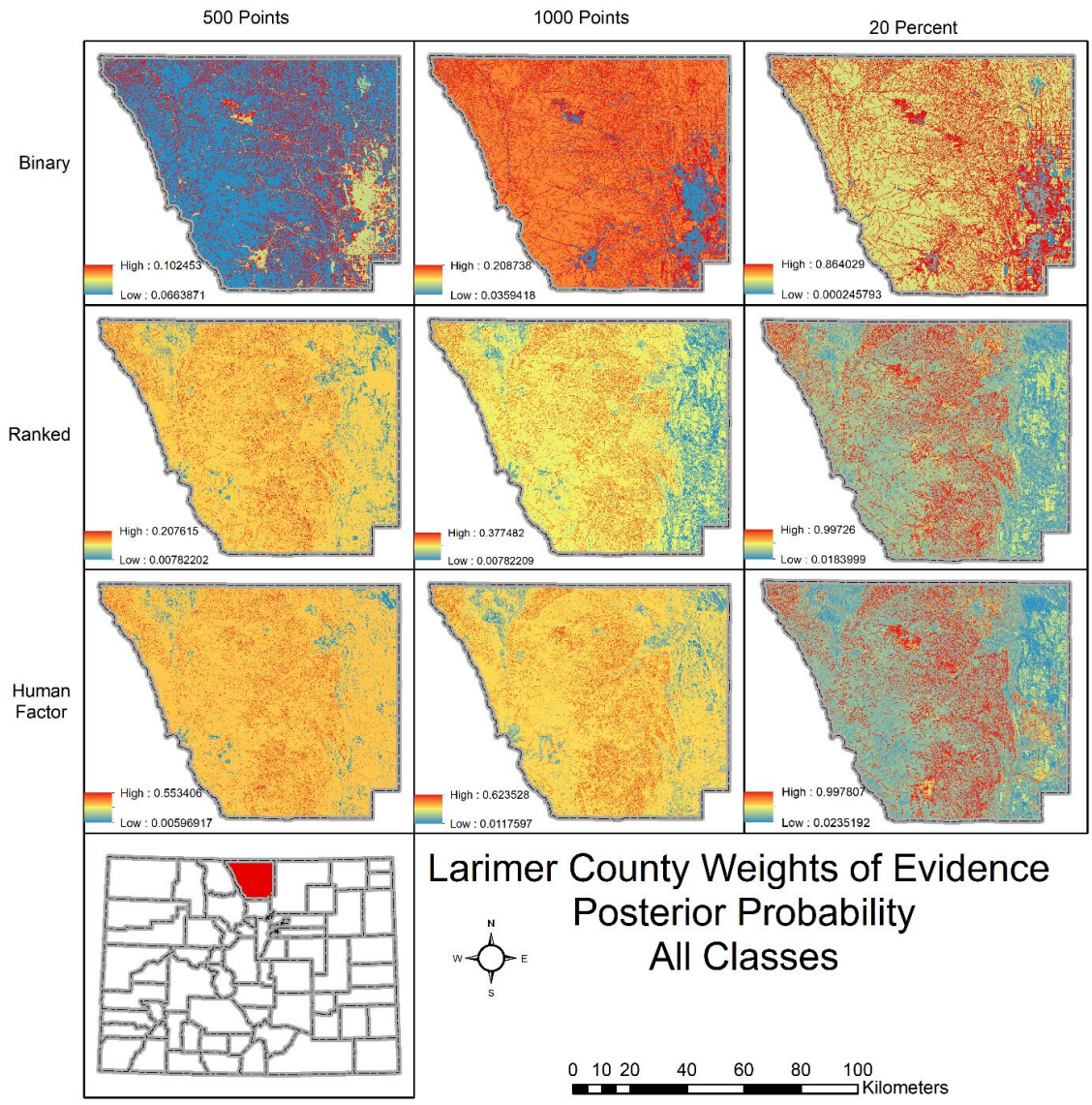

Figure 4.7. Larimer County weights of evidence posterior probability, all riskscape classes.

A subset area in Larimer County shows the WUI region of Red Feather Lakes (Figure 4.8) from the 20% training class weights of evidence posterior probability. All riskscape models demonstrate higher probability values surrounding the higher density housing areas and the transportation and hydrology network features.

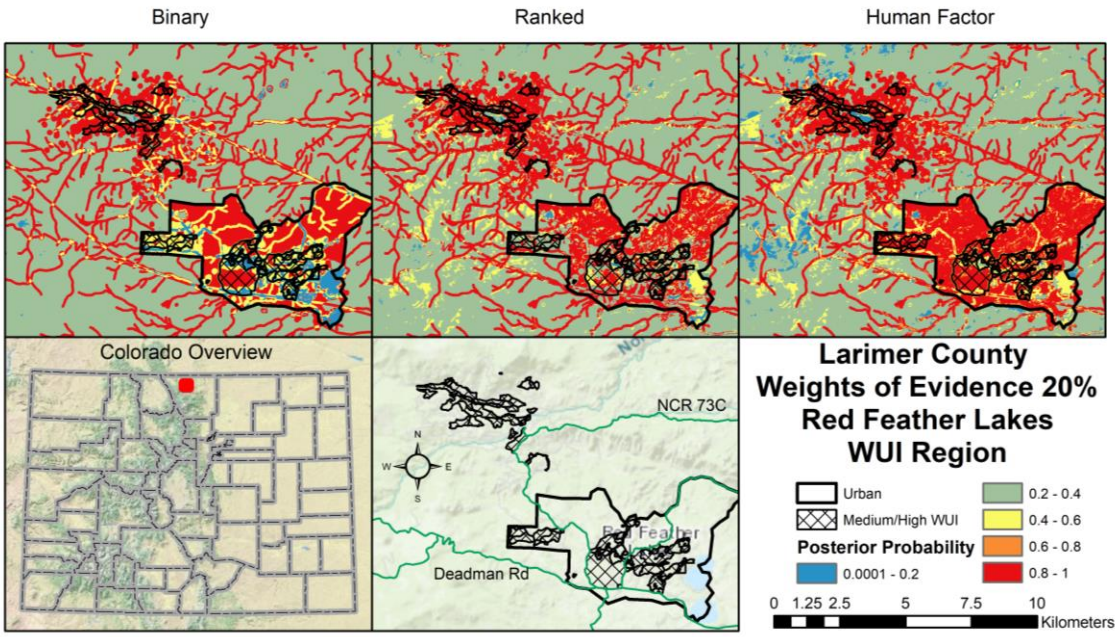

Figure 4.8. Red Feather Lakes, Larimer County. Weights of evidence posterior probability shown with wildland urban interface areas (20% point training dataset).

4.6.4 Logistic regression results

Logistic regression results show the differentiation between riskscape models. No models performed well overall, lagging behind the WOE results.

Boulder County's 1000 points training dataset outperformed both 500 points and 20% training datasets (641 points). Ranked riskscapes outperformed human factors slightly, at a high probability of 0.661 to 0.610, while binary had a high value of 0.450. The 20% dataset underperformed the 500 point training dataset, an unexpected result. This is potentially due to the random selection of training points between the landslide susceptibility cells. Urban area clustering is shown distinctly in the binary maps (500 and 1000 points) as lower values, differing form the overall trend in the human factors maps which demonstrate the urban areas as higher (Figure 4.9 A&B).

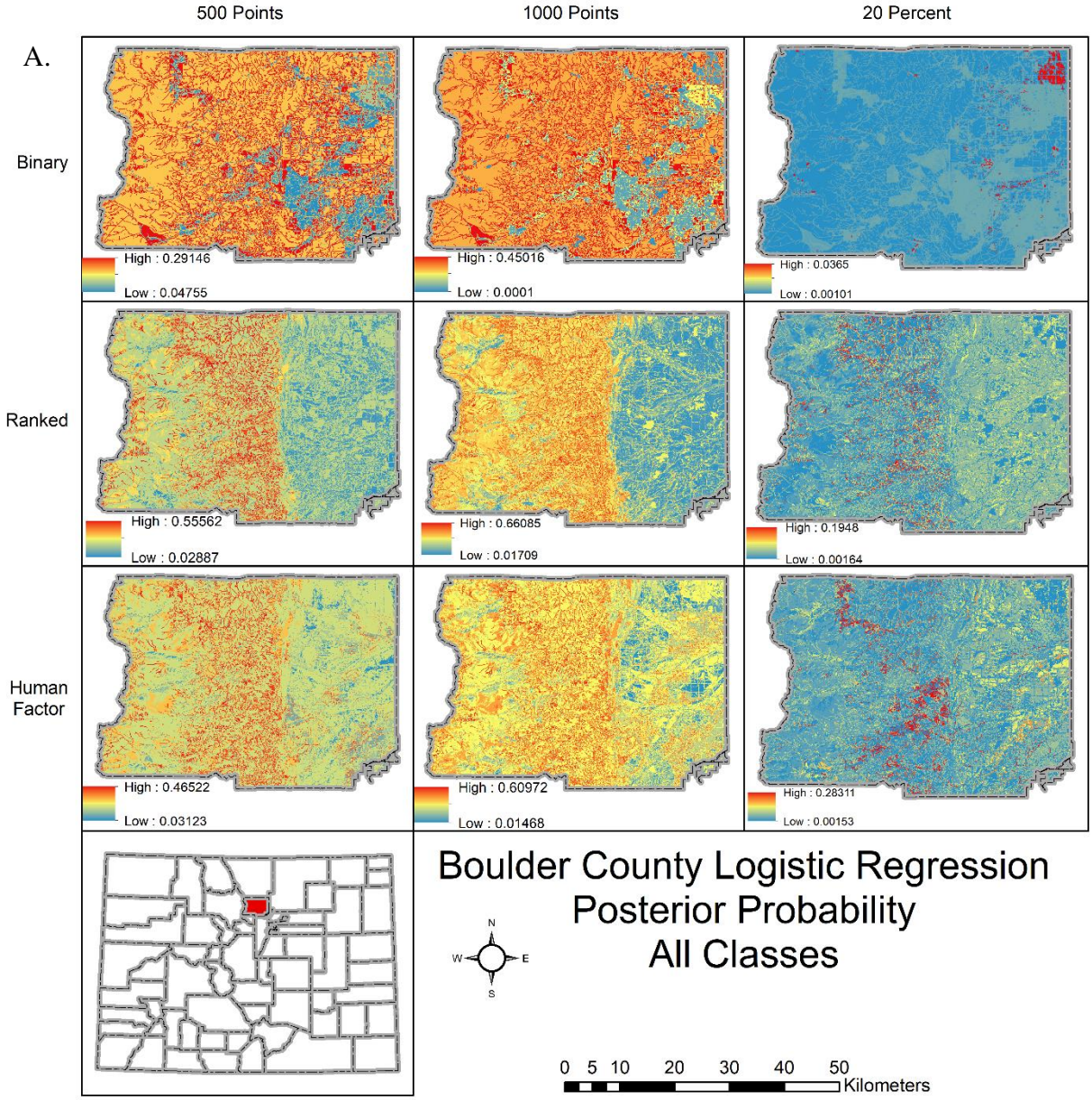
A.
500 Points
1000 Points
20 Percent
Binary
Ranked
Human Factor
High : 0.29146
Low : 0.04755
High : 0.45016
Low : 0.0001
High : 0.0365
Low : 0.00101
High : 0.55562
Low : 0.02887
High : 0.66085
Low : 0.01709
High : 0.1948
Low : 0.00164
High : 0.46522
Low : 0.03123
High : 0.60972
Low : 0.01468
High : 0.28311
Low : 0.00153
Boulder County Logistic Regression
Posterior Probability
All Classes
N
W
E
S
0 5 10 20 30 40 50
Kilometers

B.

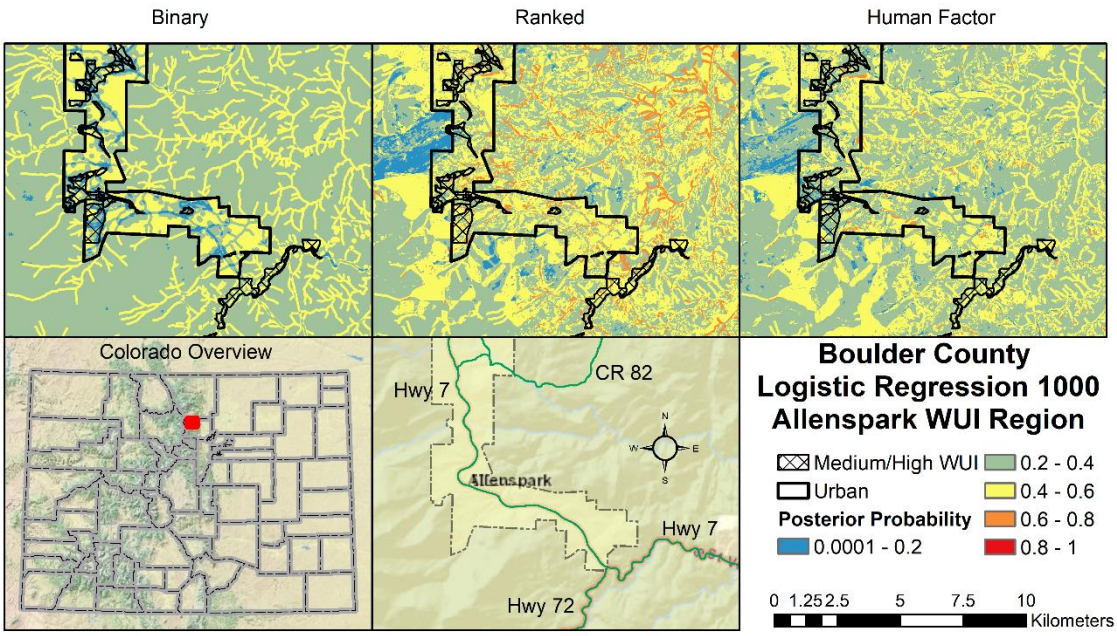

Figure 4.9. Map A: Boulder County logistic regression maps for all classes. Map B: Inset of Allenspark region (1000 point training dataset).

Larimer County logistic regression models show weaker performance (Figure 4.10 A&B). The highest values, ranked 20% and human factor 1000 points, still provided lower probability values than an acceptable range and than Boulder County results. Binary riskscapes for Larimer County ranged from 0.049 as the highest probability (20% training dataset) to 0.172 (1000 point training dataset). The ranked riskscape model's highest probability was for the 20% training dataset, with a high value of 0.348. Human factor riskscapes had a similarly high value for the 1000 point training dataset (0.384) but lower for the 20% training dataset (0.114). This may be due to the significantly larger size of the study area compared to Boulder County. The subset map of the Red Feather Lakes WUI region shows low probability values in all riskscape models, indicating the poor performance of the models.

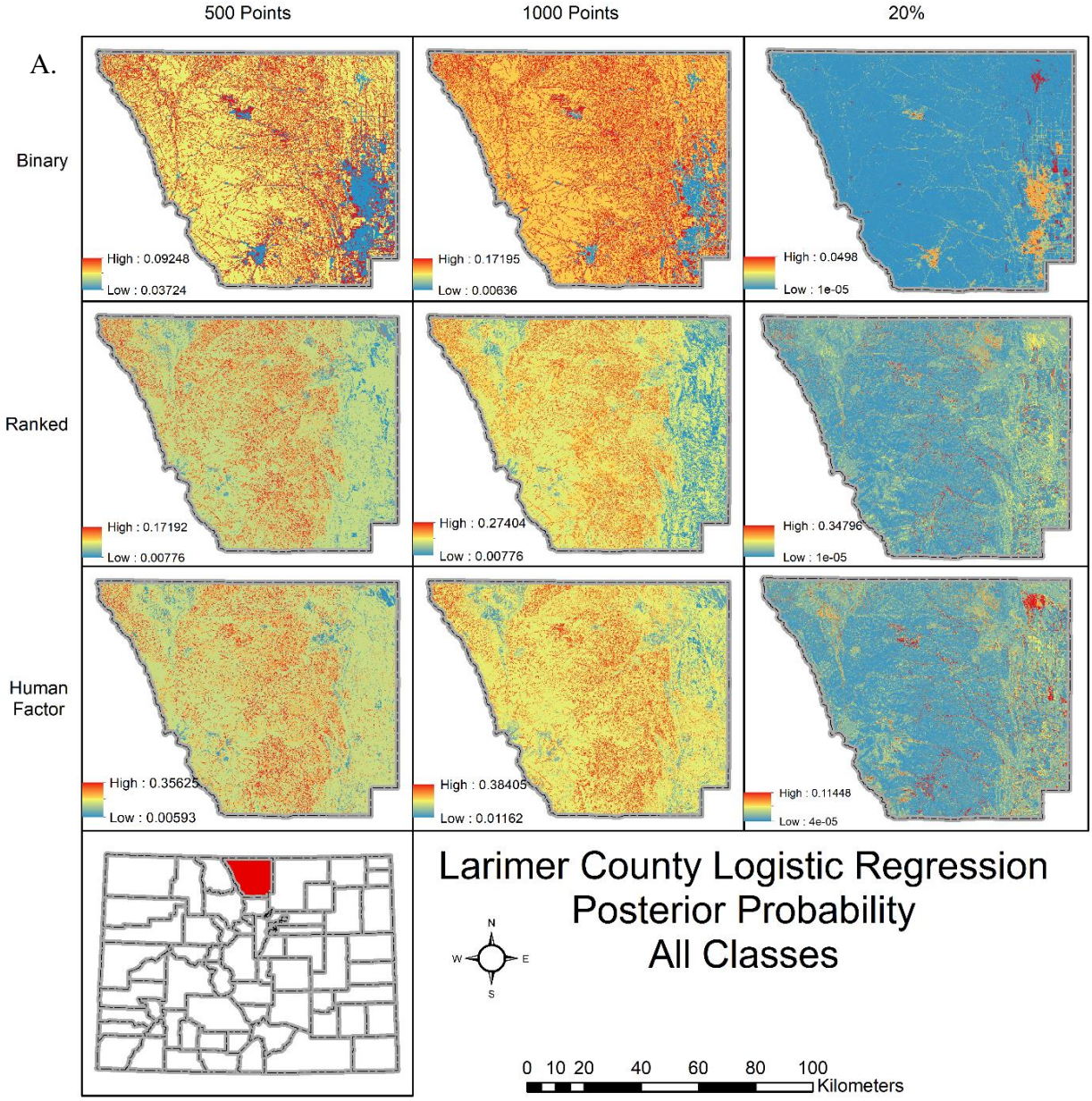
500 Points
1000 Points
20%
A.
Binary
Ranked
Human Factor
High : 0.09248
Low : 0.03724
High : 0.17195
Low : 0.00636
High : 0.0498
Low : 1e-05
High : 0.17192
Low : 0.00776
High : 0.27404
Low : 0.00776
High : 0.34796
Low : 1e-05
High : 0.35625
Low : 0.00593
High : 0.38405
Low : 0.01162
High : 0.11448
Low : 4e-05
Larimer County Logistic Regression
Posterior Probability
All Classes
N
W
E
S
0 10 20 40 60 80 100
Kilometers

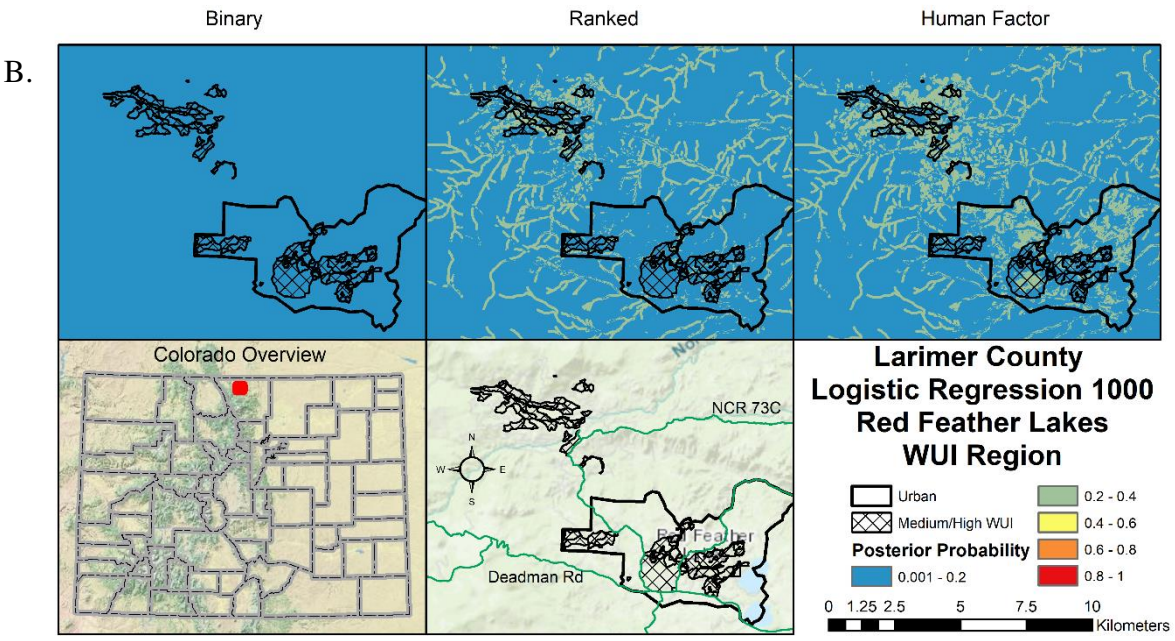

Figure 4.10. Map A: Larimer County logistic regression maps for all classes. Map B: Inset of Red Feather Lakes region (1000 point training dataset).

4.6.5 Probabilistic neural network results

Neural network approaches required the most intensive manipulations due to the configuration of the ArcSDM tools and the dependency on the GeoXplore neural network interface. Probabilistic neural network values showed distributions with greater ranges in ranked and human factor riskscapes. Probabilistic neural networks show strong alignment with riskscape outputs for the ranked and human factor values. Binary riskscapes in general ranked highly but do not have much diversity in the cell values (Figure 4.11 A&B). Ranked riskscapes show significant diversity with concentrations of high values surrounded with primarily low values, particularly demonstrated in the 20% training dataset ranked classification. Human factor riskscapes show lower probability clustering in mountainous region urban areas, exhibiting lower values than the surrounding Front Range foothills and the Plains regions. The subset maps for the

Allenspark WUI region how lower probabilities within the urban boundaries, especially in the human factor model.

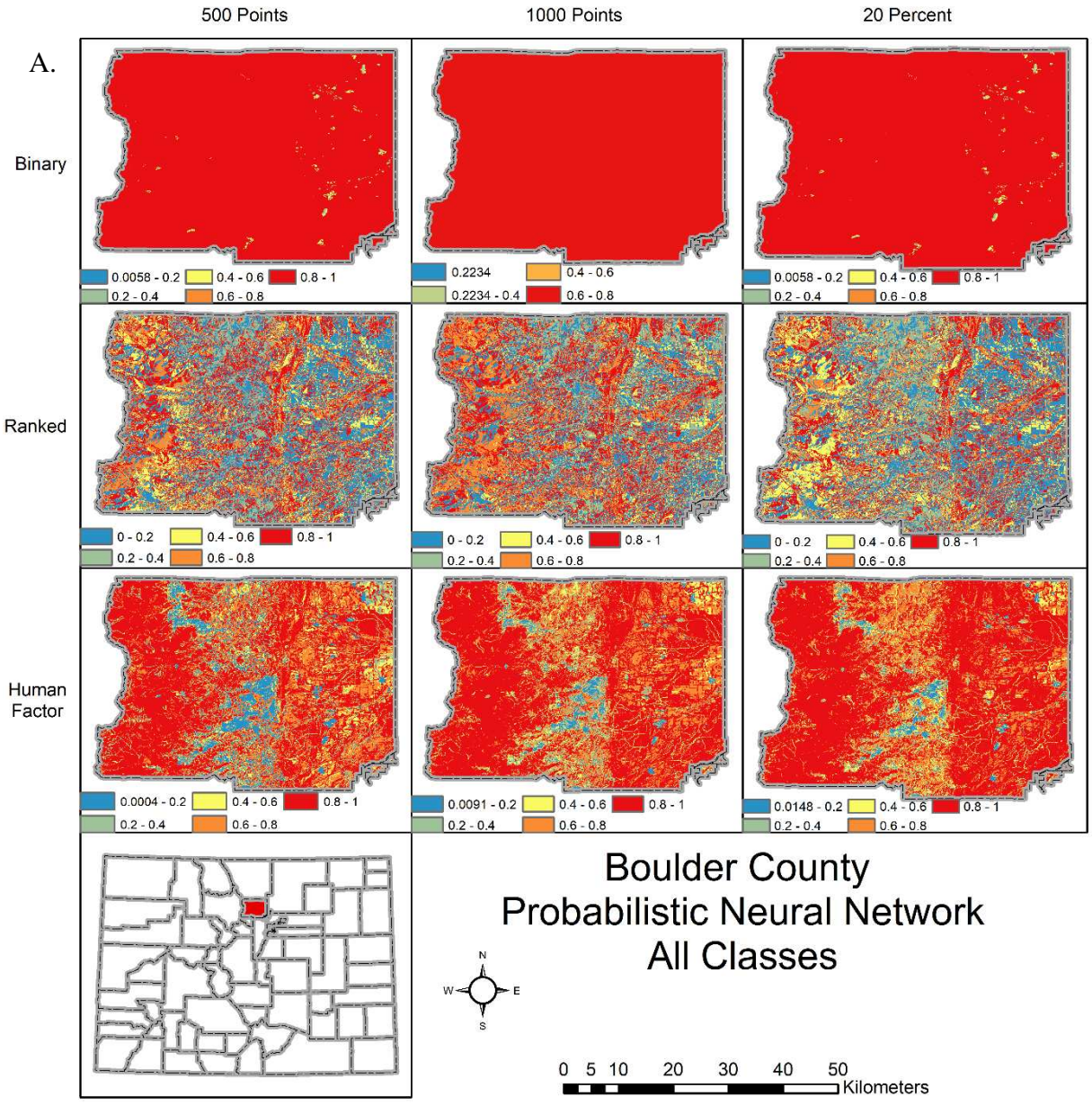

B.

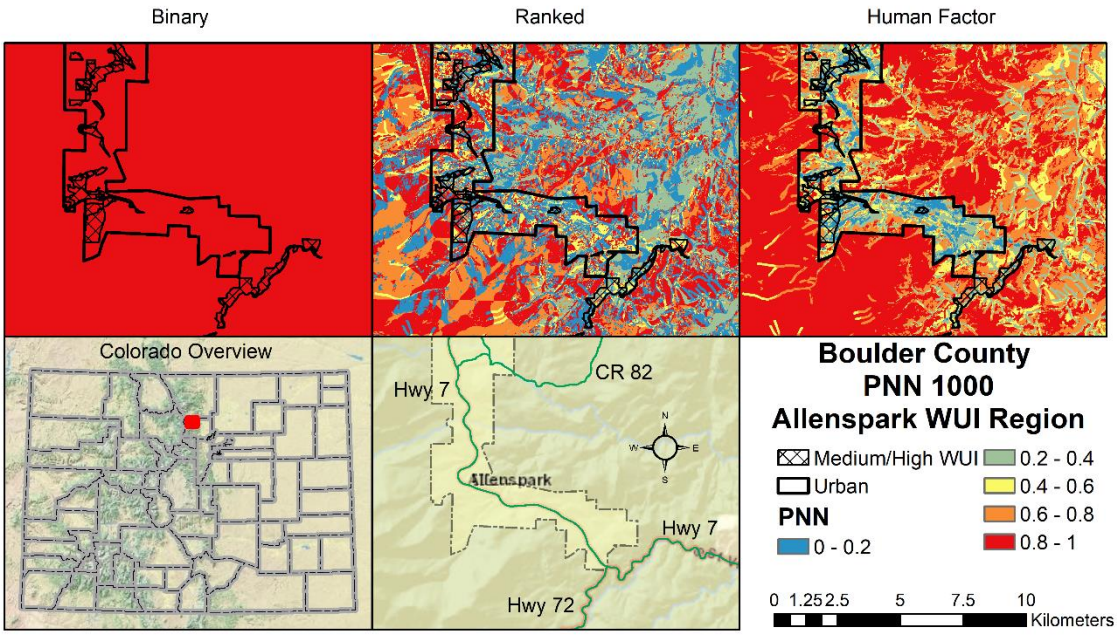

Figure 4.11. Boulder County probabilistic neural networks for all training classes. Higher values (red) indicate higher probabilities. Map B shows the Allenspark region with WUI medium and high area classifications (1000 point training dataset).

Larimer County exhibited similar trends to Boulder County. Overall, most of the region was classified as high value for prediction (red, Figure 4.12 A&B). In the binary models, most of the region is in the high range with a few lower areas that correspond to water features. Ranked riskscape models show the most diversity, with very low values on the eastern plains section. This may be due to the lack of training points in the area as there are no landslide susceptibility training cells in the region. Human factor riskscapes presented predominantly high values with smaller areas of low prediction. These low points align with urban areas and water features, surprising for the human factor model shown in in Figures 4.13 and 4.14.

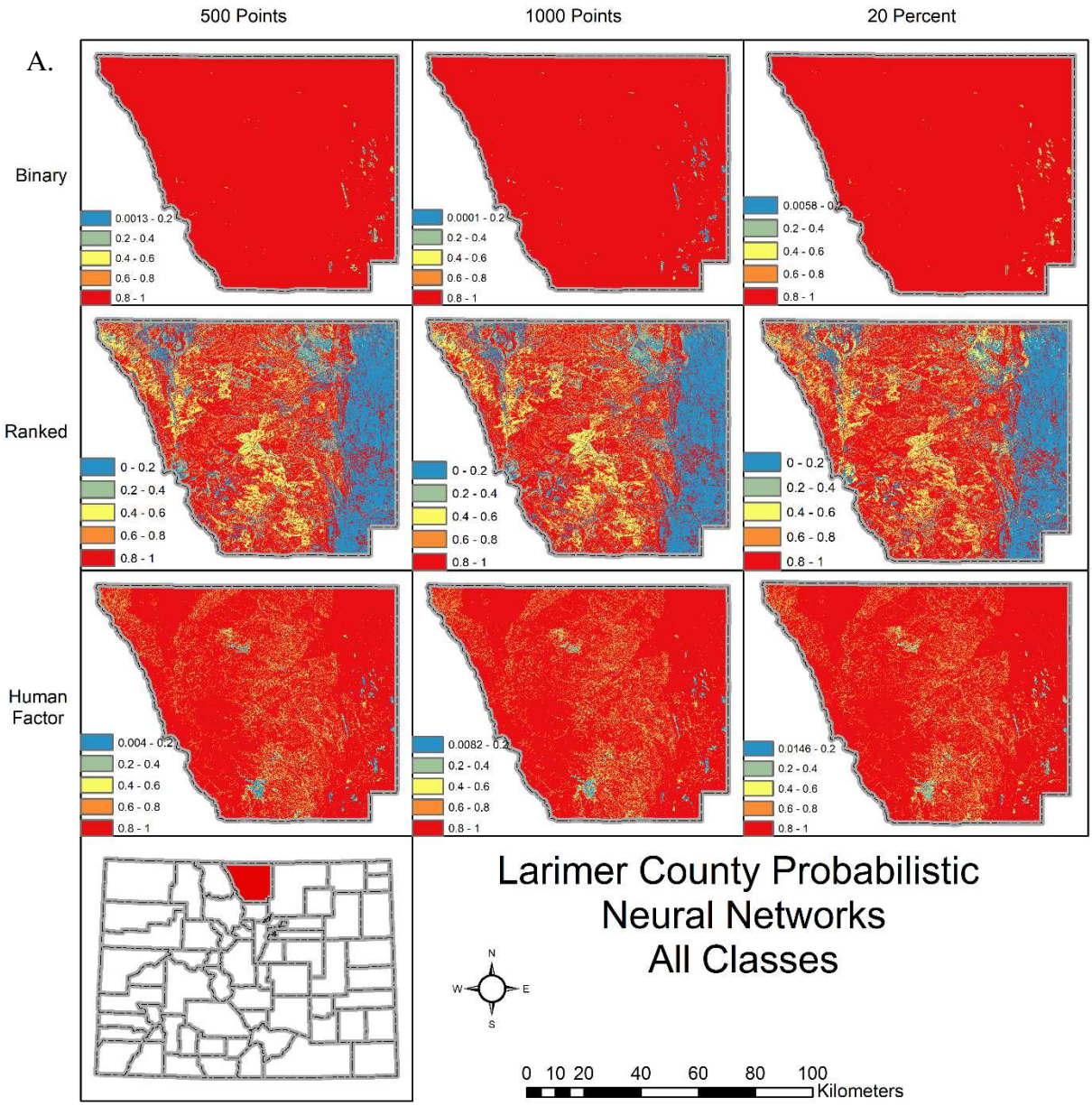
A.
500 Points
1000 Points
20 Percent
Binary
Ranked
Human Factor
0.0013 - 0.2
0.0001 - 0.2
0.0058 - 0.2
0 - 0.2
0.004 - 0.2
0.0082 - 0.2
0.0146 - 0.2
0.2 - 0.4
0.4 - 0.6
0.6 - 0.8
0.8 - 1
Larimer County Probabilistic
Neural Networks
All Classes
N
W
E
S
0 10 20 40 60 80 100
Kilometers

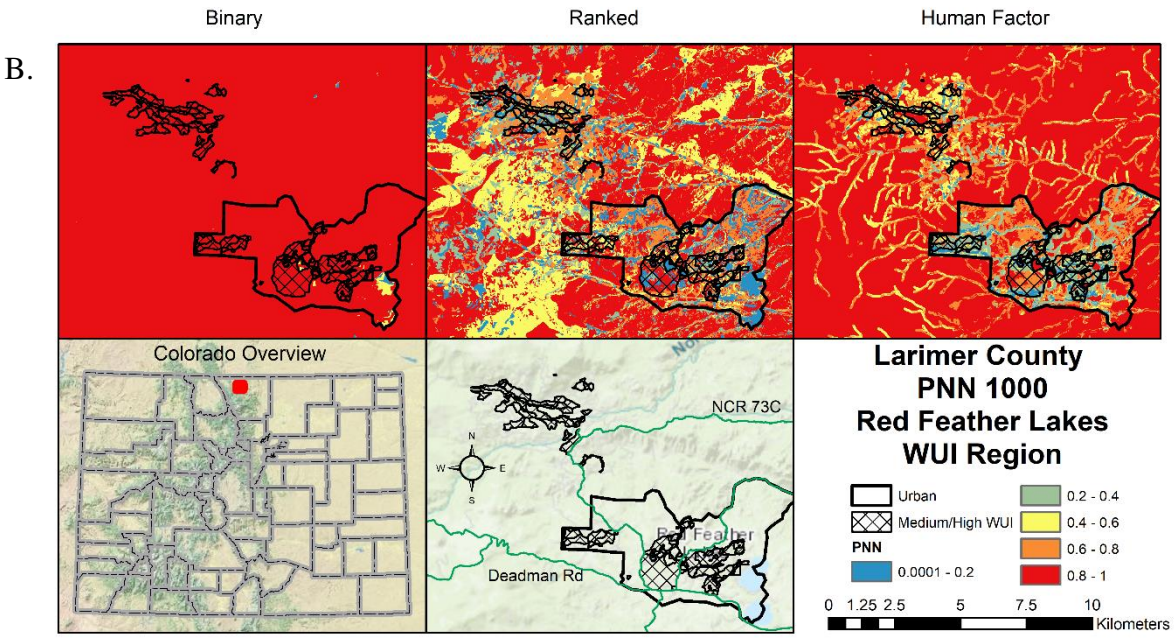

Figure 4.12. Larimer County probabilistic neural networks for all training classes. Higher values (red) indicate higher probabilities. Map B shows the Red Feather Lakes region with WUI medium and high area classifications (1000 point training dataset).

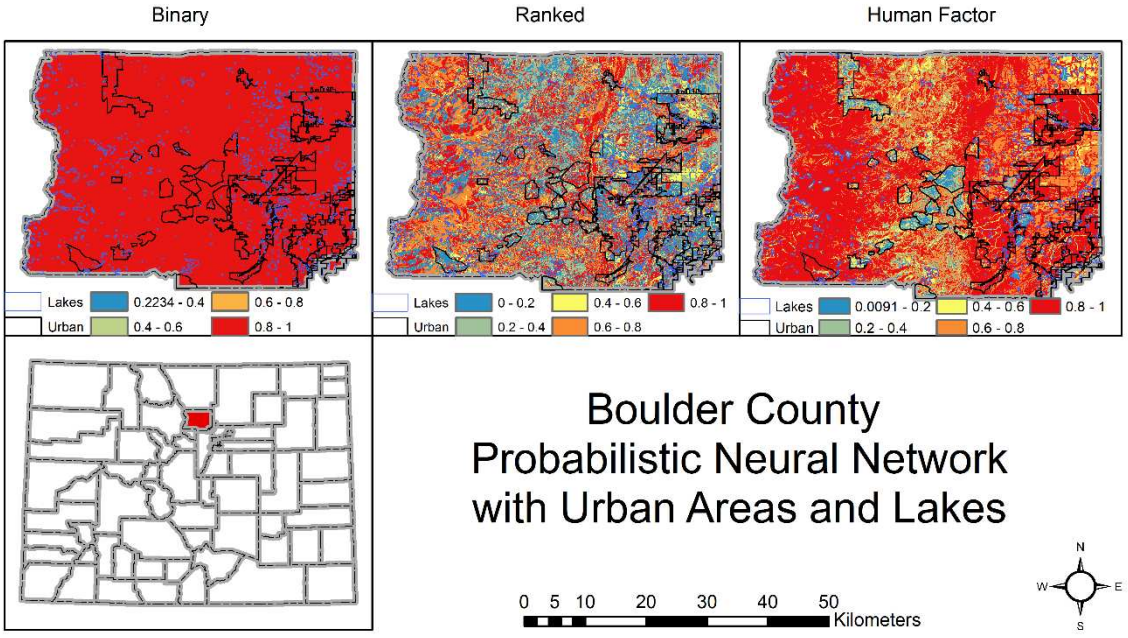

Figure 4.13. Boulder County PNN showing the coincidence of lower PNN values with lake and urban features highlighted (1000 point dataset example).

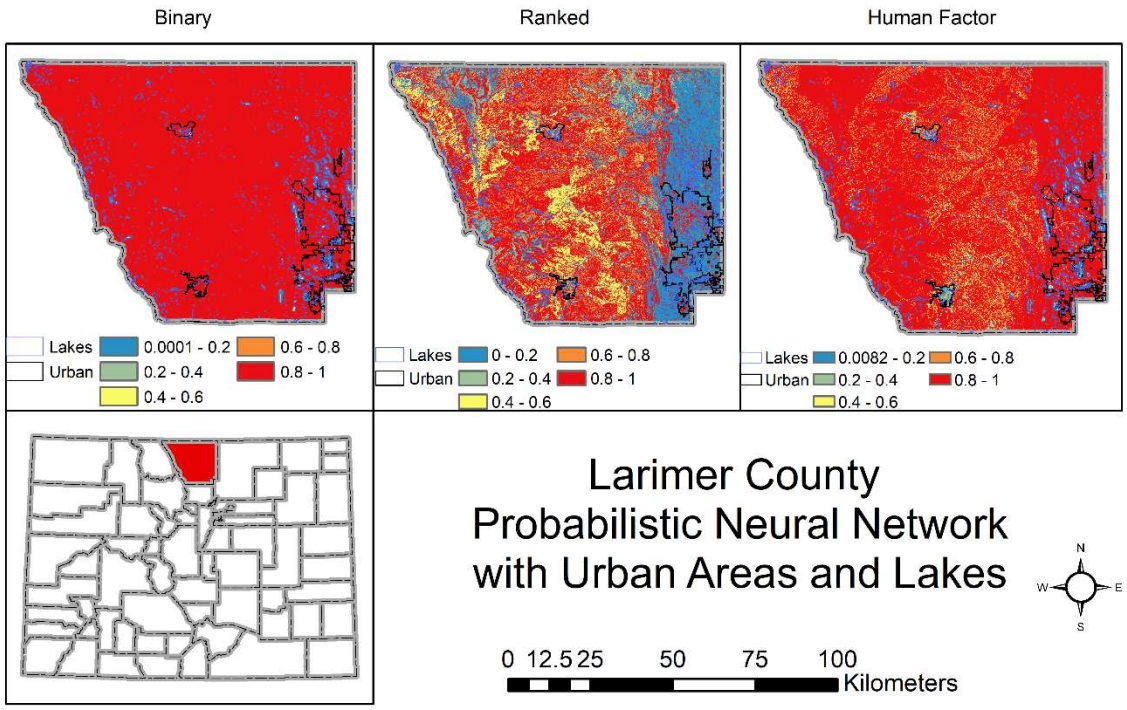

Figure 4.14. Larimer County PNN showing the coincidence of lower PNN values with lake and urban features highlighted (1000 point dataset example).

4.6.6 Validation tests

Receiver operating characteristic (ROC) curve and area under the curve (AUC) calculations were performed in ArcSDM to determine the accuracy performance of the probability tests for logistic regression and weights of evidence. These validation methods plot true positives against false positives (matrix includes true negatives and false negatives) based on known points of known locations of landslide susceptibility (landslide training points) and known locations without landslides (non-deposit training points). Values of 1 (the upper limit of the Y axis) indicate the prevalence of true positives, or a correct prediction (100%) in the model; values of 0 (the lower limit of the Y axis) indicate the reverse, where the model perfectly predicts the opposite values (e.g., true positives are listed as false positives, or 0%). Values of 0.5 indicate randomness, and the test is unable to validate the model (Nykänen et al., 2015). The larger the

area under the curve, the more significant the positive predictive power of the model (Piacentini et al., 2012), while values near the 0.5 threshold show that the model is not able to predict the output based on the training datasets. Posterior probability raster results were processed based on these training dataset inputs to test the validity of the probability outputs.

Results for Boulder County show consistently high values ranging from 0.696 to 0.797 for weights of evidence, aligning with the overall good performance of the weights of evidence models. Logistic regression also performed as a positive correlation (positive values predicted as positive), though the lowest value of 0.563 (human factor, 20%) indicates a low threshold value, close to random. Figure 4.15 shows the AUC values for the Boulder County riskscape models. The values results are shown in Table 4.4.

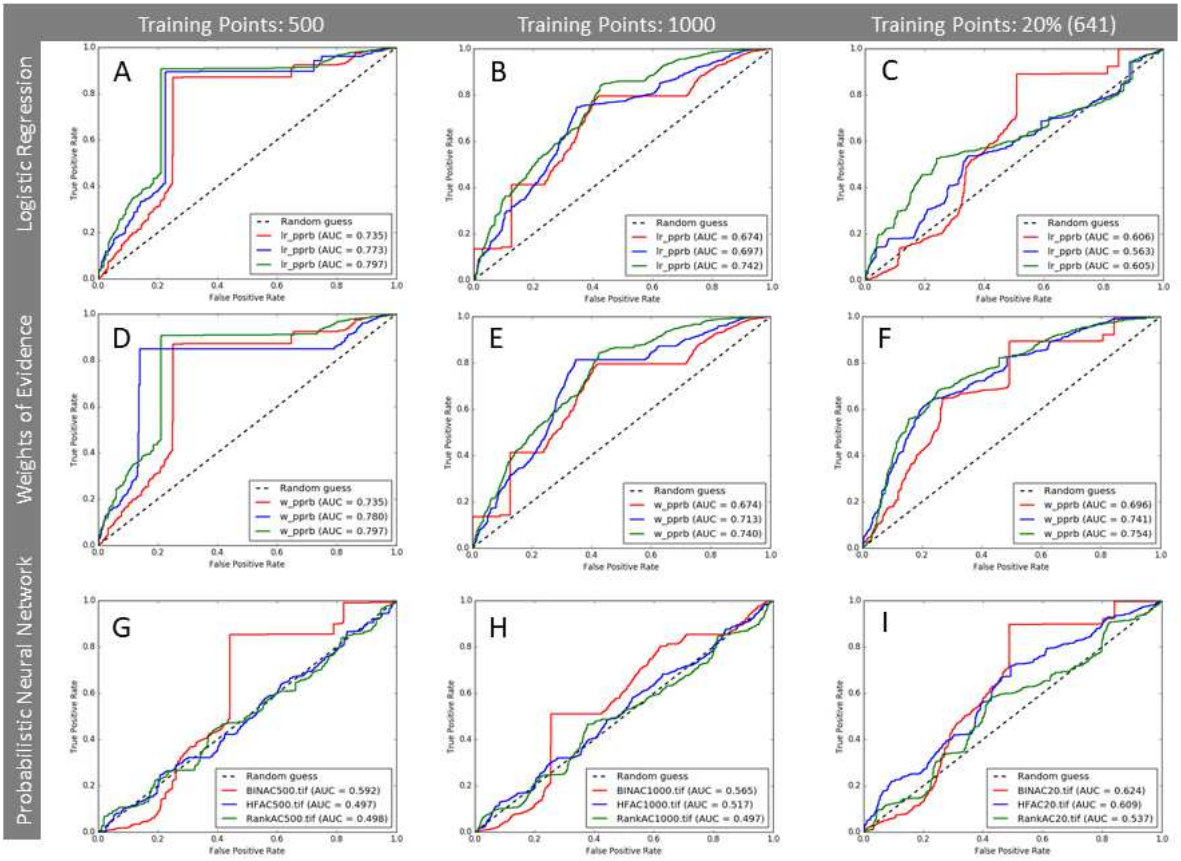

Figure 4.15. Boulder County AUC values. Red is binary riskscape, blue is human factor riskscape, and green is ranked riskscape values.

Probabilistic neural networks indicated overall poor performance for the model validation. The 500 and 1000 training point models for human factor and ranked riskscape are close to the random threshold of 0.5, indicating that these PNN models were not significant in predicting riskscapes. The binary dataset had the highest performance of the PNN riskscape validation models. This may indicate that fewer classes allowed for better validation of the model.

The lower probability ranges demonstrate dips under the random threshold line, indicating that the models are predicting the opposite of the values. These random guess threshold values are larger for the binary riskscape model, but the areas of the human riskscape model that are below the threshold line indicate the lower probability values in the urban areas (blue) in Figure 4.11. Ranked PNN in Boulder County shows a mottled pattern, demonstrating the model's inability to detect riskscape patterns.

Table 4.4. Receiver Operating Characteristic Area Under the Curve (ROC-AUC) values for Boulder County riskscapes. Values shown in red range from 0.4 – 0.6, within 0.1 of the random guess threshold of 0.5.

ARCSDM	County	Riskscape	Training Points	AUC VALUE
Logistic Regression	Boulder	Binary	500	0.735
Logistic Regression	Boulder	Binary	1000	0.674
Logistic Regression	Boulder	Binary	20%	0.606
Weights of Evidence	Boulder	Binary	500	0.735
Weights of Evidence	Boulder	Binary	1000	0.674
Weights of Evidence	Boulder	Binary	20%	0.696
Probabilistic Neural Network	Boulder	Binary	500	0.592
Probabilistic Neural Network	Boulder	Binary	1000	0.565
Probabilistic Neural Network	Boulder	Binary	20%	0.624
Logistic Regression	Boulder	Ranked	500	0.797
Logistic Regression	Boulder	Ranked	1000	0.742
Logistic Regression	Boulder	Ranked	20%	0.605
Weights of Evidence	Boulder	Ranked	500	0.797
Weights of Evidence	Boulder	Ranked	1000	0.74
Weights of Evidence	Boulder	Ranked	20%	0.754

Probabilistic Neural Network	Boulder	Ranked	500	0.498
Probabilistic Neural Network	Boulder	Ranked	1000	0.497
Probabilistic Neural Network	Boulder	Ranked	20%	0.537
Logistic Regression	Boulder	Human Factor	500	0.773
Logistic Regression	Boulder	Human Factor	1000	0.697
Logistic Regression	Boulder	Human Factor	20%	0.563
Weights of Evidence	Boulder	Human Factor	500	0.78
Weights of Evidence	Boulder	Human Factor	1000	0.713
Weights of Evidence	Boulder	Human Factor	20%	0.741
Probabilistic Neural Network	Boulder	Human Factor	500	0.497
Probabilistic Neural Network	Boulder	Human Factor	1000	0.517
Probabilistic Neural Network	Boulder	Human Factor	20%	0.609

ROC-AUC results for Larimer County show different results than Boulder County. Overall, ranked, and human factor riskscapes show higher ROC-AUC values (Figure 4.16). Both weights of evidence and logistic regression for binary riskscapes show lower values, though logistic regression shows higher values than weights of evidence in this case. All values for weights of evidence and logistic regression exceeded the 0.5 randomness threshold. Probabilistic neural networks overall had a poor performance similar to the Boulder County results. The PNN values had larger dips under the 0.5 random guess threshold for ranked and human factor riskscape models. These reversed predictions for areas of lower probability align with the lower probability areas in the maps in Figure 4.12 and 4.14. This may explain the human factor PNN results showing lower probability in urban areas. Binary PNN performed better than ranked and human factor riskscapes with higher AUC values, again indicating that fewer classes may have an influence on the overall model validation.

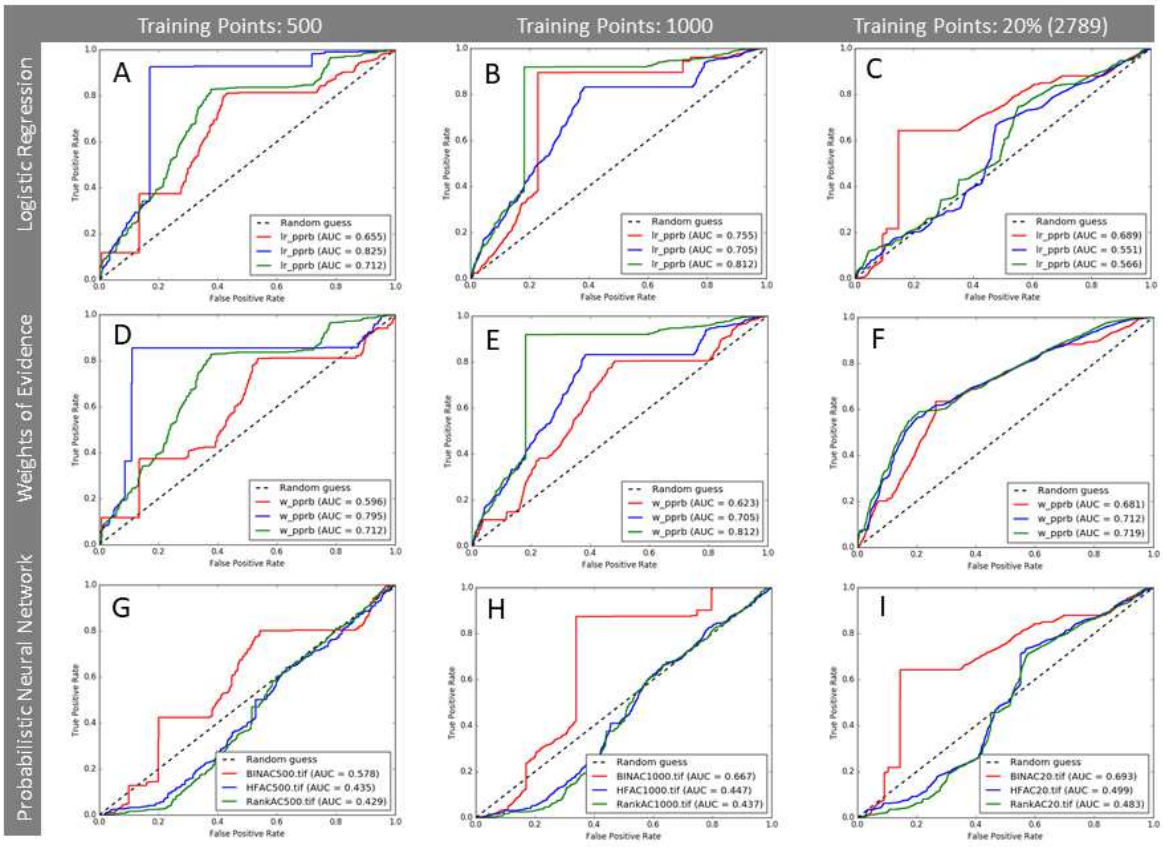

Figure 4.16. Larimer County AUC values. Red is binary riskscape, blue is human factor riskscape, and green is ranked riskscape values.

The low values for the human factor riskscape logistic regression align with the overall poor performance of logistic regression in the probability models. Human factor ROC-AUC values in this case may be lower due to the human factor model weighting human factors highly, and not the features that drive the generation of landslides. A geomorphic risk model may perform better than a riskscape model for these analyses. Notably however, the training datasets with fewer points (500 points) improved the human factor riskscape logistic regression results significantly. This is likely due to the fewer datasets and fewer non-deposit training sets allowing the model to not be as restricted to the landslide features. The values results are shown in Table 4.5.

Table 4.5. Receiver Operating Characteristic Area Under the Curve (ROC-AUC) values for Larimer County riskscapes. Values shown in red range from 0.4 – 0.6, within 0.1 of the random guess threshold of 0.5.

ARCSDM Analysis	County	Riskscape	Training Points	AUC VALUE
Logistic Regression	Larimer	Binary	500	0.655
Logistic Regression	Larimer	Binary	1000	0.755
Logistic Regression	Larimer	Binary	20%	0.689
Weights of Evidence	Larimer	Binary	500	0.596
Weights of Evidence	Larimer	Binary	1000	0.623
Weights of Evidence	Larimer	Binary	20%	0.681
Probabilistic Neural Network	Larimer	Binary	500	0.578
Probabilistic Neural Network	Larimer	Binary	1000	0.667
Probabilistic Neural Network	Larimer	Binary	20%	0.693
Logistic Regression	Larimer	Ranked	500	0.712
Logistic Regression	Larimer	Ranked	1000	0.812
Logistic Regression	Larimer	Ranked	20%	0.566
Weights of Evidence	Larimer	Ranked	500	0.712
Weights of Evidence	Larimer	Ranked	1000	0.812
Weights of Evidence	Larimer	Ranked	20%	0.719
Probabilistic Neural Network	Larimer	Ranked	500	0.429
Probabilistic Neural Network	Larimer	Ranked	1000	0.437
Probabilistic Neural Network	Larimer	Ranked	20%	0.483
Logistic Regression	Larimer	Human Factor	500	0.825
Logistic Regression	Larimer	Human Factor	1000	0.705
Logistic Regression	Larimer	Human Factor	20%	0.551
Weights of Evidence	Larimer	Human Factor	500	0.795
Weights of Evidence	Larimer	Human Factor	1000	0.705
Weights of Evidence	Larimer	Human Factor	20%	0.712
Probabilistic Neural Network	Larimer	Human Factor	500	0.435
Probabilistic Neural Network	Larimer	Human Factor	1000	0.447
Probabilistic Neural Network	Larimer	Human Factor	20%	0.499

4.7 Discussion

The weights of evidence methods demonstrated significant improvement over the logistic regression and PNN results, showing higher average AUC values for all riskscape models except the Larimer County binary riskscape logistic regression (average 0.699 compared to WOE average 0.633), shown in Table 4.6. Neural networks had intermittent success, given the restrictions on study area size and calculations. PNN did show overall higher probability mapping in both study areas but validation of the models presented as poor performance, with the AUC values close to the 0.5 threshold for random performance, and in some cases below the random guess threshold line, indicating the inverse model output. This indicates that the model did not perform well. Logistic regression results were weak for probability, but showed stronger validation AUC values, indicating that the model was more accurate.

Table 4.6. Riskscape Area Under the Curve model averages (all training datasets).

County	Riskscape	LR AUC Average	WOE AUC Average	PNN AUC Average
Boulder				
	Binary	0.671	0.701	0.593
	Ranked	0.721	0.763	0.510
	Human Factor	0.677	0.744	0.541
Larimer				
	Binary	0.699	0.633	0.646
	Ranked	0.696	0.747	0.449
	Human Factor	0.693	0.737	0.460

Riskscape processes provided an analytical framework that mitigated several challenges within the ArcSDM environment. Riskscape rasters were assembled from landslide environmental and social risk factors (listed in Table 4.1) which circumvented several of the data limitation restrictions within ArcSDM regarding number of unique condition units and processing limits. Attempts to apply all 16 riskscape factors within logistic regression failed for

the larger training datasets. Reducing the number of factors by removing those with non-influential weight classes (Table 4.2) also failed. Neural network tool requirements and limitations also were unable to process larger dataset combinations.

In data-driven models, training datasets influence the outcomes of the analyses. The randomized training point generation process will yield different results by generating different point locations each time a training dataset is created. This randomized dataset will change how prior probabilities are calculated, leading to different analytical outputs for the posterior probability mapping rasters. Using three different training datasets, the larger datasets demonstrated higher probabilities, as they are closer to the modeled riskscapes.

Findings on the applications of ArcSDM revealed that coding errors needed to be addressed frequently. Limitations in the original source code required knowledge of python coding and the ability to make changes to scripts from the open-source repository. Compiled code errors were unable to be addressed successfully, resulting in limitations in the logistic regression tool's ability to complete analyses of multiple factor inputs for the larger training datasets. Processing methods within riskscape models presented in ArcSDM require multiple applications and steps to complete for neural network analysis. ArcSDM neural network tools also are not fully contained in the ArcSDM platform and require the GeoXplore Visual C++ tool to generate the output files. Code enhancements and new releases of toolsets by the current application stewards, the Geological Survey of Finland, have provided a more robust platform. However, open-source applications do not have support and are dependent on the user community to resolve performance issues. Some tools experience performance issues running in different versions of ArcMap and ArcGIS Pro as these code updates occur.

Restrictions in cell values and number of unique condition units required data preprocessing and changing scales of datasets. Combining datasets during preprocessing can create files with unique condition units that exceed the threshold in ArcSDM. Using a riskscape model input raster eliminated this issue.

4.8 Conclusions

Riskscape models for landslides can improve our understanding of human-environment interactions. Geostatistical tools are commonly applied in landslide studies, for hazard assessments, risk assessments, and susceptibility modeling (Guzzetti, 2006). ArcSDM's origins in geologic applications can support riskscape studies, based on natural hazard datasets. Within the GIS platform, the spatial components are addressed through analytical methods, and geoprocessing geostatistical tools which evaluate these parameters not just by value but also over their spatial extent and are represented in map form.

Weights of evidence outperformed both neural networks and logistic regression and had high correlation with riskscape values for both Boulder and Larimer Counties. Overall, logistic regression had limited application, with poor response to the riskscape inputs and difficulty in completing multiple factor analysis. The supervised probabilistic neural networks performed well for probability with strong correlation to riskscape values but demonstrate lower AUC values.

Geostatistical models appear to have limited applicability in furthering our understanding of landslide riskscapes. Riskscapes as an inductively developed weighted overlay compiling factor datasets inclusive of physical and social parameters of landslide inform the spatialized risk in the study areas. These models perform inconsistently when geostatistical models used in landslide susceptibility studies are applied. Based on the results from this study, weights of

evidence models can be used to support the understanding of spatial risk based on landslide riskscapes. Logistic regression and probabilistic neural networks are not appropriate tools given their poor validation and overall poor probability performance for logistic regression. These tools are appropriate for geostatistical analysis outside of the riskscape components. Spatial models in ArcSDM present options for determining spatial statistical characteristics, however, construction of input datasets should consider the parameter restrictions.

Responses suggest that understanding the strength of the spatial relationships between datasets are important regarding the uniqueness of geostatistical approaches. Spatial distributions of acceptable landslide riskscape values may support enhanced public safety, mitigation, and planning efforts by demonstrating regions with more accurate data class values. Areas with lower accuracy may be identified to support additional study and potentially resource allocation measures.

References

Aditian, A., Kubota, T., & Shinohara, Y. (2018). Comparison of GIS-based landslide susceptibility models using frequency ratio, logistic regression, and artificial neural network in a tertiary region of Ambon, Indonesia. *Geomorphology*, *318*, 101-111. https://doi.org/10.1016/j.geomorph.2018.06.006

Agterberg, F. P., Bonham-Carter, G. F., Cheng, Q., & Wright, D. F. (1993). Weights of Evidence Modeling and Weighted Logistic Regression for Mineral Potential Mapping*. In J. C. Davis & U. C. Herzfeld (Eds.), *Computers in Geology, 25 Years of Progress* (pp. 13-32). Oxford University Press.

Agterberg, F. P., Bonham-Carter, G. F., & Wright, D. F. (1990). Statistical Pattern Integration for Mineral Exploration. In G. Gaal & D. F. Merriam (Eds.), *Computer Applications in Resource Estimation: Prediction and Assessment for Metals and Petroleum* (pp. 1-21). Elsevier Ltd. https://doi.org/10.1016/B978-0-08-037245-7.50006-8

Akgun, A. (2012). A comparison of landslide susceptibility maps produced by logistic regression, multi-criteria decision, and likelihood ratio methods: a case study at İzmir, Turkey. *Landslides*, *9*(1), 93-106. https://doi.org/10.1007/s10346-011-0283-7

Althuwaynee, O. F., Pradhan, B., & Ahmad, N. (2014). Landslide susceptibility mapping using decision-tree based chi-squared automatic interaction detection (CHAID) and logistic regression (LR) integration. *IOP Conference Series. Earth and Environmental Science*, *20*(1), @Paperno.012032-@Paperno.012032. https://doi.org/10.1088/1755-1315/20/1/012032

Ayalew, L., & Yamagishi, H. (2005). The application of GIS-based logistic regression for landslide susceptibility mapping in the Kakuda-Yahiko Mountains, central Japan. *Geomorphology*, *65*(1-2), 15-31. https://doi.org/10.1016/j.geomorph.2004.06.010

Bai, S., Lu, G., Wang, J., Zhou, P., & Ding, L. (2011). GIS-based rare events logistic regression for landslide-susceptibility mapping of Lianyungang, China. *Environmental Earth Sciences*, *62*(1), 139-149. https://doi.org/10.1007/s12665-010-0509-3

Bell, R., & Glade, T. (2004). Quantitative risk analysis for landslides - Examples from Bildudalur, NW-Iceland. *Natural Hazards and Earth Science Systems*, *4*, 14.

Borgogno Mondino, E., Giardino, M., & Perotti, L. (2009). A neural network method for analysis of hyperspectral imagery with application to the Cassas Landslide (Susa Valley, NW Italy). *Geomorphology*, *110*(1-2), 20-27. https://doi.org/10.1016/j.geomorph.2008.12.023

Bureau, U. D. o. C. U. C. (2019). *Population Estimates* [US Census Bureau population database]. https://www.census.gov/quickfacts/fact/table/larimercountycolorado,bouldercountycolorado,US/PST045219

Catani, F., Lagomarsino, D., Segoni, S., & Tofani, V. (2013). Landslide susceptibility estimation by random forests technique; sensitivity and scaling issues. *Natural Hazards and Earth System Sciences [NHESS]*, *13*(11), 2815-2831. https://doi.org/10.5194/nhess-13-2815-2013

Catani, F., Tofani, V., & Lagomarsino, D. (2016). Spatial patterns of landslide dimension: A tool for magnitude mapping. *Geomorphology*, *273*, 361-373. https://doi.org/10.1016/j.geomorph.2016.08.032

Choi, J., Oh, H. J., Lee, H. J., Lee, C., & Lee, S. (2012). Combining landslide susceptibility maps obtained from frequency ratio, logistic regression, and artificial neural network models using ASTER images and GIS. *Engineering Geology*, *124*, 12-23. https://doi.org/10.1016/j.enggeo.2011.09.011

Cresswell, T. (2013). *Geographic thought : a critical introduction*. Wiley-Blackwell.

Dahal, R. K., Hasegawa, S., Nonomura, A., Yamanaka, M., Dhakal, S., & Paudyal, P. (2008). Predictive modelling of rainfall-induced landslide hazard in the Lesser Himalaya of Nepal based on weights-of-evidence [Article]. *Geomorphology*, *102*(3-4), 496-510. https://doi.org/10.1016/j.geomorph.2008.05.041

Dahal, R. K., Hasegawa, S., Nonomura, A., Yamanaka, M., Masuda, T., & Nishino, K. (2008). GIS-based weights-of-evidence modelling of rainfall-induced landslides in small catchments for landslide susceptibility mapping. *Environmental geology (Berlin)*, *54*(2), 311-324. https://doi.org/10.1007/s00254-007-0818-3

Dai, F. C., & Lee, C. F. (2002). Landslide characteristics and slope instability modeling using GIS, Lantau Island, Hong Kong. *Geomorphology*, *42*(3), 213-228.

Dai, F. C., & Lee, C. F. (2003). A spatiotemporal probabilistic modelling of storm-induced shallow landsliding using aerial photographs and logistic regression. *Earth Surface Processes and Landforms*, *28*(5), 527-545. https://doi.org/10.1002/esp.456

Duman, T., Can, T., Gokceoglu, C., Nefeslioglu, H., & Sonmez, H. (2006). Application of logistic regression for landslide susceptibility zoning of Cekmece Area, Istanbul, Turkey. *Environmental Geology*, *51*(2), 241-256. https://doi.org/10.1007/s00254-006-0322-1

Ercanoglu, M. (2005). Landslide susceptibility assessment of SE Bartin (west Black Sea region, Turkey) by artificial neural networks. *Natural Hazards and Earth System Sciences [NHESS]*, *5*(6), 979-992.

Ermini, L., Catani, F., & Casagli, N. (2005). Artificial Neural Networks applied to landslide susceptibility assessment. *Geomorphology*, *66*, 16.

Esri. (2020). *Band Collection Statistics*. Esri. Retrieved 11/16/2020 from https://desktop.arcgis.com/en/arcmap/latest/tools/spatial-analyst-toolbox/band-collection-statistics.htm

Falaschi, F., Giacomelli, F., Federici, P. R., Puccinelli, A., Avanzi, G. D., Pochini, A., & Ribolini, A. (2009). Logistic regression versus artificial neural networks: landslide susceptibility evaluation in a sample area of the Serchio River valley, Italy [Article]. *Natural Hazards*, *50*(3), 551-569. https://doi.org/10.1007/s11069-009-9356-5

Guzzetti, F. (2006). *Landslide hazard and risk assessment: concepts, methods, and tools for the detection and mapping of landslides, for landslide susceptibility zonation and hazard assessment, and for landslide risk evaluation* [Dissertation, University of Bonn]. Bonn, Germany. http://geomorphology.irpi.cnr.it/Members/fausto/PhD-dissertation/Landslide_Hazard_and_Risk_Assessment.pdf

Harris, J. R. (2002). Processing and integration of geochemical data for mineral exploration: Application of statistics, geostatistics and GIS technology. In: ProQuest Dissertations Publishing.

Hartley, B. K. (2014). Evaluation of Weights of Evidence to Predict Gold Occurrences in Northern Minnesota's Archean Greenstone Belts. In: ProQuest Dissertations Publishing.

Heaton, J. (2017). *Non-Mathematical Introduction to Using Neural Networks*. Heaton Research. https://www.heatonresearch.com/content/non-mathematical-introduction-using-neural-networks

Hicks, H., & Laituri, M. (2020). *Geospatial applications to landslide riskscape development: a modeling approach to quantify landslide riskscapes in the Colorado Front Range [Manuscript submitted for publication]* [Manuscript]. Colorado State University.

Hicks, H., & Laituri, M. (2021). *Riskscapes as a geospatial construct: A conceptualization of the riskscapes of landslides in human-environmental systems [Manuscript submitted for publication]* [Manuscript]. Colorado State University.

Hjort, J., & Luoto, M. (2013). 2.6 Statistical Methods for Geomorphic Distribution Modeling. In J. F. Shroder (Ed.), *Treatise on Geomorphology* (pp. 59-73). Academic Press. https://doi.org/https://doi.org/10.1016/B978-0-12-374739-6.00028-2

Hosseinali, F., & Alesheikh, A. A. (2008). Weighting Spatial Information in GIS for Copper Mining Exploration. *American Journal of Applied Sciences*, *5*(9), 1187-1198. https://doi.org/10.3844/ajassp.2008.1187.1198

Kanungo, D. P., Arora, M. K., Sarkar, S., & Gupta, R. P. (2006). A comparative study of conventional, ANN black box, fuzzy and combined neural and fuzzy weighting procedures for landslide susceptibility zonation in Darjeeling Himalayas. *Engineering Geology*, *85*, 347-366.

Kouli, M., Loupasakis, C., Soupios, P., Rozos, D., & Vallianatos, F. (2014). Landslide susceptibility mapping by comparing the WLC and WofE multi-criteria methods in the west Crete Island, Greece. *Environmental Earth Sciences*, *72*(12), 5197-5219. https://doi.org/10.1007/s12665-014-3389-0

Lee, E. (2009). Landslide risk assessment: The challenge of estimating the probability of landsliding. *Quarterly Journal of Engineering Geology and Hydrogeology*, *42*, 445-458. https://doi.org/10.1144/1470-9236/08-007

Lee, J.-H., Sameen, M. I., Pradhan, B., & Park, H.-J. (2018). Modeling landslide susceptibility in data-scarce environments using optimized data mining and statistical methods. *Geomorphology*, *303*, 284-298. https://doi.org/10.1016/j.geomorph.2017.12.007

Lee, S. (2005). Application of logistic regression model and its validation for landslide susceptibility mapping using GIS and remote sensing data. *International Journal of Remote Sensing*, *26*, 1477-1491.

Lee, S. (2007). Landslide susceptibility mapping using an artificial neural network in the Gangneung area, Korea. *International Journal of Remote Sensing*, *28*, 4763-4783.

Lee, S., & Evangelista, D. G. (2006). Earthquake-induced landslide-susceptibility mapping using an artificial neural network. *Natural Hazards and Earth System Sciences [NHESS]*, *6*, 687-695.

Lee, S., Ryu, J.-H., & Kim, I.-S. (2007). Landslide susceptibility analysis and its verification using likelihood ratio, logistic regression, and artificial neural network models: case study of Youngin, Korea. *Landslides*, *4*(4), 327-338. https://doi.org/10.1007/s10346-007-0088-x

Lee, S., Ryu, J.-H., Lee, M.-J., & Won, J.-S. (2006). The application of artificial neural networks to landslide susceptibility mapping at Janghung, Korea. *Mathematical Geology*, *38*, 199-220.

Lee, S., Ryu, J.-H., Min, K., & Won, J.-S. (2003). Landslide susceptibility analysis using GIS and artificial neural network. *Earth Surface Processes and Landforms*, *28*(12), 1361-1376. https://doi.org/10.1002/esp.593

Lee, S., Ryu, J.-H., Won, J.-S., & Park, H.-J. (2004). Determination and application of the weights for landslide susceptibility mapping using an artificial neural network. *Engineering Geology*, *71*(3-4), 289-302. https://doi.org/10.1016/S0013-7952(03)00142-X

Lee, S., Ryu, J., Min, K., Choi, W., & Won, J. (2000). *Development and application of landslide susceptibility analysis techniques using geographic information system (GIS)* International Geoscience and Remote Sensing Symposium, United States.

Lee, S., Won, J.-S., Jeon, S. W., Park, I., & Lee, M. J. (2015). Spatial landslide hazard prediction using rainfall probability and a logistic regression model. *Mathematical Geosciences*, *47*(5), 565-589. https://doi.org/10.1007/s11004-014-9560-z

Looney, C. G., Wang, Z., & Raines, G. L. (2005). *GeoXplore*. In (Version 5.1) University of Nevada, Reno; United States Geological Survey.

Manzo, G., Tofani, V., Segoni, S., Battistini, A., & Catani, F. (2013). GIS techniques for regional-scale landslide susceptibility assessment: the Sicily (Italy) case study. *International journal of geographical information science : IJGIS*, *27*(7), 1433-1452. https://doi.org/10.1080/13658816.2012.693614

Morgan, M. L., White, J. L., Fitzgerald, F. S., & Berry, K. A. (2014). *Foothill and mountainous regions in Boulder County, Colorado that may be susceptible to earth and debris/mud flows during extreme precipitation events* Colorado Geological Survey. https://coloradogeologicalsurvey.org/publications/landslide-susceptibility-extreme-precipitation-boulder-colorado

Müller-Mahn, D., & Everts, J. (2013). Riskscapes: the spatial dimension of risk. In H.-D. Müller-Mahn & C. Ebooks (Eds.), *The spatial dimension of risk: How geography shapes the emergence of riskscapes*. Routledge.

Nourani, V., Pradhan, B., Ghaffari, H., & Sharifi, S. S. (2014). Landslide susceptibility mapping at Zonouz Plain, Iran using genetic programming and comparison with frequency ratio, logistic regression, and artificial neural network models. *Natural Hazards*, *71*(1), 523-547. https://doi.org/10.1007/s11069-013-0932-3

Nykänen, V., Lahti, I., Niiranen, T., & Korhonen, K. (2015). Receiver operating characteristics (ROC) as validation tool for prospectivity models — A magmatic Ni–Cu case study from the Central Lapland Greenstone Belt, Northern Finland. *Ore geology reviews*, *71*, 853-860. https://doi.org/10.1016/j.oregeorev.2014.09.007

Ohlmacher, G. C., & Davis, J. C. (2003). Using multiple logistic regression and GIS technology to predict landslide hazard in Northeast Kansas, USA. *Engineering Geology*, *69*(3-4), 331-343. https://doi.org/10.1016/S0013-7952(03)00069-3

Oyana, T. J., & Margai, F. (2016). *Spatial Analysis: Statistics, Visualization, and Computational Methods*. CRC Press. https://doi.org/10.1201/b18808

Ozdemir, A. (2011). Landslide susceptibility mapping using Bayesian approach in the Sultan Mountains (Aksehir, Turkey). *Natural Hazards*, *59*. https://doi.org/10.1007/s11069-011-9853-1

Piacentini, D., Troiani, F., Soldati, M., Notarnicola, C., Savelli, D., Schneiderbauer, S., & Strada, C. (2012). Statistical analysis for assessing shallow-landslide susceptibility in South Tyrol (south-eastern Alps, Italy). *Geomorphology (Amsterdam, Netherlands)*, *151-152*, 196-206. https://doi.org/10.1016/j.geomorph.2012.02.003

Poli, S., & Sterlacchini, S. (2007). Landslide Representation Strategies in Susceptibility Studies using Weights-of-Evidence Modeling Technique. *Natural resources research (New York, N.Y.)*, *16*(2), 121-134. https://doi.org/10.1007/s11053-007-9043-8

Pradhan, B., & Lee, S. (2007). Utilization of Optical Remote Sensing Data and GIS Tools for Regional Landslide Hazard Analysis Using an Artificial Neural Network Model. *Earth Science Frontiers*, *14*(6), 9.

Pradhan, B., & Lee, S. (2010). Landslide susceptibility assessment and factor effect analysis: backpropagation artificial neural networks and their comparison with frequency ratio and bivariate logistic regression modelling. *Environmental Modelling & Software*, *25*(6), 747-759. http://www.sciencedirect.com/science/article/B6VHC-4XWD04B-1/2/3d65635b10c7bacc6c83db25c862e61e

Prasannakumar, V., & Vijith, H. (2012). Evaluation and validation of landslide spatial susceptibility in the Western Ghats of Kerala, through GIS-based Weights of Evidence model and Area Under Curve technique. *Journal of the Geological Society of India*, *80*(4), 515-523. https://doi.org/10.1007/s12594-012-0171-3

Radeloff, V. C., Helmers, D. P., Kramer, H. A., Mockrin, M. H., Alexandre, P. M., Bar-Massada, A., Butsic, V., Hawbaker, T. J., Martinuzzi, S., Syphard, A. D., & Stewart, S. I. (2018). Rapid growth of the US wildland-urban interface raises wildfire risk. *Proceedings of the National Academy of Sciences of the United States of America*, *115*(13), 3314. https://doi.org/10.1073/pnas.1718850115

Regmi, N. R., Giardino, J. R., McDonald, E. V., & Vitek, J. D. (2014). A comparison of logistic regression-based models of susceptibility to landslides in western Colorado, USA. *Landslides*, *11*(2), 247-262. https://doi.org/10.1007/s10346-012-0380-2

Reichenbach, P., Rossi, M., Malamud, B. D., Mihir, M., & Guzzetti, F. (2018). A review of statistically-based landslide susceptibility models. *Earth-Science Reviews*, *180*, 60-91. https://doi.org/10.1016/j.earscirev.2018.03.001

Review, W. P. (2020). *World Population Review*. Retrieved January 6, 2020 from www.worldpopulationreview.com

Sawatzky, D. L., Raines, G. L., Bonham-Carter, G. F., & Looney, C. G. (2009). Spatial Data Modeller (SDM): ArcMAP 9.3 geoprocessing tools for spatial data modelling using weights of evidence, logistic regression, fuzzy logic and neural networks. http://arcscripts.esri.com/details.asp?dbid=15341

Singer, D. A., & Kouda, R. (1999). A Comparison of the Weights-of-Evidence Method and Probabilistic Neural Networks. *Natural resources research (New York, N.Y.)*, *8*(4), 287-298. https://doi.org/10.1023/A:1021606417010

Song, R., Hiromu, D., Kazutoki, A., Usio, K., & Sumio, M. (2008). Modeling the potential distribution of shallow-seated landslides using the weights of evidence method and a logistic regression model; a case study of the Sabae area, Japan. *International Journal of Sediment Research*, *23*(2), 106-118. https://doi.org/10.1016/S1001-6279(08)60010-4

Survey, U. G. (2011). *GAP/LANDFIRE National Terrestrial Ecosystems Data* US Geological Survey. https://www.usgs.gov/core-science-systems/science-analytics-and-synthesis/gap/science/land-cover-data-download?qt-science_center_objects=0#qt-science_center_objects

Tien Bui, D., Pradhan, B., Lofman, O., Revhaug, I., & Dick, O. B. (2012). Landslide susceptibility assessment in the Hoa Bihn province of Vietnam: A comparison of the Levenberg-Marquardt and Bayesian regularized neural networks. *Geomorphology*, *171*, 17.

Tobler, W. R. (1970). A Computer Movie Simulating Urban Growth in the Detroit Region. *Economic Geography*, *46*, 234-240. https://doi.org/10.2307/143141

Tweto, O. (1979). *MI-16 Geologic Map of Colorado* [Miscellaneous Investigations]. Colorado Geological Survey, Department of Natural Resources. https://coloradogeologicalsurvey.org/publications/tweto-geologic-map-colorado-1979.

van Westen, C. J. (2013). 3.10 Remote Sensing and GIS for Natural Hazards Assessment and Disaster Risk Management. In J. F. Shroder (Ed.), *Treatise on Geomorphology* (pp. 259-298). Academic Press. https://doi.org/https://doi.org/10.1016/B978-0-12-374739-6.00051-8

Wait, T. C., Morgan, M. L., Fitzgerald, F. S., Morgan, K. S., Berry, K. A., & White, J. L. (2015). *OF-15-13 Debris Flow Susceptibility Map of Larimer County, Colorado*. Golden, Colorado: State of Colorado Retrieved from https://coloradogeologicalsurvey.org/publications/debris-flow-susceptibility-map-larimer-colorado

Yesilnacar, E., & Topal, T. (2005). Landslide susceptibility mapping; a comparison of logistic regression and neural networks methods in a medium scale study, Hendek region (Turkey). *Engineering Geology*, *79*(3-4), 251-266. https://doi.org/10.1016/j.enggeo.2005.02.002

Yilmaz, I. (2009). Landslide susceptibility mapping using frequency ratio, logistic regression, artificial neural networks and their comparison; a case study from Kat landslides (Tokat-Turkey). *Computers & Geosciences*, *35*(6), 1125-1138. https://doi.org/10.1016/j.cageo.2008.08.007

Zêzere, J. L., Pereira, S., Melo, R., Oliveira, S. C., & Garcia, R. A. C. (2017). Mapping landslide susceptibility using data-driven methods. *Science of the Total Environment*, *589*(C), 250-267. https://doi.org/10.1016/j.scitotenv.2017.02.188

CHAPTER 5: LIMITATIONS OF GEOSPATIAL SCIENCE IN LANDSLIDE RISKSCAPES: PROJECTS, PRECISION, AND PARAMETERS[5]

5.1 Summary of the manuscript

Landslide riskscapes are spatial surfaces that integrate physical factors of landslide susceptibility modeling with human and built environment factors to construct a risk profile of landslides on a regional scale. The spatial datasets for landslide riskscape development are acquired or derived from authoritative sources from state, federal, and local government agencies. Multiple challenges exist with a spatial quantitative methodological approach and the dependency on secondary datasets that result in variability for riskscape development. Classification models influence the characterization of factor datasets and subsequent interpretation of a weighted sum analysis. Scales and data model resolution for raster or vector data types influence output models. Analytical selection of neighborhood thresholds, the region within the study area the algorithm uses for analysis, will alter the results of the spatial autocorrelation models. Input parameters include the neighborhood threshold size and determination of local (nearby grid cells) or global (grid cells include all cells in the dataset) operational methods. Software selection and open-source scripts also present challenges when developing geostatistical models for landslide riskscapes. Spatial Data Modeler (ArcSDM) open-source code errors show various iterations of the code can create compatibility issues with commercial-off-the-shelf (COTS) software application versions. Scale of the study needs to be considered based on limitations within ArcSDM processing. Findings show that riskscape models can provide insight into human-environment interactions regarding landslide hazards and

[5] This chapter is a manuscript co-authored with Melinda Laituri, submitted to a peer-reviewed journal for review.

can be spatially represented, but that multiple decision points within the process need to be reviewed in detail to minimize the variability of outputs.

5.2 Introduction to riskscape datasets and challenges

The development of landslide riskscapes exposes several limitations within geospatial science pertaining to the integration of natural hazards with spatial features including physical and social parameters. Issues with data create challenges with the output, accuracy, and measurements of riskscapes. Acquisition of data, data resolution, and scale parameters are considerations for analysis and modeling. Additionally, selection of parameters within the data manipulation processes, how the analyst chooses to classify and modify the data inputs, can create dissimilar outputs resulting in different interpretations of the same data. Attribute analysis and characterization of the data based on classification methods further alters outputs in unpredictable ways. These challenges need to be acknowledged as part of the geospatial analysis process for landslide riskscape model development.

Riskscapes, spatial risk landscapes for landslides, are described in Hicks and Laituri (2020, 2021a, 2021b) through the assessment of a novel methodology, a conceptual framework, and a comparative geostatistical analysis. Müller-Mahn and Everts (2013) provide a general review of riskscapes and define a riskscape as the spatial dimension of risk. The authors approach riskscapes from the social constructivist theory background and determine that riskscapes are not territorially restricted but are related to social practices (Müller-Mahn & Everts, 2013). Riskscapes defined through these social constructivist theories are portrayals of risk in a region based on the differences in perceptions amongst the constituents of the region. These risk areas have characteristics that are spatially unique, and change based on how they are envisioned by the occupants of the space. Other riskscape definitions base riskscapes as a

landscape of risk (Cutter, 1993, 1994) invoking the landscape conceptualization of a spatial expanse upon which various risks can be measured.

Riskscapes in this study are defined as the spatial extent of risk pertaining to landslide risk in Boulder and Larimer Counties, Colorado. Riskscape models applied to landslides are developed in Hicks and Laituri (2020) to explore the human-environment interaction of landslide hazards. Hicks and Laituri (2020) developed three weighted sum landslide riskscape models based on the probabilistic frequency ratio of physical and social factors coincident with landslide susceptibility zones. These applied landslide riskscape models include the human dimensions of the environment and social factor datasets with landslide susceptibility modeling (physical environmental factor) datasets. Three landslide riskscape models were developed based on binary (presence or absence of landslide susceptibility grid cells), ranked (weighted ranking of landslide susceptibility grid cells), and human factor (weighted ranking of landslide susceptibility grid cells based on human factors as the highest rank) weight models (Hicks & Laituri, 2020).

As spatially based risk analysis tools, landslide riskscapes combine the physical hazard parameters with social and built-environment features based on spatial datasets. These data include both the human factors which includes built environment and population factors (e.g., transportation network, buildings, urban designations, and population data), as well as the landslide susceptibility modeling data (e.g., geology, distance to faults, hydrology, soil, land cover, curvature, slope, aspect, and elevation). Spatializing the risk equations allows the development of riskscape maps, extending landslide risk mapping to incorporate the measurable anthropogenic features.

5.3 Data quality limitations

Datasets were accessed from various authoritative sources from governmental agencies and are all secondary datasets. Several limitations were noted in applying these datasets to riskscape development:

1. Best available data were defined as data available from the authoritative sources. However, these data may not be current. Most datasets were from 2018 and later; however, any changes to the data (especially in human factor data such as population) would change the riskscape evaluation and outputs.
2. Classification methods are difficult to portray.
    a) Natural Breaks (Jenks) method, which determines natural breaks within the data to create the classes is different in each study area for the same datasets.
    b) Data that needed to be classified based on quantity were particularly challenging as the quantities and ranges changed between the study area jurisdictions. This may be mitigated by using smaller or more homogenous study areas, but that was not the intent of this study. This issue led to one county's classes based on Natural Breaks (Jenks) being applied to the other county study area. Changing these classes would potentially change the output.
3. Environmental features change in real time. Temporal analyses or time-series analyses need to be conducted to construct real-time riskscapes for landslides. Datasets, once downloaded, are static but are reflecting dynamic features.
4. Population movement is not addressed fully. Census data indicates locations of populations based on housing, but people are not restricted to the location of a particular building. There is no temporal factor in the datasets that account for nocturnal vs diurnal population movement and how humans move throughout their environment. Those temporal population movement changes would influence the riskscape output.

5.4 Data quality factors

Data-driven processes require appropriate data inputs and management protocols to ensure correct outputs and results. Spatial data are subject to issues with data quality, completeness, currency, accuracy and precision, availability, validity or applicability, as well as subjectivity in classification methods and limited metadata inclusion. Table 5.1 defines elements of data quality and analysis challenges to be considered when applying geospatial methods to riskscape development. Issues with these spatial data are described in the following sections.

Table 5.1. Definitions of data quality measurements.

Term	Definition	Sources
A. Data quality	The quality of the data relating to positional and attribute accuracy, the appropriateness of the data to the required usage.	Bolstad (2019), Kerski and Clark (2012)
B. Completeness	Measure of how well the dataset captures all the features and attributes.	Bolstad (2019), Harmon and Anderson (2003)
C. Currency	Measure of the timeliness of the data (date in metadata) or the frequency of collection.	Bolstad (2019), Harmon and Anderson (2003)
D. Attributes	Information about data features, contained in a table.	Steinberg and Steinberg (2015)
E. Accuracy	Multiple facets relating to the quality and errors within the data. Accuracy can include positional, attribute (text) and completeness measurements.	Kennedy (2013), Bolstad (2019)
F. Precision	Consistency of the measurement.	Kennedy (2013)
G. Availability	Is the data available for use, are there any restricted uses?	Steinberg and Steinberg (2015)
H. Validity (applicability)	Do the data fit the requirement, do the data support the intended analysis?	Steinberg and Steinberg (2015)
I. Classification	A method to categorize data based on similar values.	Kennedy (2013), Bolstad (2019)
J. Metadata	Data about data, information about the geographic datasets.	Schauppenlehner and Muhar (2018), Bolstad (2019)

These data quality factors are shown in Figure 5.1 based on their alignment with locational, usage-based, and completeness factors.

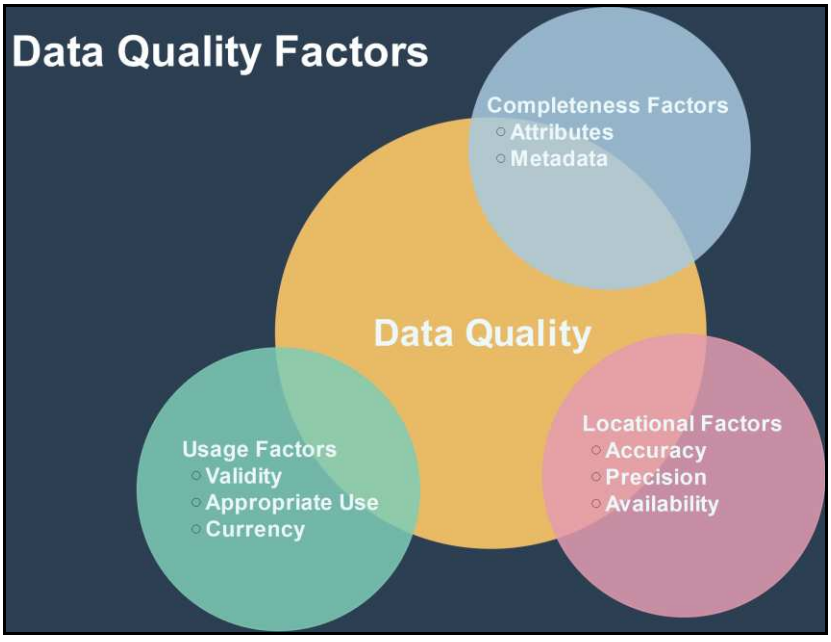

Figure 5.1. Data quality factor relationship model.

5.4.1 Data quality

Data quality (A) is reflected in the accuracy (E) and completeness (B) of the datasets. Accuracy is based on the locational precision of the data to the correct surface location. How close is this dataset location to the actual location of the feature(s) represented on the earth (surface, subsurface, or atmospheric)? Completeness refers to both the dataset's attribution – do all the fields within the dataset contain a value, or are there missing or null values, and the dataset's extent – does the same data exist across the entire area? Information on these data quality measurements may not be easily obtained. Metadata (J), or data about the data, is often not included or does not include enough information to get a sense of the viability of using a dataset and is discussed in a later section.

5.4.2 Challenges with data acquisition

Data are generally classified as primary (collected by the user or agency) or secondary (provided by an external user or agency). Primary data, where the user has collected the data through measurement or sensory tools, are often used for smaller or localized projects or by agencies responsible for developing and maintaining systems, such as local or federal government agencies. Secondary data, where the user of the data is not the data collector, creates assumptions regarding the usage of the data and the need to understand the appropriate use of the data resources as well as the limitations within the data attributes. The source of data is important as each type (primary and secondary) presents different challenges. Primary data are time-consuming and costly to collect, especially over larger areas. This may be infeasible for smaller agencies or individual users. However, primary data collection allows the researcher to control the quality and collection process, providing more fit-for-purpose data collection.

Secondary data are more readily available, and many government agencies provide these datasets freely and digitally to the public. However, secondary data are subject to existing appropriate use agreements and disclaimers. Disclaimers on secondary data can outline restrictions on usage or limit availability (time-bound) or access to the data (acceptable use) even when these data are provided by public sources. Secondary sources have considerable variability in quality and availability. Usage of secondary data requires understanding and accepting the limiting factors of the data. Limiting factors include the areal extent of the data, the areas these data represent. This assumes that the areal extent of the data denotes the same quality throughout the regional extent of the dataset; all the locations within the data areal extent are assumed to be the same quality.

5.4.3 Completeness

Dataset completeness (B) from secondary sources is variable in terms of areal extent (coverage) and non-spatial (tabular) data attribution (D). Coverage of the datasets may not be consistent across larger regions, based on data acquisition program schedules. Datasets such as the National Agriculture Imagery Program (NAIP) orthophotography in the continental United States are collected on a three-year cycle (Program, 2021). LiDAR (Light Detection and Ranging) data are available at the national level from the 3D Elevation Program from the US Geological Survey, but are not continuous over the study area used in this dissertation (Survey, 2021). If a study area crosses collection boundaries, the date of the imagery acquisitions will be different, leading to issues with consistency within the dataset. NAIP and LiDAR datasets are not included in the analysis or scope of this study, in part due to the lack of LiDAR coverage in the study area.

Attribute values (D) present another challenge with secondary datasets. Analyses are based on querying the data and combining datasets to create new information. Attribute values, the characteristics of the data contained in the data tables, are used to classify datasets. If attribute tables are incomplete or contain null values, analyses and classifications may be limited or based on incorrect information. Incomplete data influences the riskscape construction outputs due to an increase in null values, or cells that do not have values. In the riskscape analysis presented in Hicks and Laituri (2020), soil data had gaps in data completeness, with 0.47% of the soil data in Larimer county classified as unknown or data not available, and 2.29% of the soil classes in Boulder county listed as unknown or data not available (Figure 5.2).

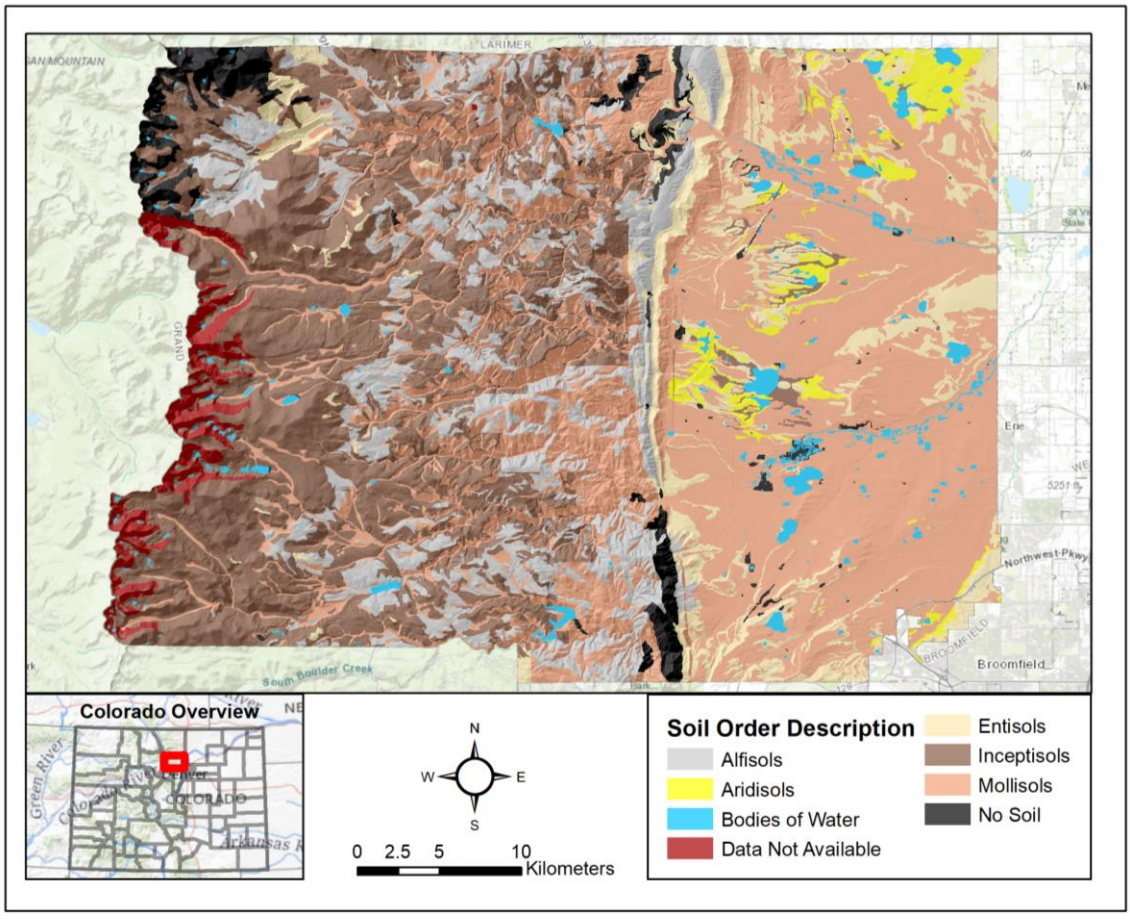

Figure 5.2. Soil data from USDS NRCS for Boulder County, Colorado. 2.29% of the study area was classified as Data Not Available.

5.4.4 Data currency

Currency of the data (C), or the date of collection, how old the data are, is another important consideration to determine the validity, or appropriateness, of the data. Data can be outdated, especially with regards to surficial features in a dynamic environment. Some data types are generally static or have a slow rate of change, such as jurisdictional boundaries that follow a political cycle with few changes as municipalities annex and de-annex regions (often near their borders) infrequently and these datasets are available from the authoritative source. Roads are built or change due to construction or damage from events. Buildings will change infrequently but may change ownership or usage, and new buildings are added regularly. While an individual building is usually static, a building dataset is very dynamic. Construction of housing developments add new buildings to the building inventory in a region. If the dataset is not maintained regularly, these changes will not be included and therefore any subsequent analyses are introducing error. This issue is related to timing and time of collection. Are these datasets static or dynamic? Once a dataset is published, the currency of the dataset needs to be understood to be useful. Understanding the currency of the dataset is important for creating an accurate analysis.

5.4.5 Metadata

Metadata (J), or data about data, are indicators of the quality of the dataset, and contain information about the development of the dataset. Metadata are not uniformly available for data accessed from public sources. Completeness of the metadata impacts our understanding of the data content. Missing information in metadata impairs the ability to judge the appropriateness of the data for analytical applications. Multiple metadata standards exist for geospatial data including ISO19115 and ISO191** (FGDC, 2021). The intent of metadata is to communicate

how the data were collected, their scale, the spatial extent, and frequency of updates among other data quality measures. Missing attributes in metadata decreases confidence in the datasets.

5.4.6 Validity (appropriateness)

Data must be valid (H) and appropriate for the intended use in the analysis. Data needs to be relevant to the study topic, area of interest, and support the analytical requirements. For landslide riskscapes, factors commonly considered as influencing landslides (primarily geophysical and environmental features) as well as the social parameters that constitute risk receptors (human, built environment, social factors) were required.

Hicks and Laituri (2020) used building units as a human built environment factor in a landslide riskscape analysis. Multiple sources for building data exist, including state and local county datasets. The county authoritative source building datasets were based on address point locations, and not on the structural size or type of building. As buildings are 3-dimensional objects, representing them as points in map does not account for the spatial extent of the features. Using polygon data to represent the size of the building is more appropriate for developing a riskscapes. Therefore, the building footprint data is preferable for these types of analyses.

A comparison of building address point data (county authoritative source) and building footprint data from Microsoft Building Footprints, Open Data Commons Open Database is shown in Figure 5.3. The county address points for houses show in the center of the parcels. The building footprint polygons show the actual locations and size of the buildings.

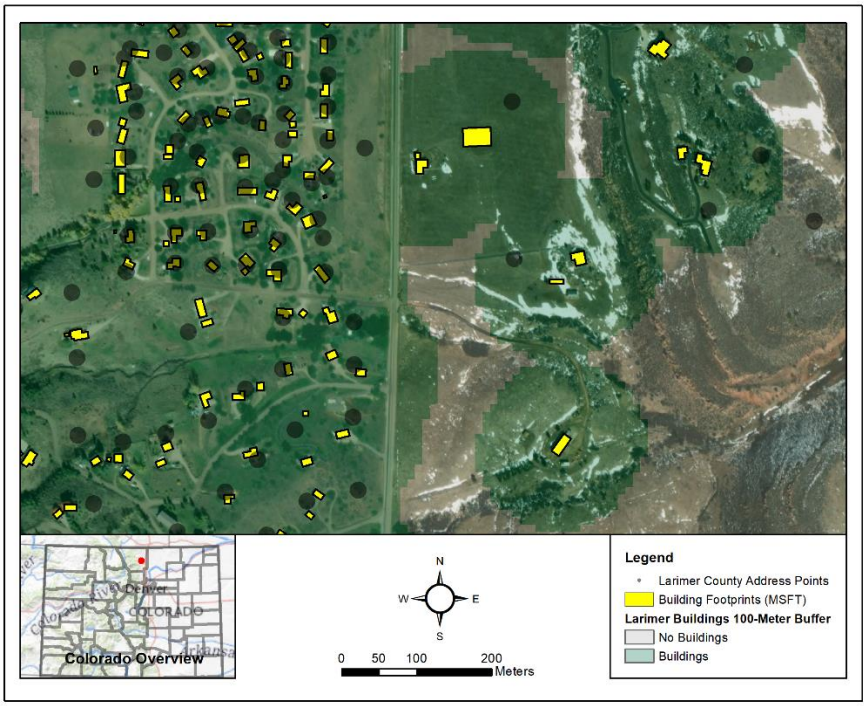

Figure 5.3. Larimer county building address points (Source: Larimer County GIS 2020) and building footprint outlines (Source: Microsoft open building, 2018). Image shows offset and areal extent differences between address points and building footprint locations. Buffer zones of 100 meters converted to raster grids for analysis show the difference between point locations, footprints, and areal extents.

5.5 Classifications issues and the challenge of subjectivity

One issue with data analysis is the process to develop user-defined classification schemes. This is exemplified in population data accessed through the U.S. Census Bureau (USCB). This source is the U.S. government agency authoritative source for U.S. population information, but also presents various challenges. First, the data are officially collected in the decadal census. The most recent official census with publicly available data was in 2010. However, the USCB creates updated datasets for annual projections and provides those datasets via the USCB GIS portal to augment the available decadal census data. These updated datasets are based on populations projections created by the American Community Survey (Bureau, 2019) are likely more accurate but not part of the decadal census count from 2010.

Second, census units are divided into tracts and blocks. The census block is the smallest unit of measurement. Census blocks are various sizes both in geographic extent and in the number of people within the block. This heterogeneity creates a map based on block features, which do not align with municipal boundaries or with environmental features. In a combined riskscape, these borders can become noticeable. This has implications for the interpretation of the riskscape and shows how the combination of human and physical factors create borders that do not align with political units or environmental units but create their own surface.

Third, classifying population is user-dependent, and this can create different maps depending on the classification scales. For example, Hicks and Laituri (2020) selected areas with 0 population within a census block to be their own unit. The goal of the riskscape is to create a uniform valuation of human and environmental factors, therefore any human population should be weighed as having higher risk. In the human factor riskscape, only census blocks with 0 population could be considered low/no risk; any human presence should be weighted equally, regardless of the population count within a census block. For the landslide riskscape model, these population datasets were designated as the highest risk value for the weighted sum analysis.

The selection of classification categories and quantities determine how data are grouped together and compiled in the analyses. These classifications settings can be based on natural groupings within the data that often lead to numerical values that are not logical to readers, with non-integer or significant figure issues. This classification, called Natural Breaks (Jenks) minimizes the intraclass variation and maximizes the interclass variation (Esri, 2021) and shows the natural tendency of the dataset. The equal interval method will divide the data into classes with the same range for each class. Using equal intervals masks features within the datasets by

altering the skew or peaks of data values by distributing them across the classes. Rounding errors can occur, which in spatial data often amounts to distance precision reduction.

Classification methods require multiple decisions to be made by the analyst. Classification tools and methods (e.g., Natural Breaks, Equal Interval) can be applied and use data-driven analysis to determine class values. The number of classes is a required input, and so choices of classification are dependent on the user's desired outcomes. When using data-driven classifications, if multiple study areas are used, the classes will be different between them or one of the study area classifications will be based on a natural data break scheme while the other is adjusted to match. This process introduces subjectivity into the analysis process. Users should have experience with these types of classification methods and understand and acknowledge the issues present in grouping data through classification methods.

Figure 5.4 demonstrates the difference between these types of classifications. Based on the same human factor riskscape input data, the maps show (A) equal interval, (B) classes matched to ranked riskscape classes, and (C) natural breaks (Jenks) classifications. While these inputs are the same dataset, the classification methods applied alters the output and can influence the interpretation of the riskscape data.

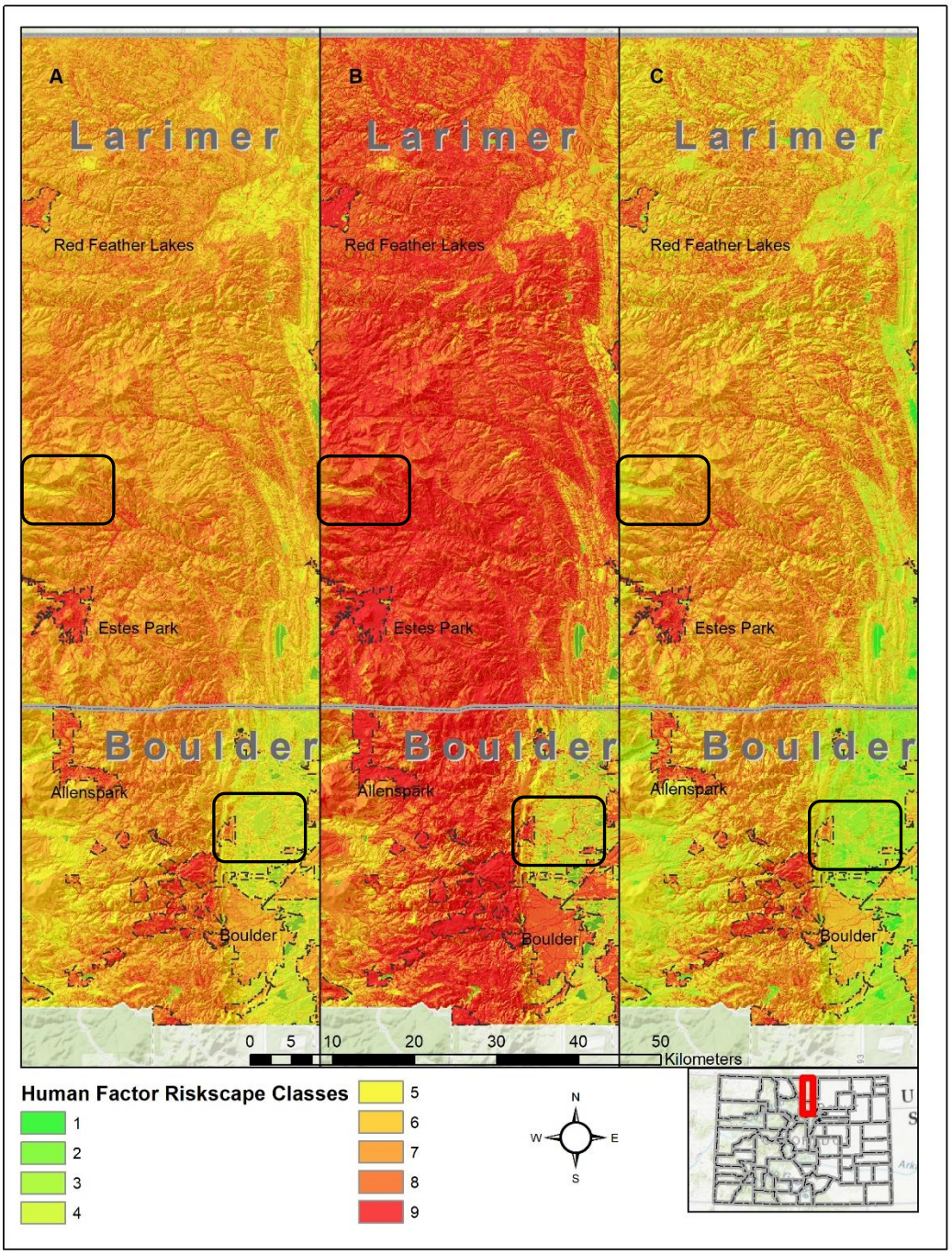
A
B
C
Larimer
Larimer
Larimer
Red Feather Lakes
Red Feather Lakes
Red Feather Lakes
Estes Park
Estes Park
Estes Park
Boulder
Boulder
Boulder
Allenspark
Allenspark
Allenspark
Boulder
Boulder
Boulder
0 5 10 20 30 40 50
Kilometers
Human Factor Riskscape Classes
1
2
3
4
5
6
7
8
9
N
W
E
S

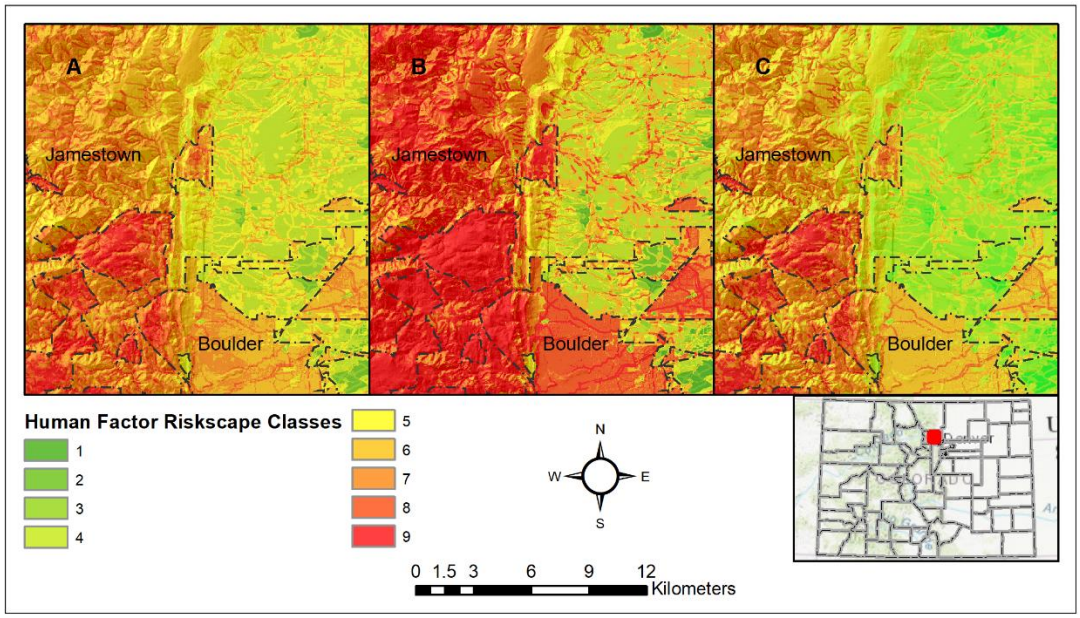

Figure 5.4. Human factor riskscapes showing differences in classification schemes. The top map shows the full urban area with areas of difference highlighted. The lower map shows an inset area in Boulder County. Map A shows human factor riskscape classes by equal interval, Map B by basing the classes on the ranked riskscape model classes and Map C by natural breaks (Jenks) method. Blocks show areas to highlight differences in rankings. Source: Hicks and Laituri (2020)

In this example, the ranked riskscape classes artificially inflated the human factor riskscape class values as the ranked classes did not have as high a range of values, so the human factor riskscape classes were grouped towards the higher end of the scale. The equal interval and natural breaks (Jenks) maps are similar, but the equal interval map has more homogenous class rankings while the natural breaks (Jenks) used the data clustering to create the classes, as observed in the larger extent of the lower class groupings. Figures 5.5 and 5.6 show the cell count and riskscape values for the three human factor riskscape models.

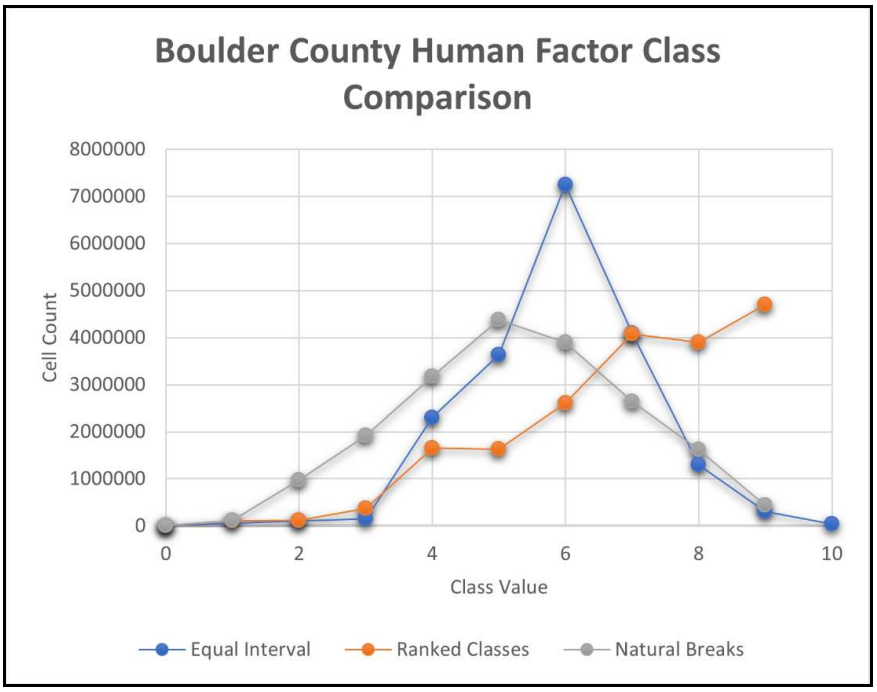

Figure 5.5. Boulder County human factor riskscape comparison. Equal interval (blue) shows the highest peak. Ranked classes (orange) show the cell counts are more heavily weighted in the upper classes, due to the higher weighting of human factor datasets. Natural Breaks (grey) shows a normal curve distribution. Data source: Hicks and Laituri (2020).

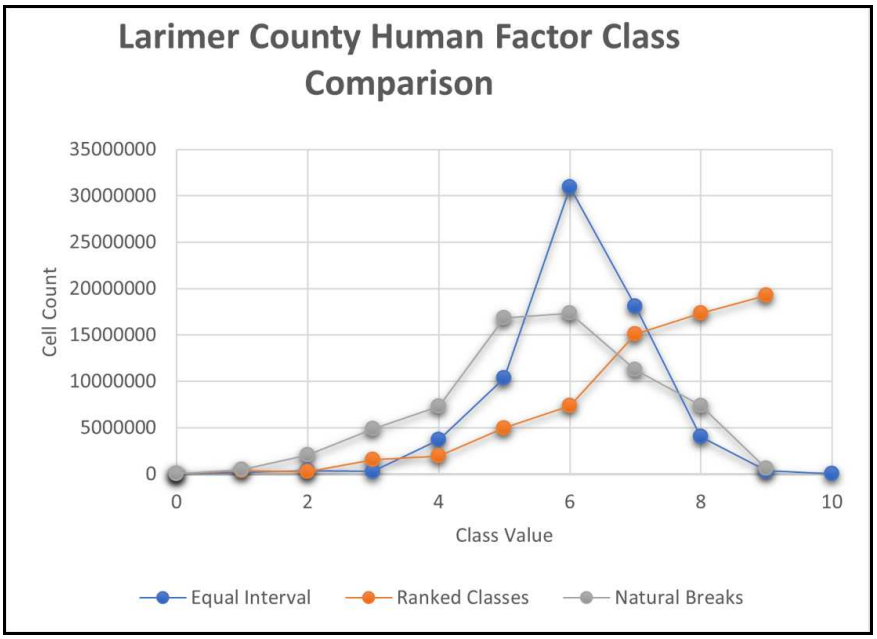

Figure 5.6. Larimer County human factor riskscape comparison. Equal interval (blue) shows the highest peak. Ranked classes (orange) show the cell counts are more heavily weighted in the

upper classes, due to the higher weighting of human factor datasets. Natural Breaks (grey) shows a normal curve distribution. Data source: Hicks and Laituri (2020).

5.6 Resolution and scale issues

Resolution and cartographic scale issues are problematic in spatial data assessments. Scale factors for data inputs is typically inconsistent, especially from governmental sources. Notably, scale and resolution differences between federal, state, and local datasets are common due to the frame of references for the agencies. National datasets are expected to be larger in areal extent than local jurisdictions that have significantly smaller areas of responsibility. Accuracy and resolution of data collected over a larger area is typically lower than data collected for smaller areas. These data are often the best available and from authoritative sources but mixing sources and scales of data of different accuracy can introduce errors into the weighted sum riskscapes analysis. For example, using 1:250,000 scale data are equivalent to 1 unit = 250,000 units of map scale, for example 1 cm equals 250,000 cm (or 2,500 meters). In a 1:10,000 map view where 1 cm = 10,000 cm (or 100 m), positional accuracy of 1 cm equals 2,500 meters does not match the visible map view. There is a visual assumption that the data are accurate, but in fact, they are not at the same positional accuracy as the view. Additionally, data that are accurate at a larger scale (1:2,000 for example) will lose information and accuracy when portrayed at a smaller scale map (1:10,000). These positional accuracy errors are generally unavoidable given the dependency on these authoritative source datasets.

Resolution is an issue related to the scales for raster data. This issue was revealed in two different ways during riskscape development. First, the modifiable area unit problem (MAUP) is a characteristic of raster data. The selection of study area boundaries defines the membership of features included in the area (Goodchild, 2001); any modifications to these boundaries will change the membership within the study area. The selection of resolution or grid size will affect

the classification of each cell. Using a larger size for a cell or a courser resolution, 1 km x 1 km as required in ArcSDM's geostatistical analysis study area grids, generalizes the data more than the input 10 x 10 meter grid (finer resolution). Classes will change based on the resolution of the data, and this issue can result in different outputs based on the selection of grid size.

Second, gridded structures use cell sizes of equal resolution to capture each thematic dataset which can lead to the mixed-pixel problem. Using 10 x 10 meter grids implies that each cell contains only one type of classification value per dataset. However, physical features do not exist in a 10 x 10 meter grid cell. Raster classifications assign the dominant class to the entire cell. Therefore, these gridded cells likely contain values that are not assigned to the class. This is generally an issue at the borders of a feature where contacts with other classifications are more likely to occur. An example of the resolution and mixed pixel problem is demonstrated in soil data for Larimer County in Figure 5.7. The border between the soil types in a vector dataset (polygons) show the borders from the soil dataset accessed from the U.S. Department of Agriculture Natural Resources Conservation Service.

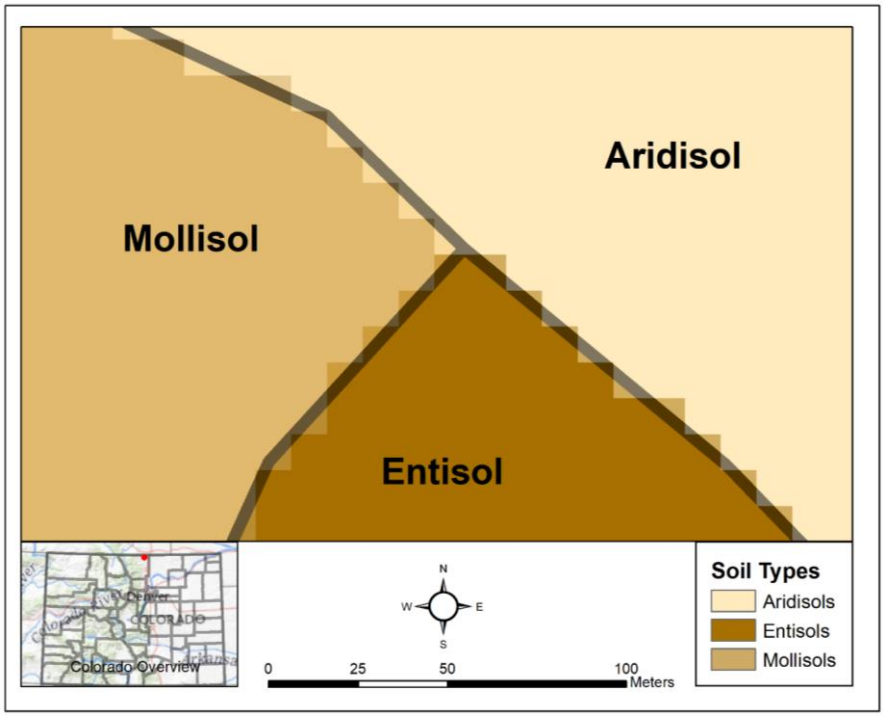

Figure 5.7. Raster data showing the mixed pixel problem. Larimer County, Colorado. Data source: USDA NRCS soils data.

5.7 Temporal scales

Issues with temporal and transitory aspects of human populations and behaviors are observed with the population datasets and interpretations of the riskscapes. Building and census data can act as a surrogate dataset for population in terms of representing human occupancy locations. However, human movement varies throughout the region. Diurnal populations are assumed to occupy office buildings and schools at a higher rate than residences. Commercial buildings and large structures may be zoned for multiple occupants that do not inhabit those structures during evenings or weekends. An event occurring during the day would potentially impact those structures more than if the event occurred during other times. Additionally, building and population datasets do not account for movement of non-residents through an area. Tourism and visitation can increase the human population risk in areas that rank low in census population

and building structure datasets. Fluctuations in diurnal and nocturnal populations, and the transient populations through a region would change the riskscape but are not easily captured with authoritative source datasets that do not contain temporal attributes or account for transient population movement.

Other temporal scales also influence riskscapes. Physical features and natural systems are dynamic (Chorley, 1962) and these changes over time can influence the input factors which may not be fully addressed in a static dataset. Temporal scales for physical attributes may be longer-duration, such as the seasonality of conditions including precipitation, snow or water fluctuations, or more immediate events such as wildland fires or avalanches. Changes to the physical environment temporally distributed across the landscape will influence the riskscapes by increasing or decreasing the potential risks for landslides.

5.8 Influences of parameter settings in a tool structure

In the development of a riskscape approach to identify areas of increase riskscape valuation for a study area in the Colorado Front Range, spatial autocorrelation tools were applied (Hicks & Laituri, 2020). These tools, designed to identify the strength of the spatial relationships of data, were used to determine the level of clustering-dispersion-randomness of riskscapes. One expectation or assumption of statistical analyses is that the data are independent and normally distributed. This assumption is often violated with spatial features due to the preconditions of certain data relationships in physical factors. Natural phenomena do not occur in a vacuum, independent of other features. They coexist and influence their surroundings. In geography, this principle is known as Tobler's First Law of Geography, defined as "everything is related to everything else, but near things are more related than distant things" (Tobler, 1970, p. 236). This

principle forms the basis for many spatial analytical approaches. The methods used in modeling riskscapes apply these spatial relationship models through the application of geoprocessing tools.

Geoprocessing tools require the application of algorithms not visible to users. Mathematical computations are components of the analyses, designed to streamline the user experience and make spatial analysis easier for common applications. To accomplish this, assumptions are made as part of the tool settings, which are configured to allow inputs but not require all potential options for inputting these settings. “Default” settings may represent the most common applications deemed by the developer whether commercial-off-the-shelf products (COTS) or open-source script-based products. These default settings influence the outputs significantly. Not all settings are appropriate for all applications, data types, and desired research questions. “Unpacking the black box” is a way of viewing this challenge.

Another observation is the parameter settings within different tools can influence output for the same datasets. For spatial autocorrelation, the selection of neighborhood type is an important input. In Esri’s ArcGIS Desktop and Pro, using the Global Moran’s *i* spatial autocorrelation tool, the type of analysis for measuring the strength of spatial relationships is directly related to the type of neighborhood tool selection. Called the “conceptualization of spatial relationships,” this forms the basis of the algorithms applied to the datasets. Accepting the default setting, Inverse Distance, may be appropriate for many applications. However, there are cases where other conceptualization methods are more appropriate. Notably, results differ for the same dataset in response to changing the conceptualization types and the subsequent distance calculation thresholds.

These differences are exemplified in the following table from human factor riskscapes developed in Hicks and Laituri (2020). Changes to the conceptualization (the method applied to

the data), the standardization (the type of neighborhood restriction to row neighbors or all neighbors), the distance threshold (using machine-driven models as default which selects a distance that will include a minimum of one neighbor or setting a distance based on user input) resulted in different outputs for p-values, Moran's *i* index value, and the determination of clustering values. For both Boulder and Larimer Counties, using the Zone of Indifference resulted in the highest (default neighborhood) and lowest (row-based neighborhood) Moran's *i* index value, though both indicated clustering. The Inverse Distance Squared setting used the default threshold for distance calculations but while the Moran's *i* index values were high and positive, indicating a high spatial autocorrelation, the p-value for the false row or default neighborhood setting (did not use row for neighborhood), was outside of the acceptable thresholds and indicated the only random (no clustering) result of all the models. Table 5.2 shows results from six human factor riskscape models that applied different conceptualization, standardization, and threshold parameters from Hicks and Laituri (2020).

Table 5.2. Comparison of spatial autocorrelation results for human factor riskscape models.

Boulder County	**Model 1**	**Model 2**	**Model 3**	**Model 4**	**Model 5**	**Model 6**
Settings						
Conceptualization	Inverse Distance	Inverse Distance	Inverse Distance Squared	Inverse Distance Squared	Zone of Indifference	Zone of Indifference
Standardization	Row (True)	Default (False)	Row (True)	Default (False)	Row (True)	Default (False)
Distance Threshold	Default (6651.41m)	Default (6651.41m)	Default (6651.41m)	Default (6651.46m)	1000 meters	1000 meters
RESULTS						
Moran's Index	0.610	0.654	0.632	0.724	0.573	0.798
Variance	0.002	0.003	0.005	0.239	0.007	0.012
Z-Score	15.224	12.877	9.426	1.505	6.776	7.370
P-Value	0.00	0.00	0.00	0.132	0.00	0.00
Results	**Clustered**	**Clustered**	**Clustered**	**Random**	**Clustered**	**Clustered**
Larimer County	**Model 1**	**Model 2**	**Model 3**	**Model 4**	**Model 5**	**Model 6**
Settings						
Conceptualization	Inverse Distance	Inverse Distance	Inverse Distance Squared	Inverse Distance Squared	Zone of Indifference	Zone of Indifference
Standardization	Row (True)	Default (False)	Row (True)	Default (False)	Row (True)	Default (False)
Distance Threshold	Default (29733.13 m)	Default (29733.13 m)	Default (29733.13 m)	Default (29733.13 m)	1000 meters	1000 meters
RESULTS						
Moran's Index	0.566	0.483	0.696	0.889	0.479	0.982

Variance	0.001	0.001	0.004	0.029	0.005	0.118
Z-Score	18.466	16.615	10.898	5.321	7.103	2.891
P-Value	0.00	0.00	0.00	0.00	0.00	0.004
Results	**Clustered**	**Clustered**	**Clustered**	**Clustered**	**Clustered**	**Clustered**

5.9 Software and coding

Software application selection forms the basis of the geospatial analysis. ArcSDM is a modeling tool developed by researchers at the U.S. Geological Survey and Geological Survey of Canada to model mineral prospects (Sawatzky et al., 2009). This tool is an external extension to Esri's ArcGIS platform. Several agencies have supported the toolset throughout its development, including the Geotechnologies Research Group at the University of Campinas and currently, the Mineral Prospectivity Modelling Project at the Geological Survey of Finland. Through the development of the ArcSDM platform and iterations of the geostatistical toolsets, the base software versions have changed from several versions of ArcGIS Desktop to several versions of ArcGIS Pro. These changes result in tools not working consistently from version to version. The current distribution model for ArcSDM is through a GitHub community. As open-source code is by definition not commercial, support is different than that of a COTS product like Esri. ArcSDM code is compiled in python and scripts are include as part of the toolset download. However, when running the scripts, most of the documentation is from the original versions of the toolsets and do not reflect the many significant changes and developments the tools have undergone.

Tools in ArcSDM are used to create geostatistical models of spatial datasets and create spatial output maps and datasets to account for the variability of probability models across space. However, as an open-source tool coded in python, and externally developed compared to the software upon which it is based, users need to be able to support and resolve issues with script

errors independently of COTS software support. Some elements of the code work in one version of the Esri software but not others. The open-source model provides a platform for accessing the ArcSDM toolbox and geostatistical modeling but requires significant user experience with coding and scripting for diagnosing and correcting errors, or a support system available to the user.

5.10 Conclusions

The basis for landslide riskscape development has multiple dependencies that influence the interpretation of results. Data quality issues are a paramount concern. If data are incomplete, the riskscape assessments will be different. Timeliness and currency of data is also a factor for concern, particularly with regards to human factor data. Population changes are not well-reflected in the decadal census datasets, and humans are transient across the landscape thereby creating challenges with using surrogate data such as building units and census blocks. A greater challenge exists with access to fluctuating human population locations on a diurnal cycle. Given human daily movements, a temporal riskscape would be more accurate for supporting decision-making during an event, but more difficult to develop given the lack of temporal data at this scale. Human encroachment into WUI areas and hazardous regions expands these areas of human-environment risk, increasing exposure of vulnerable elements at risk (Haque & Burton, 2005).

Analytical decisions as part of the process can also introduce challenges to data interpretation. These issues are particularly visible in the mapping outputs that require classification of datasets. To create visual consistency, maps are created based on a common color scheme. However, the methods of classification of the same data, as seen in Figures 5.3, 5.4, and 5.5, show that the variation in methods from equal interval to natural breaks, and a

manual classification scheme to compare to other riskscape outputs, alter the classification images and lead to different interpretations.

These differences are further exemplified in the selections of parameters within the spatial autocorrelation tools. User settings allow for changes to the type of neighborhood which determines the extent of cells to be included as the study area, the distance that is considered as part of the neighborhood, the algorithm to be applied (e.g., inverse distance weighting, zone of indifference). If the user does not specify these settings, the outputs may not be appropriate for the type of analyses.

Additionally, to more fully develop a riskscape model, other factors can be considered. Examining human perceptions of risk and multi-hazard risk assessment would create a more complete picture of risk in place. Behavioral aspects of risk can also be considered and added to a riskscape as described in Ley-García et al. (2015). While these notions are out of scope with this project, riskscapes can incorporate these elements to determine the risk environment and its social construction more fully.

The challenges encountered based on the uniqueness of spatial data need attention when applied to analytical processes. Understanding of the data inputs and the parameter selections for analyses are critical to developing an appropriate analysis with logical results. The classification schemes and inputs need to be documented. Better results are based on the understanding of these issues and the mitigation of them through the evaluation of the project requirements, precise application of the tools, and correct parameterization.

References

Bolstad, P. (2019). *GIS Fundamentals: A First Text on Geographic Information Systems* (6th ed.). XanEdu.

Bureau, U. D. o. C. U. C. (2019). *Population Estimates* [US Census Bureau population database]. https://www.census.gov/quickfacts/fact/table/larimercountycolorado,bouldercountycolorado,US/PST045219

Chorley, R. J. (1962). *Geomorphology and general systems theory*. Washington : United States Department of the Interior, Geological Survey.

Cutter, S. L. (1993). *Living with risk : the geography of technological hazards*. London ; New York : E. Arnold ; New York : Routledge, Chapman and Hall distributor.

Cutter, S. L. (1994). *Environmental risks and hazards* (S. Cutter, Ed.). Prentice Hall.

Esri. (2021). *Data Classification Methods*. Environmental Systems Research Institute. Retrieved March 16, 2021 from https://pro.arcgis.com/en/pro-app/latest/help/mapping/layer-properties/data-classification-methods.htm

FGDC, F. G. D. C. (2021). *ISO Geospatial Metadata Standards*. FGDC.gov. Retrieved 01/13/2021 from https://www.fgdc.gov/metadata/iso-standards

Goodchild, M. F. (2001). Models of Scale and Scales of Modelling In N. J. Tate & P. M. Atkinson (Eds.), *Modelling Scale in Geographical Information Science*. Wiley.

Haque, C. E., & Burton, I. (2005). Adaptation Options Strategies for Hazards and Vulnerability Mitigation: An International Perspective. In C. E. Haque (Ed.), *Mitigation of Natural Hazards and Disasters: International Perspectives*. Springer.

Harmon, J. E., & Anderson, S. J. (2003). *The Design and Implementation of Geographic Information Systems* (1. Aufl. ed.). Wiley.

Hicks, H., & Laituri, M. (2020). *Geospatial applications to landslide riskscape development: a modeling approach to quantify landslide riskscapes in the Colorado Front Range [Manuscript submitted for publication]* [Manuscript]. Colorado State University.

Hicks, H., & Laituri, M. (2021a). *Geostatistical assessments of landslide riskscapes: a comparison of logistic regression, weights of evidence, and neural networks [Manuscript submitted for publication]* [Manuscript]. Colorado State University.

Hicks, H., & Laituri, M. (2021b). *Riskscapes as a geospatial construct: A conceptualization of the riskscapes of landslides in human-environmental systems [Manuscript submitted for publication]* [Manuscript]. Colorado State University.

Kennedy, M. D. (2013). *Introducing Geographic Information Systems with ArcGIS: A Workbook Approach to Learning GIS* (3. Aufl. ed.). Wiley.

Kerski, J., & Clark, J. (2012). *GIS Guide to Public Domain Data*. Esri Press.

Ley-García, J., Denegri de Dios, F. M., & Ortega Villa, L. M. (2015). Spatial dimension of urban hazardscape perception: The case of Mexicali, Mexico. *International Journal of Disaster Risk Reduction*, *14*, 487-495. https://doi.org/10.1016/j.ijdrr.2015.09.012

Müller-Mahn, D., & Everts, J. (2013). Riskscapes: the spatial dimension of risk. In H.-D. Müller-Mahn & C. Ebooks (Eds.), *The spatial dimension of risk: How geography shapes the emergence of riskscapes*. Routledge.

Program, U. N. N. A. I. (2021). Farm Service Agency. Retrieved 1/15/2021 from https://www.fsa.usda.gov/programs-and-services/aerial-photography/imagery-programs/naip-imagery/

Sawatzky, D. L., Raines, G. L., Bonham-Carter, G. F., & Looney, C. G. (2009). Spatial Data Modeller (SDM): ArcMAP 9.3 geoprocessing tools for spatial data modelling using weights of evidence, logistic regression, fuzzy logic and neural networks. http://arcscripts.esri.com/details.asp?dbid=15341

Schauppenlehner, T., & Muhar, A. (2018). Theoretical Availability versus Practical Accessibility: The Critical Role of Metadata Management in Open Data Portals. *Sustainability (Basel, Switzerland)*, *10*(2), 545. https://doi.org/10.3390/su10020545

Steinberg, S. L., & Steinberg, S. J. (2015). *GIS Research Methods: Incorporating Spatial Perspectives*. Redlands: Esri Press.

Survey, U. G. (2021). *3D Elevation Program (3DEP)*. National Geospatial Program. Retrieved January 28, 2021 from https://www.usgs.gov/core-science-systems/ngp/3dep/what-is-3dep?qt-science_support_page_related_con=0#qt-science_support_page_related_con

Tobler, W. R. (1970). A Computer Movie Simulating Urban Growth in the Detroit Region. *Economic Geography*, *46*, 234-240. https://doi.org/10.2307/143141

CHAPTER 6: CONCLUSIONS

This chapter summarizes the four studies included in this dissertation and discusses the contributes to our understanding of riskscapes as a spatial construction of risk. A summary of the contributions from this research and the implications of landslide riskscape analysis is presented. A synopsis of the results and limiting factors of spatial data are discussed with recommendations on future work, data parameter and method considerations.

6.1 Summary of contributions and implications for landslide riskscape methodologies

This dissertation presents several findings with implications for further development of landslide riskscapes and riskscape models in general. This study focused on the guiding question, how is space measured in a landslide riskscape? This was addressed through four primary research questions, outlined in Table 6.1 with the key findings.

Table 6.1. Research questions and key findings.

Chapter	Research Question	Key Findings
2	1. What is a riskscape, how do riskscapes relate to other landslide analysis methods, and can a landslide riskscape conceptual model be developed?	• Modified riskscape theoretical frameworks to include spatial theory. • Created a landslide riskscape conceptual model. • The addition of environmental systems and risk theoretical frameworks provides a method to quantify riskscapes. • Spatial theory introduced to riskscapes provides a method to measure the spatial influence of riskscape models.
3	1. What is a landslide riskscape for Boulder and Larimer Counties, Colorado? 2. Can spatial characteristics of landslide riskscapes be	• Created a landslide riskscape method to generate an information surface for human-environment interactions based on landslide risk factors. • Developed three weighted sum riskscapes to operationalize the spatial

	measured? 3. How does spatial autocorrelation help us understand landslide riskscapes?	risk equation. • Quantified strength of spatial relationships based on spatial autocorrelation methods. • Models indicated clustering.
4	1. Do geostatistical models support riskscape analysis? 2. How do probabilistic neural networks, logistic regression, and weights of evidence geostatistical tools compare in the development of landslide riskscapes for Boulder and Larimer Counties, Colorado?	• Compared geostatistical analysis of riskscapes using logistic regression, weights of evidence, and probabilistic neural networks. • Provided AUC validation of models. • Weights of evidence and logistic regression had valid models. • Probabilistic neural networks had limited utility.
5	1. Based on these analyses, what are the limitations of spatial data in these landslide riskscape applications?	• Assessed limitations of spatial processes in landslide riskscape development. • Classification and parameterization processes will influence the results of models.

6.2 Riskscape frameworks

A synthesis of riskscape definitions and evolutions is presented in Chapter Two to address the gap in a riskscape conceptual framework through the incorporation of spatial modeling methodologies. The interdisciplinary approach to riskscapes through the application of spatial methods and landslide modeling frameworks provided an operational model to quantify the spatial aspects of riskscapes. Defining the relationship between riskscapes and quantitative landslide studies furthers our understanding of space as it applies to the emergent nature of risk and the physical properties of landslides. Landslide risk studies frequently use GIS methods to determine areas of hazard and risk, and leverage multiple geostatistical methods (See Reichenbach et al. (2018) for a review of these statistical approaches).

Riskscapes are defined based on an integration of theoretical frameworks in combination with quantitative landslide risk studies and the conceptualization of space from spatial theory. While risk is an emergent property, so too are riskscapes. From the literature, riskscapes emerge in the social constructivist theory applications (Cutter, 2001; Müller-Mahn & Everts, 2013; Müller-Mahn et al., 2018; Müller-Mahn, 2013). However, to define risk as having a spatial dimension implies that that space has dimensions that can be measured. This function is notably absent in the literature on riskscapes. Introducing spatial theory to the riskscape structure is one approach to mitigate that deficiency. A conceptual diagram was proposed to incorporate human and social factors (roads, railroads, airports, building units, urban area classifications, and population by census block) in a quantitative risk assessment approach to landslide models. A second contribution in this chapter is the development of a landslide riskscape theoretical framework and spatial risk equation modification by adding spatial measurements to a natural hazard risk equation framework.

Landslide risk assessments in general, when focused on quantitative studies, apply discrete formulae to specific areas to measure loss and damage potential. Yet these risk equations do not account for the measurable spatial extents of the risk factors, whether considering the hazard, the elements at risk, or the consequences for vulnerable elements. The addition of spatial theory methods can account for the spatial dimensions of applied landslide riskscapes. By developing a landslide riskscape formula based on modifications to the risk equation model, I add spatial components to the risk equation model to address this lack of spatial extent modeling. Riskscapes as a constructivist model can then be used to measure landslide features by incorporating the spatial attributes of those features.

Riskscapes as developed in this conceptual model blend social constructivist theory of risk as a constructed and emergent property with risk approaches from spatial theory by creating a framework to include spatial calculations. Understanding and recognizing the anthropogenic influences on the Earth's surface and humans as agents occupying and modifying the spaces they inhabit suggests that the inclusion of social factors in landslide riskscapes can create a more complete understanding of the spatial dimensions of these human-environment interactions.

6.3 Riskscape spatial modeling

The development of a quantitative spatial weighted sum riskscape modeling methodology for landslide riskscapes in Chapter Three yields two important results. First, a mechanism to create the riskscape models is developed and applied to study areas in Colorado. This chapter defines riskscapes for landslides spatially by developing a weighted sum model and analyzing the strength of the spatial relationships between the riskscape factors. Weighting models are developed in three methods, a binary (presence/absence) model, a ranked model based on the frequency ratio of contributing factors, and a human factor weighted model, designed to emphasize the social structures and vulnerable social and human factor elements.

Binary riskscapes have fewer classes and therefore limited utility for detailed assessments though are simple to create and can be easily classified into logical class groupings. Ranked riskscapes emphasize the physical datasets and their interaction with landslide susceptibility features. The standard weighting scheme applied the probabilistic frequency ratio values equally across all physical and human factor features. Human factor riskscapes apply a higher value to all human-related datasets (population, urban classification, building units). This valuation changes the human factor riskscapes to highlight areas where human habitation and activity are more common. The weighting schemes applied in ranked and human factor riskscapes resulted in

significantly more classes due to the weighted sum process. This allows for more detailed view of the interaction of the data features but presents challenges in data visualization. Classification methods need to be applied to reduce the total classes (88 unique values for human factor, and 79 for ranked) to a suitable number. Applications of riskscapes should consider the type of analysis required to determine appropriate weighting schemes.

Second, the inclusion of spatial autocorrelation supports the assessment of spatial relationships between the landslide riskscape factors. The application of spatial autocorrelation can increase the accuracy of assessing the spatial relationships of riskscapes and landslide modeling. Space is a measurable feature and spatial science methods can improve our understanding of landslide riskscapes and risk analyses. The weighted riskscape maps are analyzed using spatial autocorrelation to establish the strength of the spatial relationships between the riskscape factors. Ranked and human factor riskscape models have significant results for spatial autocorrelation clustering, using Global and Anselin Local Moran's *i* analyses. Binary riskscapes demonstrated clustering effect, but due to the limited data classifications, ranked and human riskscape models are preferred. It is important to note that the definitions of parameters in spatial autocorrelation can have significant effect on the degree of outcomes for clustering or dispersion determinations. The spatial definition of neighborhood, distance threshold, and standardization types are important to consider when performing both global and local spatial autocorrelation analyses. Raster classification methods for multi-part (based on classified riskscape factors) or single-part (based on cell value) rasters will also influence the number of cells included in each defined neighborhood. Differences were noted in the Anselin Local Moran's *i* between Boulder and Larimer Counties, due to the influence of the neighborhood function which is based on the size of the study area. Larimer County is

approximately 3.5 times as large as Boulder County, and the neighborhood distance threshold was significantly larger. When the datasets were merged and a consistent neighborhood distance threshold was calculated, the discrepancies disappeared. This indicates that the spatial settings can influence the results of the analysis and therefore should be defined before the analysis.

The spatial modeling methods used to develop these landslide riskscapes can be adapted and generalized to other riskscapes, types of risk, or regions. Spatial workflows presented in Figure 3.2 can be modified to apply other input data types and study area locations to develop riskscapes based on other practices. Further, augmenting these processes with other datasets, temporal data, human-social behavioral data will improve the understanding of complex human-environment interactions.

6.4. Geostatistical riskscapes

The third area of contribution is the geostatistical methodology development to assess landslide riskscapes using logistic regression, probabilistic neural networks, and weights of evidence models in Chapter Four. This approach adapts ArcSDM tools, originally developed to support mineral exploration (Hartley, 2014; McDonnell et al., 2008; Sawatzky et al., 2009) and applied to landslide modeling in Manzo et al. (2013); Poli and Sterlacchini (2007); Prasannakumar and Vijith (2012) to analyze landslide riskscape models. ArcSDM and GeoXplore are open-source toolsets and programs, developed by Looney et al. (2005); Sawatzky et al. (2009) that contain geostatistical tools, including response-based weights of evidence, logistic regression, and neural networks. These tools can be used directly in the Esri GIS products (ArcGIS Desktop and ArcGIS Pro) to create spatially distributed maps of geostatistical probabilities of data inputs.

In Chapter Four, I developed three geostatistical models to establish the probability of landslide riskscapes within the study areas of Boulder and Larimer Counties, Colorado. Weights of evidence models were found to have strong performance, especially for ranked and human factor riskscape models. Logistic regression did not perform as well, resulting in lower probabilities. Neural networks had limited success, with probabilistic neural networks indicating strong probabilities but low AUC values. Significant findings show the weights of evidence model correctly predicted the probability models, whereas logistic regression did not perform as well. Neural networks had high probability models using the probabilistic neural network tool. However, probabilistic neural networks had the lowest validation scores, with AUC values approximating the 0.5 random guess threshold and the lowest area under the curve values. This suggests that riskscape models do not perform in a similar manner to deductively based processes such as landslide susceptibility modeling. As an integrated conceptualization combining human and environmental features, riskscapes are built from spatialized datasets. These datasets are not related by causal relationships but rather spatial, geographic ones. This may explain the overall poor results of logistic regression and neural networks models.

6.5 Spatial data limitations in riskscapes

During the assessments and analyses performed in this dissertation, several limitations in spatial data science were identified, and presented in Chapter Five. Data quality issues are not unique to spatial analyses, but several examples of the influence of spatial data were identified. Authoritative source datasets, those that are publicly available from the agencies responsible for their content, are time-bound. Agencies have collection, maintenance, and publication cycles. Data for the population figures for example are obtained from the U.S. Census Bureau. Decadal census data were dated at the time of this analysis; estimated population data figures are

collected at a smaller scale by the American Community Survey program. These datasets are from the authoritative source agency and represent the best data available but are not "official" population figures from the decadal census counts. Other temporal factors include human behavioral aspects and movements of populations. Physical temporal scales are a consideration as natural systems experience cyclical or abrupt changes (Hungr et al., 2014; Varnes, 1958).

Selection of classification schemes and parameters for analysis also greatly influence the results of the studies. Riskscape data are classified for mapping purposes, as viewing the full calculated classes (13 for Binary, 79 for Ranked, 88 for Human Factor) are not discernable in the maps. Classification schemes in GIS can be manually entered, but default to a natural breaks method (Natural Breaks, Jenks), which classifies data based on an algorithm to maximize the distance between groupings. When using two study areas, as in these studies, natural breaks for one county was not the same as the natural breaks for the other county. To compare the maps effectively, natural break values were rounded and converted to logical numbers (wholes or halves, instead of six decimal places). This made the outputs easier to read but did modify the classification schemes.

Parameter settings were also found to influence data analysis. In evaluating the Global Moran's *i* spatial autocorrelation models, multiple parameters were used. Changes to the conceptualization of space (the algorithm applied such as inverse distance, inverse distance squared, or zone of indifference), the standardization (row neighborhood true or false), and the distance threshold (the area the model is using to define the neighborhood) all influenced the spatial autocorrelation outputs for p-value, z-score, and Moran's index (Chapter Five, Table 5.2).

6.6 Summary of riskscape modeling

Riskscapes for natural hazard risks are complex interactions between humans and their environment. Natural hazard analyses use geospatial tools. As a natural hazard, landslide analysis uses multiple geospatial and geostatistical methods to determine probability of risk and areas susceptible to landslides. Riskscapes demonstrate the spatial dimension of risk by introducing spatial components into natural hazard and landslide risk approaches. Current riskscape literature focuses on the social aspects of risk (Cutter, 2001; Müller-Mahn, 2013) often spatially based on the distribution of vulnerability (Cutter, 1996; Cutter, 1993; Hewitt & Burton, 1971). Quantifiable riskscapes, integrating risk with space in an analytical approach, are a method to use spatial tools to create integrated riskscapes maps. The RiskScape Project approaches natural hazard multi-risk mapping as a loss-modeling tool through an open-source geospatial program (RiskScape, 2016). The approach developed in this dissertation created a weighted sum analysis, applied spatial autocorrelation tools, and used geostatistical methods to determine probabilities of landslide riskscapes in two study areas in Colorado (Figure 6.1). Riskscapes were quantified by combining the physical, human, and infrastructure (built-environment) factors as an integrated human-environment assessment to determine priority areas for landslide mitigation and response planning.

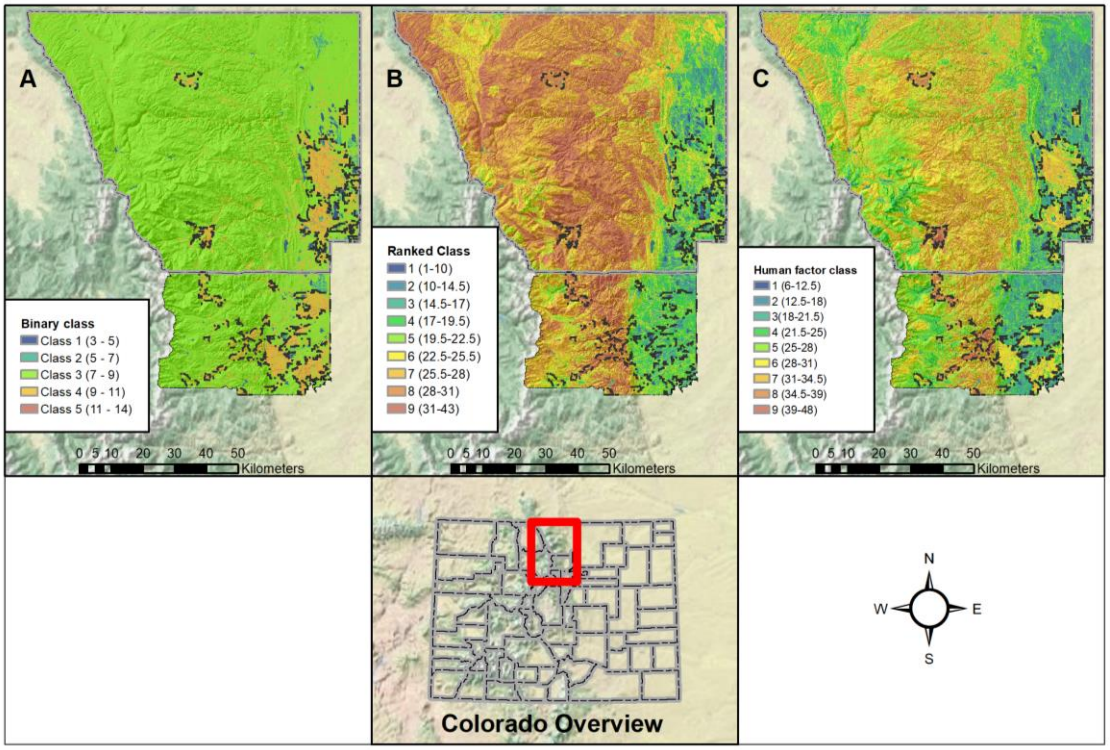

Figure 6.1. Landslide riskscapes in Boulder and Larimer Counties, Colorado. Map A shows binary riskscape values for all classes. Map B is the classified ranked riskscape. Map C is the classified human factor riskscape.

As scientists discuss a new geologic epoch, the Anthropocene (Bohle, 2014; Huang, 2018; Steffen et al., 2007), and human-environment interactions at a geomorphic scale, termed anthropogenic geomorphology (James et al., 2013), a riskscape identifies this human-environment interaction where humans as agents of change are a factor with the same spatial significance as physical geologic and environmental factors. As a timescale reference for measuring geologic time has changed and recognized the human era as a distinct era, this can shift how we evaluate risks. Riskscapes can provide a mechanism to support this transition. Humans are not victims of the geomorphic processes and hazard events, separated from the outcomes only related to perceptions and vulnerability studies. Human and built-environment features are part of the existing landscape and modify the spaces they occupy. Approaching

human factors as contributing surficial features that can be measured in a riskscape approach creates a model for land-use planning, disaster response, and improving our understanding of the spatial distribution of risk.

6.7 Recommendations and future work

6.7.1 Data types and features

Riskscapes can provide a framework to expand our understanding of human-environmental interactions. However, the secondary datasets used in this study are time-bound, and current as of the collection date. Temporal data inclusion for physical features, the study area conditions, and social behavior would enhance the development of riskscapes in several ways. First, diurnal, and nocturnal populations data would improve the ability to understand locations of populations through time. Currently in this study, building datasets acted as a surrogate for population locations (but not numbers). However, these datasets do not reveal the human behavioral aspects or how much time the population occupies the building. The riskscape would change between diurnal and nocturnal residences due to population movement (to offices, schools, or other business activities during the day for example *non-pandemic example). Therefore, planning agencies may need to take the daily schedule for populations into account when evaluating riskscape applications.

Environmental characteristics of the landscape also change over time, sometimes rapidly, sometimes seasonally, or over longer durations. These changes are not reflected in the static datasets. Usage of primary data, or more current data (remote imaging, field data collection) would improve the accuracy of the riskscape models and can improve the usability of the datasets for detailed measurements in local areas. However, focusing on a smaller region would change the characteristics of the riskscape, and may not capture the neighboring influential

factors and human behavioral movements at a regional scale. Additionally, other proximal events that change the characteristics of the landscape, such as wildland fire or building construction will impact the riskscape analysis. Timeliness of data as well as completeness are considerations when using authoritative source datasets. While the timeliness issue may be mitigated by improved data collection practices, this may not be available over a larger region. Data access and availability for spatial datasets are improving, but users do need to understand the currency of the data to determine appropriate use, limitations, and the impact on the analysis.

There are several areas that may be beneficial to investigate as riskscapes and geospatial processing methods continue to evolve. First, a standard, national-level landslide inventory database would be beneficial for all studies of this nature. Landslide data are challenging to obtain at a regional scale. Much effort has been made towards this goal, and that will only serve to improve the accuracy of the analyses and outcomes of the decision-making information. The inclusion of susceptibility factors would assist practitioners and planners in understanding the specific risks landslides present to their communities. Real-time data sources would also improve the modeling for riskscapes.

6.7.2 Methods and approaches

Geostatistical tools are evolving with software application development practices. ArcGIS Pro has expanded to include spatial statistical models previously unavailable in native GIS platforms. Statistical approaches are applied to landslide studies, but often lack the spatial relationship classifications that are provided within spatial science. Expansion of spatial autocorrelation methods would support increased understanding of the relevance space has on landslide factors and riskscapes. Recent work has been done applying fractal methods to

landslide studies (Li et al., 2012; Zhang et al., 2019) and exploring these tools for landslide riskscapes would be a next step.

Another element that would benefit riskscape model development is the evaluation of disaster response-based GIS applications such as HAZUS-MH in the US, which currently does not have a landslide module. HAZUS currently includes seismic, flood, tsunami, and hurricane modules (FEMA, 2021). Given the anticipated effects of climate change, and the projected increase in extreme weather effects, modeling landslides becomes more important and providing more modeling frameworks in the national hazard loss estimation tool would be step forward.

ArcSDM is a robust tool with challenges pertaining to open source supported python code. These issues required additional support from python users to edit the scripts based on missing script components. Changes from the original toolset scripts require revisions to locate input scripts that are stored in new locations. To apply this toolset to future studies, familiarity with scripting and python code is recommended. Ongoing work from sponsoring agencies provides frequent updates to the toolsets, which may eliminate this need in the future. However, due to the open-source development history of this product, support is limited. As the community of practice grows, this may change in the future. Given the number of scripts used to execute each analytical function, it was not uncommon to encounter scripting errors that required debugging procedures. Understanding how to resolve these errors is important for the use of the tools. As ArcGIS Pro replaces ArcGIS Desktop gradually, I recommend using the tools in the ArcGIS Pro environment first, as fewer errors were encountered in the newer GIS product.

6.7.3 Expanding geographies of riskscapes

The quantitative riskscape models presented in these studies can be applied to other regions, other hazards, and other datasets. Specific to landslide riskscapes, applying these methods to

areas of known landslide hazards would be a beneficial study to test the validity of these methods and geostatistical models. Evaluating the scale of studies to determine if larger or smaller regional studies improve modeling outputs in terms of validation and applicability or utility would further our understanding of the limitations of these quantitative models. Expanding quantitative riskscape models to other hazards, and ideally, multiple hazards as suggested by Schmidt et al. (2011) would create a more complete picture of risk within its situational context, and expand our abilities to respond to comprehensive risk in these areas.

6.8 Conclusions

Several key observations are made during this dissertation. First, space matters, but research in landslides and riskscapes do not measure space with spatial tools. Spatial autocorrelation is applied in a limited way to landslide studies (Catani et al., 2016; Erener & Düzgün, 2010; Yang et al., 2019) and not included in riskscape studies. While riskscapes from social constructivist theory may largely focus on qualitative approaches, for natural hazards such as landslides, applying tools to measure the strength of spatial relationships can improve the outcomes of the studies. Spatial autocorrelation allows researchers to determine if space really does matter, and if so, where.

Second, risk and hazards are still defined based on the context for individual research projects, studies, or discussions. Cutter defines risk as a subset of a hazard, or a property of a hazard (2001). Müller-Mahn (2013) approaches risk for riskscapes as an emergent property based on social practices and behaviors of people. A more uniform approach to these commonly used terms would be beneficial, and an attempt to bridge the gap between these approaches is made to establish a common framework for landslide riskscapes.

Riskscapes emerge through the analytical integration of human-environment datasets. Geospatial technology is a platform for integrating information from multiple disciplines into a synthesized view of our world. Natural hazards are effectively increasing, in part due to human factors both direct and indirect, such as development in hazardous areas, climate impacts, and altered land use (James et al., 2013). As populations move into areas that had not previously been developed – for example, the WUI, more people are exposed to landslide hazards. Urbanization as a global phenomenon is also increasing, causing more risky areas to be developed and expanding into sensitive geologic zones (van Westen, 2013)

These landslide risk factors can be combined into a geographically based view of risk, or a riskscape. Typical landslide susceptibility models or risk assessments focus on the geologic and causal factors for landslides to develop geologically based models of where future landslides may occur. The inclusion of the social and human factors, population, infrastructure, political or jurisdictional data, leads to a more robust view of the impacts of landslides occurring in these areas. This inclusive assessment is necessary for the best possible policy development and for decision-makers to have access to the most current and inclusive information.

Looking at riskscapes as a geospatial phenomenon instead of solely a socially emergent one allows us to evaluate the spatial relevance of the riskscape. The inclusion of the spatial domain can enhance our understanding of the emergent properties of space as well as social risk at a new level.

References

Bohle, M. (2014). Recording the Onset of the Anthropocene. In G. Lollino, M. Arattano, M. Giardino, R. Oliveira, & S. Peppoloni (Eds.), *Engineering Geology for Society and Territory* (Vol. 7, pp. 161-163). Springer International Publishing.

Catani, F., Tofani, V., & Lagomarsino, D. (2016). Spatial patterns of landslide dimension: A tool for magnitude mapping. *Geomorphology*, *273*, 361-373. https://doi.org/10.1016/j.geomorph.2016.08.032

Cutter, S. (1996). Societal responses to environmental hazards. *International Social Science Journal*, *48*(4), 525-536.

Cutter, S. L. (1993). *Living with risk : the geography of technological hazards*. London ; New York : E. Arnold ; New York : Routledge, Chapman and Hall distributor.

Cutter, S. L. (2001). *American hazardscapes : the regionalization of hazards and disasters*. Washington, D.C. : Joseph Henry Press.

Erener, A., & Düzgün, H. (2010). Improvement of statistical landslide susceptibility mapping by using spatial and global regression methods in the case of More and Romsdal (Norway). *Landslides*, *7*(1), 55-68. https://doi.org/10.1007/s10346-009-0188-x

FEMA. (2021). *What is Hazus?* U.S. Department of Homeland Security. https://www.fema.gov/flood-maps/tools-resources/flood-map-products/hazus/about

Hartley, B. K. (2014). Evaluation of Weights of Evidence to Predict Gold Occurrences in Northern Minnesota's Archean Greenstone Belts. In: ProQuest Dissertations Publishing.

Hewitt, K., & Burton, I. (1971). *The hazardousness of a place : a regional ecology of damaging events*. University of Toronto Press.

Huang, S.-M. (2018). Understanding disaster (in)justice: Spatializing the production of vulnerabilities of indigenous people in Taiwan. *Environment and planning. E, Nature and space (Print)*, *1*(3), 382-403. https://doi.org/10.1177/2514848618773748

Hungr, O., Leroueil, S., & Picarelli, L. (2014). The Varnes classification of landslide types, an update. *Landslides*, *11*(2), 167-194. https://doi.org/10.1007/s10346-013-0436-y

James, L. A., Harden, C. P., & Clague, J. J. (2013). 13.1 Geomorphology of Human Disturbances, Climate Change, and Hazards. In J. F. Shroder (Ed.), *Treatise on Geomorphology* (pp. 1-13). Academic Press. https://doi.org/https://doi.org/10.1016/B978-0-12-374739-6.00339-0

Li, C., Ma, T., Sun, L., Li, W., & Zheng, A. (2012). Application and verification of a fractal approach to landslide susceptibility mapping. *Natural Hazards*, *61*(1), 169-185. https://doi.org/10.1007/s11069-011-9804-x

Looney, C. G., Wang, Z., & Raines, G. L. (2005). *GeoXplore*. In (Version 5.1) University of Nevada, Reno; United States Geological Survey.

Manzo, G., Tofani, V., Segoni, S., Battistini, A., & Catani, F. (2013). GIS techniques for regional-scale landslide susceptibility assessment: the Sicily (Italy) case study. *International journal of geographical information science : IJGIS*, *27*(7), 1433-1452. https://doi.org/10.1080/13658816.2012.693614

McDonnell, P., Jordan, C., Carney, J., Thomas, C., & Survey, B. G. (2008). *Mineral prospectivity modelling in Ghana's Volta Basin : utilizing ArcSDM to model geological and geophysical data*. Geological Survey of Denmark and Greenland.

Müller-Mahn, D., & Everts, J. (2013). Riskscapes: the spatial dimension of risk. In H.-D. Müller-Mahn & C. Ebooks (Eds.), *The spatial dimension of risk: How geography shapes the emergence of riskscapes*. Routledge.

Müller-Mahn, D., Everts, J., & Stephan, C. (2018). RISKSCAPES REVISITED - EXPLORING THE RELATIONSHIP BETWEEN RISK, SPACE AND PRACTICE. *Erdkunde*, *72*(3), 197-213. https://doi.org/10.3112/erdkunde.2018.02.09

Müller-Mahn, H.-D. (2013). *The spatial dimension of risk: how geography shapes the emergence of riskscapes*. Routledge.

Poli, S., & Sterlacchini, S. (2007). Landslide Representation Strategies in Susceptibility Studies using Weights-of-Evidence Modeling Technique. *Natural resources research (New York, N.Y.)*, *16*(2), 121-134. https://doi.org/10.1007/s11053-007-9043-8

Prasannakumar, V., & Vijith, H. (2012). Evaluation and validation of landslide spatial susceptibility in the Western Ghats of Kerala, through GIS-based Weights of Evidence model and Area Under Curve technique. *Journal of the Geological Society of India*, *80*(4), 515-523. https://doi.org/10.1007/s12594-012-0171-3

Reichenbach, P., Rossi, M., Malamud, B. D., Mihir, M., & Guzzetti, F. (2018). A review of statistically-based landslide susceptibility models. *Earth-Science Reviews*, *180*, 60-91. https://doi.org/10.1016/j.earscirev.2018.03.001

RiskScape, P. (2016). *The RiskScape Project: About the Project*. New Zealand Foundation for Reseaerch, Science, and Technology. Retrieved October 1, 2016 from https://riskscape.niwa.co.nz/about-the-project/funding

Sawatzky, D. L., Raines, G. L., Bonham-Carter, G. F., & Looney, C. G. (2009). Spatial Data Modeller (SDM): ArcMAP 9.3 geoprocessing tools for spatial data modelling using weights of evidence, logistic regression, fuzzy logic and neural networks. http://arcscripts.esri.com/details.asp?dbid=15341

Schmidt, J., Matcham, I., Reese, S., King, A., Bell, R., Henderson, R., Smart, G., Cousins, J., Smith, W., & Heron, D. (2011). Quantitative multi-risk analysis for natural hazards: a framework for multi-risk modeling. *Natural Hazards*, *58*, 1169-1192.

Steffen, W., Crutzen, P. J., & McNeill, J. R. (2007). The Anthropocene: Are Humans Now Overwhelming the Great Forces of Nature. *AMBIO*, *36*(8), 614-621. https://doi.org/10.1579/0044-7447(2007)36[614:TAAHNO]2.0.CO;2

van Westen, C. J. (2013). 3.10 Remote Sensing and GIS for Natural Hazards Assessment and Disaster Risk Management. In J. F. Shroder (Ed.), *Treatise on Geomorphology* (pp. 259-298). Academic Press. https://doi.org/https://doi.org/10.1016/B978-0-12-374739-6.00051-8

Varnes, D. J. (1958). *Landslide types and processes* (Landslides and engineering practice Issue. N. R. Council.

Yang, J., Song, C., Yang, Y., Xu, C., Guo, F., & Xie, L. (2019). New method for landslide susceptibility mapping supported by spatial logistic regression and GeoDetector: A case study of Duwen Highway Basin, Sichuan Province, China. *Geomorphology (Amsterdam, Netherlands)*, *324*, 62-71. https://doi.org/10.1016/j.geomorph.2018.09.019

Zhang, T.-y., Han, L., Zhang, H., Zhao, Y.-h., Li, X.-a., & Zhao, L. (2019). GIS-based landslide susceptibility mapping using hybrid integration approaches of fractal dimension with index of entropy and support vector machine. *Journal of mountain science*, *16*(6), 1275-1288. https://doi.org/10.1007/s11629-018-5337-z

CHAPTER 7: RECOMMENDATIONS AND REFLECTION

This chapter is a reflection on the graduate school experience; my perspectives on the role of spatial analysis and riskscapes, both in natural hazard applications and in higher education; and some reflections on my personal experience as a 'forever' graduate student.

7.1 Riskscape processes and geospatial science, what is next?

7.1.1 Data

There are several areas of recommended further study based on the conclusions found herein, and some were discussed in Chapter Six. Challenges with data access and quality were described in Chapter Five, but bear repeating here. I believe the primary focus for spatial studies should be on data, as quality and access can be challenges. These challenges extend well beyond this paper into many fields and to spatial data in general. Notably, authoritative source data can be hard to find and to identify the quality once you do find it. Data currency and completeness are not always documented in metadata (if available) or other information available on the datasets. As a community of practice, we need to do better at data stewardship. While there is temptation to overshare data using cloud-based mapping applications, such as ArcGIS Online from the Esri GIS application suite, or other online data clearinghouses, some of these data sources are not curated or maintained. This is problematic for data consumers, and the extent of this issue is unknown.

Key observation: Results from any analysis are dependent on data quality. Data quality documentation is sporadic. Data consumers need to recognize these limitations.

7.1.2 Geostatistical methods

As geostatistical software evolves, other geostatistical comparisons, standardization, or level-setting on methods for landslide assessments would be beneficial. This comparison and quantitative work is lacking in riskscape modeling as well. Much work is being done using different statistical models for landslide susceptibility studies, highlighted in the statistical method review work by Reichenbach et al. (2018). Fractal methods are being investigated in works by Lei et al. (2016); Liu et al. (2019); Zhang et al. (2019). There are many options to perform geostatistical analyses developing within commercial GIS software, and even more are available in open-source or specialized statistical software integration. The challenge remains to adequately measure the spatial components of spatial features within these statistical frameworks. More research into how these methods compare would be useful to inform modeling practices.

A concern with GIS modeling and geostatistical tools is how easy they are to access and use. These readily available tools allow users to access many specialized geostatistical models; however, users must be aware of the appropriateness of the toolsets given the desired analytical processes. Active academic research in this area can support business workflows by demonstrating the applicability of geostatistical methods and comparison of those methods to align with the data manipulation and analysis processes.

Key observation: Spatial statistics are relevant in the measurement and study of spatial features, and space matters. GIS interfaces allow for advanced analytical assessments, but users do not necessarily have the knowledge to understand the spatial statistical appropriateness of the tools. Comparative research is one mechanism to inform users of the applications of these tools.

7.1.3 Geographic engagement through technology

GIS technology has undergone tremendous development throughout my career and over the past 60 or so years since it first evolved as a technology application, starting with the Canadian land system in the 1960s and the early works by Roger Tomlinson. It has become ubiquitous; spatial information is everywhere even if it is not referenced or acknowledged as "spatial information." We have seen the emergence of "passive geographers" – people who use the interaction of different environments or systems in the same geographic location as part of their daily routines. People are paying attention to this as a function in their everyday lives. In our current social structure, people have locational information available with smart devices (phones, watches, tablets) and make spatially-based decisions all the time (in actions such as determining which restaurants are nearby or summoning a ride service). As people become more geographically aware for routine information gathering, their awareness of the space they occupy increases.

Key Observation: Geography is re-emerging as a daily activity. Locational awareness is part of our social decision-making processes.

7.1.4 Spatial representation in spatial structures

Riskscapes can support the study of the interface between people and their environment and can be developed to model multiple hazard types at regional scales. As populations are mobile, the riskscape may in fact fluctuate spatially and temporally, depending on criteria applied. This temporal component is well-documented in risk studies (Brenning, 2005) but incorporating that temporal aspect with space is also necessary as the spatial attributes fluctuate in both the human/social and physical environmental factors. Spatial autocorrelation functions

also contribute to our understanding of the spatial aspects of the relationships between features based on the strength of these relationships distributed in space.

Key observation: Both space and time matter in risk analysis, but space needs to also include the dependent nature of spatial autocorrelations, not just locations.

7.1.5 Riskscapes and the Internet of Things (IoT)

Riskscapes as demonstrated in this work can be quantified and operationalized to create a spatially-distinct object to provide insights into the relationships between human and environmental features. However, temporal aspects of riskscapes are difficult to develop due to the fluctuating nature of human movement throughout a landscape and the limitations of available data. Mobile devices and the internet of things – the interconnectedness of devices, and people through their access to these devices, may present an opportunity to address some of these issues with people transacting through the landscape and our ability to provide timely warnings.

Geofencing is a term associated with GIS software, and establishes a threshold boundary that provides notification of movement across the boundary (e.g., objects with tracking devises such as GPS-connected vehicles). Combining the connectedness data from mobile devices through which people share their locations with the population datasets for riskscapes might improve the input data for human factors. A similar model has been used for contact tracing during the COVID-19 pandemic, with residents in Colorado being offered the opportunity to opt in to a mobile device notification systems (Center, 2020). IoT connectedness opportunities exist and could provide data inputs to improve the granularity and temporal data aspects and a notification platform available to people as they transact through risk landscapes.

Key observation: Additional technology applications can support riskscape modifications, through understanding the movements of people through risk landscapes as well as the capability to notify people of the risks present in areas they enter.

7.1.6 Summary of thoughts on riskscapes

Riskscapes are an existing framework from social constructivist theories that place risk spatially, envisioned as a landscape, but rooted in the social constructs related to perception Müller-Mahn (2013). This implies the spatial components are part of the riskscape. These spatial components are not included as measured features in social theory. Borrowing quantitative methods from landslide literature, which is rich in methods to assess risk factors related to landslide hazards, can create a new form of riskscape, one in which space is measured. A quantitative method for riskscapes allows for a different perspective of risk. The landslide riskscape methods presented form a framework to establish these riskscapes in a quantitative model. However, there are many more models that could expand this quantitative riskscape, related to multiple hazards, and adding in more social theory components such as perception and vulnerability as discrete, spatially-mapped factors.

7.2 Potential for a riskscape role in natural hazards educational content

Riskscapes are a newer concept in natural hazards though they have been present for decades in social and vulnerability studies (Cutter, 1996; Cutter, 1994), and they have not yet been deployed to landslide studies at the same rate as to other natural hazard areas, such as multiple hazard studies (Schmidt et al., 2011), or flooding and tsunamis (RiskScape, 2016). Many other analysis methods exist in landslide susceptibility modeling and risk assessment (Guzzetti, 2006; Reichenbach et al., 2018). So how can the information derived from the natural hazard and landslide literature and the processes derived from spatial technology support the

educational platforms for communication of landslide riskscape information? How can we change the story to incorporate the social aspects of risk into a natural hazards framework?

I proposed a framework for practical steps and methods that would evolve the conversation on landslide hazard and risk modeling to incorporate the findings from the literature into some new takeaways that can inform the educational processes on technology applications in landslide hazard assessments. We all know that education is important. This applies to the evolving methods of approaching natural hazard response and study. Landslides, with few restrictions on their locational distributions, occur globally and need to be included in academic approaches as well as community-based education initiatives. As stated by Rouhban (2013) in the forward of Sassa et al (2013), "awareness and education on landslide risk are values which must be raised, and mitigation of the risk is an imperative which must be observed." (Sassa et al., 2013, p. v).

Natural hazards are a special topic in higher education courses. Natural hazard studies offer an interdisciplinary view into the human experience while firmly based in the physical sciences, often framed in geologic and geomorphic processes. Natural hazards occur globally, in many cases unpredictably, and can literally and figuratively reshape the world. Students, in my experience, express amazement at the number of different hazards that occur globally in any given day. Due to the immense scale of many hazard events, there are many communities at risk and different populations that benefit from the prevention and study of natural hazards, and the outcomes of natural hazard assessment and identification.

One challenge to teaching natural hazards through technology applications such as geospatial analysis in the higher-educational realm is the lack of availability of current information in the form of textbooks. There are several challenges when evaluating texts for

undergraduate- or graduate-level courses. One of the primary issues is that with so many hazards to cover, and events occurring daily, some of the best case studies to review are recent enough that they cannot be included in printed, static texts. Catastrophic events can change how responses are planned and developed for future events, create significant loss of life, become media sensations, and of course, completely devastate and reshape the community and global perspectives. Journal articles present an alternative, but do not generally cover basic background information in sufficient depth to set the framework for hazard analyses. Media reporting is often sensationalized and incomplete. What methods then can be used to inform on emerging events in a time-sensitive manner within a classroom context? Perhaps available and flexible technology tools, and models such as a riskscape approach, can be leveraged to act as a response-simulation tool or a reconstruction model to augment instruction in a timeframe that is accessible to coursework and more timely than a textbook edition cycle.

Another challenge in teaching natural hazard courses is the lack of available technology applications specifically focused on natural hazard topics, such as identification, preparation, mitigation, response, and recovery for natural hazard events. Another way of looking at the issue is that texts that are more specific to natural hazard topics generally focus only on the natural hazards themselves, their geologic, geomorphic, or atmospheric context, their geographic distribution globally, and their triggering mechanisms. Occasionally, texts will discuss some of the practices associated with the tactical responses or the preparative steps required to mitigate damages as much as is feasible. These texts are often focused on US-based or "western" types of environments and geographies, perhaps because they may consider those readers to be their audience; to be fair, I am considering English-language textbooks, which further narrows the market. Case studies in these texts discuss how building practices, or engineering developments

can support or help prepare wealthy communities (local to national scales) for natural-hazard defense. But a great many events take place in communities that do not have the same requirements for engineering or building codes, the same transportation networks, or similar economies. These vastly different areas are not always highlighted as having different requirements for the same types of events in terms of how to prepare and mitigate when the basic infrastructure is so different.

Despite GIS being commonly used in the governmental or support agencies responsible for responding to an event, or the availability of the technology to those deployed to a devastated region after an event as part of a response team, these technologies are not often found in the reference materials available to natural hazards education. The GIS applications that are used daily, as part of the preparedness phase in many regions, and critically during event occurrences, are not discussed as a practical solution to the stages of a response scenario.

GIS can be used in a variety of ways for natural hazard assessments and the teaching of these applied practices. Geospatial methods are more focused on each hazard as a separate entity and few processes demonstrate interrelatedness. GIS has evolved into its own academic discipline as distinct from its origins as a technology tool to support environmental research. GIS is considered to have originated in the 1960s in Canada as part of a project to support the Canadian land inventory (see works on Roger Tomlinson). It has evolved significantly over the past 60 years of its existence to be a more computational platform, and has maintained alignment with information technology trends, including protocols such as enterprise data management structures and web-based or cloud tools and mapping systems as well as system enhancements such as advanced processing speeds and storage capabilities.

Communication challenges exist at the multiple levels of natural hazard response. The agencies responsible for stewarding areas, as well as emergency-response situations need to communicate, in some cases immediately, with the local populations as well as transient populations coming through the affected areas. Residents of areas that are prone to landslides, both urban and non-urban, also need to have access to communications from emergency response agencies and the scientific community to best prepare or respond to a landslide event or potential for an event. Evacuation plans need to be available and understood.

For students, understanding the protocols used by local and national agencies for response is valuable if they plan to support or have a career as a GIS practitioner in this field. Standard analytical practices need to be blended with rationales for applications, tools appropriate to the required scopes, as well as data available and plans for workarounds when data are not available. How these studies and outcomes are communicated to the appropriate end-user must also be considered.

These strategies should form a cohesive framework for communicating information appropriate to the community at the appropriate time and level of detail. Technology is a strategic tool to prepare the analysis and communicate and visualize in certain situations. Other situations may not rely on a technology solution if for example, the communication infrastructure is damaged, if there are power station outages, power lines are disrupted, or communication towers damaged, in which case other methods must be used. The scope of this framework does not apply to a critical-level event where no communication systems are available.

Riskscapes can set a context for the programs and processes as related to any natural hazard, but landslides do not have much riskscape background despite the massive amount of literature available on landslide risks. Riskscapes can be used as a communication tool, based in

a technology platform. Specifically, geospatial methods that create riskscapes can be applied to the education about landslides and provide a training platform to demonstrate practical and critical knowledge in multiple aspects of urban planning for disasters and disaster-mitigation strategies. By incorporating riskscapes into technology applications, more applied work can be generated. The focus of a riskscape is more inclusive and holistic in terms of the relationship of the feature, the risk, and the community.

7.3 Personal reflections

My path through graduate school was non-traditional as a classification, though it seems that this term has less meaning as education changes to meet the demands of new markets and generations, and currently, global pandemics. It was marked with life experiences, and extended for well over a decade, almost two. As a working professional, graduate school was never a full-time endeavor for me. I think doctoral students can agree, a certain amount of tenacity is required to remain focused on school and reach the desired outcome. In my case, that desire was moderated by and conflicted with other time commitments. My children were both born while I was completing my master's degree and Ph. D. program. We moved. I changed jobs several times, working full-time as a GIS leader in multiple industries. I teach. My family is engaged in many activities, and as my children grew, so did their own time demands. It is a difficult balancing act, and one you cannot master. But the key for me was focusing on my objective and knowing that doing nothing was not an option – I really wanted to finish school. It is easy to want to stop. It is hard to keep going. Projects change in scope. Data go missing. Life happens. My motivation was that as a teacher, in addition to my other roles, I wanted to demonstrate to my students that goals are achievable. I wanted to model learning behaviors for my children as well. But mostly, I wanted this degree for me. I think of graduate school as a calling. You must want it

enough to put up with the challenges that go along with it. I think the graduate student success equation is:

Equation 7.1.

Desire for degree + tolerance for challenges ≥ challenges to deal with

Also note, I did have another word in mind here.

One challenge I discovered through this process is that I am by trait an inductive person in what is substantively a deductive process. My natural proclivity is to find common ground, act as a collaborator and coordinator; professionally, most of my job functions require a meeting of the minds or enterprise-based approaches. This is the grown-up version of share your toys, play nice, do not run with scissors. Through my childhood academics in a Quaker primary and secondary school system, this tendency to act as peacemaker and observe shared perspectives was reinforced. To find the opposite in dissertation writing, to carve out successively smaller boxes and containers in which to fit your ideas until your ideas are unique and specialized, (and in your mind, maybe profound as well) felt unnatural and confining. The insights came for writing, however, when the boxes were more fully defined, and I had to approach this personal challenge differently. I had to define those successively smaller containers of ideas by determining the commonalities (and gaps) in the other existing small boxes of ideas. Once I was able to switch to that mentality, had that insight, I was able to start gathering and stacking the boxes into a more cohesive narrative. So, if you like to think of yourself as a "big picture" person, a "strategic thinker" and less "detail-oriented", maybe that observation will be helpful to you. I do still want to stomp on the boxes, and break down the walls and barriers between entities, to identify that common and shared space of knowledge, and of humanity. But in this

case, you need to carefully cultivate and refine your boxes to be uniquely you. That was hard for me and took me literally years to figure out.

This is also a challenging time for our discipline, as researchers, scientists, and women in science. Throughout history, people have fought and argued for the right to "science," outside of the confines of church and the state. We are privileged to have the responsibility to create and share knowledge in support of the human endeavor. It becomes a responsibility to communicate, to disseminate, to inform. In this incredibly hostile global environment, with increased attacks on truth, fact, data, scientific methods, so called "intellectualism"—all things which should be cherished yet seem to be vilified, it is hard to stand tall for the pursuit of knowledge. Yet that is the task. I hope this changes. It needs to.

One thing that everyone told me, in particular my advisor who specifically requested this dissertation chapter as a reflection piece, that I did not give proper weight to until the end stages of working on this dissertation was that it does in fact change you. I had heard that and read it in many of the dissertation guidebooks I have perused over the years. But I must admit, I did not really give it much thought. After all, I am a busy, working mother of two and wife, who also works two additional teaching jobs – how could a writing project change me? How could studying a topic more in-depth make a difference to me or my approaches, or my thoughts and behaviors, when my whole life is overscheduled as it is? I did not really think, at my age either, that this process could change me. Dr. Laituri, you were absolutely right. This was a transformation. As I am writing this chapter, throughout 2020 (which is an entirely other story altogether), not quite complete with the rest of the document, I can say that this process does change you. That is because the process is about change. It is not only about the contribution to knowledge; that contribution is the *minimum* requirement to enter the academy. The contribution

is what makes it “official.” But the change, the transformation, must occur within you; you must become the scholar, the peer. I had heard and read of course that only someone who has gone through it can understand that transformation. I find that to be true as well. I did not understand that. The process changes you and only when you change can you complete the journey. Put another way, your journey is not complete unless you have experienced that change, that shift from student to scholar, scientist, researcher, whatever your chosen title may be. I think my teaching workload impeded my acceptance or realization of this, or my understanding of the impact of the shift in mindset, and what it would feel like when that happened. By working and teaching in my subject, I thought I was already in the transition. I was not. I did not recognize that until the writing process was nearing submission completion. So, the first piece of advice I have for other and future students: Pay attention to this transition. I underestimated it, and that hindered my writing. Now that I feel I understand that part of the process better, everything is easier. Also, listen to your advisor.

Advice for future students? Just write. Even when you think you have nothing to say, it is important to write. When you get stuck on one section, move to another. This is another solution that is likely completely obvious to most people that took me forever to resolve in my own mind. When I got stuck, I would think about my problem for weeks and months, and not be as productive as I wanted to be. I should have identified that earlier and switched to working on other sections of the project. Lesson learned. Be prepared for more paperwork than you expect. The academy has a bureaucracy too. I told my kids to “respect the game” when they played lacrosse. I think the same applies to graduate school, especially a doctoral degree. I made the least progress when I lost focus or got lost in the details and all of the inevitable tangents of information that you can discover, or when I forgot that my project had value and that this work

is valuable, and when I forgot about the academic process and paperwork; this was easy for me to do with my professional workload and family commitments. Sometimes you lose yourself in the process and get overwhelmed. It is designed to make you want to give up, which is a shame; this is something I think the academy needs to spend some time reflecting upon. It is actually a beacon of knowledge and enlightenment, and can be a lot of fun, if only at your personal academic level. But any institutional bureaucracy can be tiring, so finding the best way to navigate that is important. Ask for help. Find a writing group or a cohort. If you can keep focused on the good you are doing, the additions to knowledge you are making, you can get through. It is a beautiful journey, and you should be proud.

…

I would be completely remiss if I did not again reiterate my pure gratitude for my advisor, Dr. Melinda Laituri. She has inspired me, motivated me, challenged me, and I would not be here without her. Thank you.

And to my committee, who had to cope with an unusual student, I am grateful for your support; I hope this was not too burdensome. COVID certainly did not help us get together for meetings. I can tell you that I was always excited to see emails from all of you, and it made me feel like progress was possible. And of course, I appreciate your questions regarding this work, as it helped me frame the project differently, and contributed to ideas that eventually formed an additional manuscript to highlight some of the challenges you asked about.

I also again need to acknowledge the support of my family, my parents David and Alice, and my sister Amanda.

My teams at work, all of them, have heard about this project long enough, so I knew it was time to finish so I could start telling new stories. My students and my ever-patient Academic

Directors at the University of Denver and Johns Hopkins University were always an inspiration. My cohort at the WTDD Stuck-to-Unstoppable group are also hard-working, inspirational women working on their advanced degrees, and it was helpful to connect with others in a similar position.

And for my husband Matthew, and my beloved sons Erik and Logan. I love you. Thanks for putting up with me. Sorry this took so long. Mamma is done.

References

Brenning, A. (2005). Spatial prediction models for landslide hazards: review, comparison and evaluation. *Natural Hazards and Earth System Sciences*, *5*(6), 853-862. https://doi.org/10.5194/nhess-5-853-2005

Center, C. S. E. O. (2020). *Exposure Notification*. Colorado Department of Health and Environment. https://covid19.colorado.gov/Exposure-notifications

Cutter, S. (1996). Societal responses to environmental hazards. *International Social Science Journal*, *48*(4), 525-536.

Cutter, S. L. (1994). *Environmental risks and hazards* (S. Cutter, Ed.). Prentice Hall.

Guzzetti, F. (2006). *Landslide hazard and risk assessment: concepts, methods, and tools for the detection and mapping of landslides, for landslide susceptibility zonation and hazard assessment, and for landslide risk evaluation* [Dissertation, University of Bonn]. Bonn, Germany. http://geomorphology.irpi.cnr.it/Members/fausto/PhD-dissertation/Landslide_Hazard_and_Risk_Assessment.pdf

Lei, G., Kunlong, Y., & Thomas, G. (2016). Landslide displacement analysis based on fractal theory, in Wanzhou District, Three Gorges Reservoir, China. *Geomatics, natural hazards and risk*, *7*(5), 1707-1725. https://doi.org/10.1080/19475705.2015.1137241

Liu, L., Li, S., Li, X., Jiang, Y., Wei, W., Wang, Z., & Bai, Y. (2019). An integrated approach for landslide susceptibility mapping by considering spatial correlation and fractal distribution of clustered landslide data. *Landslides*, *16*(4), 715-728. https://doi.org/10.1007/s10346-018-01122-2

Müller-Mahn, H.-D. (2013). *The spatial dimension of risk: how geography shapes the emergence of riskscapes*. Routledge.

Reichenbach, P., Rossi, M., Malamud, B. D., Mihir, M., & Guzzetti, F. (2018). A review of statistically-based landslide susceptibility models. *Earth-Science Reviews*, *180*, 60-91. https://doi.org/10.1016/j.earscirev.2018.03.001

RiskScape, P. (2016). *The RiskScape Project: About the Project*. New Zealand Foundation for Reseaerch, Science, and Technology. Retrieved October 1, 2016 from https://riskscape.niwa.co.nz/about-the-project/funding

Sassa, K., Rouhban, B., Briceño, S., McSaveney, M., & He, B. (2013). *Landslides: Global Risk Preparedness* (1 ed.). Springer-Verlag. https://doi.org/10.1007/978-3-642-22087-6

Schmidt, J., Matcham, I., Reese, S., King, A., Bell, R., Henderson, R., Smart, G., Cousins, J., Smith, W., & Heron, D. (2011). Quantitative multi-risk analysis for natural hazards: a framework for multi-risk modeling. *Natural Hazards*, *58*, 1169-1192.

Zhang, T.-y., Han, L., Zhang, H., Zhao, Y.-h., Li, X.-a., & Zhao, L. (2019). GIS-based landslide susceptibility mapping using hybrid integration approaches of fractal dimension with index of entropy and support vector machine. *Journal of mountain science*, *16*(6), 1275-1288. https://doi.org/10.1007/s11629-018-5337-z

APPENDICES

APPENDIX A: DATA SOURCES

Table A.1. Data sources for riskscape development.

Type	Source	Title	Date Publication
Landslide susceptibility areas	Colorado Geological Survey Open File Reports	Landslide Susceptibility Modeled data	2014 and 2015
Elevation	USGS National Map	Digital Elevation model	2018
Elevation	USGS National Map	Aspect*	2018
Elevation	USGS National Map	Slope degrees*	2018
Elevation	USGS National Map	Curvature*	2018
Geologic Units	Colorado Geological Survey	Lithology	2018
Faults	USGS/Mineral Resources	Faults	2005
Hydrology	USGS National Hydrography Dataset (NHD)	Flowlines (rivers and streams)	2018
Hydrology	USGS National Hydrography Dataset (NHD)	Waterbodies (lakes and reservoirs)	2018
Land cover	USGS GAP	GAP Land cover	2018
Soil	USDA NRCS	Soil	2018
Buildings	Microsoft Open Buildings	Building footprints	2018
Transportation Network	Colorado Department of Transportation	Roads	2018
Transportation Network	Colorado Department of Transportation	Railways	2018
Transportation Network	Colorado Department of Transportation	Airports	2018
Census Population	U.S. Census Bureau	2018 TIGER/Line Shapefiles	2018
Census Urban Areas	U.S. Census Bureau	2018 TIGER/Line Shapefiles	2018

APPENDIX B: APPENDIX TO CHAPTER 3 MANUSCRIPT

B.1 Data sources

Table B.1. List of data sources (* denotes data derived from DEM source)

Type	Source	Title	Date Publication	Type Class
Landslide susceptibility areas	Colorado Geological Survey Open File Reports	Landslide Susceptibility Modeled data	2014 and 2015	Physical hazard
Elevation	USGS National Map	Digital Elevation model	2018	Hazard Factor
Elevation	USGS National Map	Aspect*	2018	Hazard Factor
Elevation	USGS National Map	Slope degrees*	2018	Hazard Factor
Elevation	USGS National Map	Curvature*	2018	Hazard Factor
Geologic Units	Colorado Geological Survey	Lithology	11/20/2013	Hazard Factor
Faults	USGS/Mineral Resources	Faults	2005	Hazard Factor
Hydrology	USGS National Hydrography Dataset (NHD)	Flowlines (rivers and streams)	2018	Hazard Factor
Hydrology	USGS National Hydrography Dataset (NHD)	Waterbodies (lakes and reservoirs)	2018	Hazard Factor
Land cover	USGS GAP	GAP Land cover	2018	Hazard Factor
Soil	USDA NRCS	Soil	2018	Hazard Factor
Buildings	Microsoft Open Buildings	Building footprints	2018	Infrastructure
Transportation Network	Colorado Department of Transportation	Roads	2018	Infrastructure
Transportation Network	Colorado Department of Transportation	Railways	2018	Infrastructure
Transportation Network	Colorado Department of Transportation	Airports	2018	Infrastructure
Census Population	U.S. Census Bureau	2018 TIGER/Line Shapefiles	9/28/2018	Human Factor
Census Urban Areas	U.S. Census Bureau	2018 TIGER/Line Shapefiles	2018	Human Factor

B.2 Methods specifications

1. Settings for GIS parameters and environments settings

The environmental settings were set for each data layer for reclassification:

Changed classes to one class and valued at 1, nodata to 0.

- Cell size was set to 10 meters.
- Processing extent and mask were set to the study area boundaries.

2. Classification

Factors were classified using manual classification based on rounded Natural Breaks (Jenks)

Three classes were used for the Binary reclassification, nine classes were used for both ranked and human factor reclassifications.

3. Spatial Autocorrelation setting (Global Moran's *i*)

a. Input <Feature class>

b. Input Field: <Gridcode>

c. Generate Report: True

d. Conceptualization of Spatial Relationships:

    i. Inverse Distance

    ii. Inverse Distance Square

    iii. Zone of Indifference

    iv. Contiguity edges corners

e. Distance Method: Euclidian

f. Standardization:

    i. None

    ii. Row (true)

g. Distance Band or Threshold Distance:

i. Default system calculations (blank)

ii. 1000 meters (Zone of Indifference)

h. Weight Matrix File:

i. None

APPENDIX C: RESULTS TABLES

This appendix includes the results tables for sixteen factors analyzed for riskscape development in Chapter 3. Areal percent calculations and landslide zonal statistics were used to create the cell percent of areas with and without landslide susceptibility cells.

Table C.1. Landslide percentage for Boulder and Larimer Counties, Colorado. Data source: Colorado Geological Survey. CGS Open File Report datasets 14-02 (Boulder County) and 15-13 (Larimer County). (Morgan, White et al. 2014, Wait, Morgan et al. 2015)

Landslide susceptibility cell status	**Boulder cell count**	**Boulder landslide percent**	**Larimer cell count**	**Larimer landslide percent**
No landslide	17950535	93.68	60000099	88.02
Landslide	1210165	6.32	8167504	11.98
Total landslide cells	19160700	100.00	68167603	100.00

Table C.2. Aspect classes for Boulder and Larimer Counties, showing slope face direction. Data derived from U.S. Geological Survey Digital Elevation Model data.

Aspect class (degrees)	**Boulder aspect class name**	**Boulder slope class percent**	**Boulder no landslide cell count**	**Boulder landslide cell count**	**Boulder landslide percent per slope class**	**Probabilistic Frequency Ratio**	**Binary Weight**	**Ranked Weight**
No Data	No Data	0.11	20833	622	0.05	0.46	0	0
-1-0	Flat	1.30	249111	400	0.03	0.03	1	0.5
0-22.5 and 337.5-360	North	14.36	2563778	188475	15.57	**1.08**	1	1
22.5-67.5	Northeast	15.84	2841269	194651	16.08	**1.02**	1	3
67.5-112.5	East	17.99	3264825	181472	15.00	0.83	1	3
112.5-157.5	Southeast	16.61	3019372	163266	13.49	0.81	1	3
157.5-202.5	South	12.95	2310296	170078	14.05	**1.09**	1	3
202.5-247.5	Southwest	7.40	1284536	134289	11.10	**1.50**	1	3
247.5-292.5	West	5.72	1012314	83334	6.89	**1.20**	1	1
292.5-337.5	Northwest	7.71	1384201	93578	7.73	**1.00**	1	1
Aspect class (degrees)	**Larimer aspect class name**	**Larimer slope class percent**	**Larimer no landslide cell count**	**Larimer landslide cell count**	**Larimer landslide percent per slope class**	**Probabilistic Frequency Ratio**	**Binary Weight**	**Ranked Weight**
No Data	No Data	0.05	34558	825	0.01	0.19	0	0
-1-0	Flat	1.07	725911	1559	0.02	0.02	1	0.5
0-22.5 and 337.5-360	North	13.06	7714542	1185747	14.52	**1.11**	1	1.5
22.5-67.5	Northeast	14.22	8500838	1194150	14.62	**1.03**	1	3
67.5-112.5	East	15.72	9571561	1147074	14.04	0.89	1	3
112.5-157.5	Southeast	14.15	8693194	954944	11.69	0.83	1	3
157.5-202.5	South	13.41	8070673	1073329	13.14	0.98	1	3
202.5-247.5	Southwest	10.06	5923159	934397	11.44	**1.14**	1	3
247.5-292.5	West	8.91	5232541	838746	10.27	**1.15**	1	3

292.5-337.5	Northwest	9.34	5533122	836733	10.24	**1.10**	1	3

Table C.3. Slope classes in degrees for Boulder and Larimer Counties. Data derived from U.S. Geological Survey Digital Elevation Model data.

Slope class (degrees)	**Boulder slope class cell count**	**Boulder slope class percent**	**Boulder no landslide cell count**	**Boulder landslide cell count**	**Boulder landslide percent per slope class**	**Probabilistic Frequency Ratio**	**Binary Weight**	**Ranked Weight**
No Data	21455	0.11	20833	622	0.05	0.46	1	0
0-4	6334949	**33.06**	6316056	18893	1.56	0.05	1	1
4.001-10	3436787	17.94	3303129	133658	11.04	0.62	1	3
10.001-15	2412595	12.59	2246409	166186	13.73	**1.09**	1	3
15.001-20	2100030	10.96	1916450	183580	15.17	**1.38**	1	3
20.001-25	1727220	9.01	1539792	187428	15.49	**1.72**	1	3
25.001-30	1303831	6.80	1129237	174594	14.43	**2.12**	1	3
30.001-35	883911	4.61	737775	146136	12.08	**2.62**	1	3
35.001-40	507659	2.65	404434	103225	8.53	**3.22**	1	1
40.001-86	432263	2.26	336420	95843	7.92	**3.51**	1	1
Slope class (degrees)	**Larimer slope class cell count**	**Larimer slope class percent**	**Larimer no landslide cell count**	**Larimer landslide cell count**	**Larimer landslide percent per slope class**	**Probabilistic Frequency Ratio**	**Binary Weight**	**Ranked Weight**
NoData	35383	0.05	34558	825	0.01	0.19	1	0
0-4	18242880	26.76	17974353	268527	3.29	0.12	1	1
4.001-10	16097024	23.61	14824218	1272806	15.58	0.66	1	3
10.001-15	10625660	15.59	9170424	1455236	17.82	**1.14**	1	3
15.001-20	8338827	12.23	6885655	1453172	17.79	**1.45**	1	3
20.001-25	6051635	8.88	4769720	1281915	15.70	**1.77**	1	3
25.001-30	4053163	5.95	3042699	1010464	12.37	**2.08**	1	3
30.001-35	2456621	3.60	1751345	705276	8.64	**2.40**	1	1
35.001-40	1299963	1.91	889166	410797	5.03	**2.64**	1	1
40.001-86	966447	1.42	657961	308486	3.78	**2.66**	1	1

Table C.4. Elevation classes in meters for Boulder and Larimer Counties. Data derived from U.S. Geological Survey Digital Elevation Model data.

Boulder DEM Elevation in meters	**Boulder elevation class percent**	**Boulder no landslide cell count**	**Boulder landslide cell count**	**Boulder landslide percent per elevation class**	**Probabilistic Frequency Ratio**	**Binary Weight**	**Ranked Weight**
1400 - 1800	38.04	7223929	65037	5.37	0.14	1	1
1800 - 2200	12.60	2119898	295265	24.40	**1.94**	1	3
2200 - 2600	20.13	3537734	319119	26.37	**1.31**	1	3
2600 - 3000	12.98	2385682	101980	8.43	0.65	1	1

3000 - 3400	9.80	1697038	181170	14.97	**1.53**	1	3
3400 - 3800	5.69	866808	223028	18.43	**3.24**	1	3
3800 - 4200	0.74	117645	24444	2.02	**2.72**	1	1
4200 - 4400	0.01	1801	122	0.01	1.00	1	0.5
Larimer DEM Elevation in meters	**Larimer elevation class percent**	**Larimer no landslide cell count**	**Larimer landslide cell count**	**Larimer landslide percent per elevation class**	**Probabilistic Frequency Ratio**	**Binary Weight**	**Ranked Weight**
1400 - 1800	23.10	15296400	449583	5.50	0.24	1	1
1800 - 2200	18.47	10824654	1765249	21.61	**1.17**	1	3
2200 - 2600	23.26	13632224	2223413	27.22	**1.17**	1	3
2600 - 3000	18.82	11009919	1817269	22.25	**1.18**	1	3
3000 - 3400	12.60	7270336	1319699	16.16	**1.28**	1	3
3400 - 3800	3.47	1804115	563792	6.90	**1.99**	1	1
3800 - 4200	0.28	162451	28499	0.35	**1.25**	1	0.5
4200 - 4400	0.00	0	0	0.00	0.00	0	0

Table C.5. Combined curvature classes for Boulder County. Data derived from U.S. Geological Survey Digital Elevation Model data.

Combined Curvature Classes	**Curvature class name**	**Combined curve class percent**	**Landslide percent per curve class**	**Probabilistic Frequency Ratio**	**Binary Weight**	**Ranked Weight**
-2.737 - -0.000001	Negative	49.97	59.51	**1.19**	1	5
-0.000001 - 0.000001	Neutral	1.39	0.05	0.04	0	0
0.000001 - 3.680	Positive	48.65	40.43	0.83	1	5

Table C.6. Combined curvature classes for Larimer County. Data derived from U.S. Geological Survey Digital Elevation Model data.

Combined Curvature Classes	**Curvature class name**	**Areal percent combined curve class**	**Landslide percent by combined curve class**	**Probabilistic Frequency Ratio**	**Binary Weight**	**Ranked Weight**
-1.989861 - -0.000001	Negative	49.20	57.87	**1.18**	1	5
-0.000001 - 0.000001	Neutral	1.14	0.03	0.03	0	0
0.000001 - 2.478489	Positive	49.66	42.10	0.85	1	5

Table C.7. Boulder County hydrology flowlines (50-meter buffer) and landslides percentages.

Near Flowline Status	Areal percent near flowline (50-meters)	Percent landslide near flowline (50-meters)	Probabilistic Frequency Ratio	Binary Weight	Ranked Weight
No Flowline	80.01	57.24	0.72	0	0
Flowline	19.99	42.76	**2.14**	1	5

Table C.8. Boulder County waterbodies (50-meter buffer) and landslides percentages.

Near waterbody status	Areal percent near waterbody (50-meters)	Percent landslide near waterbody (50-meters)	Probabilistic Frequency Ratio	Binary Weight	Ranked Weight
No Waterbody	96.48	98.24	**1.02**	0	0
Waterbody	3.52	1.76	0.50	1	1

Table C.9. Larimer County hydrology flowlines (50-meter buffer) and landslides percentages.

Near flowline status	Areal percent near flowline (50-meters)	Percent landslide near flowline (50-meters)	Probabilistic Frequency Ratio	Binary Weight	Ranked Weight
No Flowline	77.14	62.21	0.81	0	0
Flowline	22.86	37.79	**1.65**	1	5

Table C.10. Larimer County waterbodies (50-meter buffer) and landslides percentages.

Near waterbody status	Areal percent near waterbody (50-meters)	Percent landslide near waterbody (50-meters)	Probabilistic Frequency Ratio	Binary Weight	Ranked Weight
No waterbody	97.36	99.24	**1.02**	0	0
Waterbody	2.64	0.76	0.29	1	1

Table C.11. Boulder County lithologic types and landslide percentages.

Lithologic type	Class	Areal percent lithology	Percent landslides by rock type	Probabilistic Frequency Ratio	Binary Weight	Ranked Weight
Alluvium	1	3.20	0.03	0.01	1	0.5
Shale	2	13.33	1.62	0.12	1	1
Granite	3	35.36	53.34	**1.51**	1	5
Sandstone	4	16.35	6.65	0.41	1	1
Biotite gneiss	5	12.95	25.97	**2.01**	1	3
Glacial drift	6	5.75	3.77	0.66	1	1
Water	7	0.57	0.19	0.33	0	0
Dune sand	8	2.92	0.00	0.00	0	0
Gravel	9	5.31	0.14	0.03	1	0.5
Granitoid	10	2.71	4.02	**1.48**	1	1
Siltstone	11	0.80	3.53	**4.40**	1	1

Felsic gneiss	12	0.73	0.76	**1.03**	1	0.5

Table C.12. Boulder County faults (50-meter buffer) and landslides percentages.

Seismic Value	Areal percent near faults (50-meters)	Percent landslide near faults (50-meters)	Probabilistic Frequency Ratio	Binary Weight	Ranked Weight
No Faults	98.43	98.42	1.00	0	0
Faults	1.57	1.58	1.00	1	1

Table C.13. Larimer County lithologic types and landslide percentages.

Lithologic Type	Class	Areal percent lithology	Percent landslides by rock type	Probabilistic Frequency Ratio	Binary Weight	Ranked Weight
Alluvium	1	1.33	0.06	0.05	1	0.5
Sandstone	2	9.72	4.91	0.50	1	1
Mudstone	3	2.33	1.17	0.50	1	1
Granite	4	34.23	42.05	**1.23**	1	5
Felsic gneiss	5	11.11	13.07	**1.18**	1	3
Shale	6	11.81	0.79	0.07	1	0.5
Siltstone	7	1.15	0.90	0.78	1	0.5
Landslide	8	0.07	0.03	0.37	1	0.5
Biotite gneiss	9	17.80	32.17	**1.81**	1	5
Water	10	0.66	0.04	0.07	0	0
Gravel	11	4.43	0.55	0.12	1	0.5
Clastic	12	0.07	0.15	**2.06**	1	0.5
Glacial drift	13	2.73	2.97	**1.09**	1	1
Ash-flow tuff	14	0.16	0.19	**1.17**	1	0.5
Plutonic rock (phaneritic)	15	0.01	0.02	**1.14**	1	0.5
Dune sand	16	1.86	0.00	0.00	0	0
Intermediate volcanic rock	17	0.51	0.93	**1.81**	1	0.5

Table C.14. Larimer County faults (50-meter buffer) and landslides percentages.

Seismic Value	Areal percent near faults (50-meters)	Percent landslide near faults (50-meters)	Probabilistic Frequency Ratio	Binary Weight	Ranked Weight
No Faults	98.50	97.48	0.99	0	0
Faults	1.50	2.52	**1.68**	1	1

Table C.15. Boulder County soil classification and landslide percentages.

Soil order	Areal percent soil order	No landslide cell count	Landslide cell count	Percent landslide per soil order	Probabilistic Frequency Ratio	Binary Weight	Ranked Weight

Inceptisols	28.86	5142148	388251	32.08	**1.11**	1	5
Entisols	8.77	1612548	68309	5.64	0.64	1	1
Alfisols	12.50	2258689	136124	11.25	0.90	1	3
Mollisols	39.99	7348678	314044	25.95	0.65	1	3
Bodies of Water	1.97	374331	3565	0.29	0.15	0	0
No Soil	3.26	461365	163364	13.50	**4.14**	1	3
Aridisols	2.35	448907	875	0.07	0.03	1	0.5
Unknown/Data Not Available	2.29	303869	135633	11.21	**4.89**	1	3

Table C.16. Larimer County soil classification and landslide percentages.

Soil order	Areal percent soil order	No landslide cell count	Landslide cell count	Percent landslides per soil order	Probabilistic Frequency Ratio	Binary Weight	Ranked Weight
Inceptisols	28.89	16417876	3274320	40.09	**1.39**	1	5
Mollisols	37.26	22856144	2539699	31.10	0.83	1	5
Entisols	5.86	3821087	174736	2.14	0.36	1	1
Alfisols	18.81	11473553	1345751	16.48	0.88	1	3
Unknown/Data Not Available	0.47	200229	121618	1.49	**3.15**	1	1
Bodies of Water	1.33	882607	22419	0.27	0.21	0	0
No Soil	3.15	1545503	600369	7.35	**2.34**	1	1
Aridisols	3.77	2555288	13152	0.16	0.04	1	1
Histosols	0.01	3051	359	0.00	0.88	0	0
Spodosols	0.47	243784	75081	0.92	**1.97**	1	1

Table C.17. Boulder County land cover and landslide percentages.

GAP Type Value	Land cover description	Areal percent land cover class	Percent landslide per land cover class	Probabilistic Frequency Ratio	Binary Weight	Ranked Weight
145	Inter-Mountain Basins Aspen-Mixed Conifer Forest and Woodland	0.01	0.02	**3.79**	1	0.5
148	Rocky Mountain Aspen Forest and Woodland	0.56	0.80	**1.43**	1	0.5
149	Rocky Mountain Lodgepole Pine Forest	12.69	7.38	0.58	1	1
151	Rocky Mountain Subalpine Dry-Mesic Spruce-Fir Forest and Woodland	3.26	3.34	**1.03**	1	1
152	Rocky Mountain Subalpine Mesic Spruce-Fir Forest and Woodland	3.49	4.46	**1.28**	1	1
153	Rocky Mountain Subalpine-Montane Limber-Bristlecone Pine Woodland	0.01	0.00	0.32	0	0

155	Southern Rocky Mountain Dry-Mesic Montane Mixed Conifer Forest and Woodland	1.03	2.87	**2.78**	1	1
156	Southern Rocky Mountain Mesic Montane Mixed Conifer Forest and Woodland	4.14	7.57	**1.83**	1	1
158	Southern Rocky Mountain Ponderosa Pine Woodland	21.24	31.56	**1.49**	1	5
183	Great Basin Pinyon-Juniper Woodland	0.00	0.00	**3.30**	0	0
189	Southern Rocky Mountain Pinyon-Juniper Woodland	0.00	0.00	0.00	0	0
192	Western Great Plains Floodplain	0.49	0.00	0.00	0	0
194	Western Great Plains Riparian Woodland and Shrubland	1.30	0.11	0.08	1	0.5
270	Rocky Mountain Lower Montane Riparian Woodland and Shrubland	0.03	0.11	**3.45**	1	0.5
272	Rocky Mountain Subalpine-Montane Riparian Woodland	0.51	0.99	**1.94**	1	0.5
312	Northern Rocky Mountain Montane-Foothill Deciduous Shrubland	0.00	0.00	0.41	0	0
315	Southern Rocky Mountain Montane-Subalpine Grassland	0.76	0.59	0.78	1	0.5
316	Rocky Mountain Gambel Oak-Mixed Montane Shrubland	0.44	0.76	**1.72**	1	0.5
317	Rocky Mountain Lower Montane-Foothill Shrubland	3.64	6.67	**1.83**	1	1
323	Rocky Mountain Subalpine-Montane Mesic Meadow	0.07	0.01	0.10	1	0.5
326	Western Great Plains Foothill and Piedmont Grassland	2.75	1.12	0.41	1	1
329	Western Great Plains Sandhill Steppe	0.02	0.00	0.05	0	0
331	Western Great Plains Shortgrass Prairie	0.73	0.01	0.01	1	0.5
438	Rocky Mountain Alpine-Montane Wet Meadow	0.14	0.21	**1.46**	1	0.5
439	Rocky Mountain Subalpine-Montane Riparian Shrubland	1.27	1.96	**1.54**	1	1
443	North American Arid West Emergent Marsh	0.00	0.00	0.00	0	0
458	Inter-Mountain Basins Playa	0.02	0.03	**1.51**	1	0.5
485	Inter-Mountain Basins Mixed Salt Desert Scrub	0.00	0.00	0.00	0	0
489	Inter-Mountain Basins Big Sagebrush Shrubland	0.01	0.01	**1.39**	1	0.5
491	Inter-Mountain Basins Montane Sagebrush Steppe	0.49	0.38	0.78	1	0.5
502	Rocky Mountain Alpine Fell-Field	0.35	0.36	**1.04**	1	0.5
503	Rocky Mountain Alpine Turf	2.10	2.84	**1.35**	1	1
529	Rocky Mountain Cliff, Canyon and Massive Bedrock	0.17	0.63	**3.80**	1	0.5

536	Southwestern Great Plains Canyon	0.01	0.00	0.12	0	0
537	Western Great Plains Cliff and Outcrop	0.01	0.00	0.13	0	0
545	Inter-Mountain Basins Active and Stabilized Dune	0.00	0.00	0.00	0	0
549	Rocky Mountain Alpine Bedrock and Scree	4.63	20.96	**4.53**	1	3
554	North American Alpine Ice Field	0.05	0.41	**8.50**	1	0.5
556	Cultivated Cropland	12.04	0.05	0.00	1	0.5
557	Pasture/Hay	4.07	0.09	0.02	1	0.5
558	Introduced Upland Vegetation - Annual Grassland	0.03	0.01	0.28	1	0.5
559	Introduced Upland Vegetation - Perennial Grassland and Forbland	2.65	0.50	0.19	1	0.5
561	Introduced Upland Vegetation - Shrub	0.59	0.55	0.93	1	0.5
562	Introduced Riparian and Wetland Vegetation	0.00	0.00	0.00	0	0
566	Recently Logged Areas	0.00	0.00	0.00	0	0
567	Harvested Forest - Grass/Forb Regeneration	0.01	0.00	0.43	0	0
568	Harvested Forest-Shrub Regeneration	0.00	0.00	0.00	0	0
570	Recently Burned	0.00	0.00	**3.07**	0	0
574	Disturbed/Successional - Grass/Forb Regeneration	0.12	0.02	0.21	1	0.5
575	Disturbed/Successional - Shrub Regeneration	0.42	0.49	**1.19**	1	0.5
579	Open Water (Fresh)	1.84	0.16	0.09	0	0
580	Quarries, Mines, Gravel Pits and Oil Wells	0.00	0.00	0.97	0	0
581	Developed, Open Space	3.44	1.01	0.29	1	1
582	Developed, Low Intensity	5.58	0.84	0.15	1	0.5
583	Developed, Medium Intensity	2.23	0.10	0.04	1	0.5
584	Developed, High Intensity	0.56	0.00	0.01	0	0

Table C.18. Larimer County land cover and landslide percentages.

GAP Type Value	**Land cover description**	**Areal percent land cover class**	**Percent landslides per land cover class**	**Probabilistic Frequency Ratio**	**Binary Weight**	**Ranked Weight**
137	Middle Rocky Mountain Montane Douglas-fir Forest and Woodland	0.00	0.00	0.00	0	0
138	Northern Rocky Mountain Dry-Mesic Montane Mixed Conifer Forest	0.05	0.06	**1.21**	1	0.5
140	Northern Rocky Mountain Mesic Montane Mixed Conifer Forest	0.15	0.23	**1.51**	1	0.5
144	Rocky Mountain Foothill Limber Pine-Juniper Woodland	1.82	1.06	0.58	1	1

145	Inter-Mountain Basins Aspen-Mixed Conifer Forest and Woodland	0.01	0.04	**3.33**	1	0.5
148	Rocky Mountain Aspen Forest and Woodland	0.76	1.34	**1.76**	1	0.5
149	Rocky Mountain Lodgepole Pine Forest	18.27	18.88	**1.03**	1	3
151	Rocky Mountain Subalpine Dry-Mesic Spruce-Fir Forest and Woodland	5.30	6.04	**1.14**	1	1
152	Rocky Mountain Subalpine Mesic Spruce-Fir Forest and Woodland	4.56	7.64	**1.68**	1	1
153	Rocky Mountain Subalpine-Montane Limber-Bristlecone Pine Woodland	0.01	0.00	0.64	0	0
155	Southern Rocky Mountain Dry-Mesic Montane Mixed Conifer Forest and Woodland	0.69	1.83	**2.65**	1	1
156	Southern Rocky Mountain Mesic Montane Mixed Conifer Forest and Woodland	2.41	4.88	**2.02**	1	1
158	Southern Rocky Mountain Ponderosa Pine Woodland	13.75	21.56	**1.57**	1	3
183	Great Basin Pinyon-Juniper Woodland	0.00	0.00	**1.75**	0	0
184	Inter-Mountain Basins Curl-leaf Mountain Mahogany Woodland and Shrubland	0.00	0.00	0.00	0	0
187	Colorado Plateau Pinyon-Juniper Woodland	0.10	0.03	0.34	1	0.5
189	Southern Rocky Mountain Pinyon-Juniper Woodland	0.00	0.00	0.00	0	0
191	Northwestern Great Plains Riparian	0.00	0.00	0.42	0	0
192	Western Great Plains Floodplain	0.13	0.00	0.00	0	0
194	Western Great Plains Riparian Woodland and Shrubland	0.37	0.10	0.27	1	0.5
270	Rocky Mountain Lower Montane Riparian Woodland and Shrubland	0.02	0.02	**1.14**	1	0.5
272	Rocky Mountain Subalpine-Montane Riparian Woodland	0.27	0.69	**2.56**	1	0.5
312	Northern Rocky Mountain Montane-Foothill Deciduous Shrubland	0.00	0.00	0.08	0	0
315	Southern Rocky Mountain Montane-Subalpine Grassland	1.44	1.40	0.97	1	1
316	Rocky Mountain Gambel Oak-Mixed Montane Shrubland	0.20	0.41	**2.10**	1	0.5
317	Rocky Mountain Lower Montane-Foothill Shrubland	8.39	11.85	**1.41**	1	3
323	Rocky Mountain Subalpine-Montane Mesic Meadow	0.06	0.07	**1.14**	1	0.5
325	Northwestern Great Plains Mixedgrass Prairie	0.76	0.19	0.26	1	0.5

326	Western Great Plains Foothill and Piedmont Grassland	4.32	3.28	0.76	1	1
329	Western Great Plains Sandhill Steppe	0.06	0.01	0.15	1	0.5
331	Western Great Plains Shortgrass Prairie	4.64	0.25	0.05	1	0.5
398	Rocky Mountain Subalpine-Montane Fen	0.00	0.00	0.00	0	0
427	Western Great Plains Open Freshwater Depression Wetland	0.01	0.00	0.05	0	0
438	Rocky Mountain Alpine-Montane Wet Meadow	0.06	0.08	**1.21**	1	0.5
439	Rocky Mountain Subalpine-Montane Riparian Shrubland	1.34	1.94	**1.45**	1	1
443	North American Arid West Emergent Marsh	0.01	0.00	0.08	0	0
445	Western Great Plains Saline Depression Wetland	0.10	0.08	0.75	1	0.5
457	Inter-Mountain Basins Greasewood Flat	0.02	0.00	0.07	0	0
458	Inter-Mountain Basins Playa	0.07	0.02	0.22	1	0.5
484	Inter-Mountain Basins Mat Saltbush Shrubland	0.08	0.00	0.02	0	0
485	Inter-Mountain Basins Mixed Salt Desert Scrub	0.17	0.00	0.03	0	0
486	Inter-Mountain Basins Wash	0.01	0.00	0.03	0	0
489	Inter-Mountain Basins Big Sagebrush Shrubland	0.04	0.05	**1.30**	1	0.5
490	Inter-Mountain Basins Big Sagebrush Steppe	2.85	0.79	0.28	1	0.5
491	Inter-Mountain Basins Montane Sagebrush Steppe	4.02	2.78	0.69	1	1
495	Wyoming Basins Dwarf Sagebrush Shrubland and Steppe	0.67	0.17	0.25	1	0.5
498	Inter-Mountain Basins Semi-Desert Shrub Steppe	0.04	0.01	0.24	1	0.5
502	Rocky Mountain Alpine Fell-Field	0.37	0.36	0.95	1	0.5
503	Rocky Mountain Alpine Turf	1.69	2.65	**1.56**	1	1
529	Rocky Mountain Cliff, Canyon and Massive Bedrock	0.15	0.32	**2.13**	1	0.5
536	Southwestern Great Plains Canyon	0.02	0.00	0.15	0	0
537	Western Great Plains Cliff and Outcrop	0.06	0.00	0.07	0	0
545	Inter-Mountain Basins Active and Stabilized Dune	0.00	0.00	**8.35**	0	0
546	Inter-Mountain Basins Cliff and Canyon	0.00	0.00	0.31	0	0
547	Inter-Mountain Basins Shale Badland	0.00	0.00	0.39	0	0
549	Rocky Mountain Alpine Bedrock and Scree	1.99	5.78	**2.90**	1	1
554	North American Alpine Ice Field	0.01	0.04	**3.95**	1	0.5
556	Cultivated Cropland	7.52	0.21	0.03	1	0.5

557	Pasture/Hay	1.89	0.19	0.10	1	0.5
558	Introduced Upland Vegetation - Annual Grassland	0.04	0.02	0.57	1	0.5
559	Introduced Upland Vegetation - Perennial Grassland and Forbland	1.46	0.46	0.31	1	0.5
561	Introduced Upland Vegetation - Shrub	0.16	0.14	0.92	1	0.5
562	Introduced Riparian and Wetland Vegetation	0.00	0.00	0.00	0	0
566	Recently Logged Areas	0.01	0.00	0.40	0	0
567	Harvested Forest - Grass/Forb Regeneration	0.37	0.08	0.23	1	0.5
568	Harvested Forest-Shrub Regeneration	0.01	0.00	0.16	0	0
570	Recently Burned	0.00	0.00	0.83	0	0
572	Recently burned shrubland	0.00	0.00	0.79	0	0
574	Disturbed/Successional - Grass/Forb Regeneration	0.10	0.03	0.32	1	0.5
575	Disturbed/Successional - Shrub Regeneration	0.20	0.26	**1.31**	1	0.5
579	Open Water (Fresh)	1.26	0.08	0.06	0	0
580	Quarries, Mines, Gravel Pits and Oil Wells	0.06	0.01	0.23	1	0.5
581	Developed, Open Space	1.69	1.01	0.59	1	1
582	Developed, Low Intensity	1.90	0.48	0.25	1	0.5
583	Developed, Medium Intensity	0.80	0.06	0.08	1	0.5
584	Developed, High Intensity	0.19	0.01	0.04	1	0.5

Table C.19. Boulder County urban area classifications and landslide percentages.

Urban Classification	Areal percent urban area	Percent landslides in urban areas	Probabilistic Frequency Ratio	Binary Weight	Ranked Weight	Human Factors Weight
Not Urban	78.85	91.36	**1.16**	0	0	0
Urban	21.15	8.64	0.41	1	5	5

Note: Urban class includes urban place and urban cluster from US Census Bureau.

Table C.20. Larimer County urban area classifications and landslide percentages.

Urban Classification	Areal percent urban area	Percent landslides in urban areas	Probabilistic Frequency Ratio	Binary Weight	Ranked Weight	Human Factors Weight
Not Urban	93.28	99.18	**1.06**	0	0	0
Urban	6.72	0.82	0.12	1	5	5

Note: Urban class includes urban place and urban cluster from US Census Bureau.

Table C.21. Boulder County building buffer (100-meter) and landslide percentages.

Building Presence	Areal percent buildings	Percent buildings near landslides	Probabilistic Frequency Ratio	Binary Weight	Ranked Weight	Human Factors Weight

No Buildings	77.74	92.59	**1.19**	0	0	0
Buildings	22.26	7.41	0.33	1	5	5

Table C.22. Larimer County building buffer (100-meter) and landslide percentages.

Building Presence	Areal percent buildings	Percent buildings near landslides	Probabilistic Frequency Ratio	Binary Weight	Ranked Weight	Human Factors Weight
No Buildings	89.56	95.48	**1.07**	0	0	0
Buildings	10.44	4.52	0.43	1	5	5

Table C.23. Boulder County population values within Census blocks and landslide percentages.

Population Range	Areal percent population by block	Percent landslides by population block	Probabilistic Frequency Ratio	Binary Weight	Ranked Weight	Human Factors Weight
No Data	0.02	0.00	0.24	0	0	0
0	18.62	24.03	**1.29**	1	3	5
1-25	37.98	37.74	0.99	1	5	5
25-100	28.79	28.49	0.99	1	3	5
100-300	12.71	9.51	0.75	1	1	5
300-500	1.29	0.22	0.17	1	0.5	5
500-1000	0.54	0.00	0.00	0	0	0
>1000	0.05	0	0.00	0	0	0

Table C.24. Larimer County population values within Census blocks and landslide percentages.

Population Range	Areal percent population by block	Percent landslides by population block	Probabilistic Frequency Ratio	Binary Weight	Ranked Weight	Human Factors Weight
No Data	0.00	0.00	0.03	0	0	0
<1	39.32	36.89	0.94	1	5	5
1 - 25	34.92	38.28	**1.10**	1	5	5
25 - 100	16.63	15.87	0.95	1	3	5
100 - 300	7.82	8.22	**1.05**	1	1	5
300 - 500	1.15	0.74	0.64	1	0.5	5
500 - 1000	0.16	0.00	0.00	0	0	5
>1000	0.01	0.00	0.00	0	0	5

Table C.25. Boulder County transportation and landslide percentages.

Transportation Type	Areal Percent Roadways	Areal Percent Landslides near Roads (50-meter)	Probabilistic Frequency Ratio	Binary Weight	Ranked Weight
No Roads	87.13	94.80	**1.09**	0	0
Roads	12.87	5.20	0.40	1	1

	Areal Percent Railroads	Areal Percent Landslides near Railroads (50-meter)	Probabilistic Frequency Ratio	Binary Weight	Ranked Weight
No Railroads	99.37	99.80	**1.00**	0	0
Railroads	0.63	0.20	0.32	1	1
	Areal Percent Airports	**Areal Percent Landslide near Airport (500-meters)**	**Probabilistic Frequency Ratio**	**Binary Weight**	**Ranked Weight**
No Airports	99.92	100	**1.00**	0	0
Airports	0.08	0	0.00	1	1

Table C.26. Larimer County transportation and landslide percentages.

Transportation Type	Areal Percent Roadways	Areal Percent Landslides near Roads (50-meter)	Probabilistic Frequency Ratio	Binary Weight	Ranked Weight
No Roads	93.96	96.68	**1.03**	0	0
Roads	6.04	3.32	0.55	1	1
	Areal Percent Railroads	**Areal Percent Landslides near Railroads (50-meter)**	**Probabilistic Frequency Ratio**	**Binary Weight**	**Ranked Weight**
No Railroads	99.71	99.95	**1.00**	0	0
Railroads	0.29	0.05	0.17	1	1
	Areal Percent Airports	**Areal Percent Landslide near Airport (500-meters)**	**Probabilistic Frequency Ratio**	**Binary Weight**	**Ranked Weight**
No Airports	99.99	100.00	**1.00**	0	0
Airports	0.01	0.00	0	1	1

APPENDIX D: MODELBUILDER DATA PROCESSING MODELS

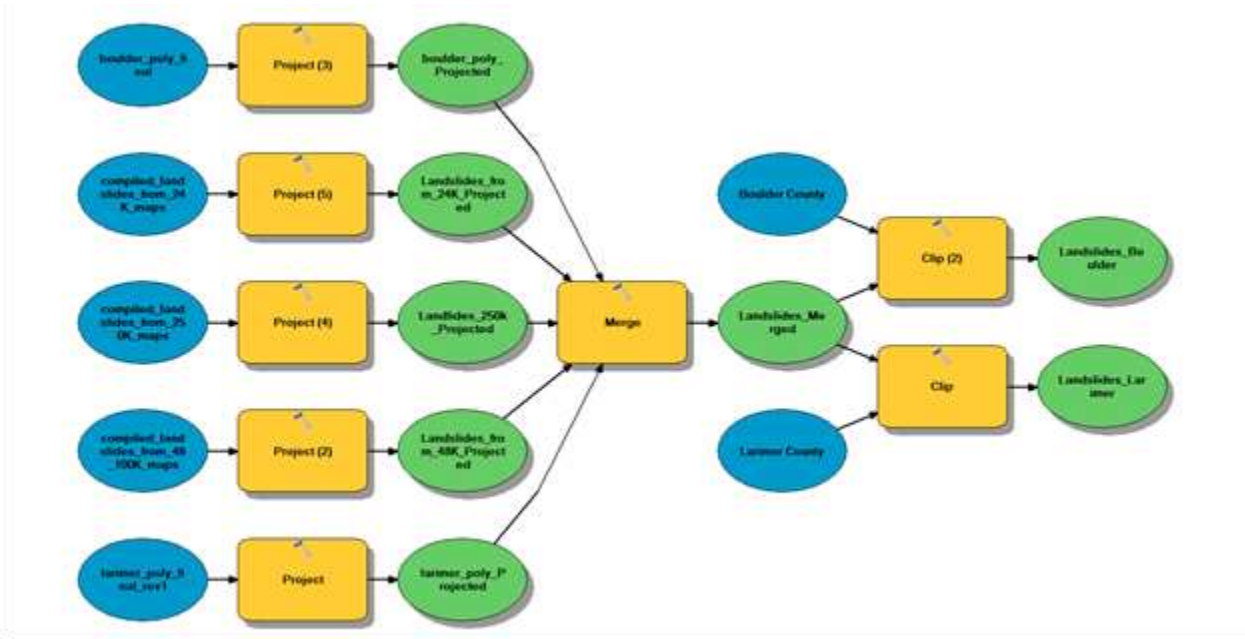

Figure D.1. Landslide preprocessing model.

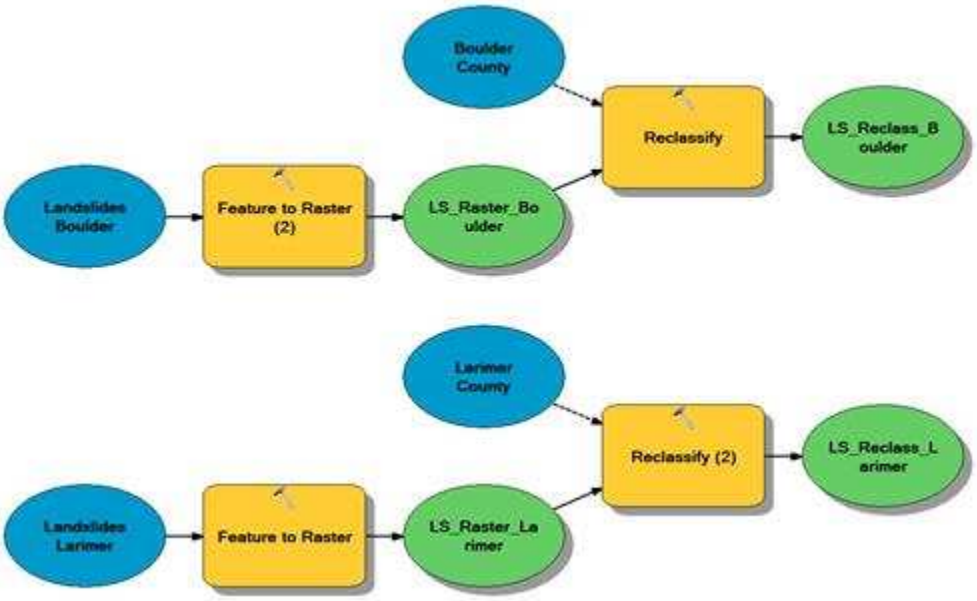

Figure D.2. Landslide processing model.

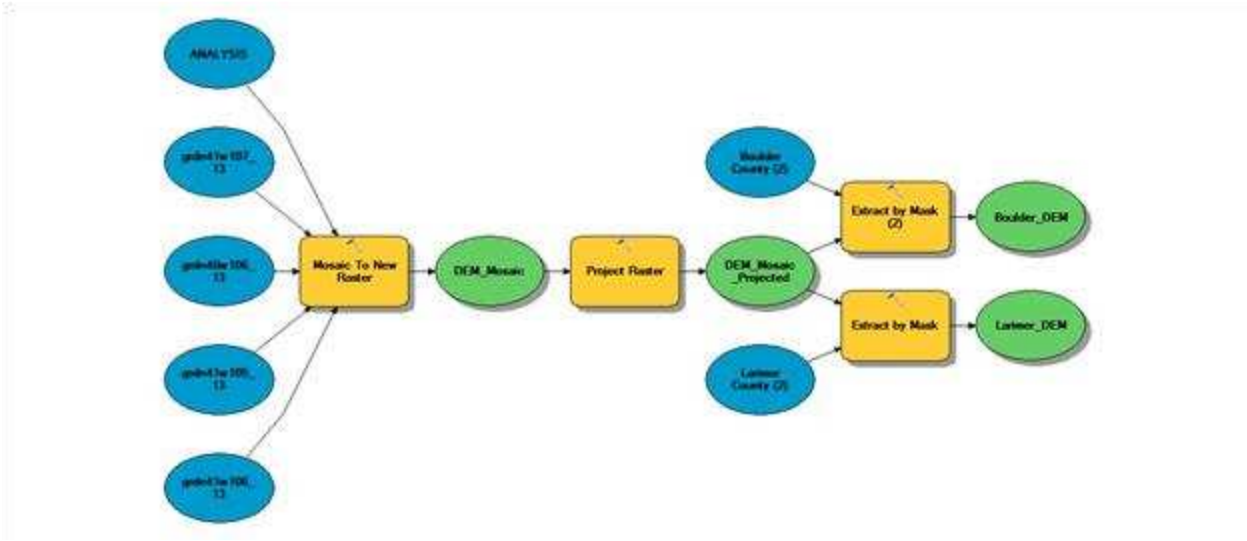

Figure D.3. DEM processing model.

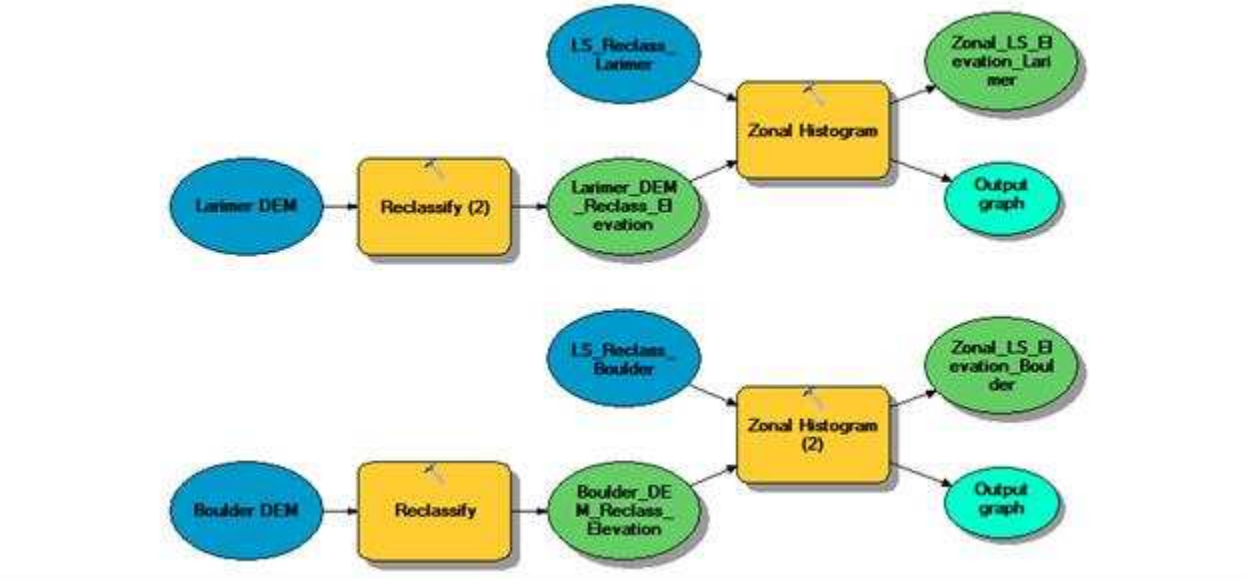

Figure D.4. Elevation reclassification model.

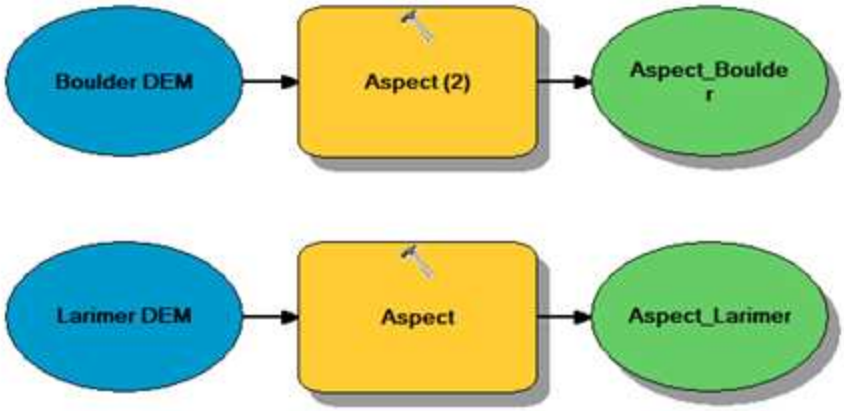

Figure D.5. DEM to aspect model.

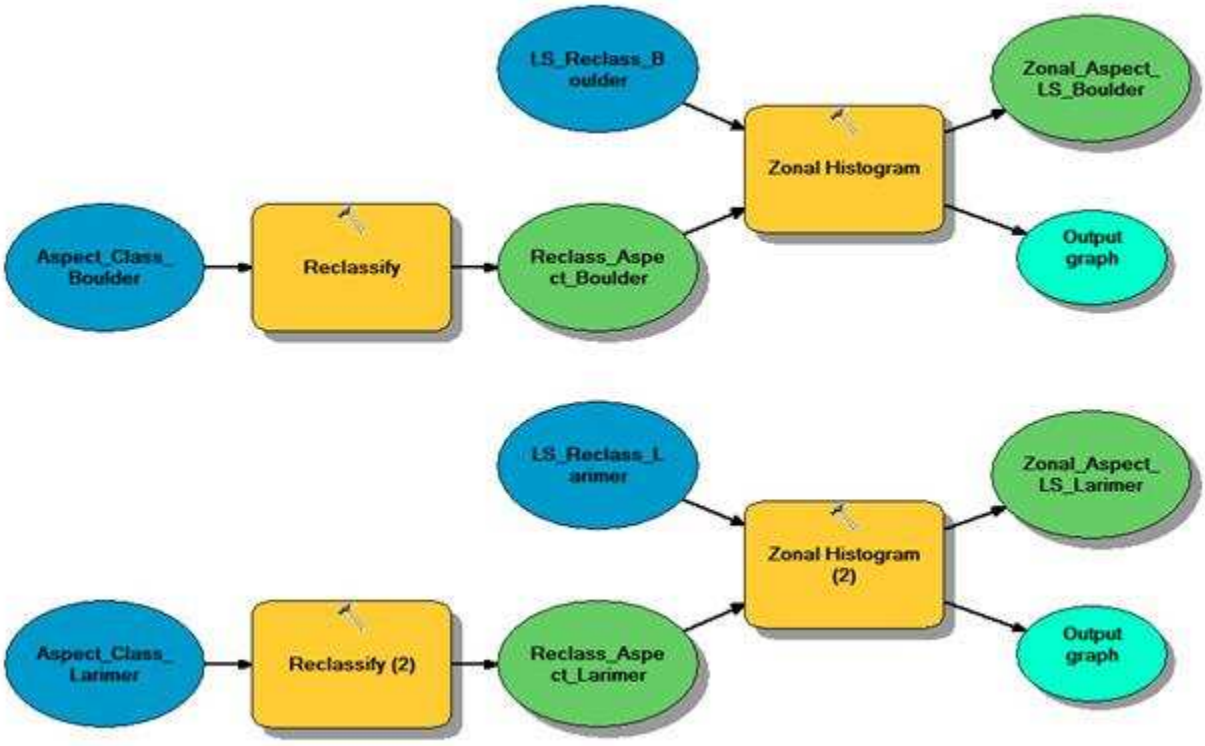

Figure D.6. Aspect processing model.

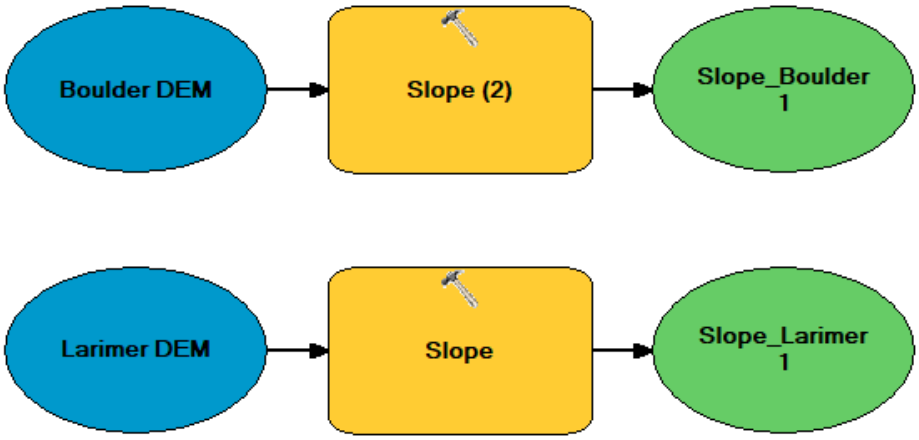

Figure D.7. Slope preprocessing model.

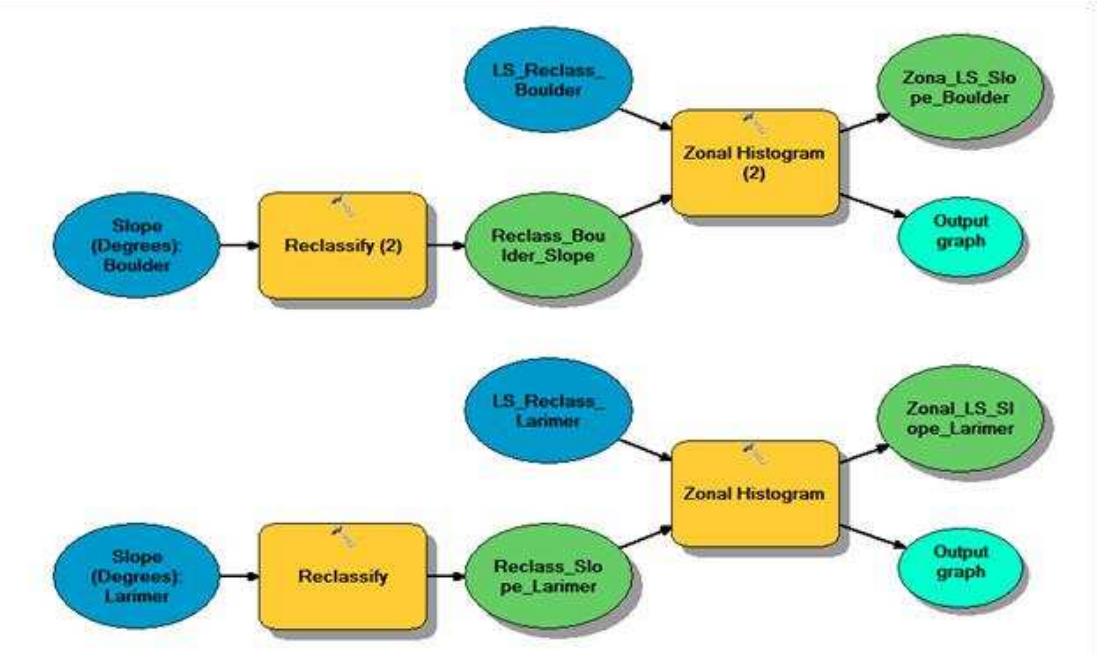

Figure D.8. Slope processing model.

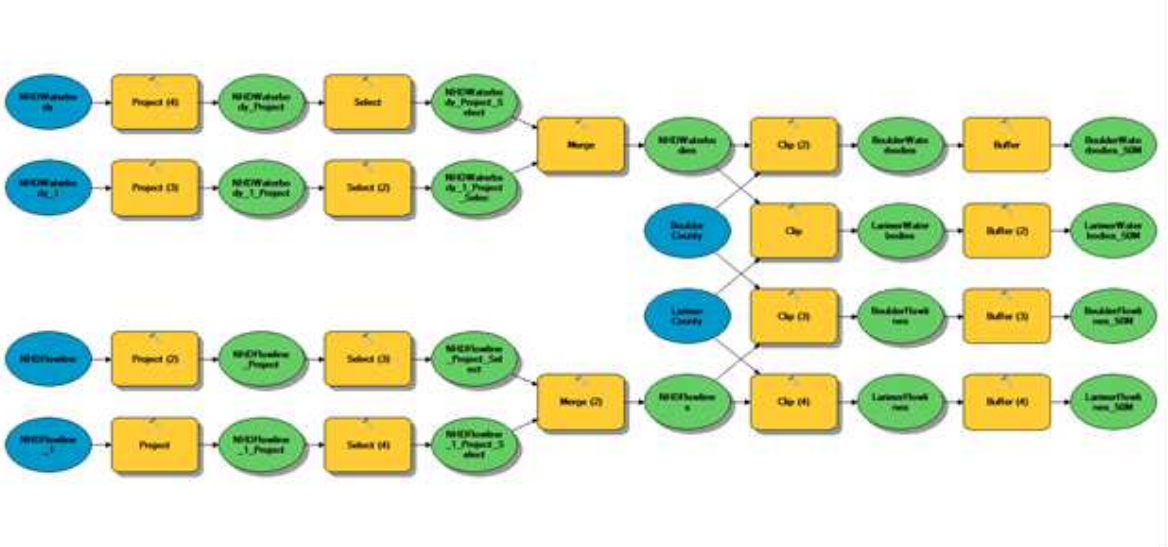

Figure D.9. Hydrology preprocessing model.

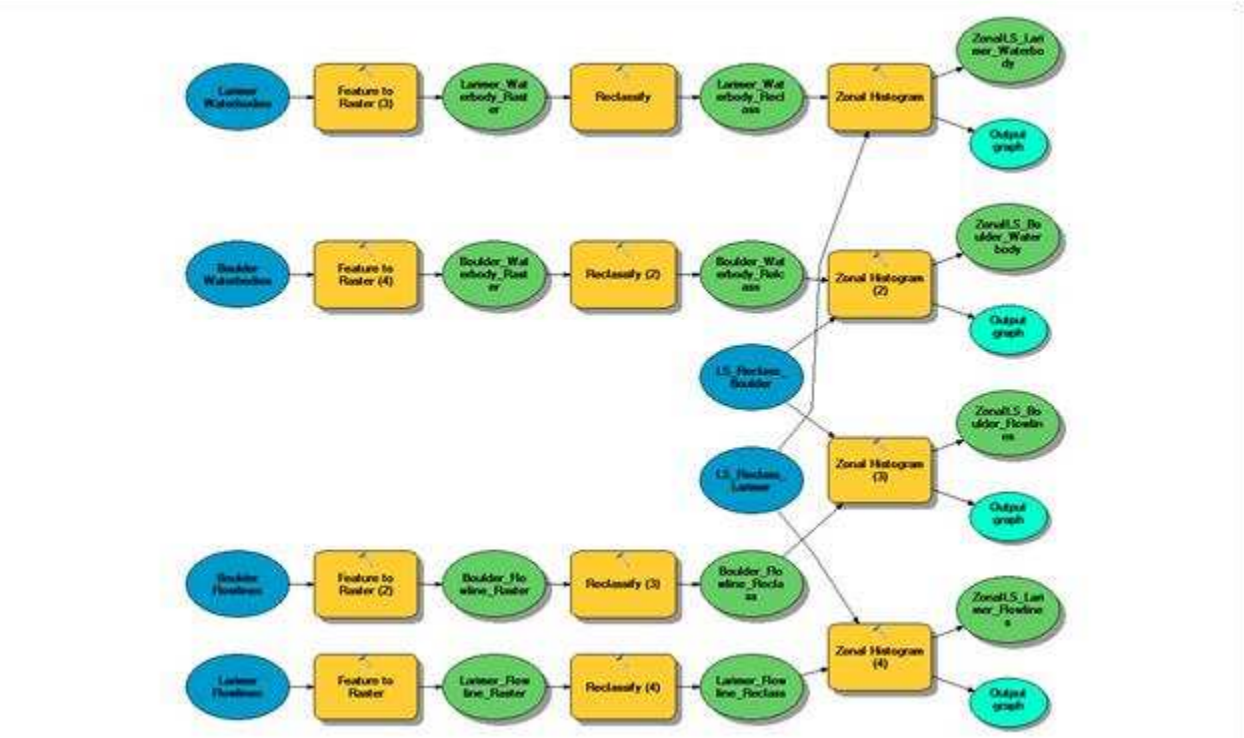

Figure D.10. Hydrology processing model.

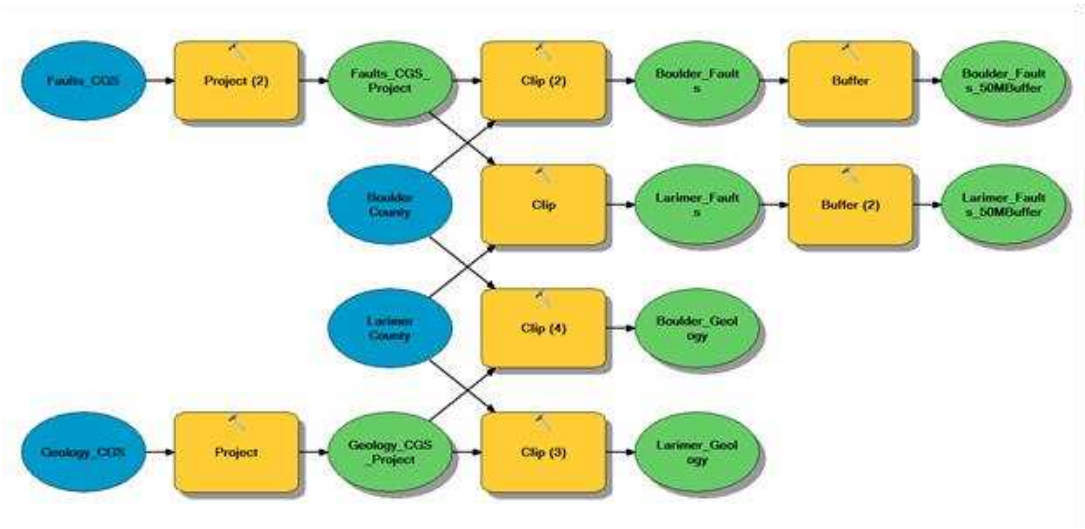

Figure D.11. Geology preprocessing model.

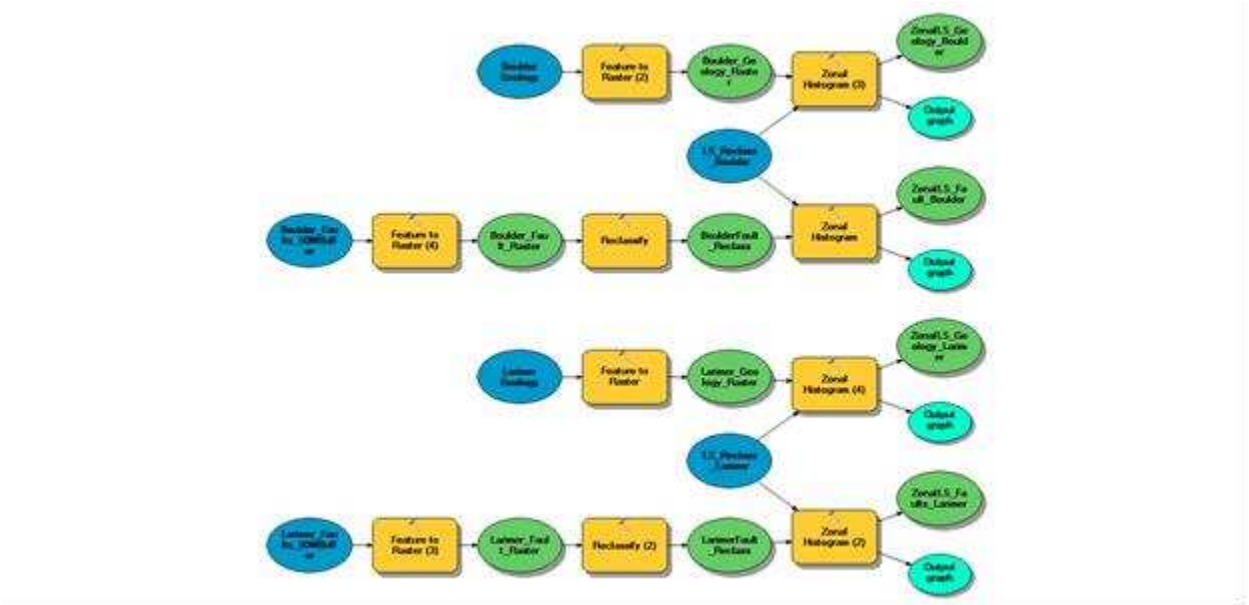

Figure D.12. Geology processing model.

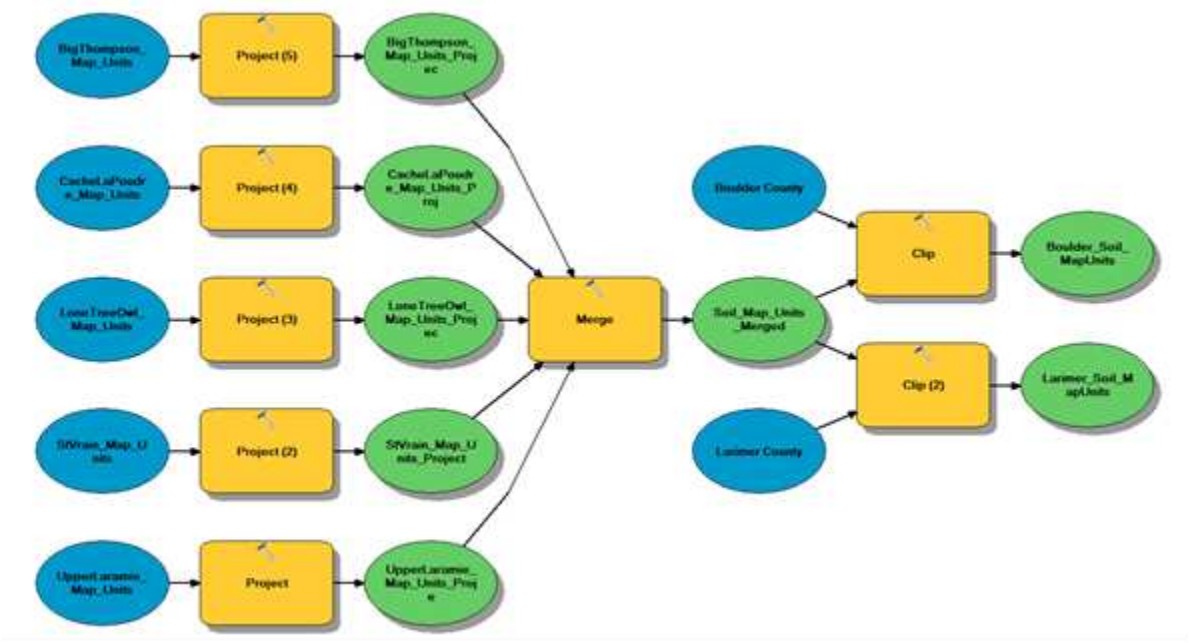

Figure D.13. Soil preprocessing model.

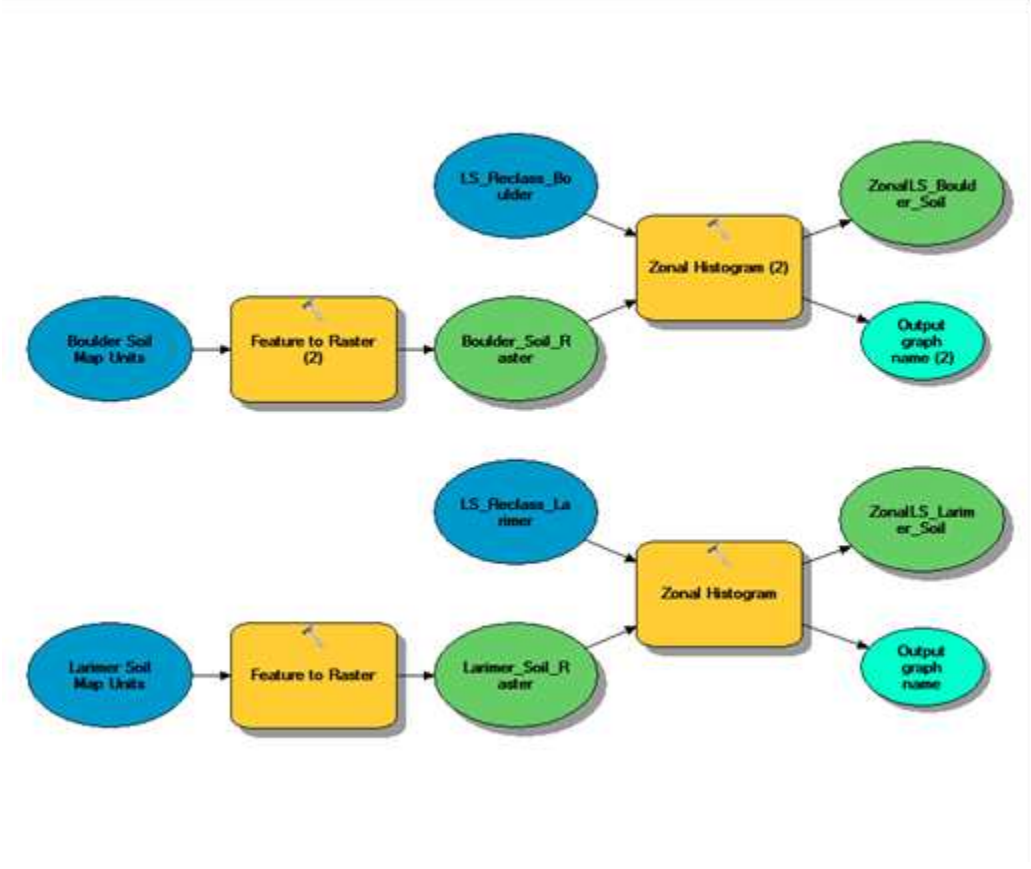

Figure D.14. Soil processing model.

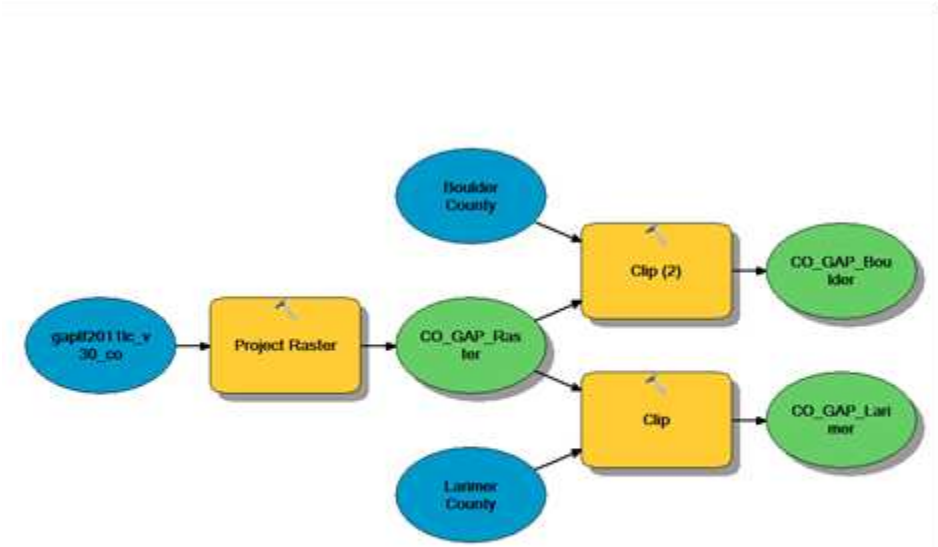

Figure D.15. Land cover preprocessing model.

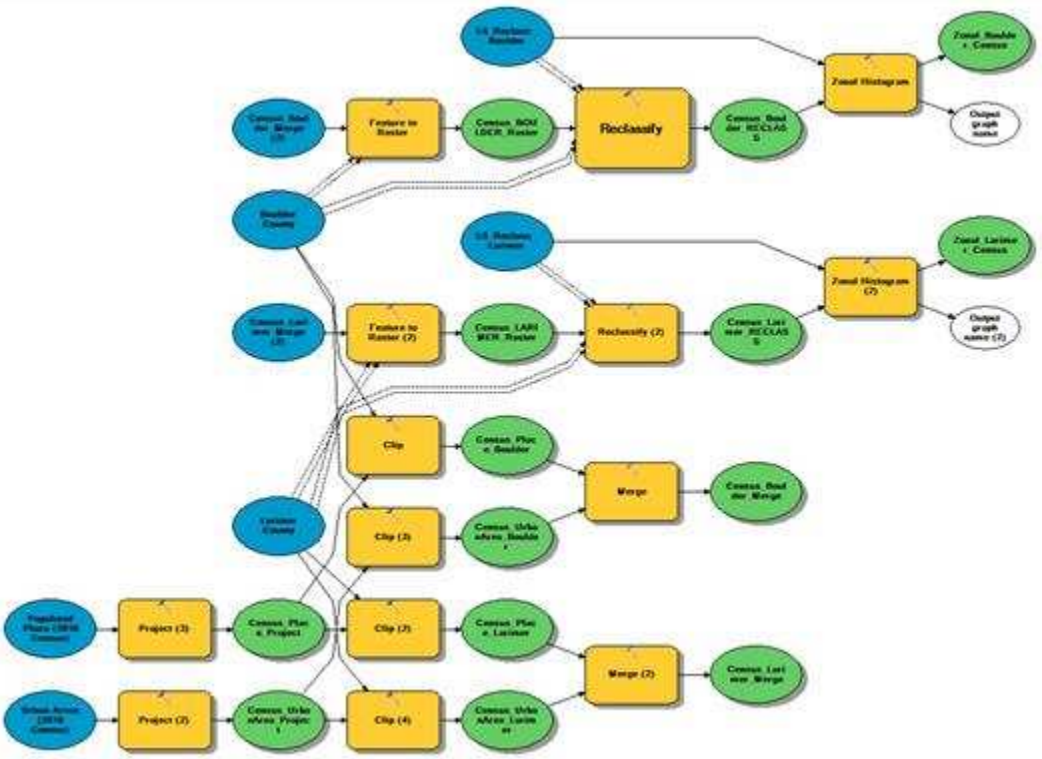

Figure D.16. Urban areas processing model.

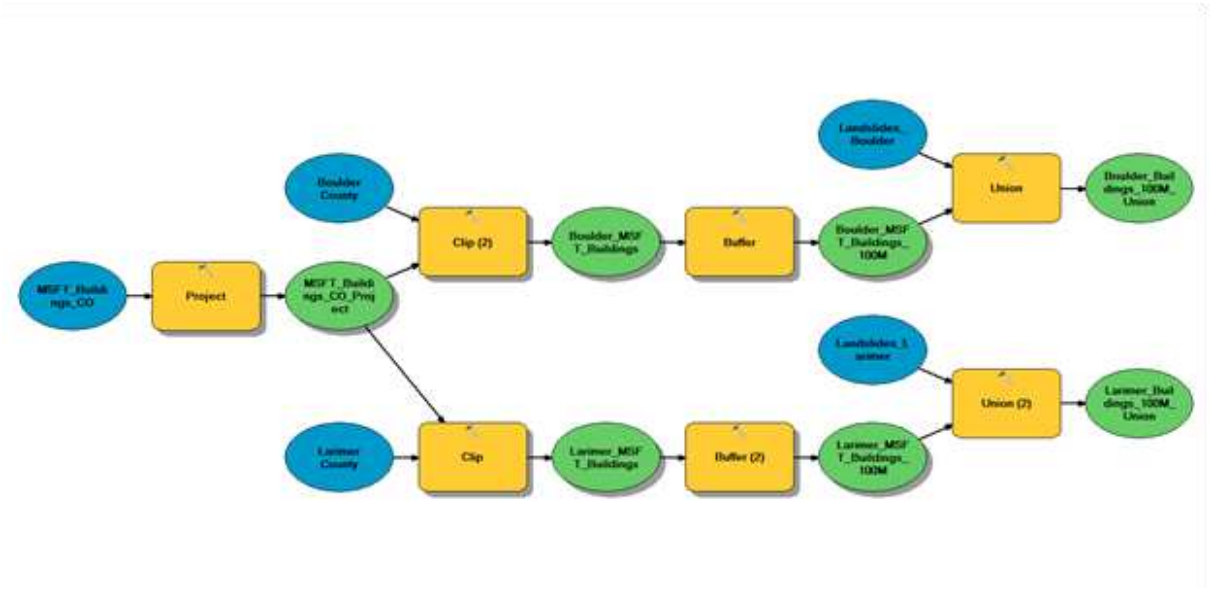

Figure D.17. Building preprocessing model.

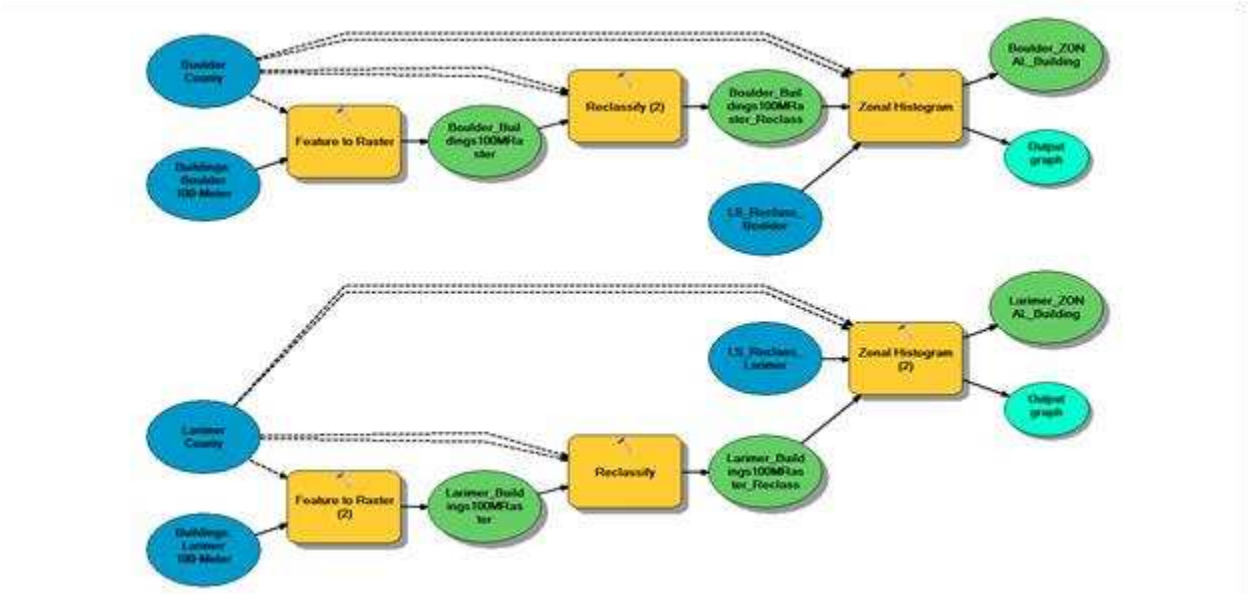

Figure D.18. Building processing model.

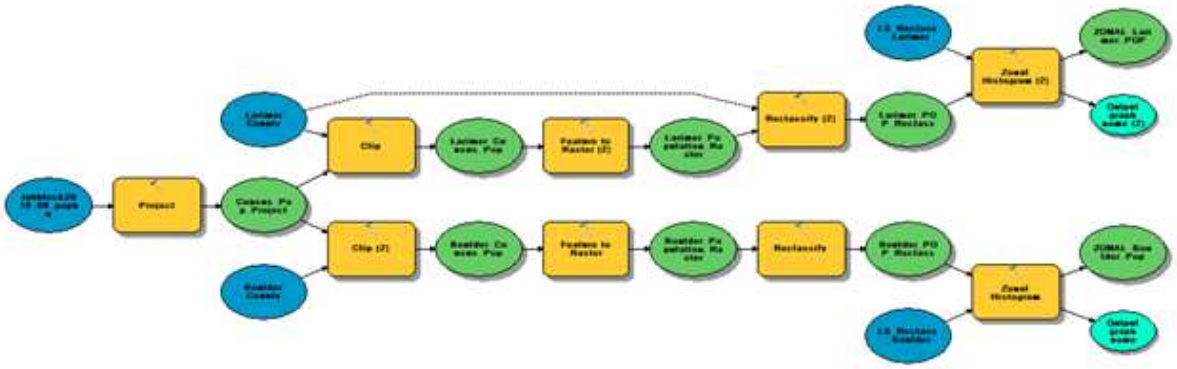

Figure D.19. Population processing model.

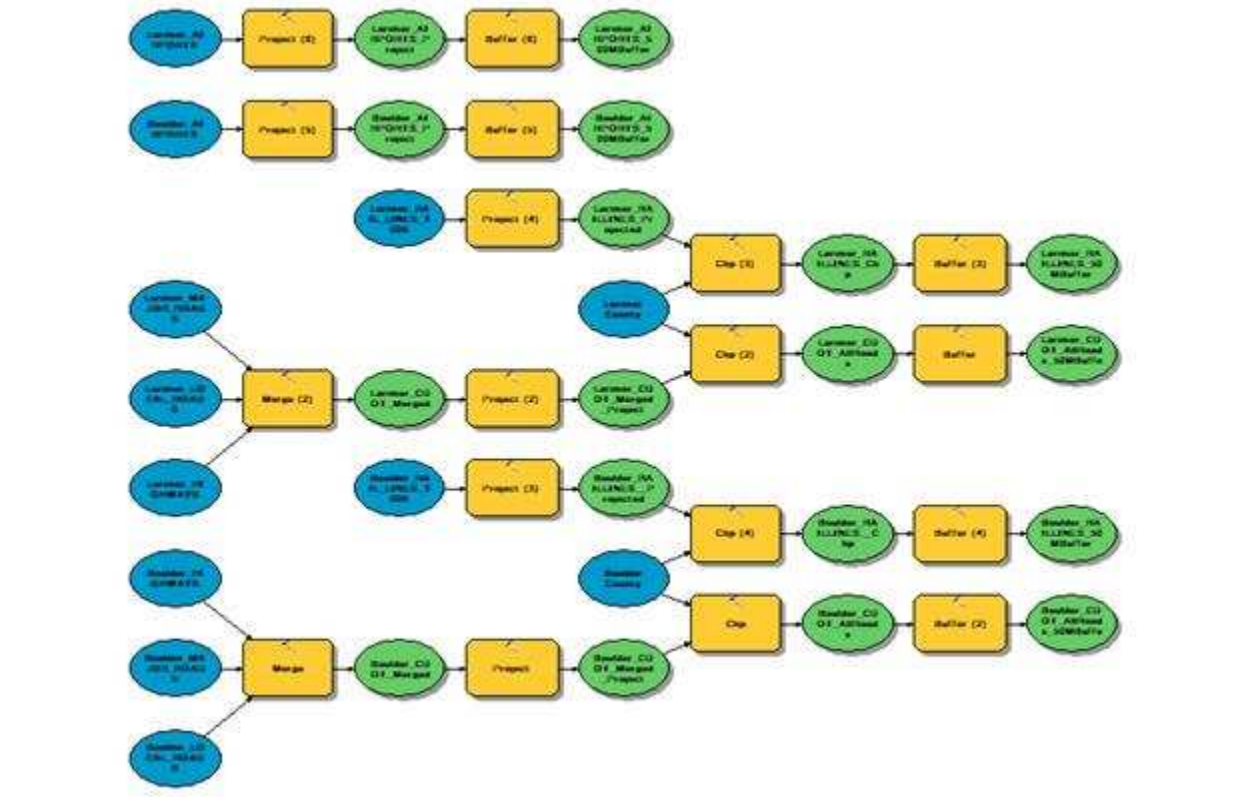

Figure D.20. Transportation preprocessing model.

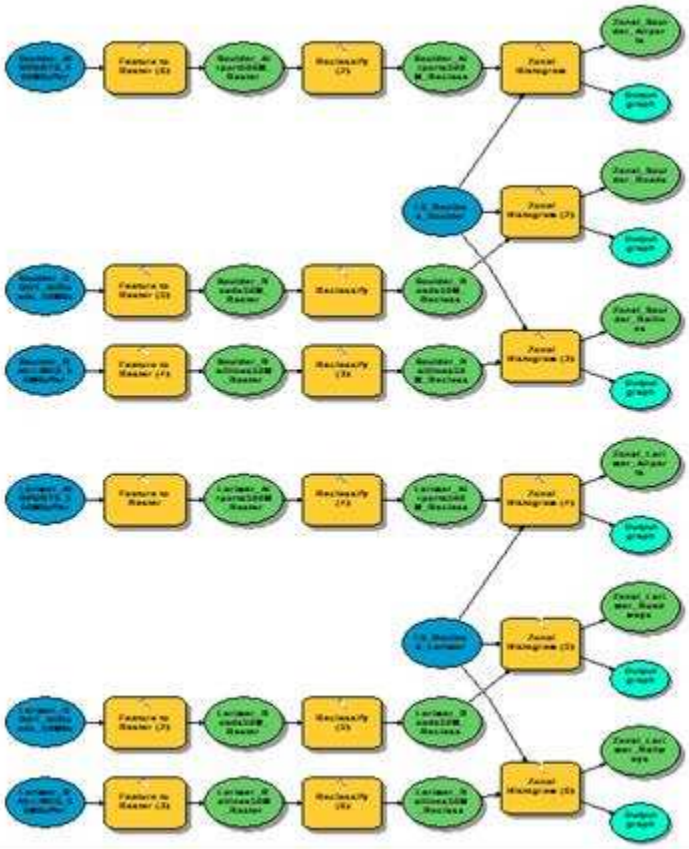

Figure D.21. Transportation processing model.

APPENDIX E: MAPS

Appendix E includes the factor and riskscape maps for individual factors from Chapter 3.

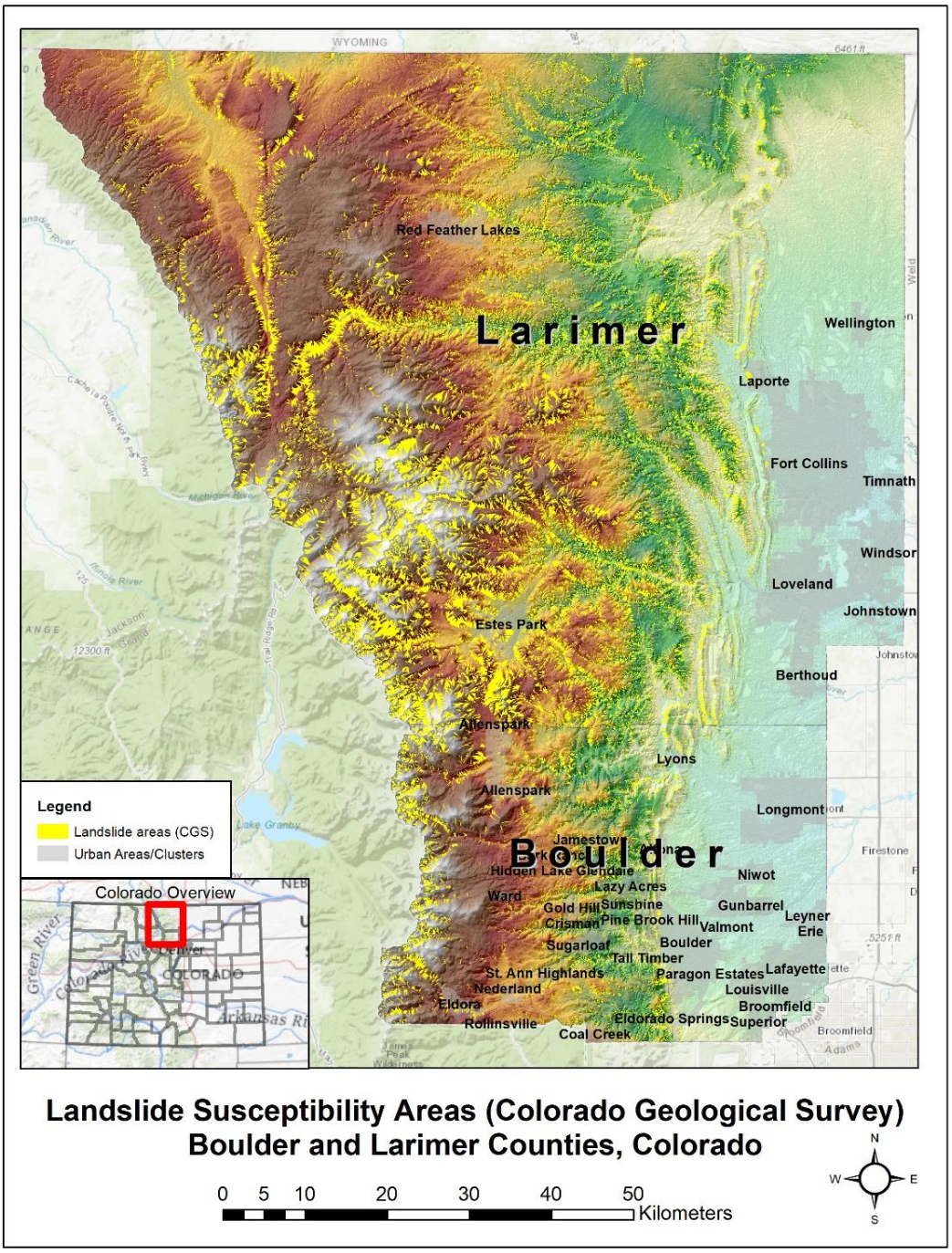

Figure E.1. Landslide susceptibility areas for Boulder and Larimer Counties, Colorado. Data source: Colorado Geological Survey. CGS Open File Report datasets 14-02 (Boulder County) and 15-13 (Larimer County). (Morgan et al., 2014; T. Wait et al., 2015)

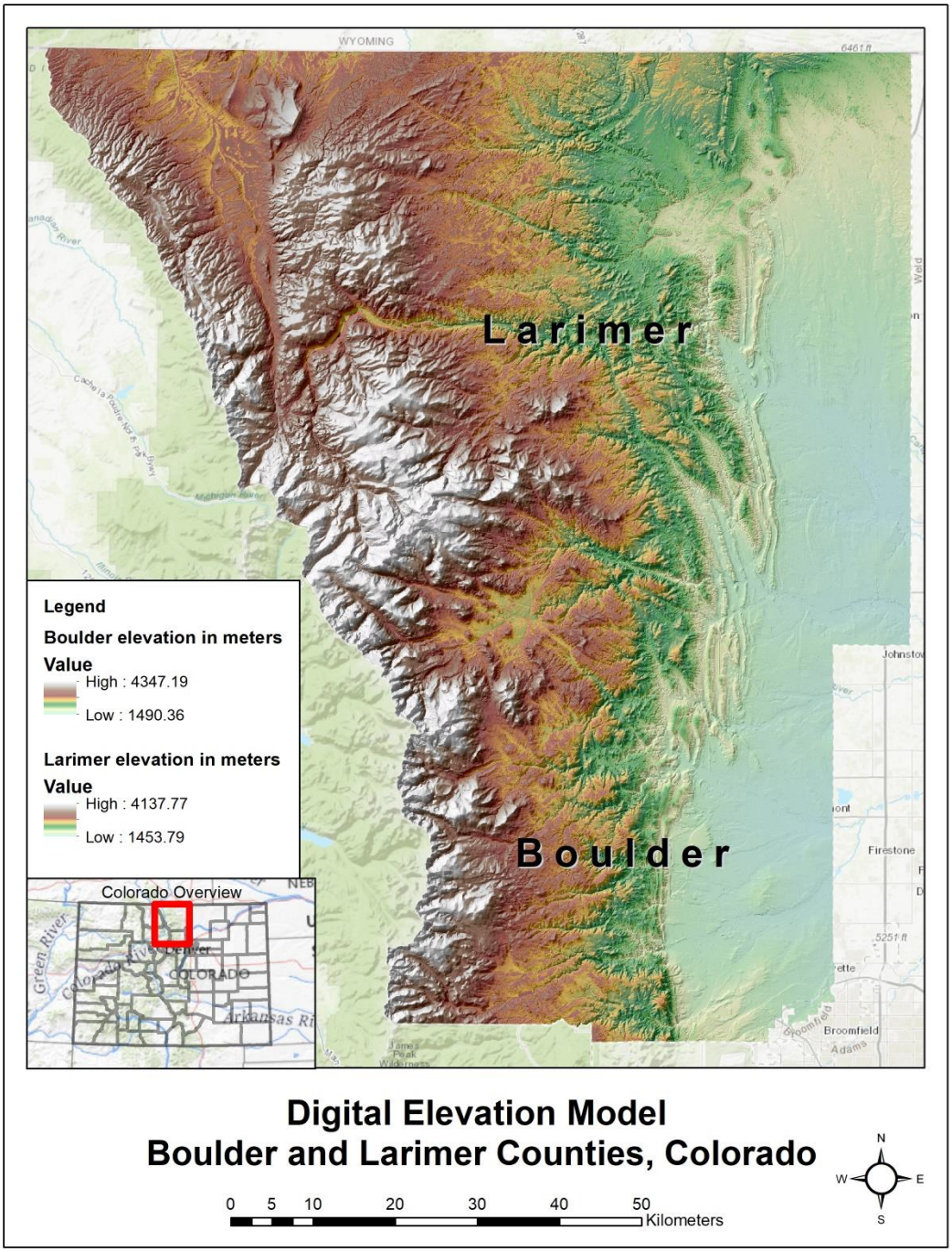

Figure E.2. Colorado Digital Elevation Model (DEM) for Boulder and Larimer Counties, Colorado. Data source: U.S. Geological Survey Digital Elevation Model data.

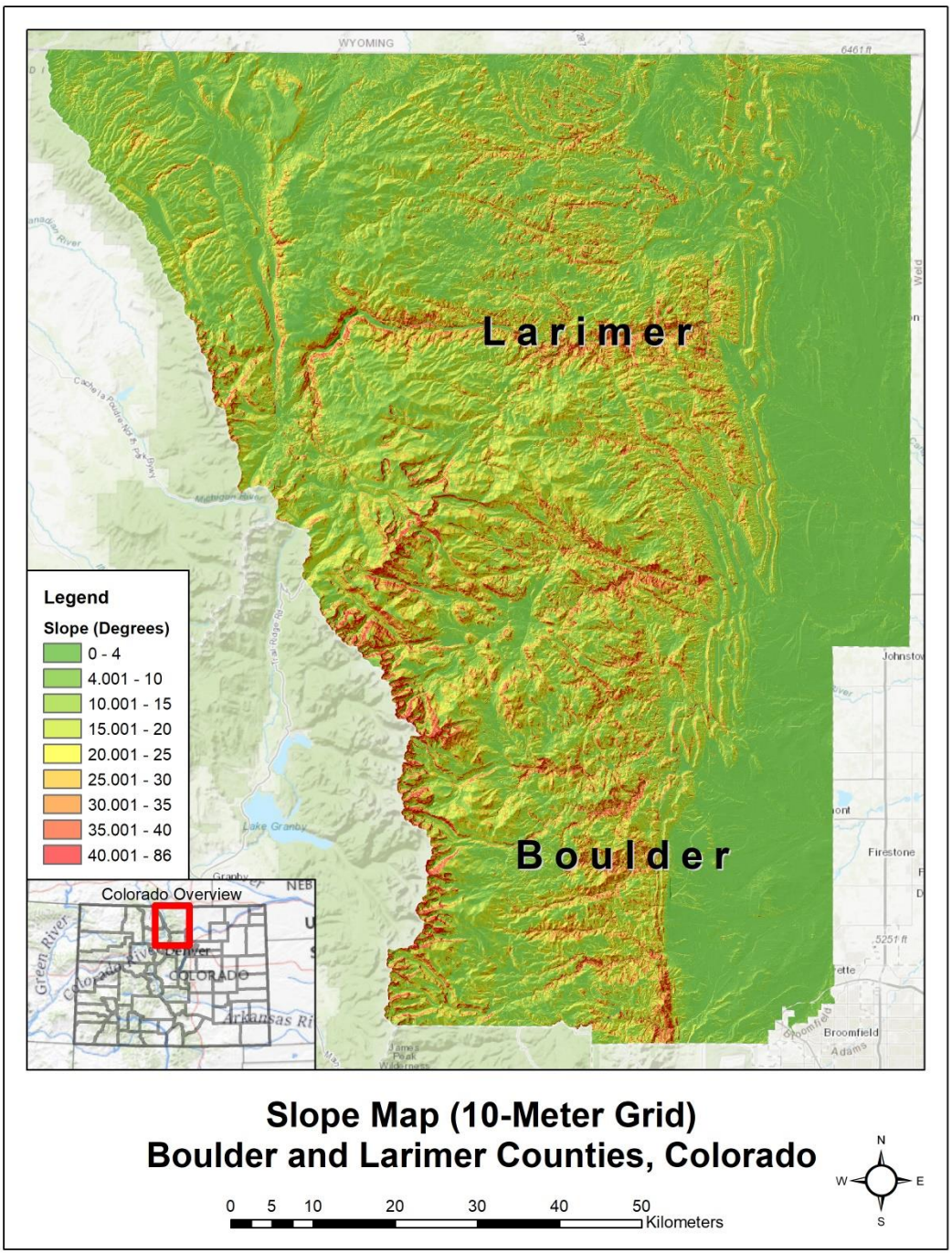

Figure E.3. Slope classifications in degrees for Boulder and Larimer Counties, Colorado. Data derived from U.S. Geological Survey Digital Elevation Model data.

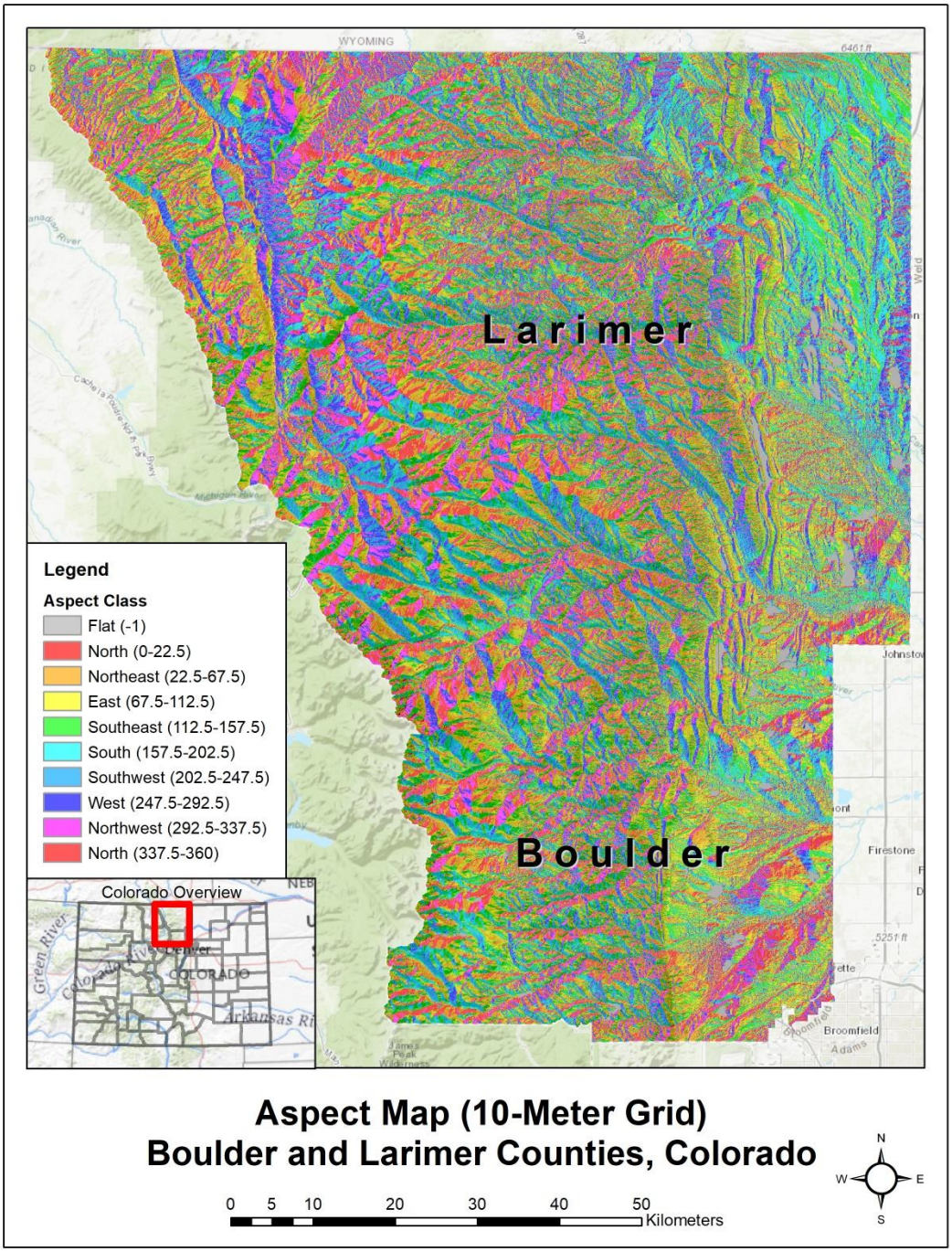

Figure E.4. Slope aspect showing direction of slope face (orientation) for Boulder and Larimer Counties, Colorado. Data derived from U.S. Geological Survey Digital Elevation Model data.

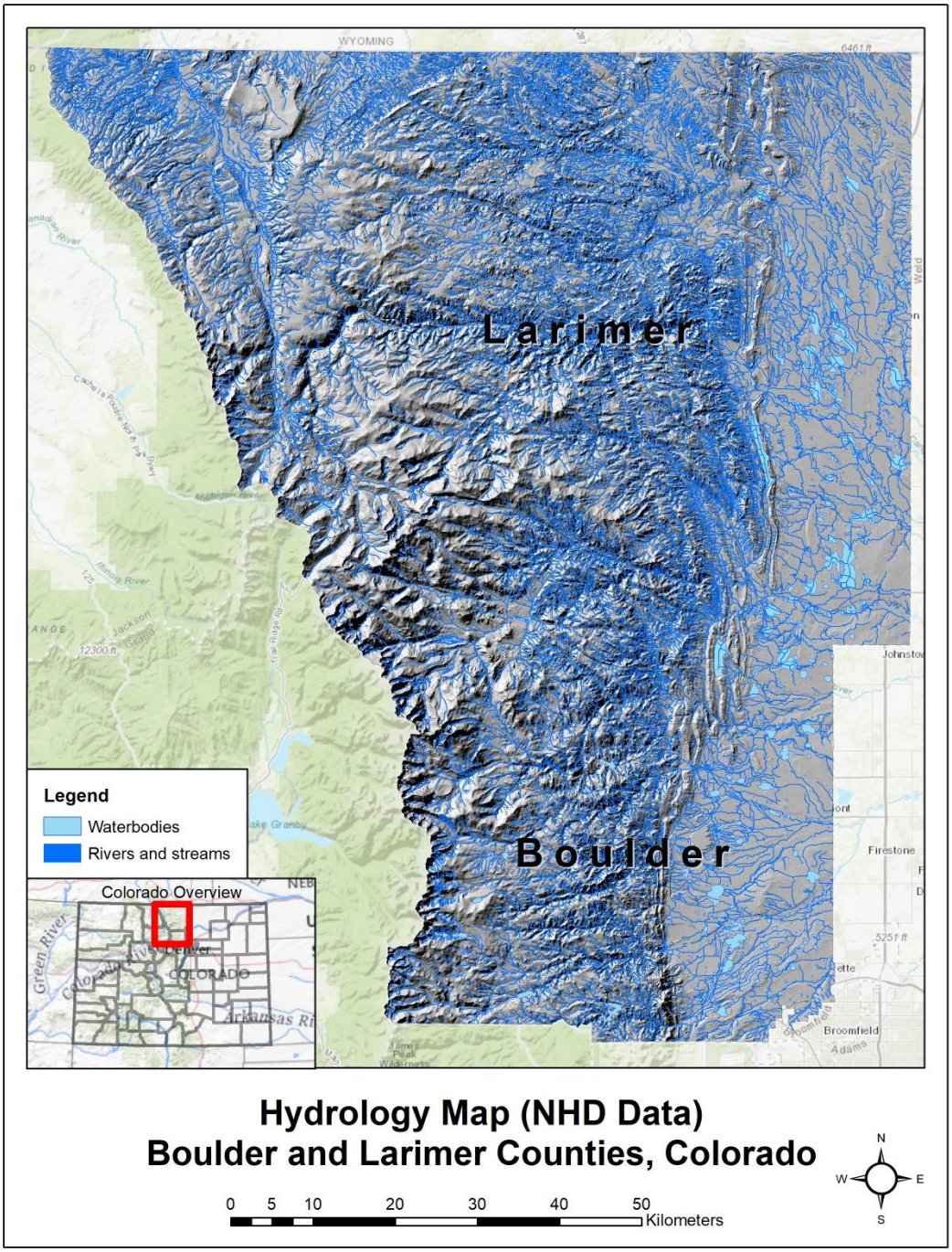

Figure E.5. Hydrology network showing areas within 50 meters of waterbodies (lakes and reservoirs) and flowlines (rivers and streams) for Boulder and Larimer Counties, Colorado. Data source: U.S. Geological Survey National Hydrology Dataset (NHD).

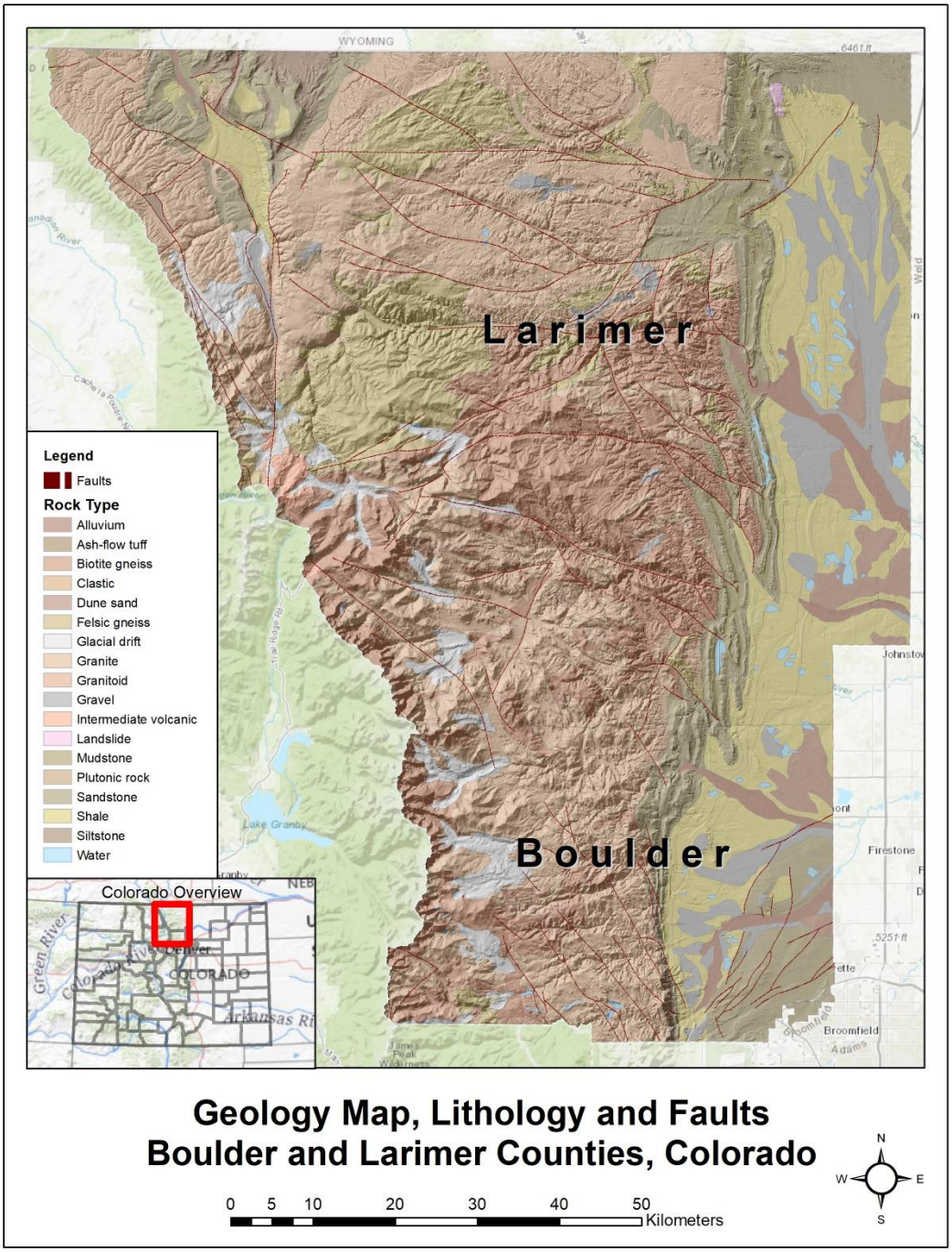

Figure E.6. Geology including lithology classes and proximity to faults (50-meter buffer), Boulder and Larimer Counties, Colorado. Data source: Colorado Geological Survey.

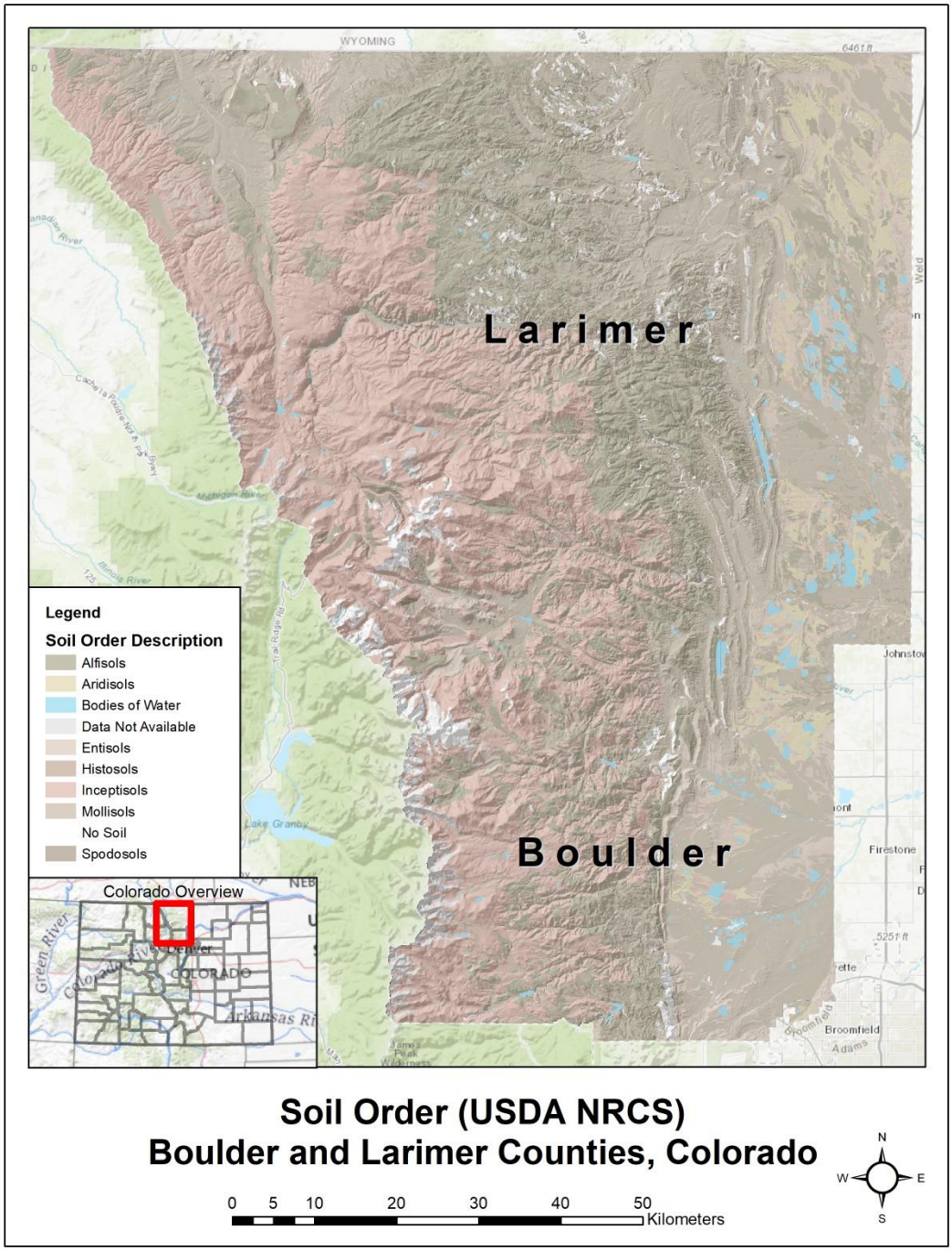

Figure E.7. Soil order classes, Boulder and Larimer Counties, Colorado. Data source: U.S. Department of Agriculture Natural Resources Conservation Service (NRCS).

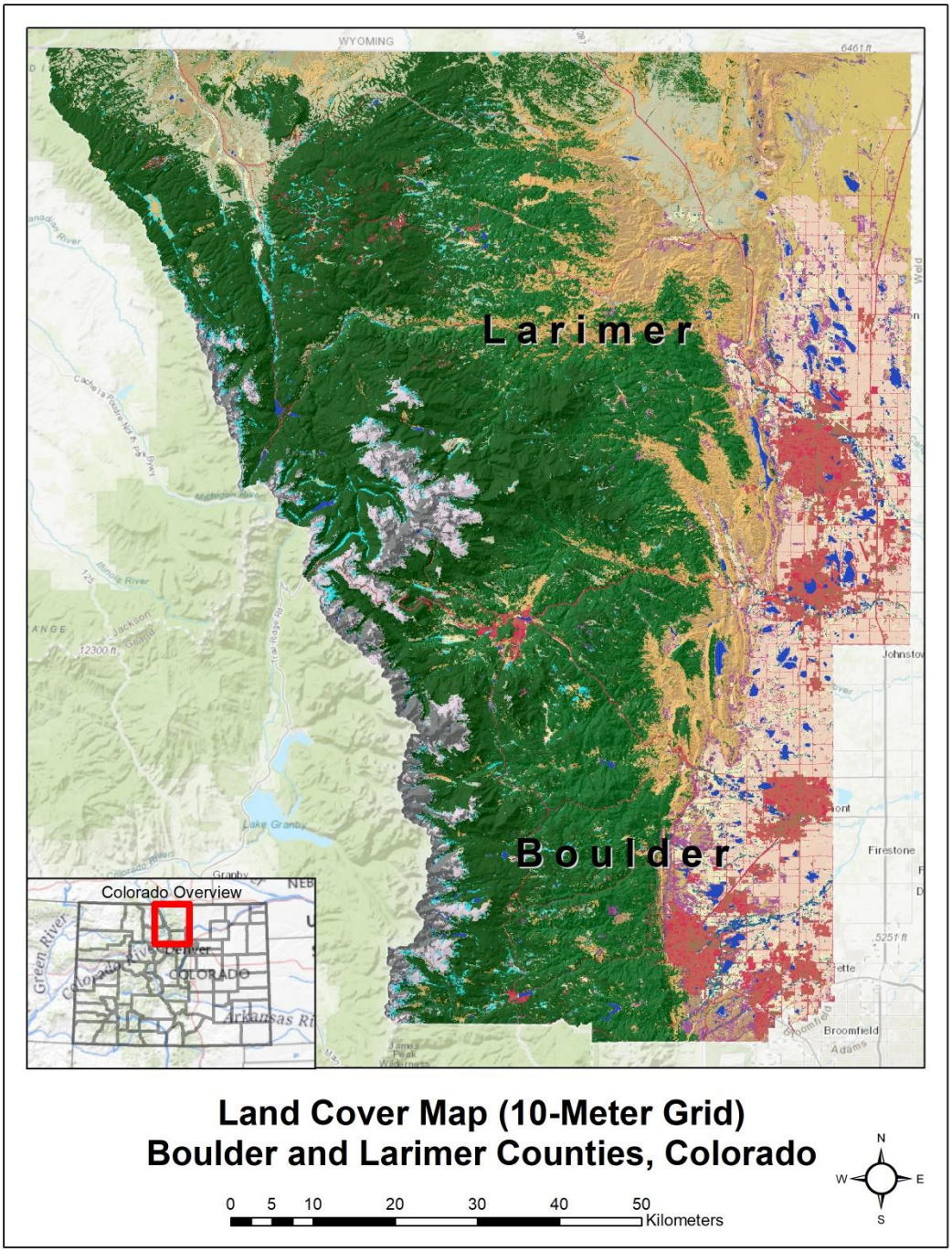

Figure E.8. Land cover vegetation classes, Boulder and Larimer Counties, Colorado. Data source: U.S. Geological Survey, GAP Analysis Project.

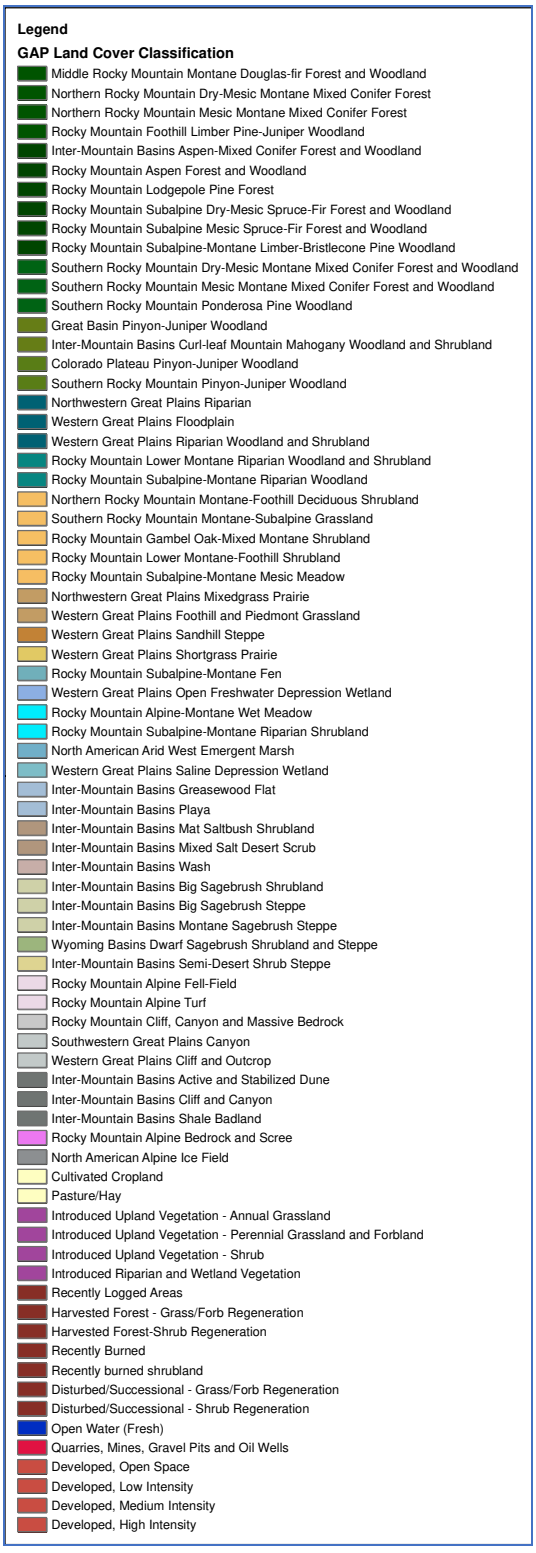

Figure E.9. GAP land cover symbology.

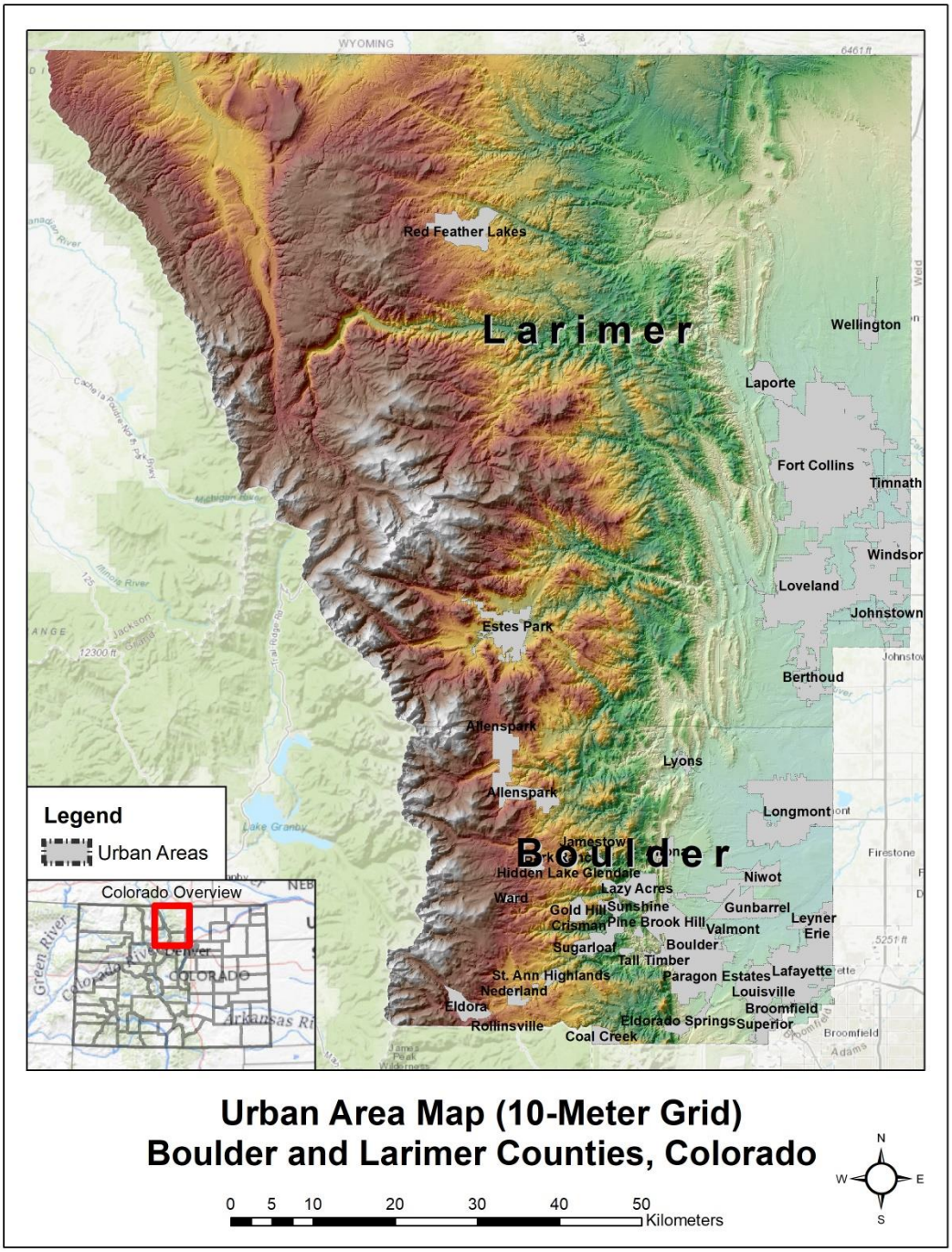

Figure E.10. Urban area classes for Boulder and Larimer Counties, Colorado. Data source: U.S. Census Bureau.

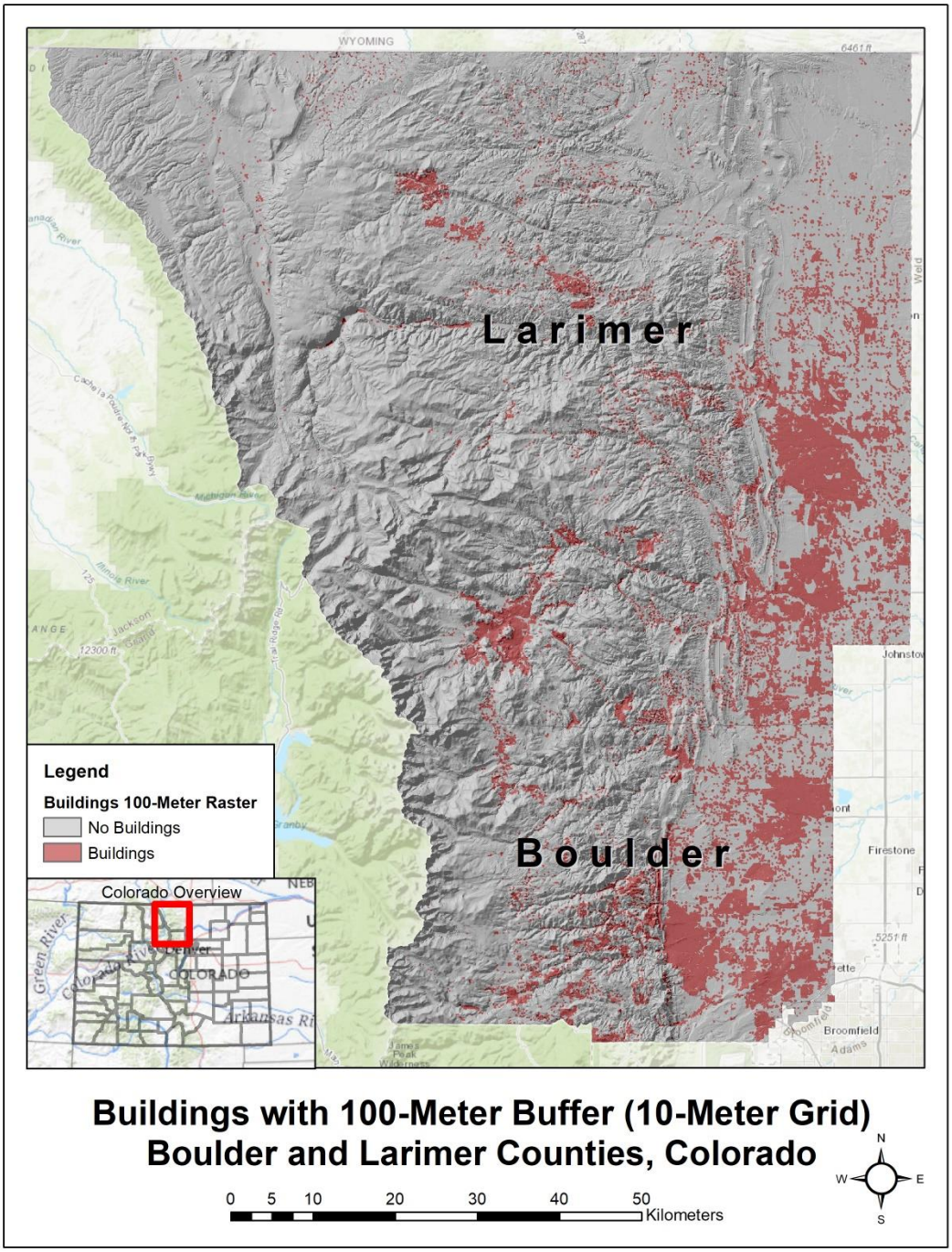

Figure E.11. Buildings with 100-meter buffer for Boulder and Larimer Counties, Colorado. Data source: Microsoft building footprint data 2018.

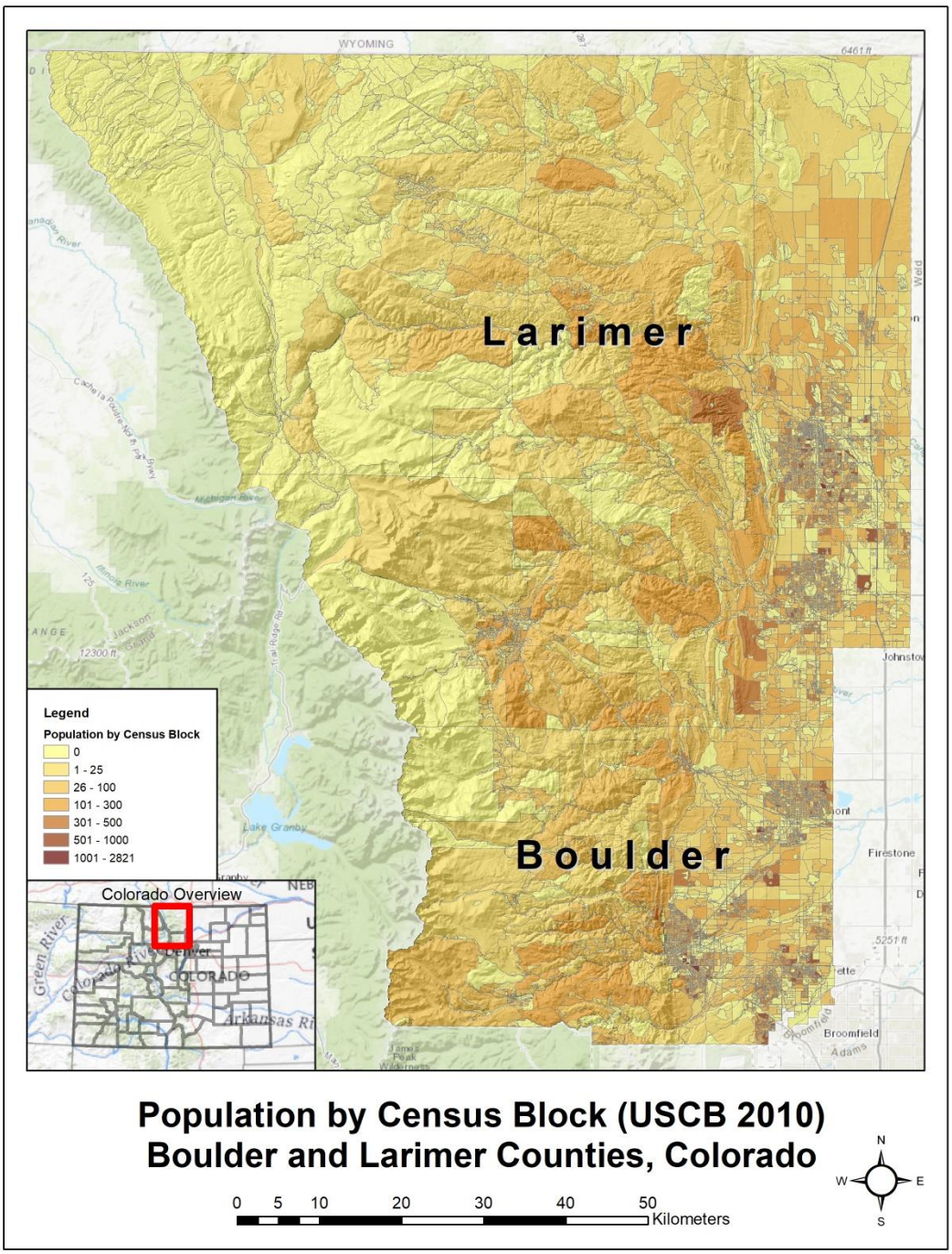

Figure E.12. Population by census block for Boulder and Larimer Counties, Colorado. Data source: U.S. Census Bureau.

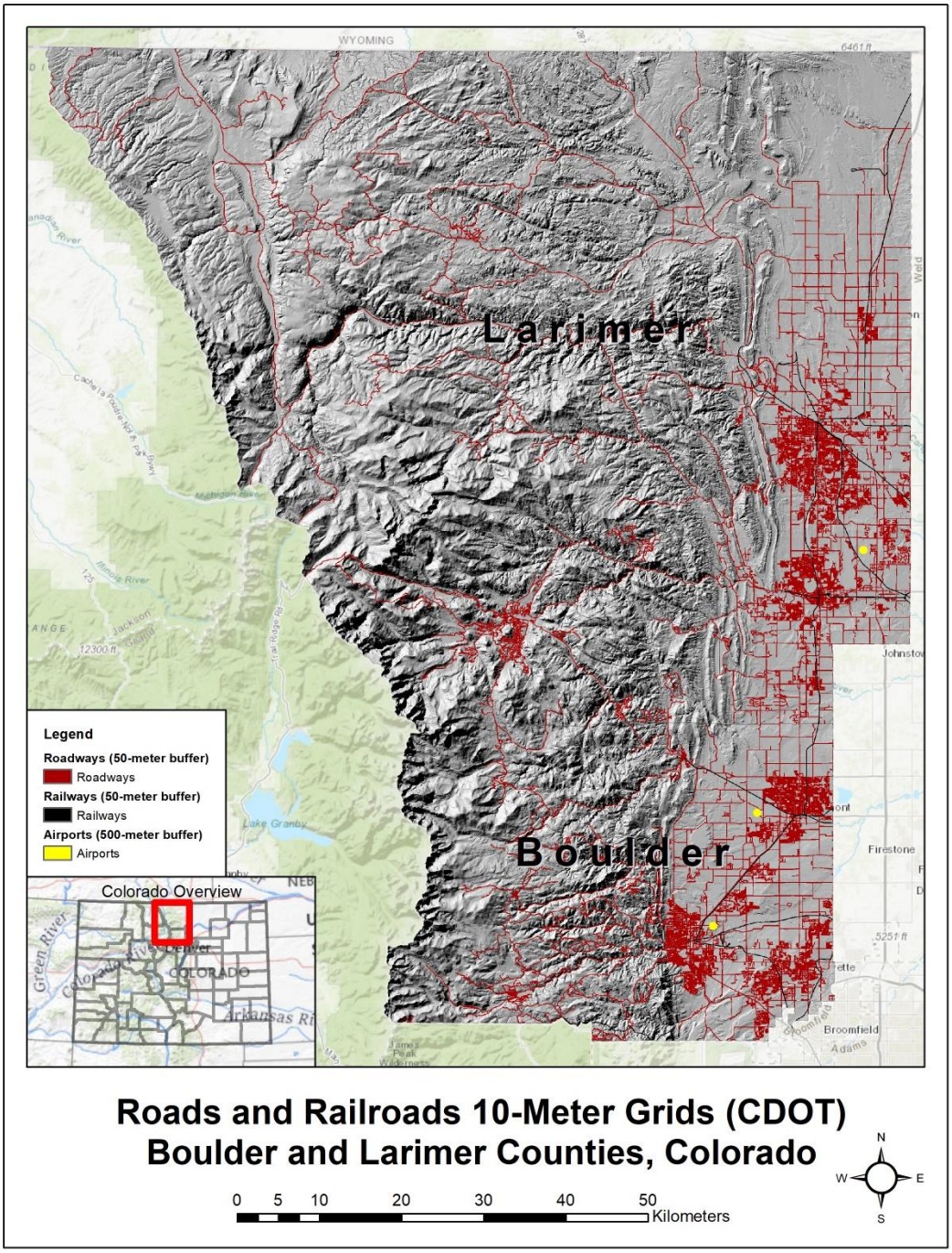

Figure E.13. Transportation classes for Boulder and Larimer Counties, Colorado including 50-meter buffer for railroads and roadways, and 500-meter buffer for airports. Data sources: Colorado Department of Transportation, Boulder County, and Larimer County.

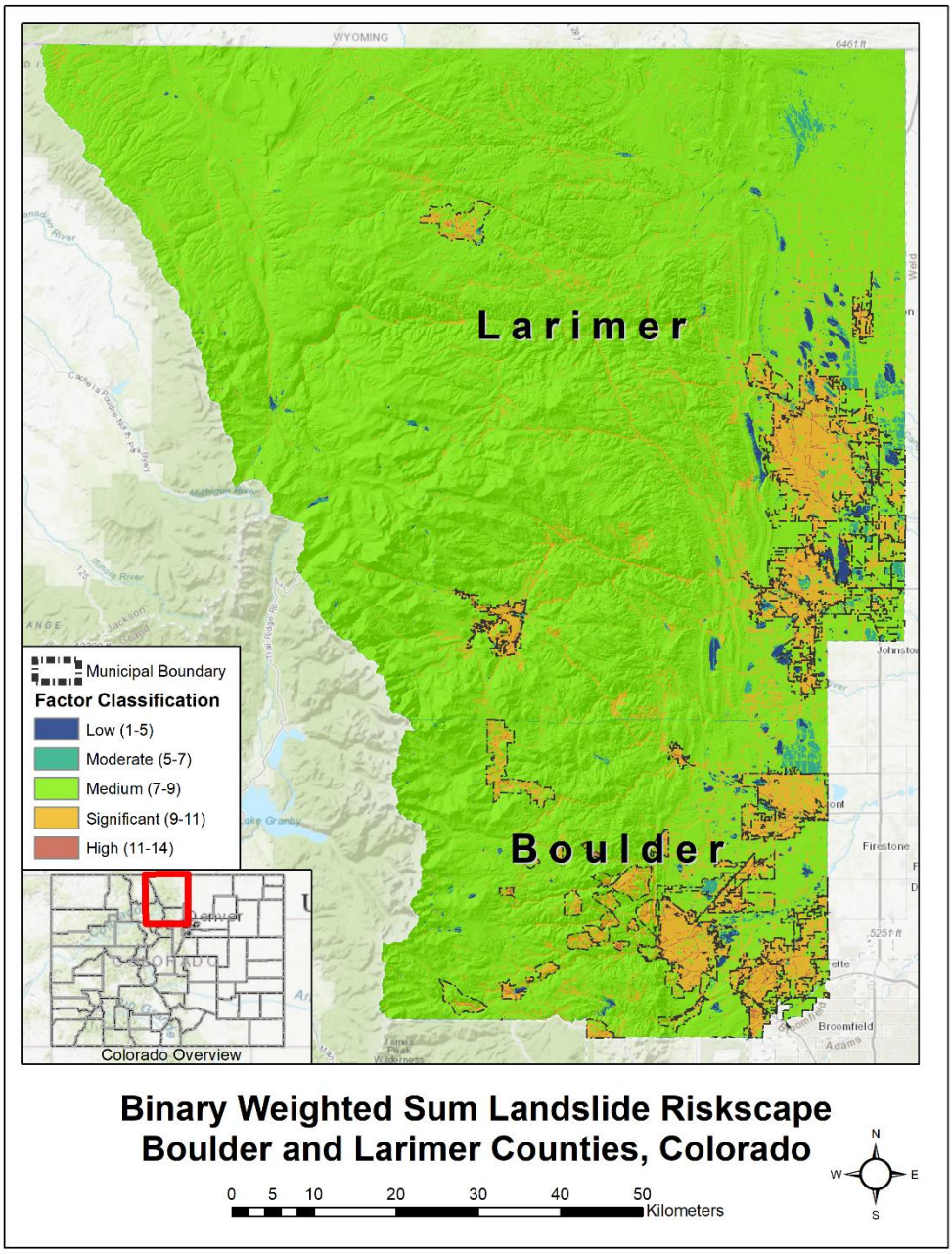

Figure E.14. Binary weighted-sum riskscape for Boulder and Larimer Counties, Colorado indicating number of factors present in 10-meter grid locations.

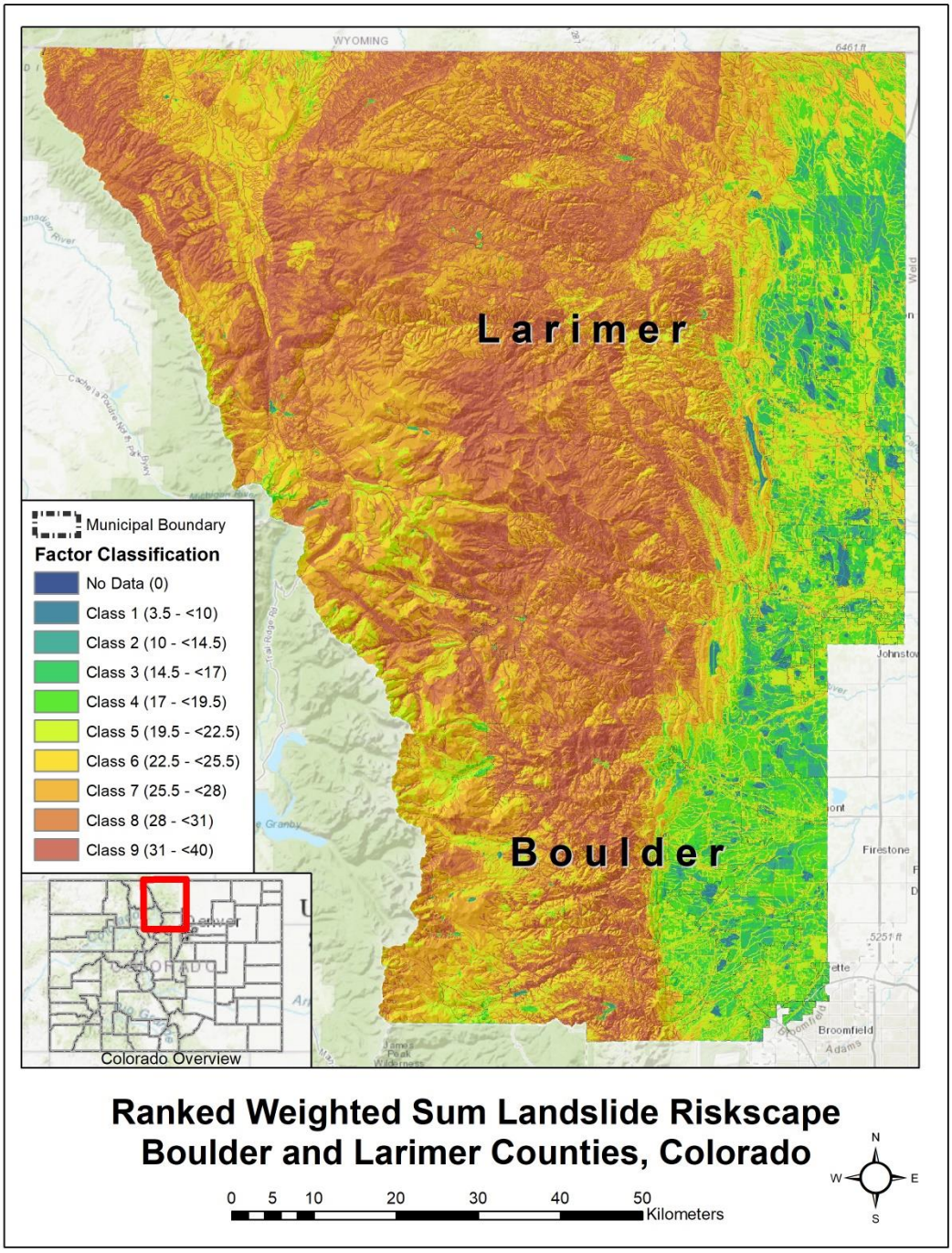

Figure E.15. Ranked weighted-sum riskscape for Boulder and Larimer Counties, Colorado indicating number of factors present in 10-meter grid locations.

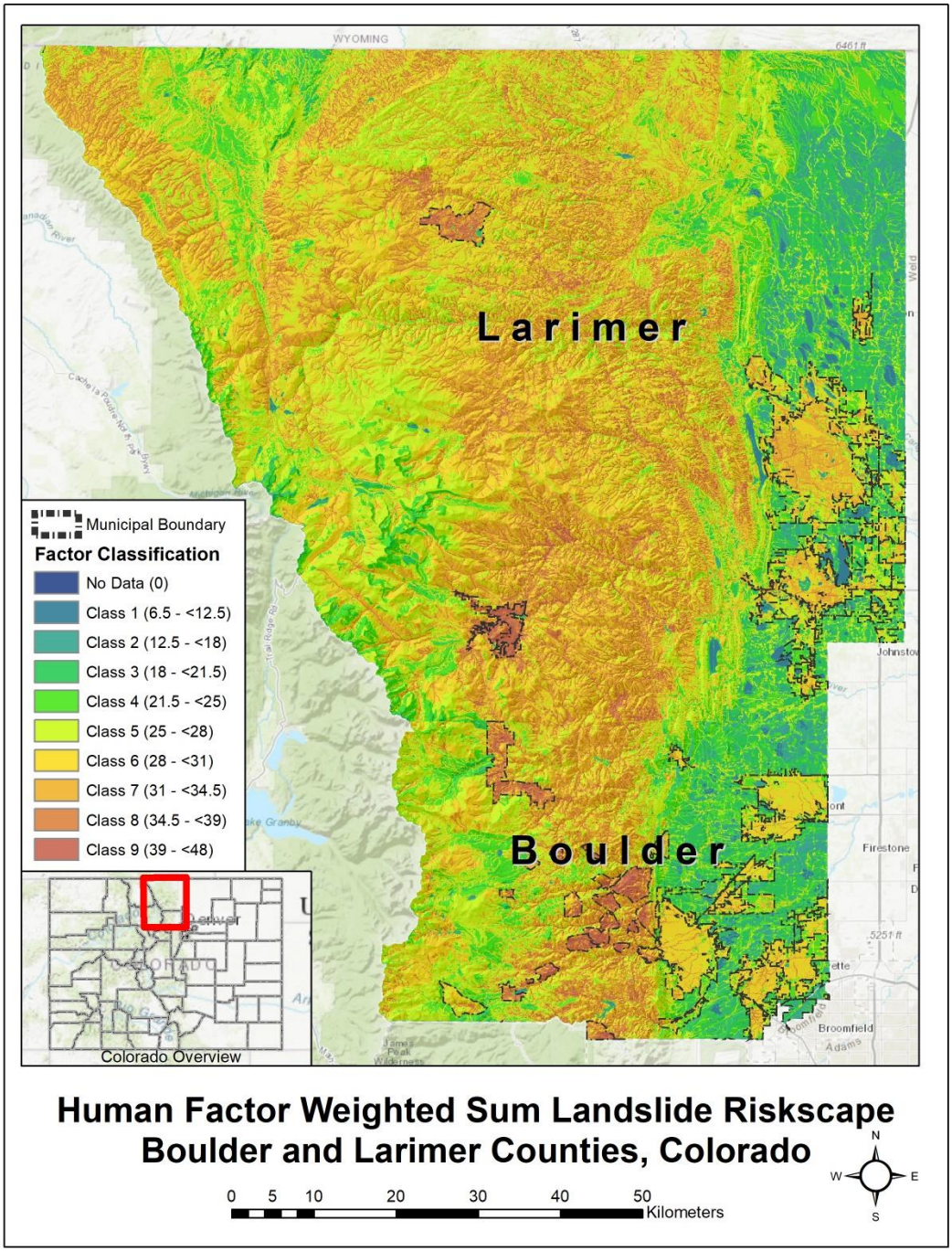

Figure E.16. Human factor weighted-sum riskscape for Boulder and Larimer Counties, Colorado indicating number of factors present in 10-meter grid locations.

APPENDIX F: RESULTS CHARTS

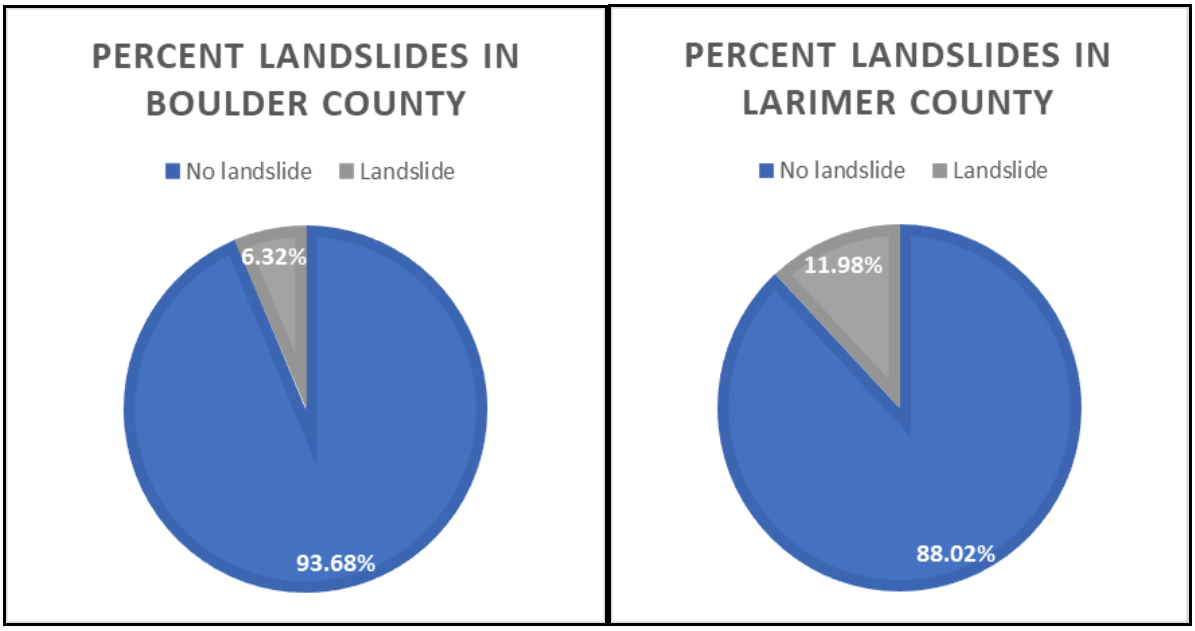

Figure F.1. Landslide percentage for Boulder and Larimer Counties, Colorado. Data source: Colorado Geological Survey. CGS Open File Report datasets 14-02 (Boulder County) and 15-13 (Larimer County). (Morgan et al., 2014; T. Wait et al., 2015)

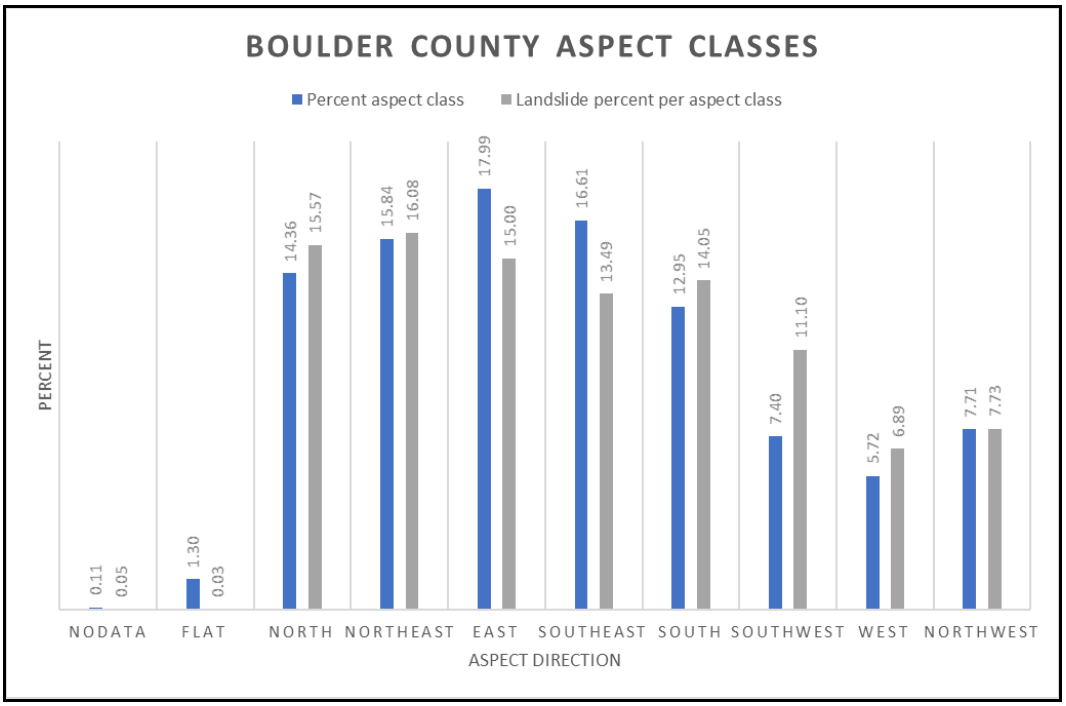

Figure F.2. Aspect classes for Boulder County, showing slope face direction. Data derived from U.S. Geological Survey Digital Elevation Model data.

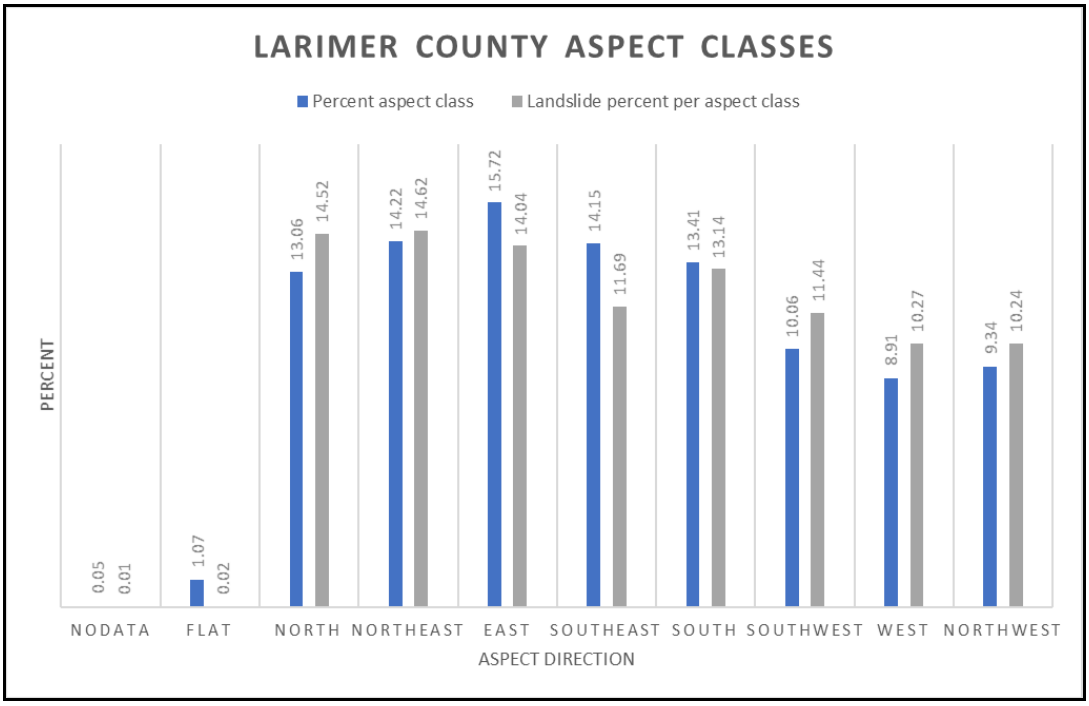

Figure F.3. Aspect classes for Larimer County, showing slope face direction. Data derived from U.S. Geological Survey Digital Elevation Model data.

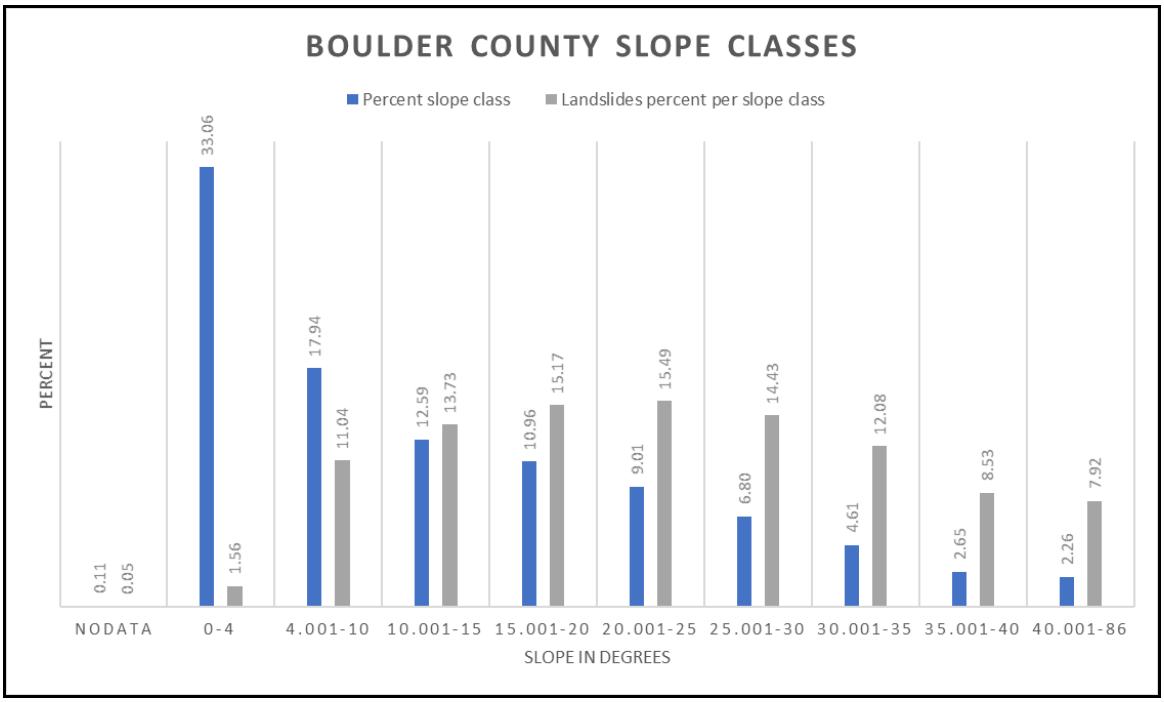

Figure F.4. Slope classes in degrees for Boulder County. Data derived from U.S. Geological Survey Digital Elevation Model data.

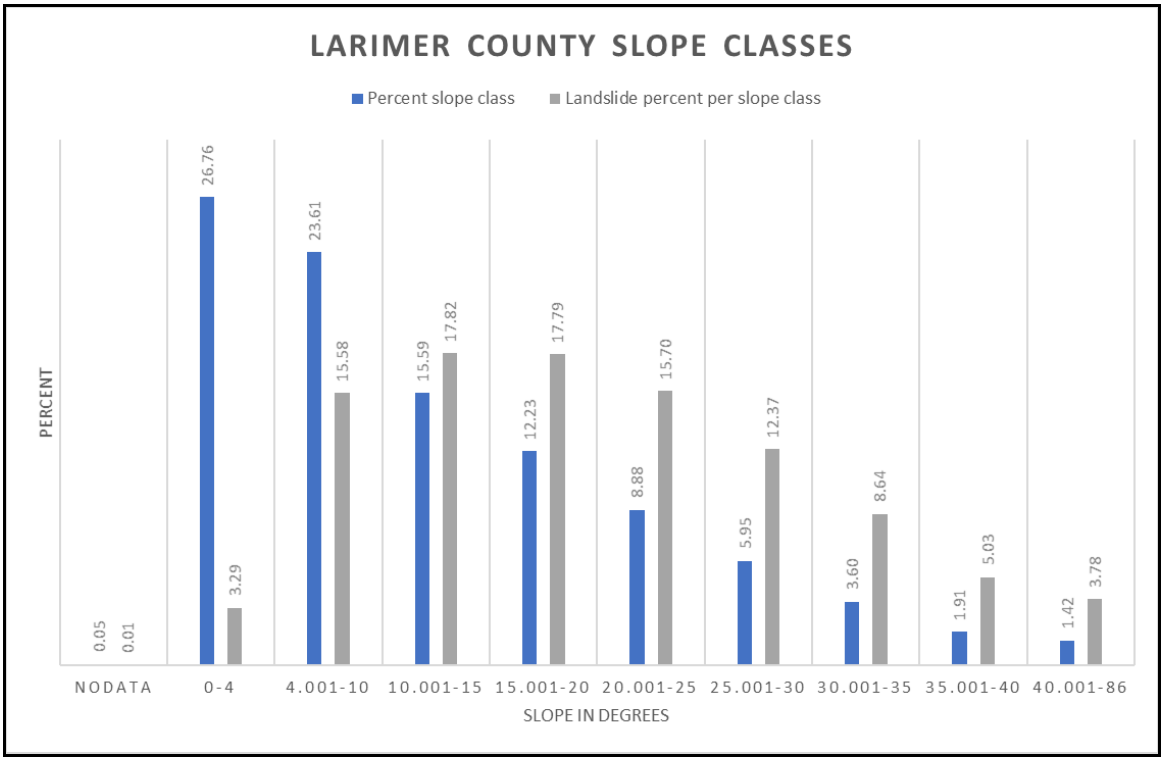

Figure F.5. Slope classes in degrees for Larimer County. Data derived from U.S. Geological Survey Digital Elevation Model data.

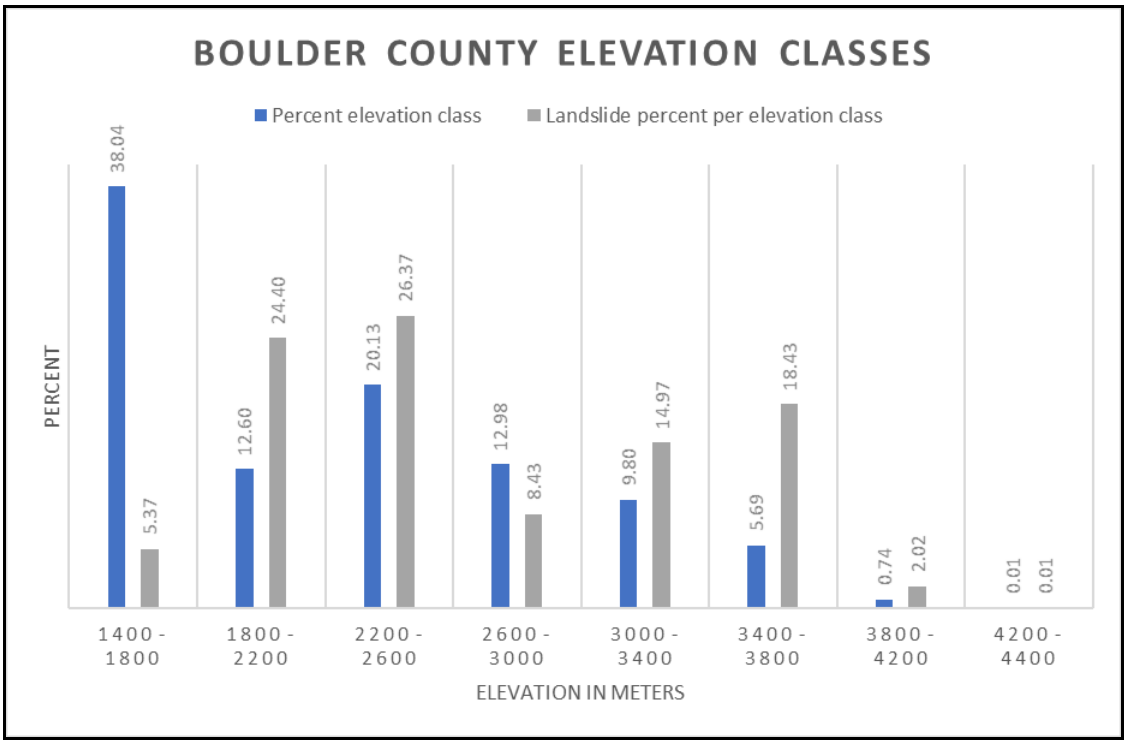

Figure F.6. Elevation classes in meters for Boulder County. Data derived from U.S. Geological Survey Digital Elevation Model data.

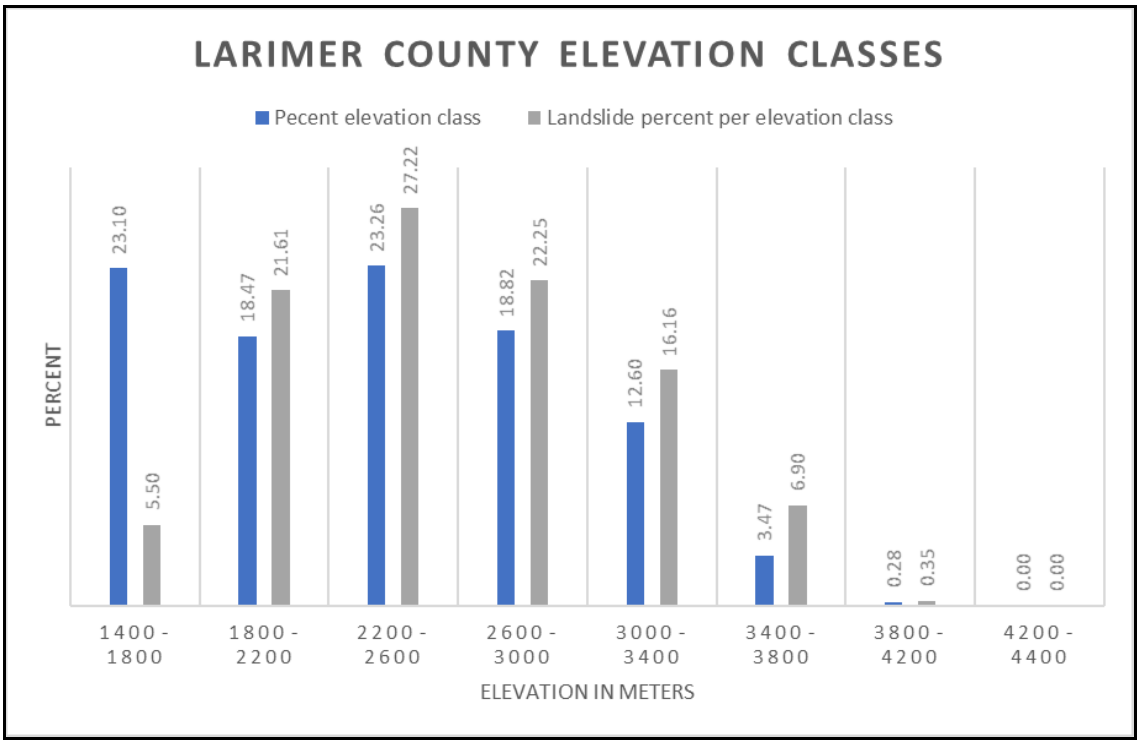

Figure F.7. Elevation classes in meters for Larimer County. Data derived from U.S. Geological Survey Digital Elevation Model data.

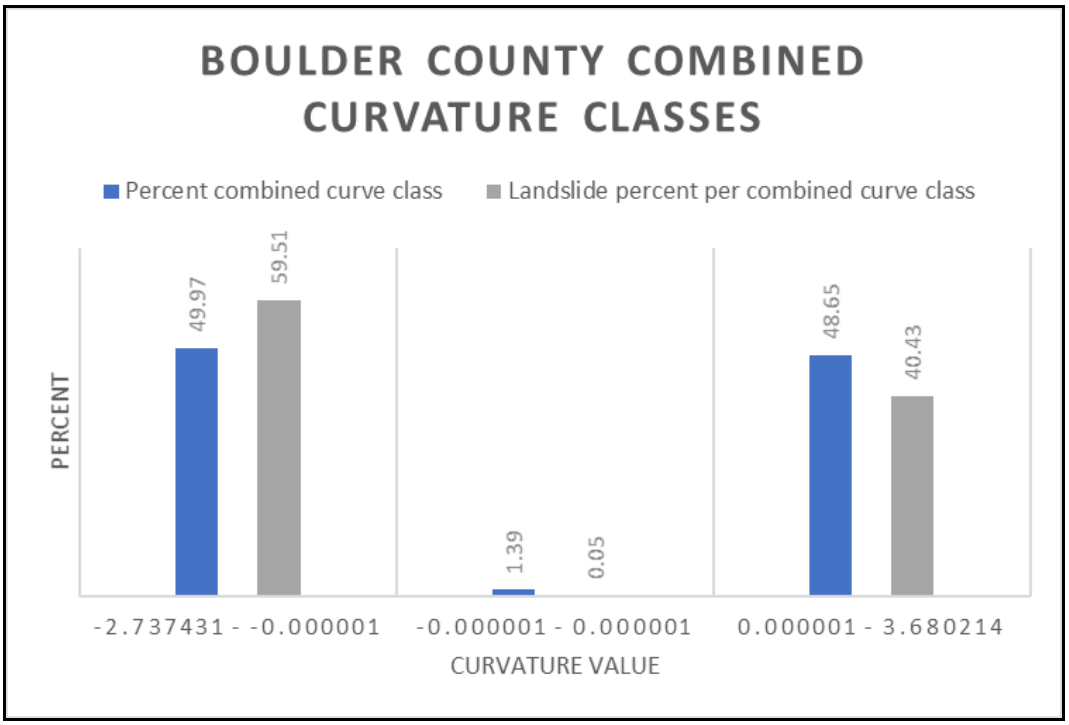

Figure F.8. Combined curvature (planimetric and profile) classes for Boulder County. Data derived from U.S. Geological Survey Digital Elevation Model data.

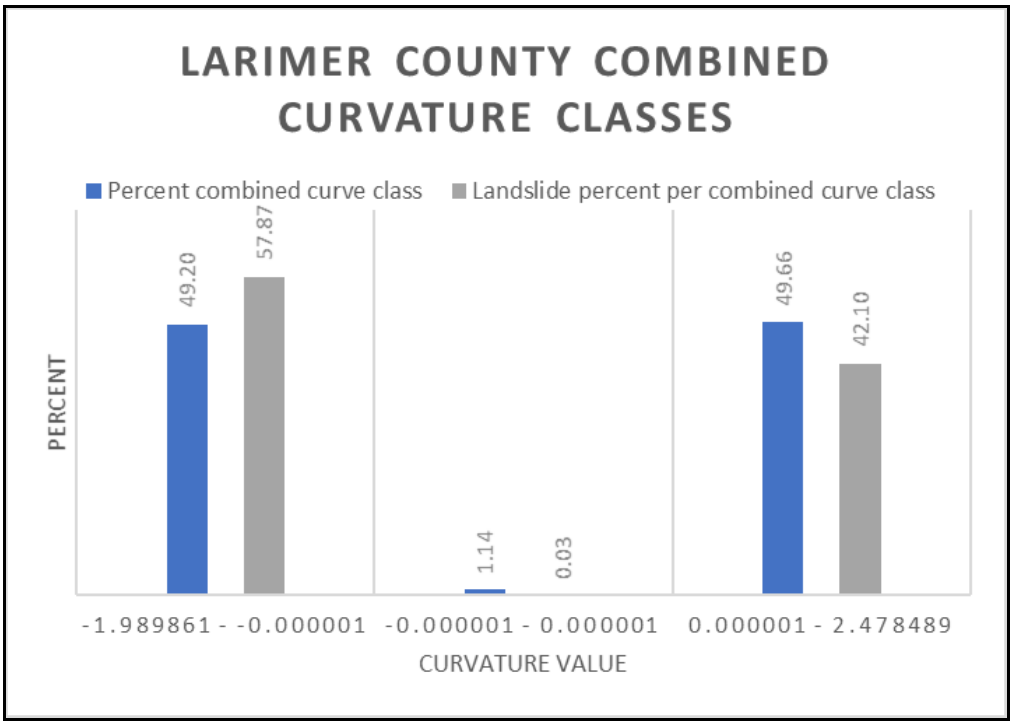

Figure F.9. Combined curvature (planimetric and profile) classes for Larimer County. Data derived from U.S. Geological Survey Digital Elevation Model data.

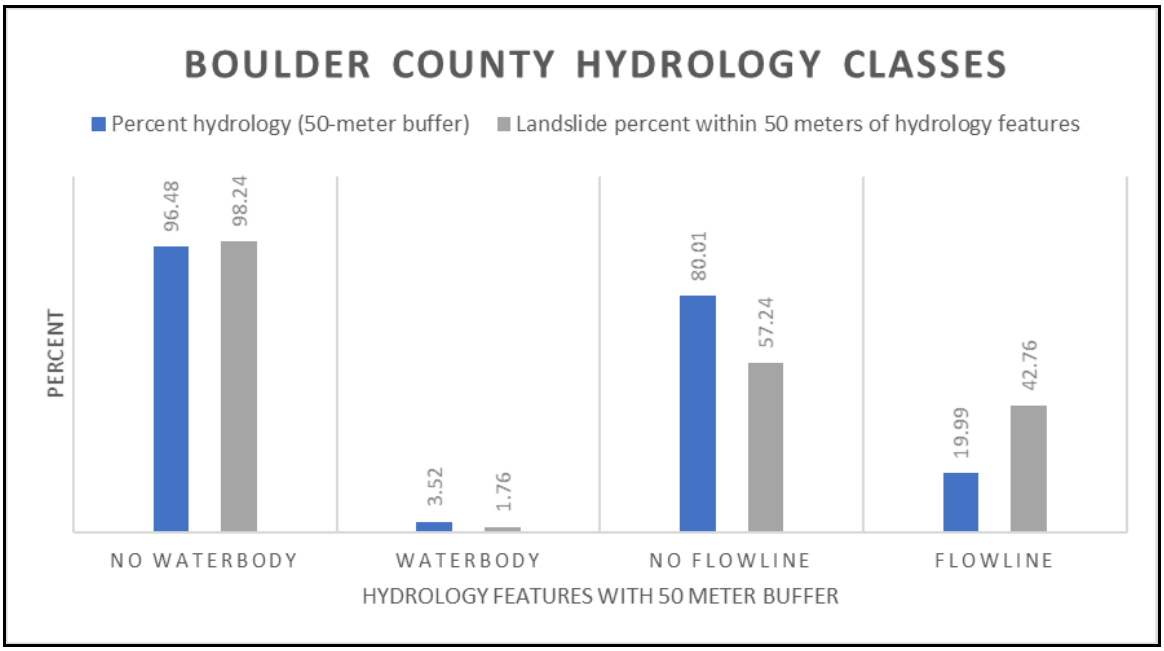

Figure F.10. Hydrology classes for Boulder County, showing areas within 50 meters of waterbodies (lakes and reservoirs) and flowlines (rivers and streams). Data source: U.S. Geological Survey National Hydrology Dataset (NHD) data.

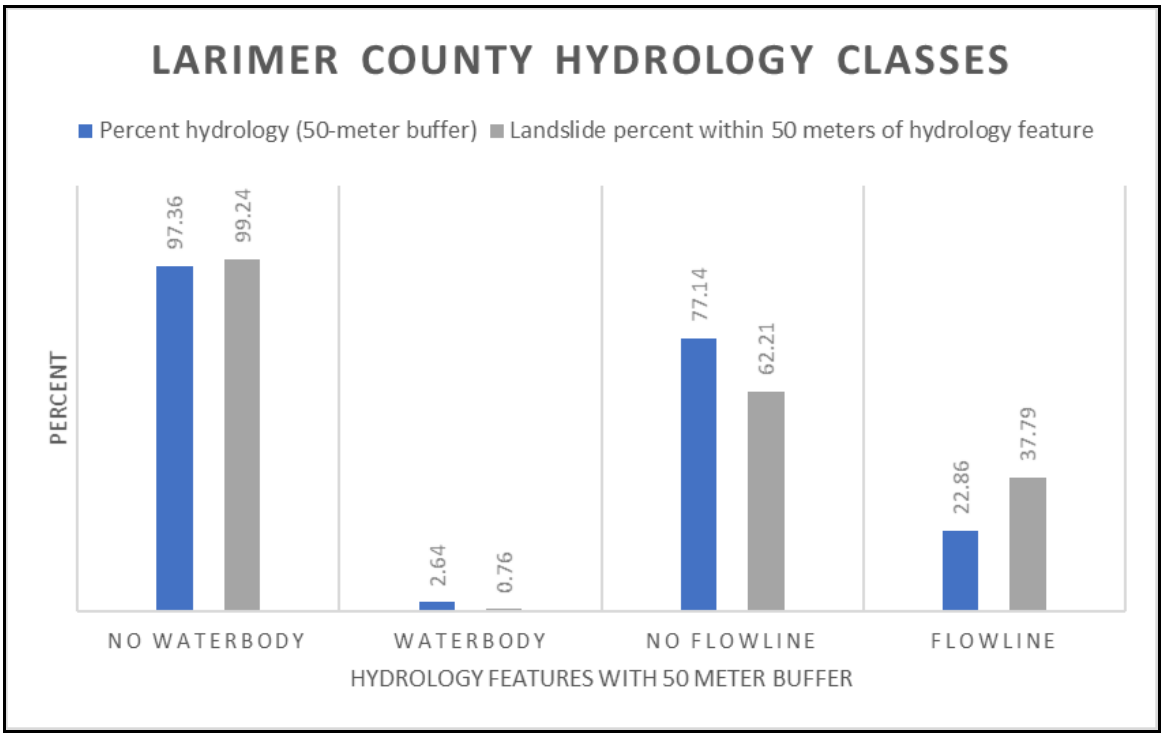

Figure F.11. Hydrology classes for Larimer County, showing areas within 50 meters of waterbodies (lakes and reservoirs) and flowlines (rivers and streams). Data source: U.S. Geological Survey National Hydrology Dataset (NHD) data.

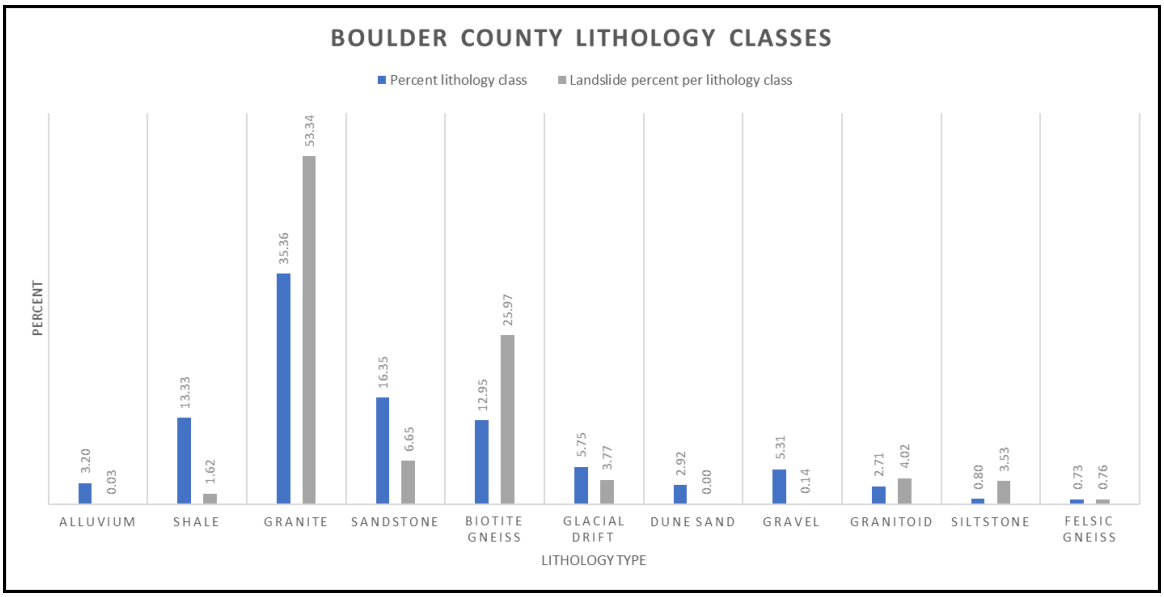

Figure F.12. Fault classes (presence or absence), Boulder and Larimer Counties, showing areas within 50 meters of fault lines. Data source: Colorado Geological Survey.

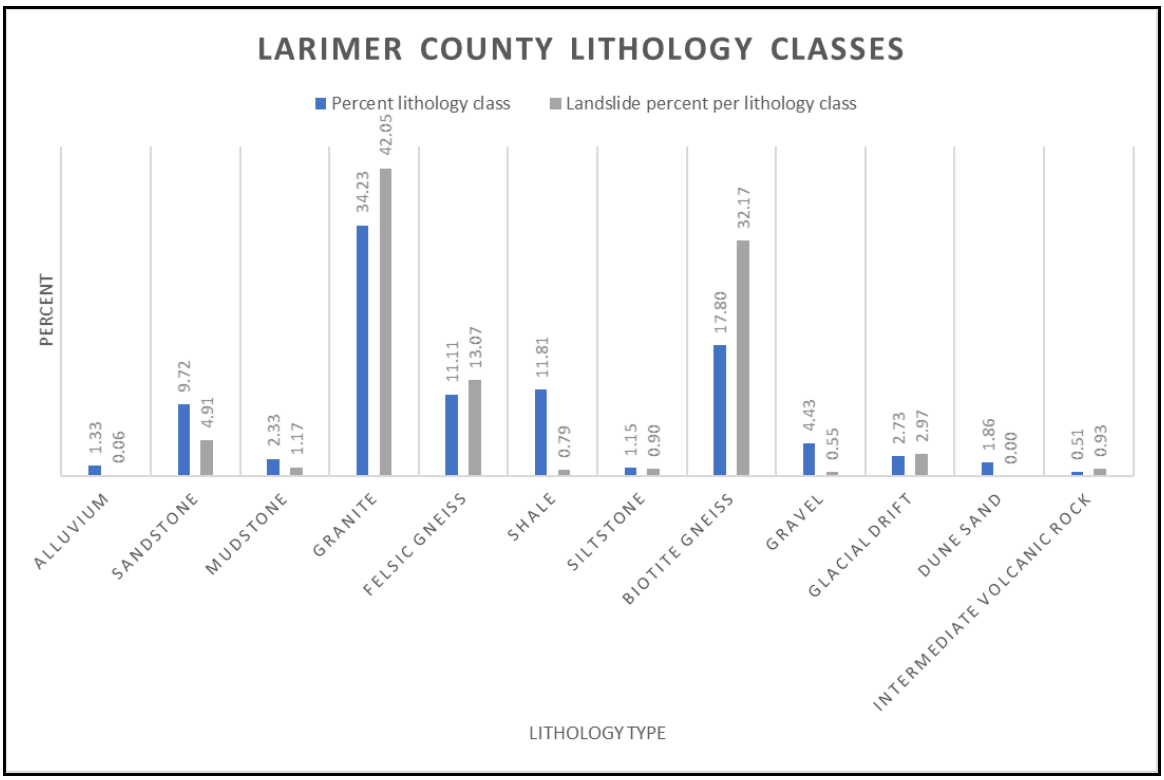

Figure F.13. Lithology classes, Larimer County (classes with less than 0.5% areal extent and water classes were removed from chart). Data source: Colorado Geological Survey.

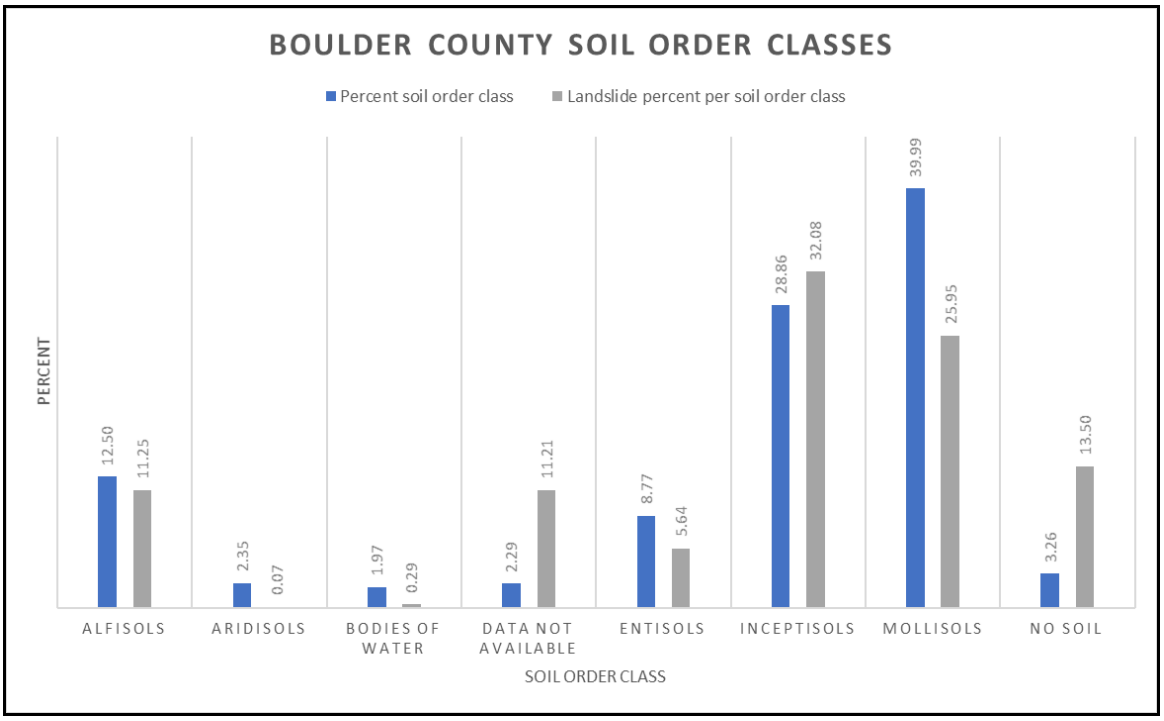

Figure F.14. Soil order classes, Boulder County. Data source: U.S. Department of Agriculture Natural Resources Conservation Service (NRCS).

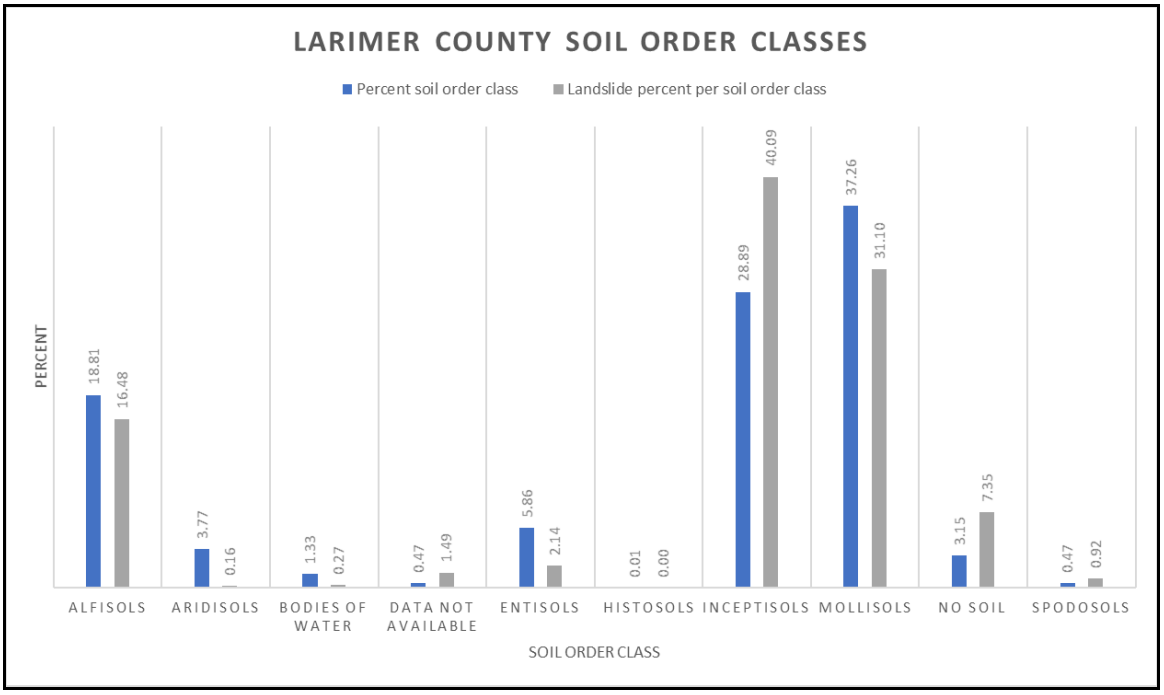

Figure F.15. Soil order classes, Larimer County. Data source: U.S. Department of Agriculture Natural Resources Conservation Service (NRCS).

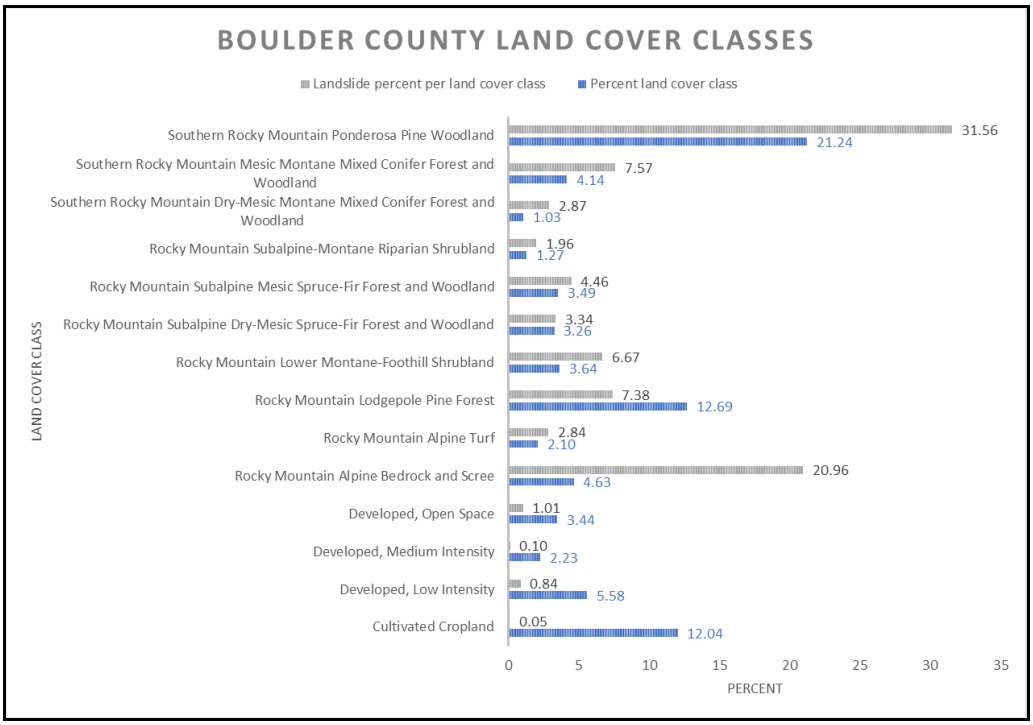

Figure F.16. Land cover classes, Boulder County (with classes for water and pasture removed). Data source: U.S. Geological Survey, GAP Analysis Project.

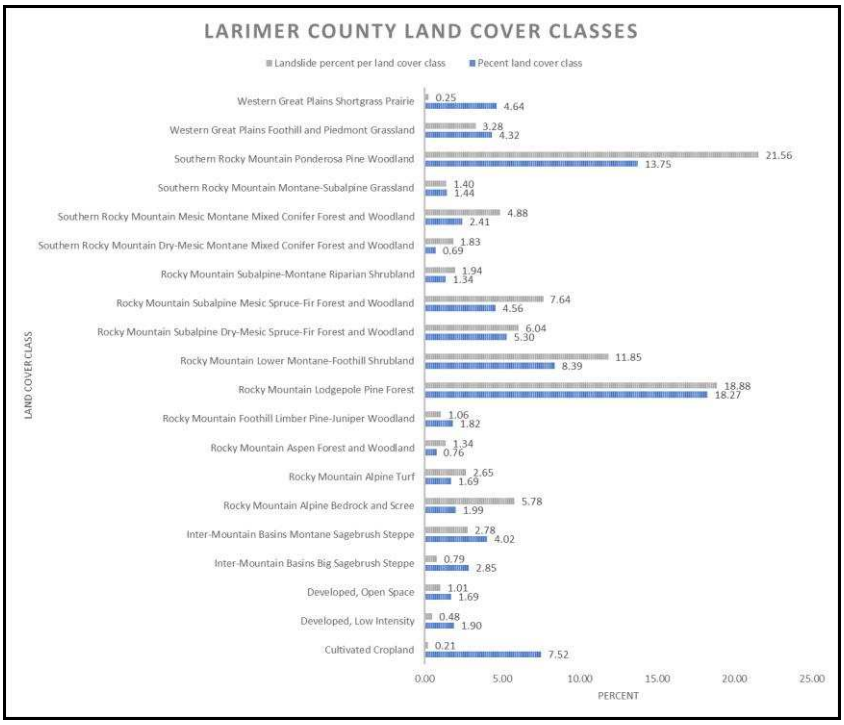

Figure F.17. Land cover classes, Larimer County (with classes for water and pasture removed). Data source: U.S. Geological Survey, GAP Analysis Project.

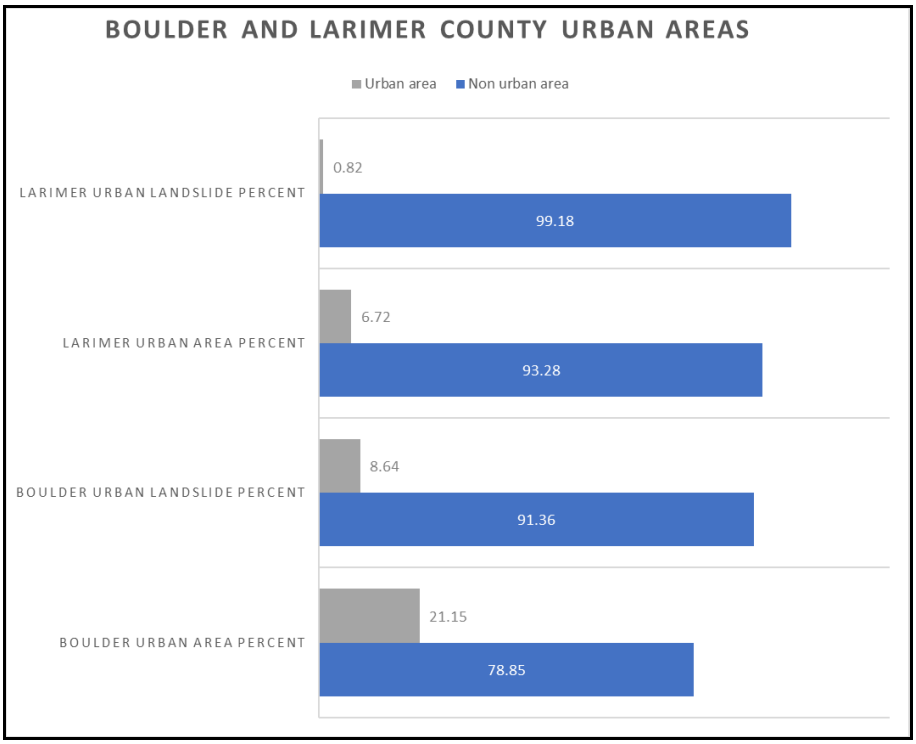

Figure F.18. Urban area classes for Boulder and Larimer Counties. Data source: U.S. Census Bureau.

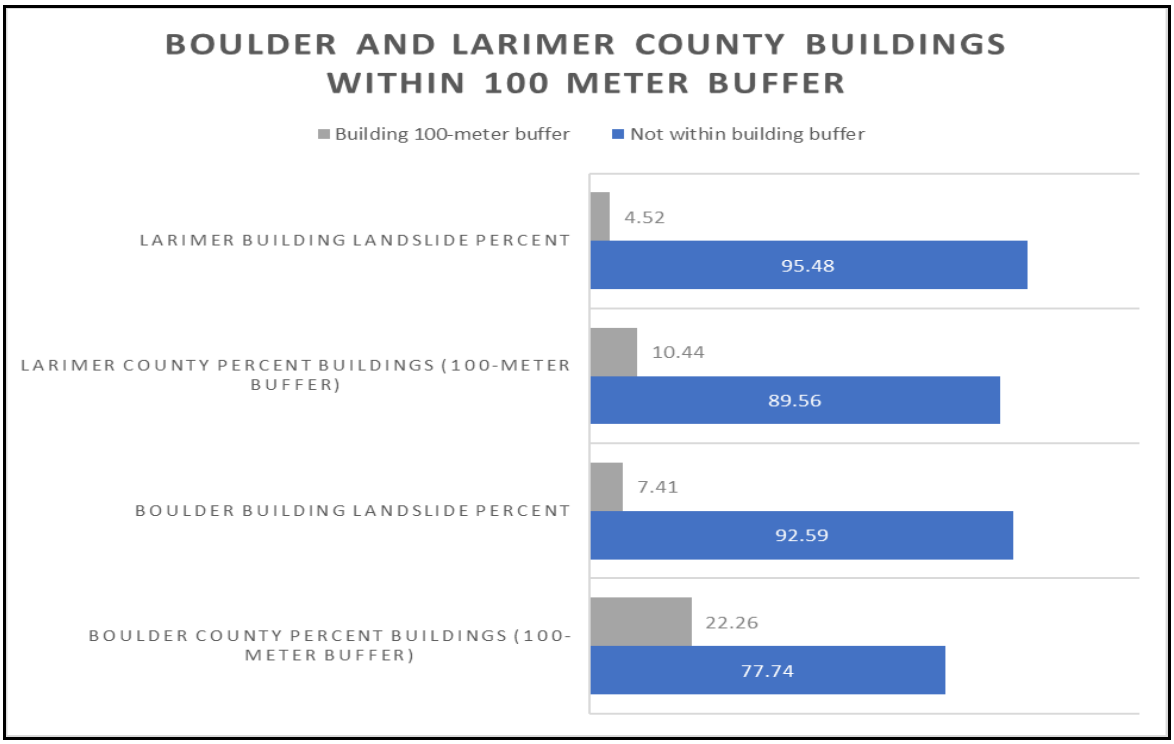

Figure F.19. Building classes for Boulder and Larimer Counties, with 100-meter buffer. Data source: Microsoft building footprints (2018).

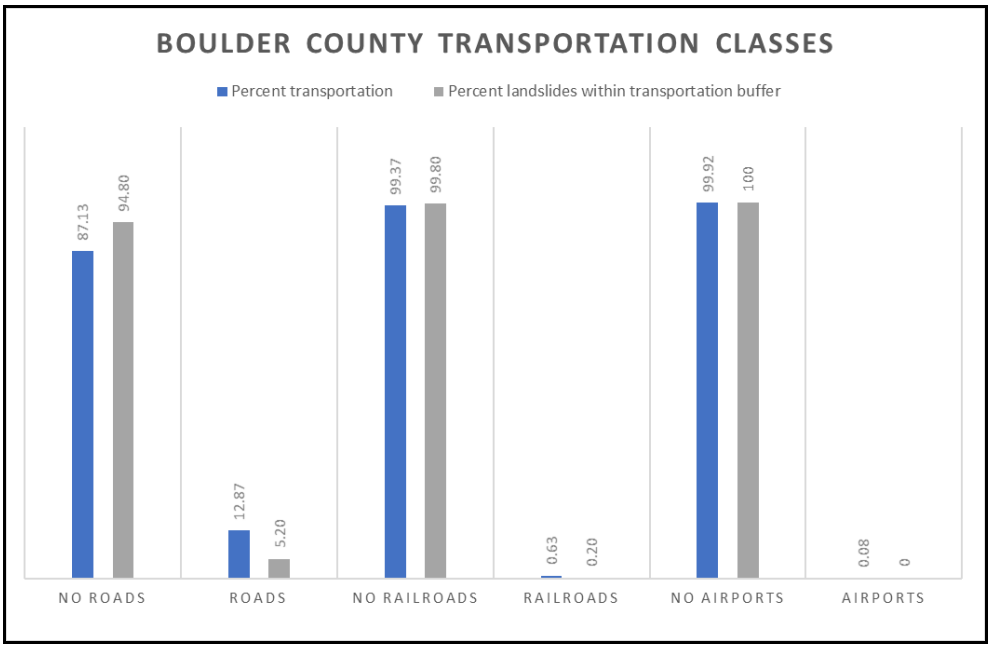

Figure F.20. Transportation classes for Boulder County, with 50-meter buffer for railroads and roadways, and 500-meter buffer for airports. Data source: Colorado Department of Transportation and Boulder County.

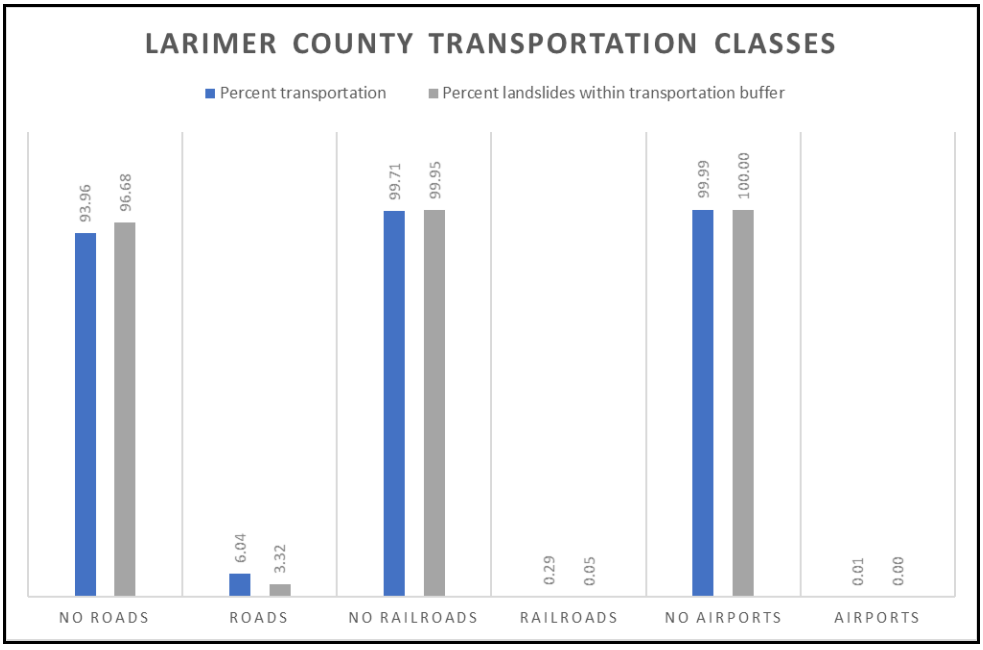

Figure F.21. Transportation classes for Larimer County, with 50-meter buffer for railroads and roadways, and 500-meter buffer for airports. Data source: Colorado Department of Transportation and Larimer County.

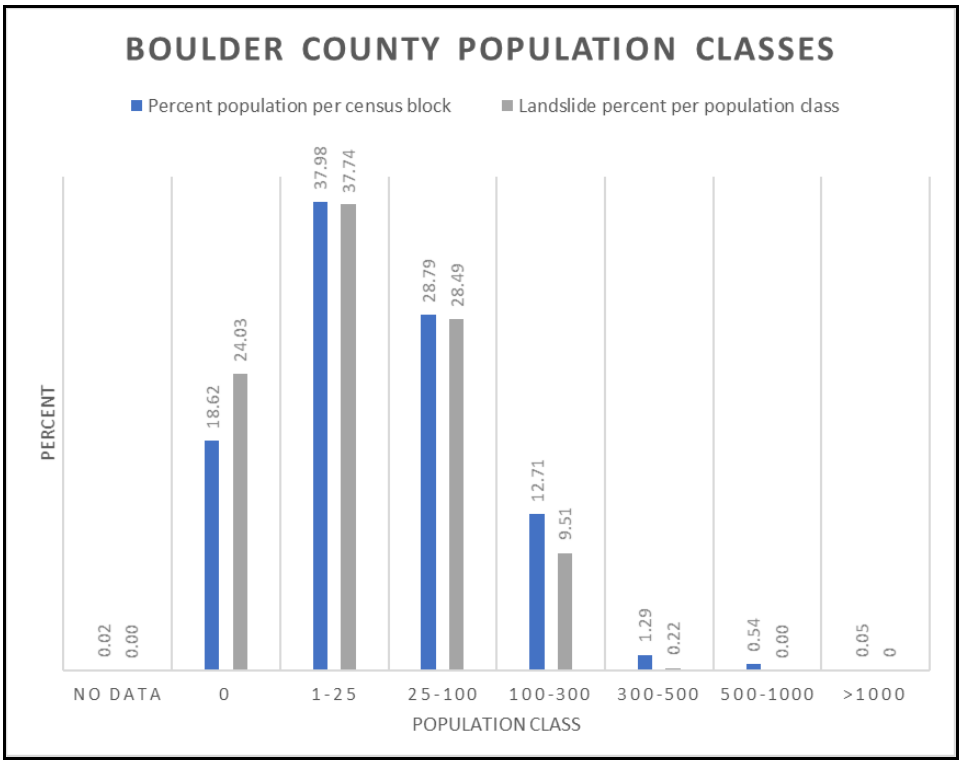

Figure F.22. Population classes for Boulder County. Data source: U.S. Census Bureau.

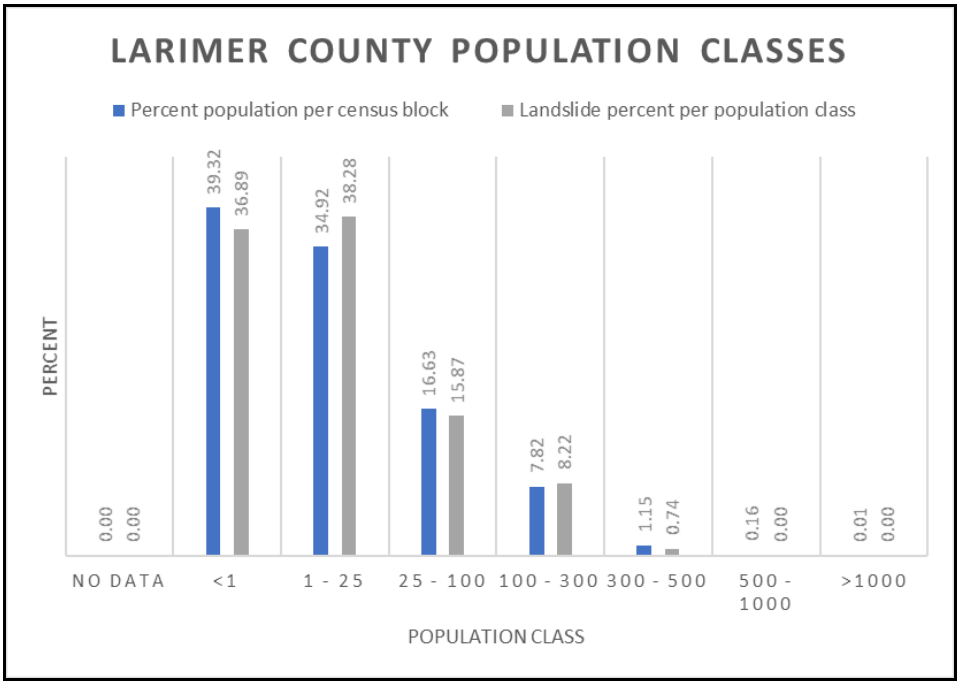

Figure F.23. Population classes for Larimer County. Data source: U.S. Census Bureau.

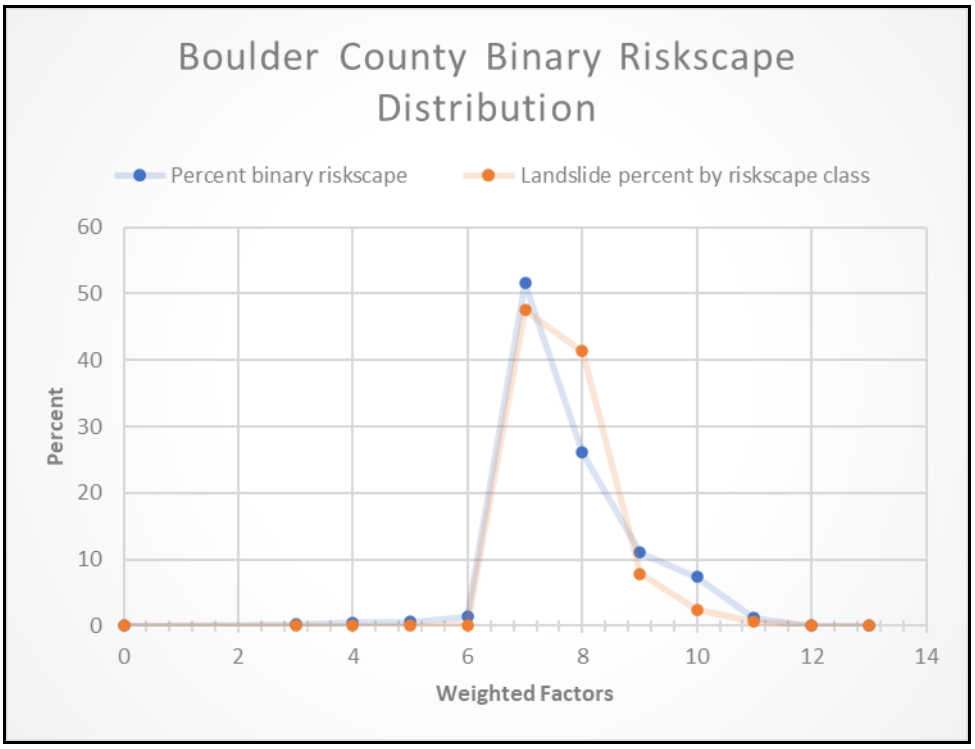

Figure F.24. Boulder County binary riskscape weighted factors and landslide percentages.

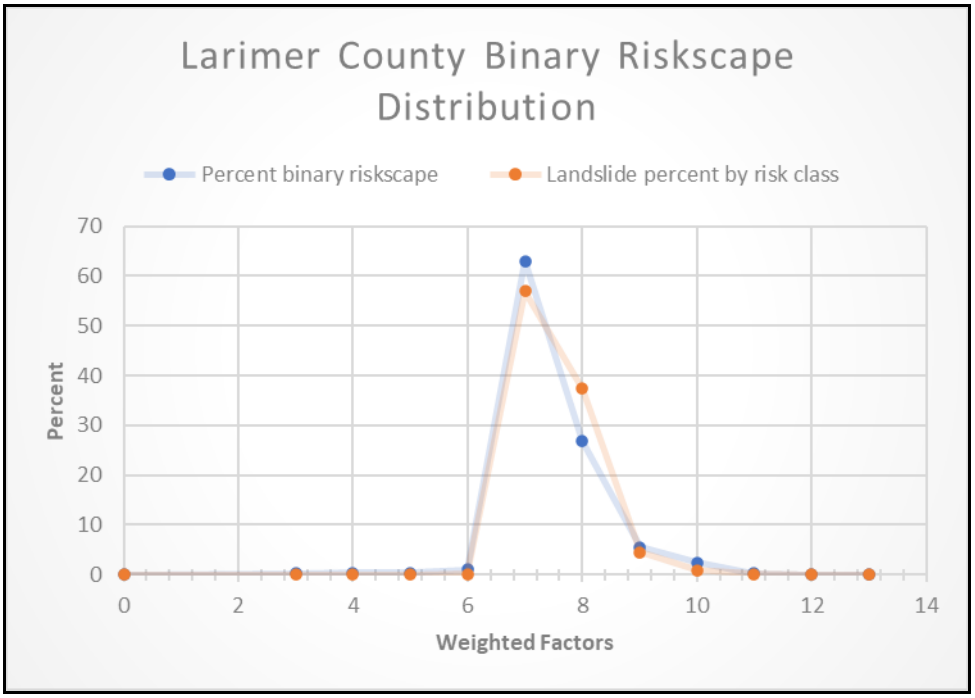

Figure F.25. Larimer County binary riskscape weighted factors and landslide percentages.

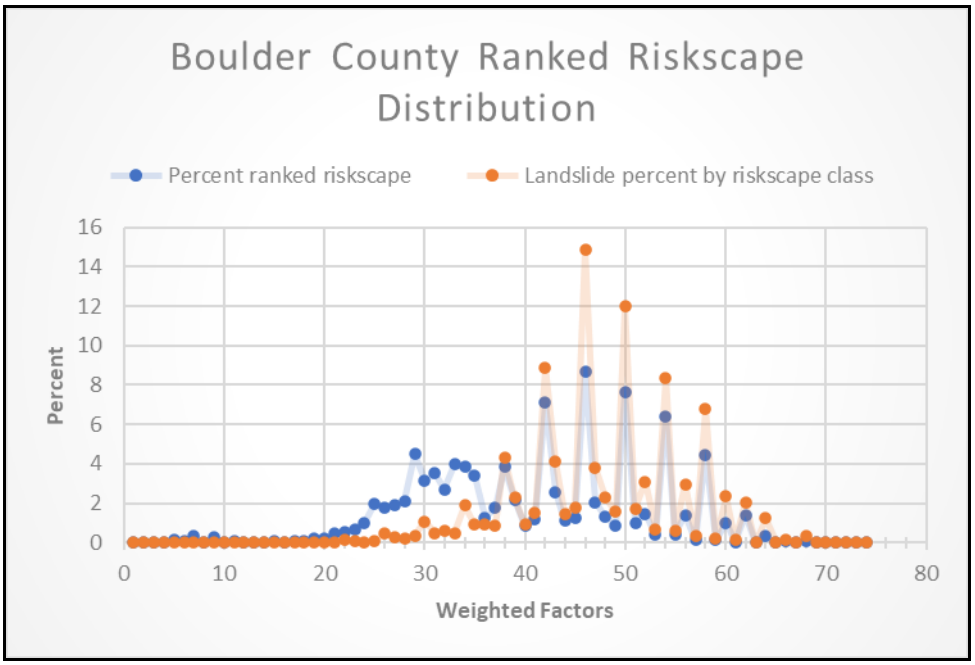

Figure F.26. Boulder County ranked riskscape weighted factors and landslide percentages.

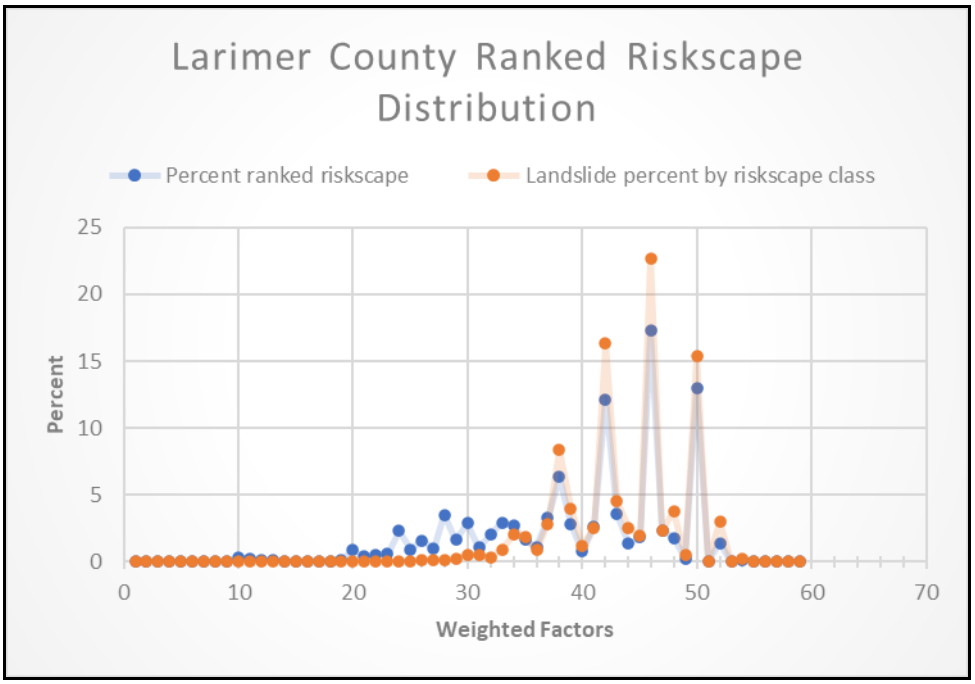

Figure F.27. Larimer County ranked riskscape weighted factors and landslide percentages.

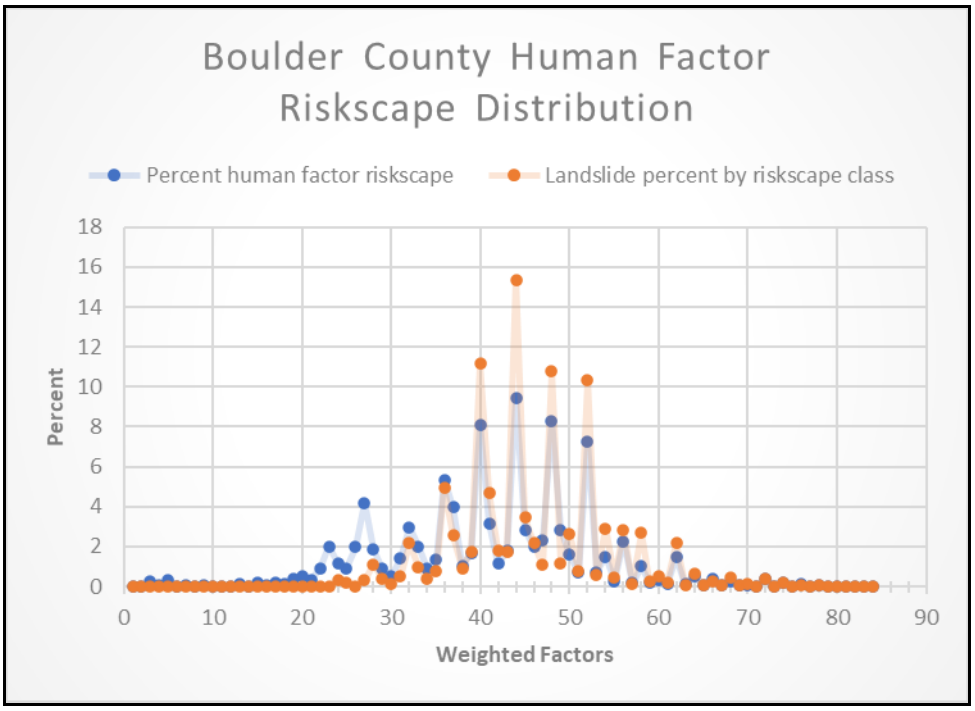

Figure F.28. Boulder County human factor riskscape weighted factors and landslide percentages.

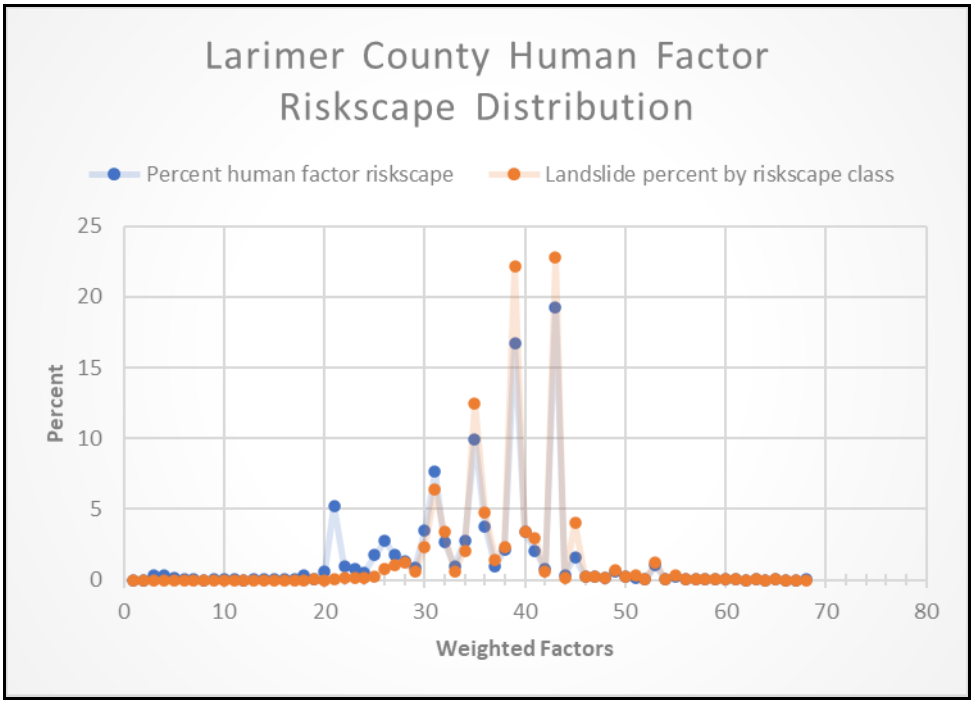

Figure F.29. Larimer County human factor riskscape weighted factors and landslide percentages.

APPENDIX G: GEOSTATISTICAL MAPS

Appendix G includes the geostatistical maps for logistic regression and weights of evidence analyses showing confidence, standard deviation, and posterior probability raster data from Chapter 4.

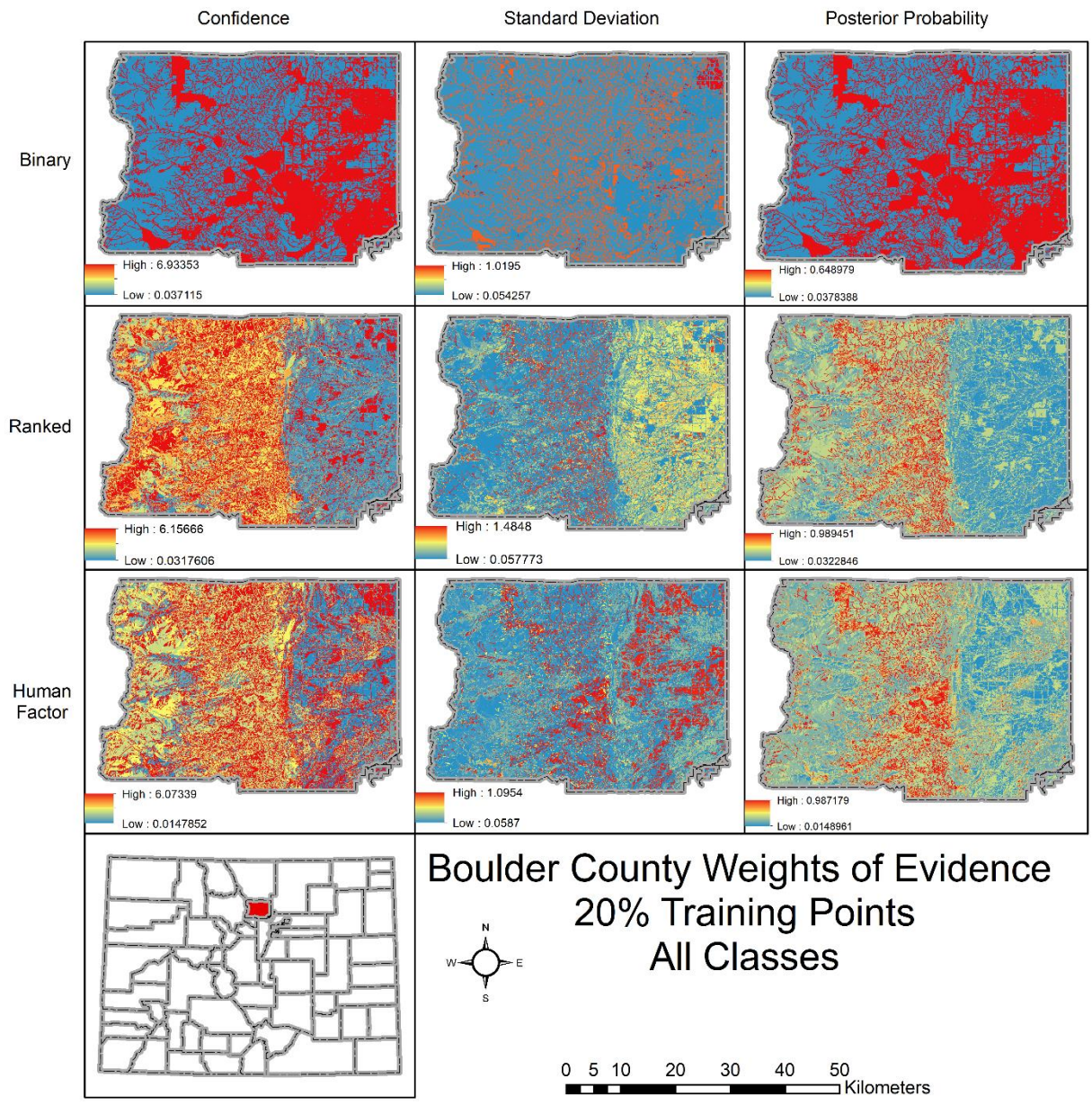

Figure G.1. Boulder County weights of evidence posterior probability maps using 20% training point dataset.

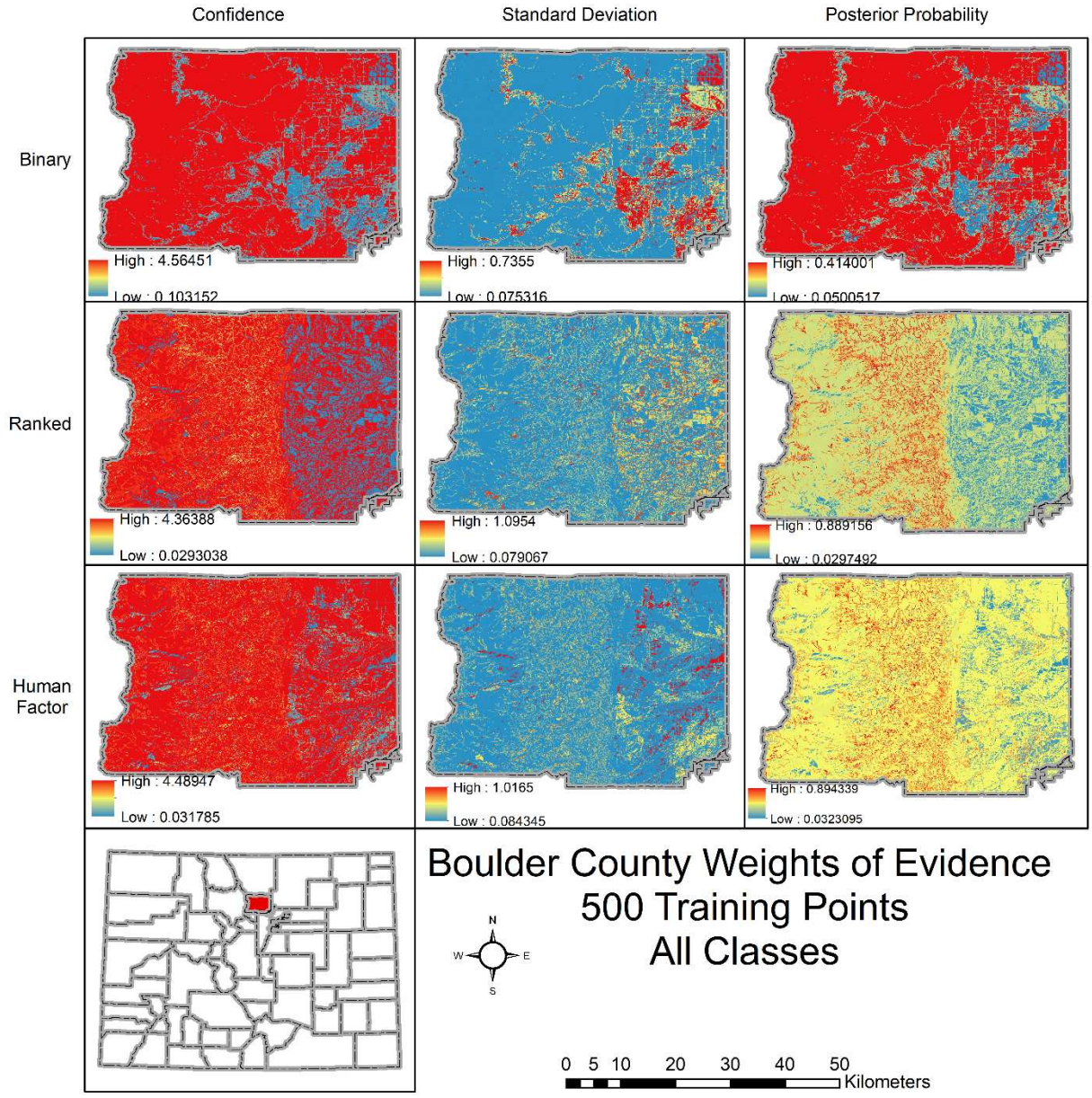

Figure G.2. Boulder County weights of evidence posterior probability maps using 500 point training point dataset.

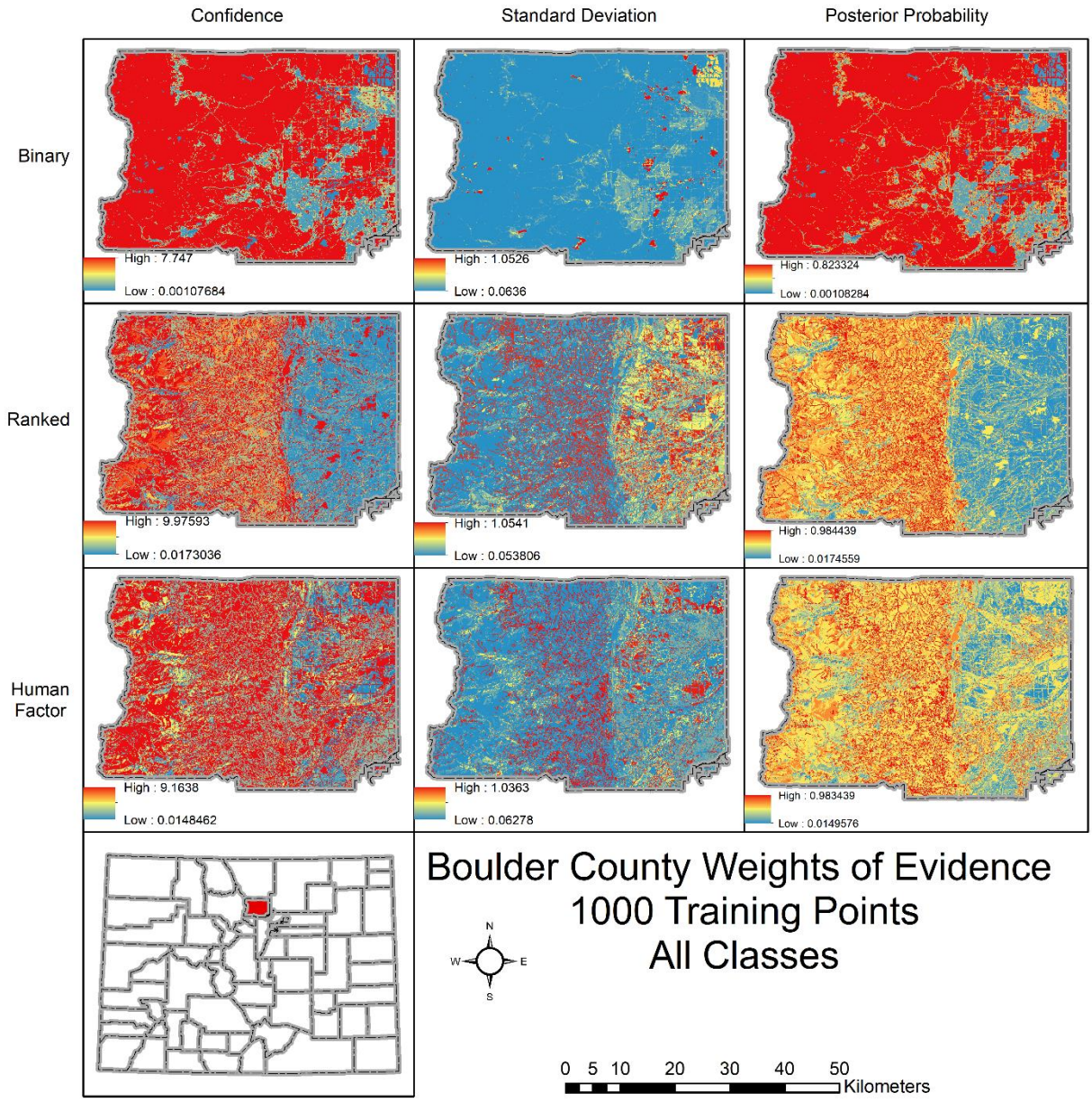

Figure G.3. Boulder County weights of evidence posterior probability maps using 1000 point training point dataset.

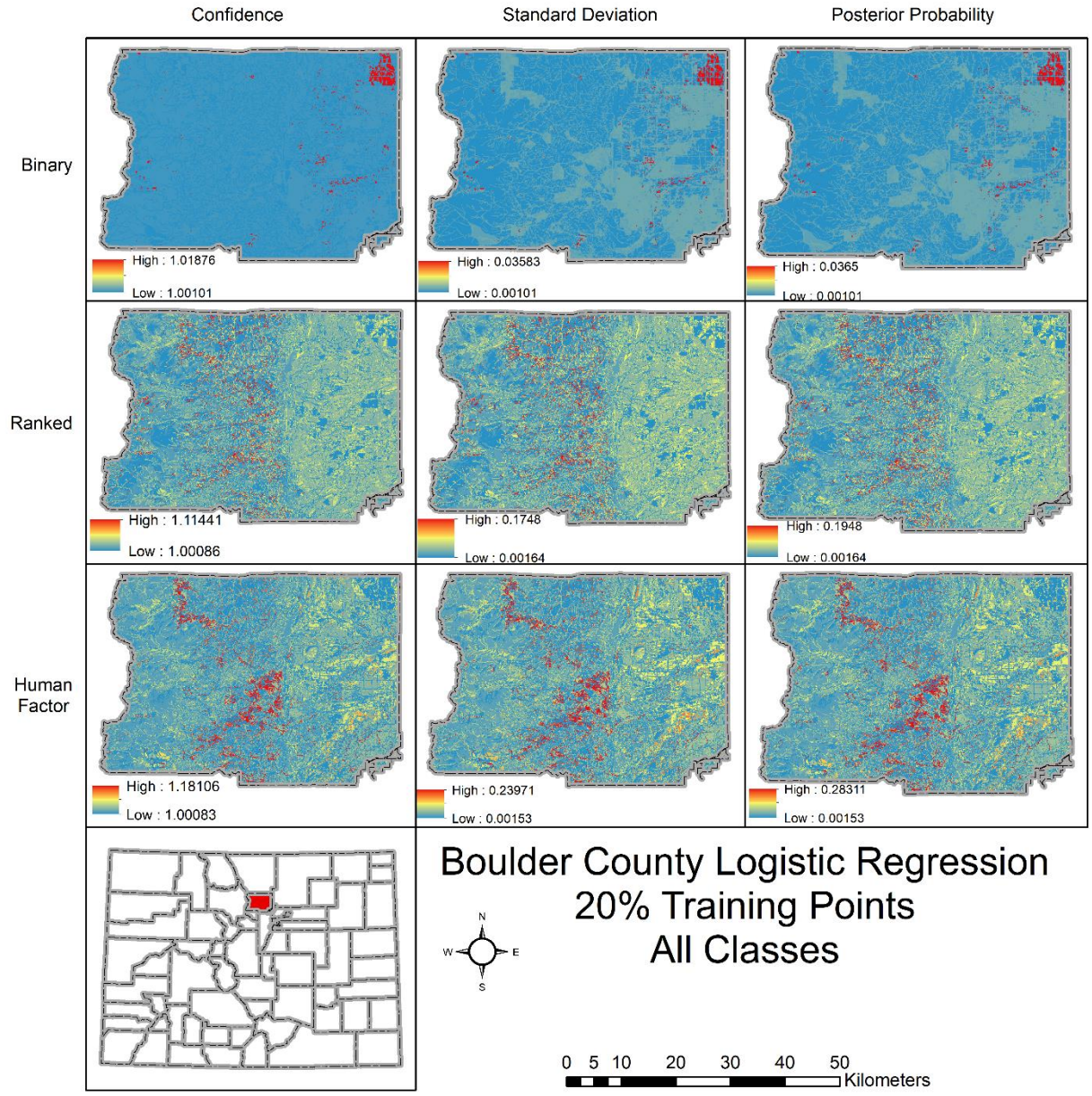

Figure G.4. Boulder County logistic regression posterior probability maps using 20% training point dataset.

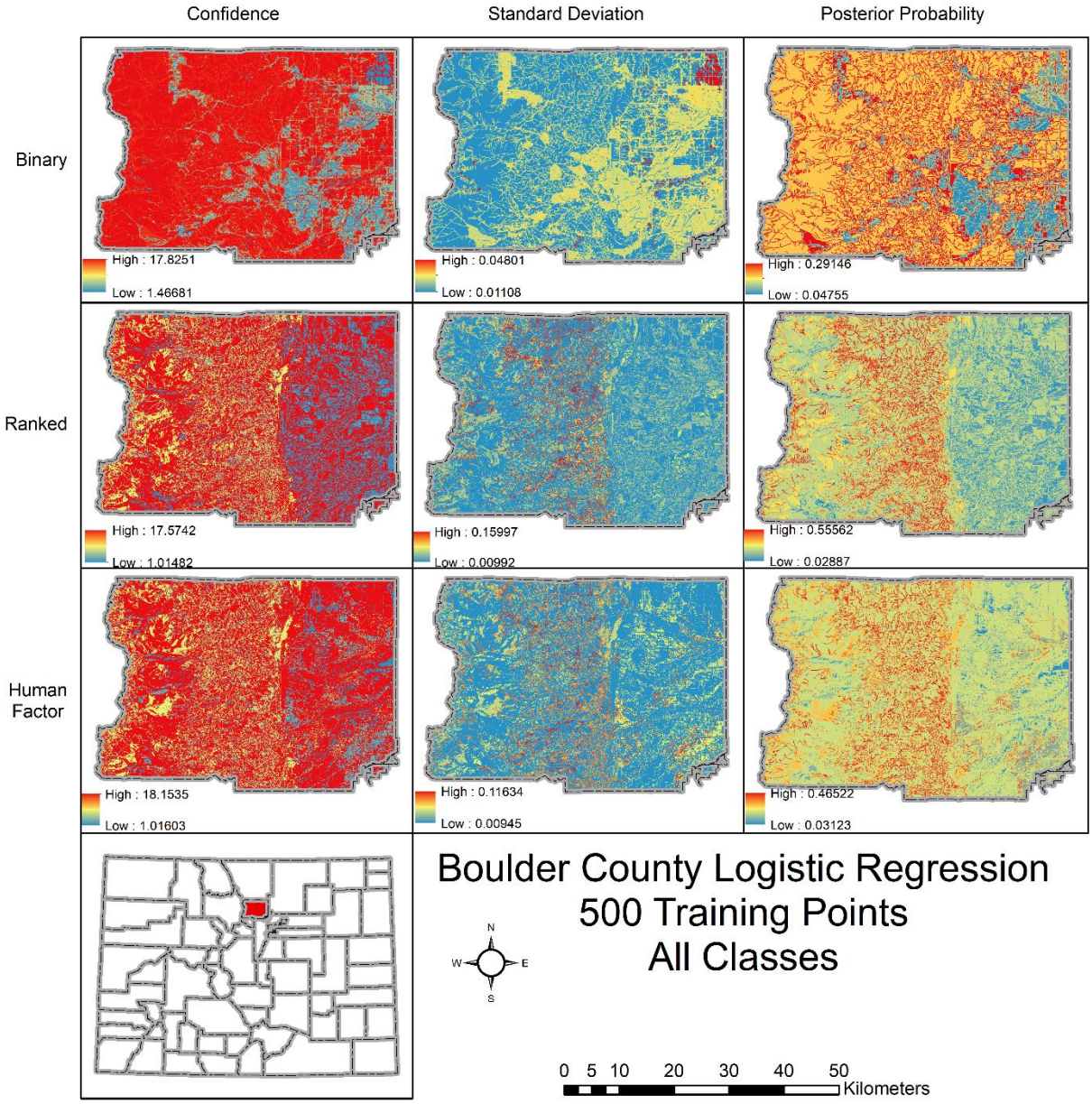

Figure G.5. Boulder County logistic regression posterior probability maps using 500 point training point dataset.

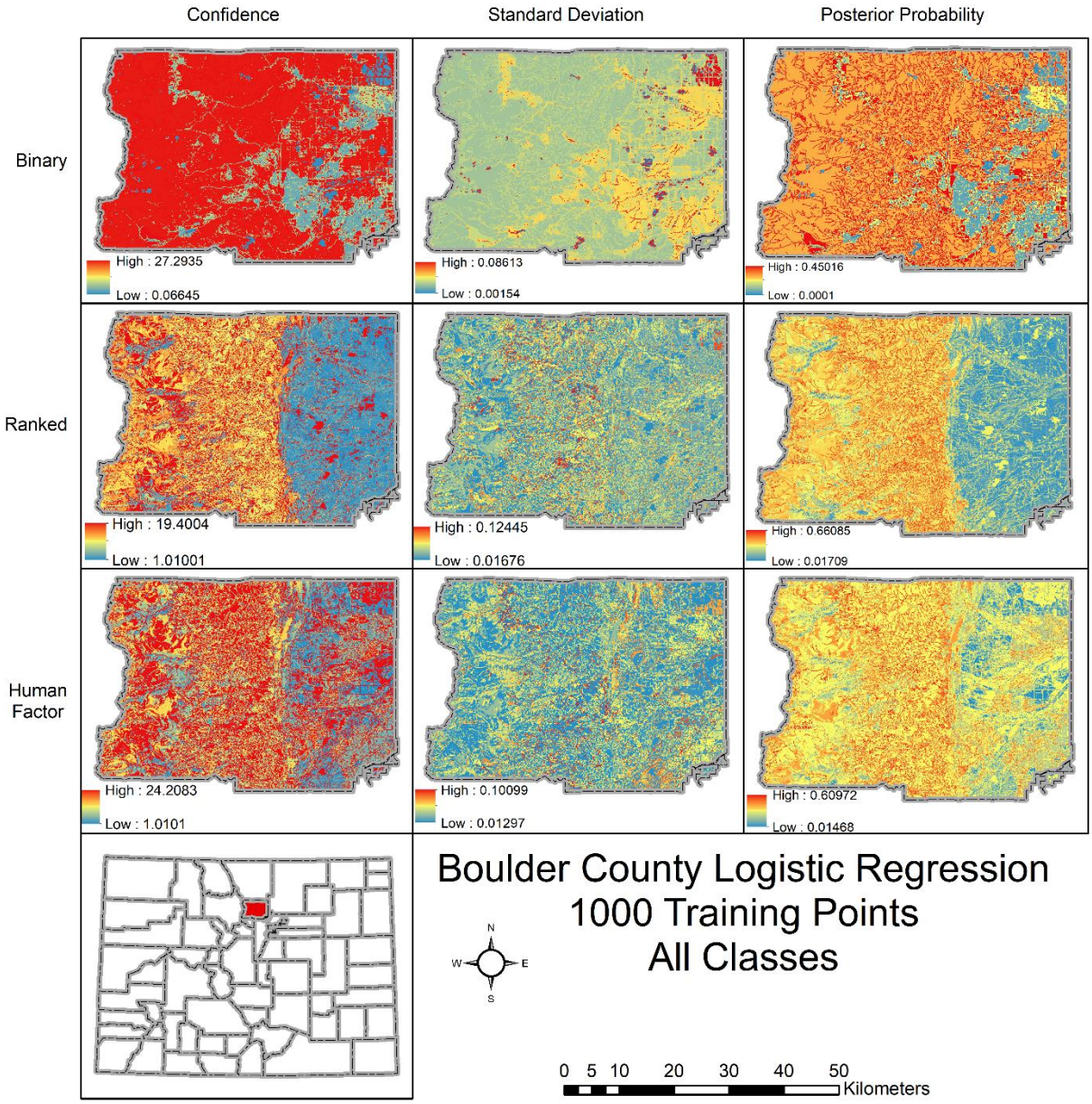

Figure G.6. Boulder County logistic regression posterior probability maps using 1000 point training point dataset.

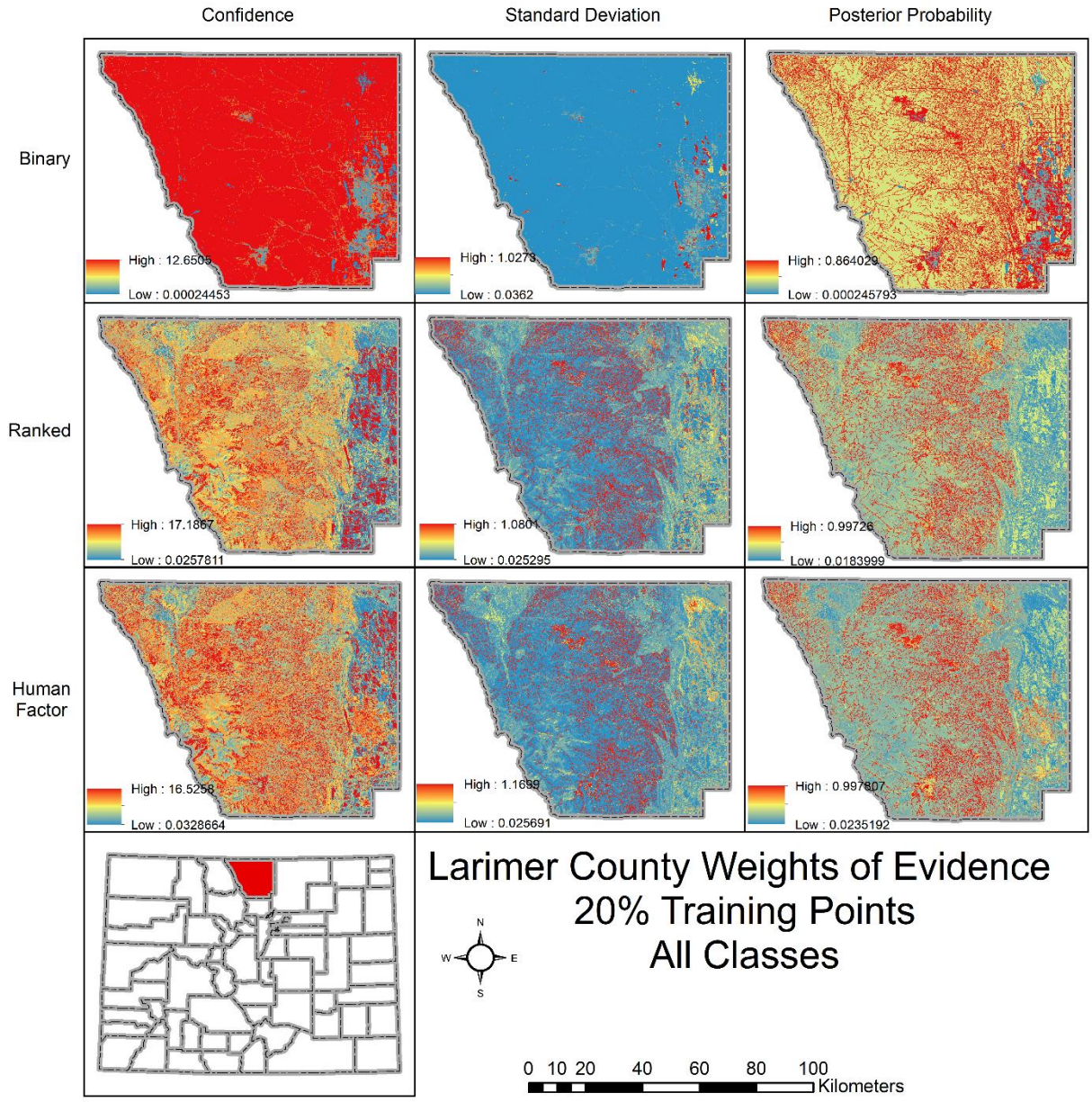

Figure G.7. Larimer County weights of evidence posterior probability maps using 20% training point dataset.

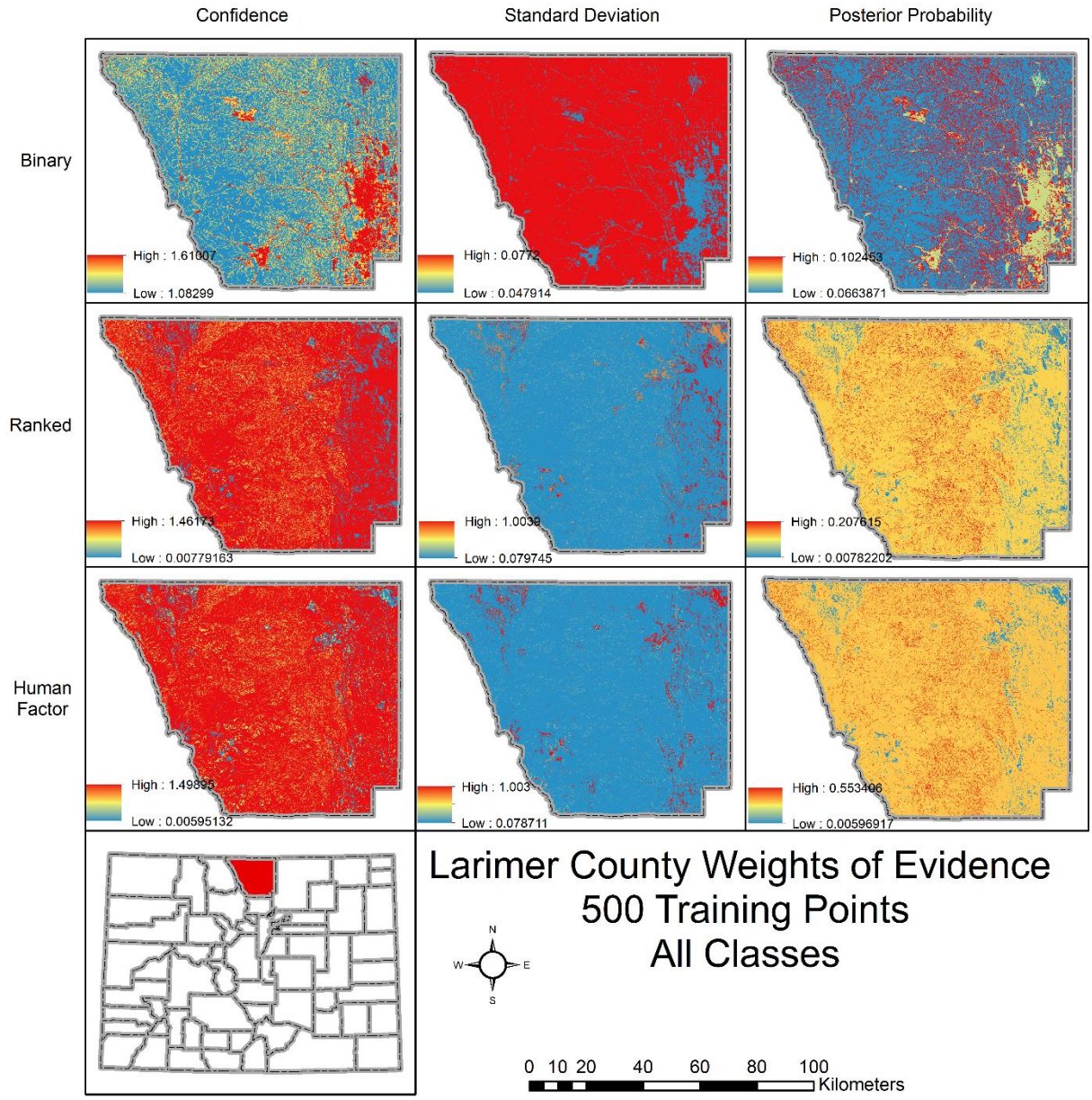

Figure G.8. Larimer County weights of evidence posterior probability maps using 500 point training point dataset.

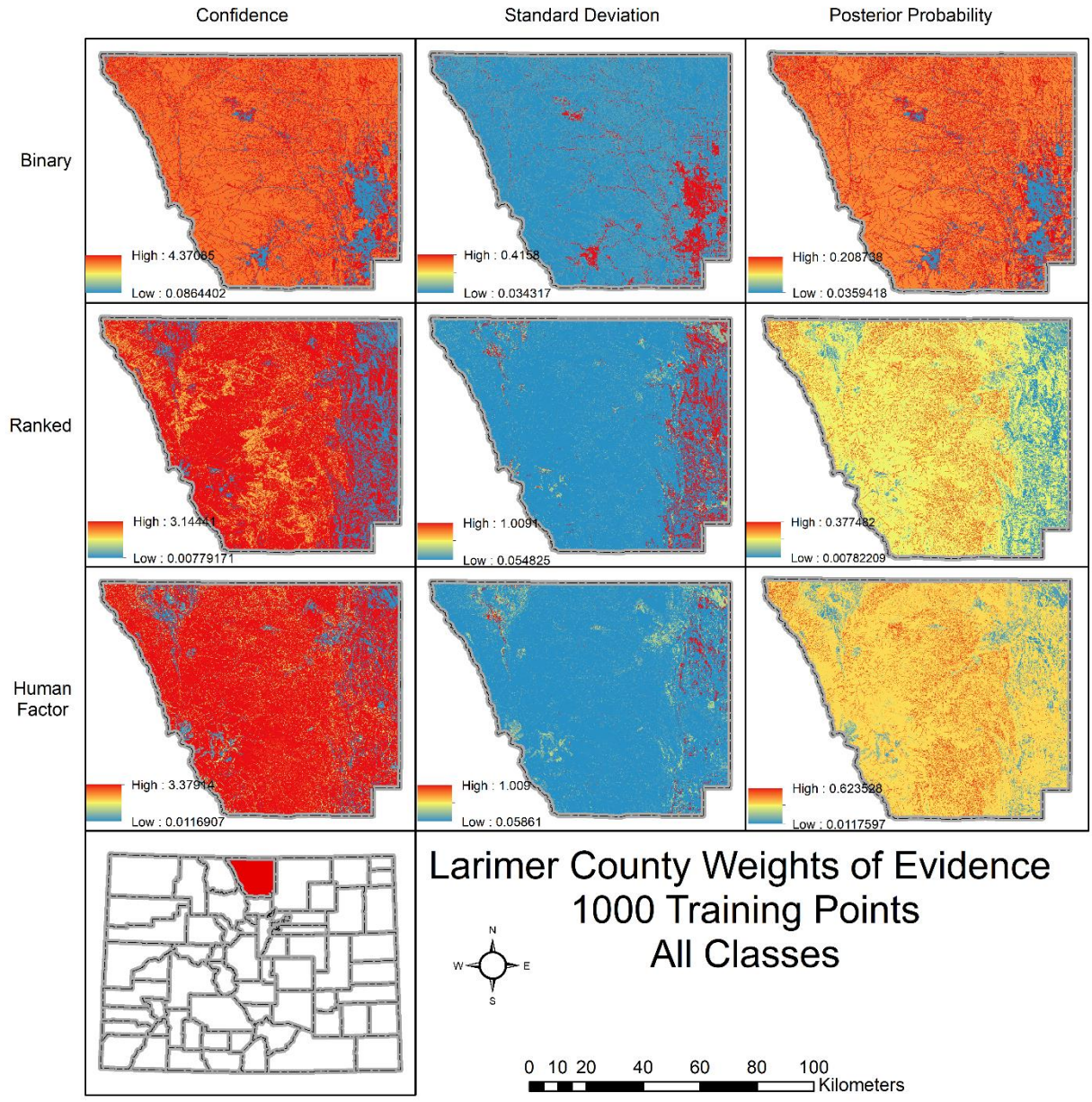

Figure G.9. Larimer County weights of evidence posterior probability maps using 1000 point training point dataset.

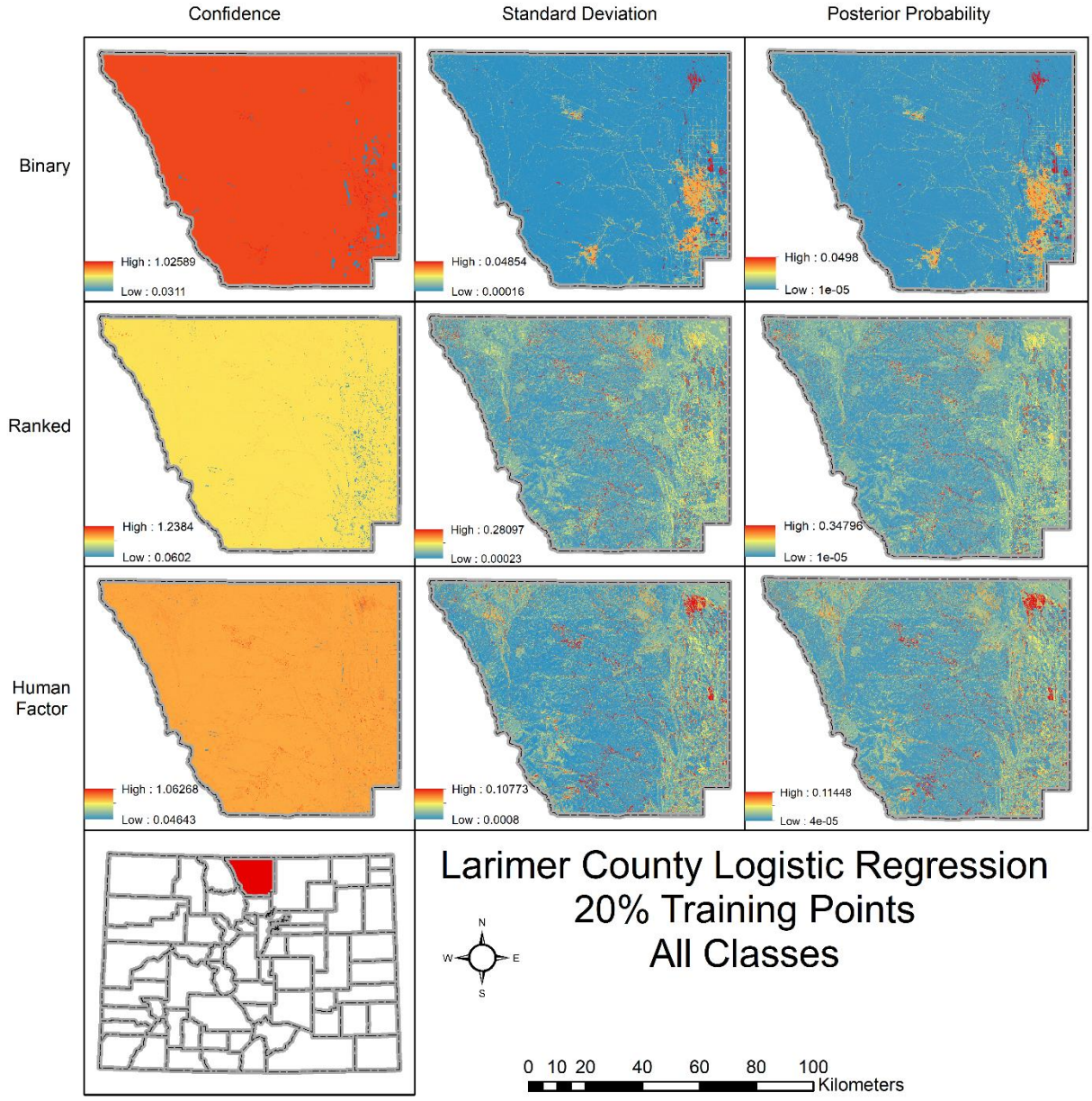

Figure G.10. Larimer County logistic regression posterior probability maps using 20% training point dataset.

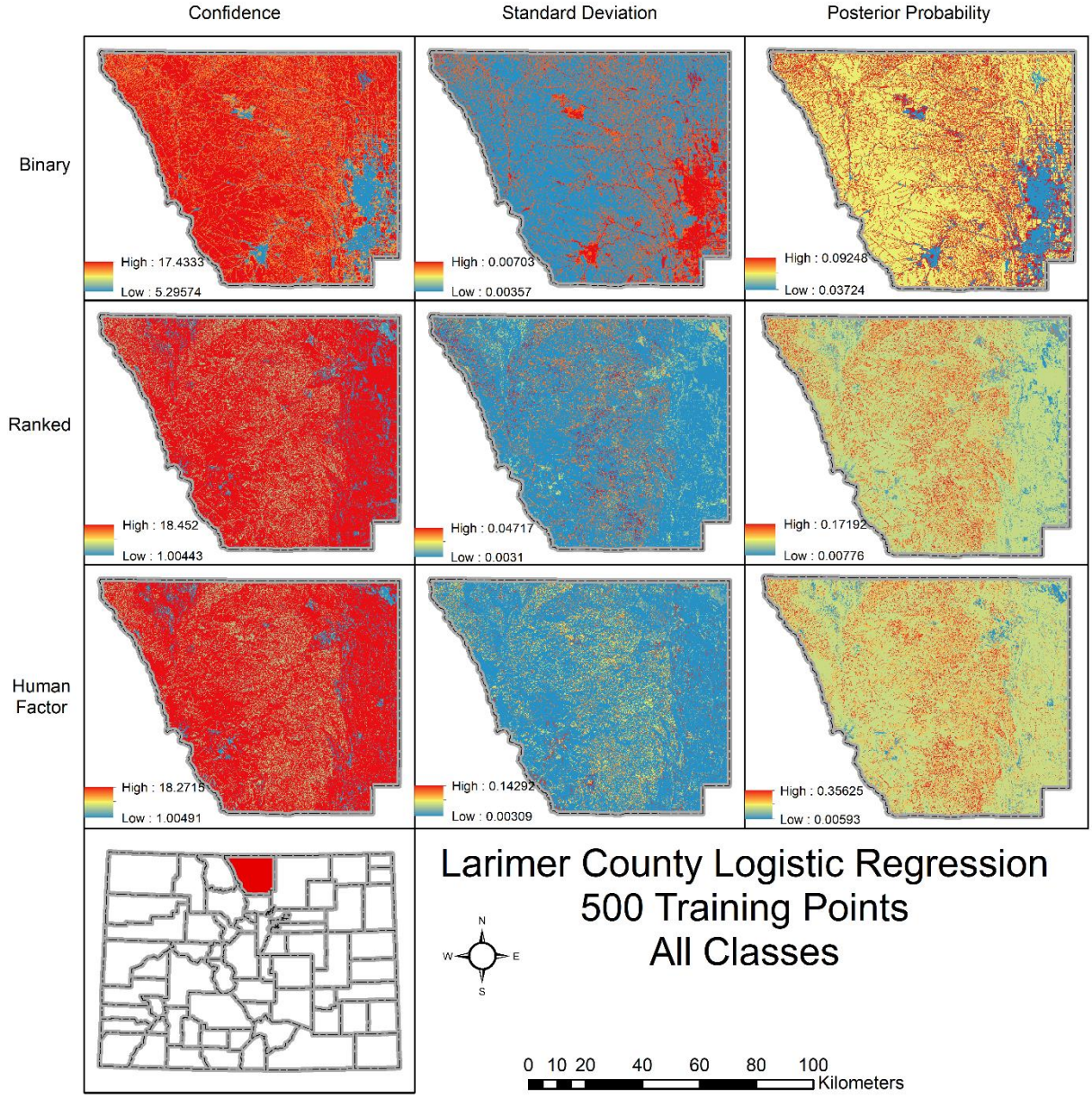

Figure G.11. Larimer County logistic regression posterior probability maps using 500 point training point dataset.

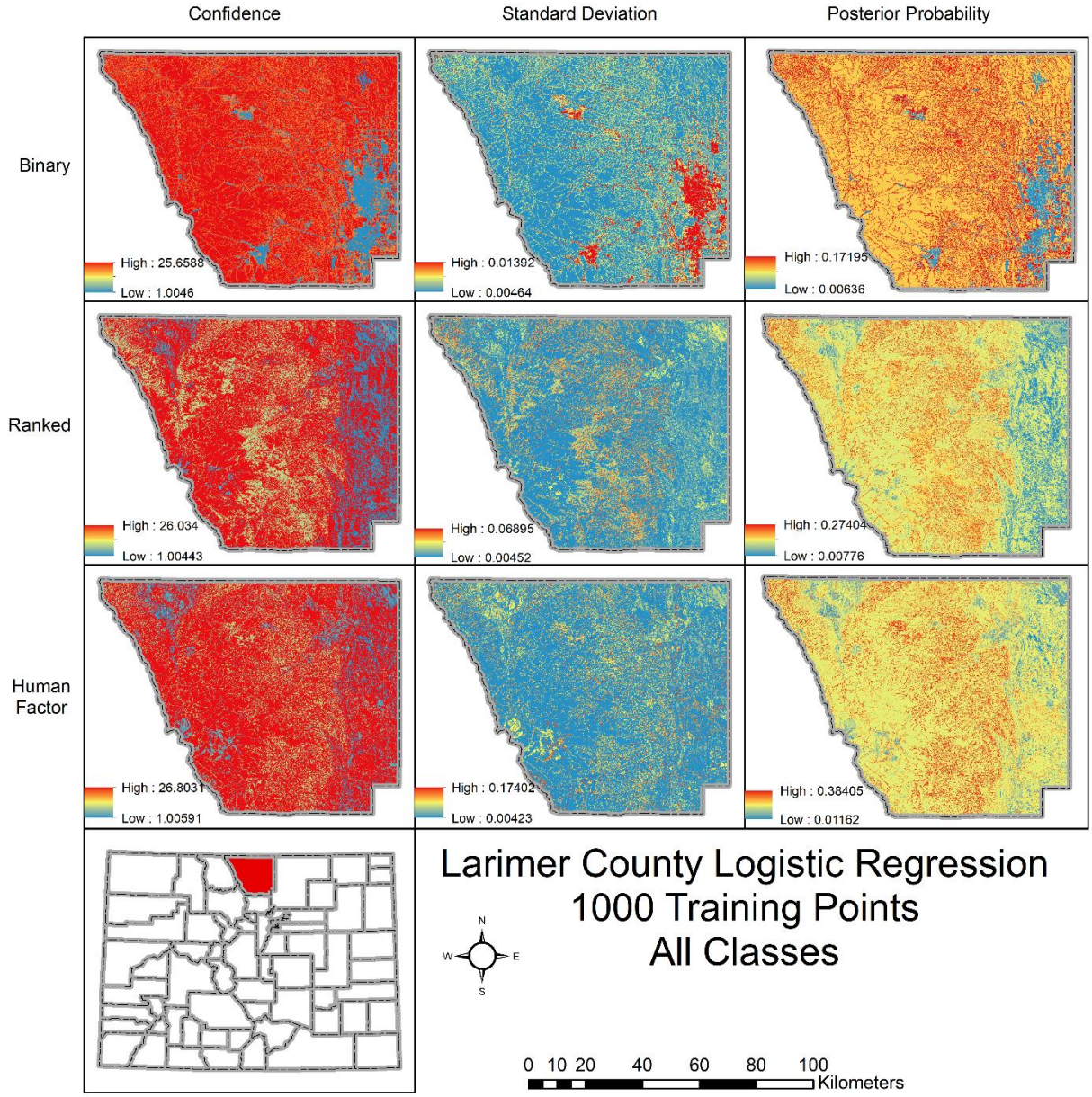

Figure G.12. Larimer County logistic regression posterior probability maps using 1000 point training point dataset.

APPENDIX H: CALCULATE WEIGHTS TABLES

Table H.1. Boulder County, binary riskscapes, all classes, calculate weights tables (classes with no points were removed, 6 from 500 training points, 5 from 1000 training points, and 6 from 20% training points).

Boulder binary 500 training points							
CLASS	AREA_SQ_KM	NO_POINTS	WPLUS	S_WPLUS	WMINUS	S_WMINUS	CONTRAST
6	26.4274	2	-1.4588	0.7355	0.0134	0.0523	-1.4722
7	988.4614	253	-0.0234	0.0729	0.0246	0.0744	-0.048
8	500.7828	207	0.6936	0.0907	-0.3035	0.0657	0.9971
9	211.8238	28	-0.838	0.2029	0.0812	0.0542	-0.9192
10	140.2123	7	-1.9023	0.3878	0.0846	0.053	-1.9869
11	22.0342	2	-1.2606	0.7416	0.0102	0.0522	-1.2708
CLASS	AREA_SQ_KM	NO_POINTS	S_CONTRAST	STUD_CNT	GEN_CLASS	WEIGHT	W_STD
6	26.4274	2	0.7373	-1.9966	6	-1.4588	0.7355
7	988.4614	253	0.1041	-0.4608	99	0.086896	0.075316
8	500.7828	207	0.112	8.901	8	0.6936	0.0907
9	211.8238	28	0.21	-4.3778	9	-0.838	0.2029
10	140.2123	7	0.3914	-5.0767	10	-1.9023	0.3878
11	22.0342	2	0.7434	-1.7094	99	0.086896	0.075316
Boulder binary 1000 training points							
CLASS	AREA_SQ_KM	NO_POINTS	WPLUS	S_WPLUS	WMINUS	S_WMINUS	CONTRAST
4	10.2622	1	-2.3094	1.0526	0.0091	0.0459	-2.3186
6	26.4274	3	-2.1388	0.6132	0.0228	0.0461	-2.1616
7	988.4614	486	-0.1168	0.0636	0.1251	0.066	-0.2419
8	500.7828	412	1.4514	0.117	-0.4307	0.054	1.8821
9	211.8238	74	-0.7054	0.1441	0.0856	0.0486	-0.791
10	140.2123	18	-1.9989	0.2525	0.1247	0.0477	-2.1235
11	22.0342	4	-1.5895	0.5527	0.0158	0.046	-1.6053
CLASS	AREA_SQ_KM	NO_POINTS	S_CONTRAST	STUD_CNT	GEN_CLASS	WEIGHT	W_STD
4	10.2622	1	1.0536	-2.2006	4	-2.3094	1.0526
6	26.4274	3	0.6149	-3.5152	6	-2.1388	0.6132
7	988.4614	486	0.0917	-2.6381	7	-0.1168	0.0636
8	500.7828	412	0.1289	14.6064	8	1.4514	0.117
9	211.8238	74	0.1521	-5.2008	9	-0.7054	0.1441
10	140.2123	18	0.2569	-8.2649	10	-1.9989	0.2525
11	22.0342	4	0.5546	-2.8945	11	-1.5895	0.5527
Boulder binary 20% training points							
CLASS	AREA_SQ	NO_	WPLUS	S_WPLUS	WMINUS	S_WMINUS	CONTRAST

	_KM	POINTS					
6	26.4274	1	-2.5481	1.0195	0.0186	0.0486	-2.5667
7	988.4614	188	-0.761	0.081	0.6411	0.0657	-1.4021
8	500.7828	325	1.3023	0.0936	-0.5589	0.0638	1.8613
9	211.8238	78	0.1479	0.1425	-0.0189	0.0515	0.1668
10	140.2123	39	-0.2659	0.1885	0.0199	0.0501	-0.2859
11	22.0342	10	0.5026	0.4279	-0.0062	0.0487	0.5088
CLASS	AREA_SQ_KM	NO_POINTS	S_CONTRAST	STUD_CNT	GEN_CLASS	WEIGHT	W_STD
6	26.4274	1	1.0206	-2.5148	6	-2.5481	1.0195
7	988.4614	188	0.1043	-13.4407	7	-0.761	0.081
8	500.7828	325	0.1133	16.4256	8	1.3023	0.0936
9	211.8238	78	0.1515	1.101	99	0.020525	0.054257
10	140.2123	39	0.195	-1.4658	99	0.020525	0.054257
11	22.0342	10	0.4307	1.1814	99	0.020525	0.054257

Table H.2. Boulder County, ranked riskscapes, all classes, calculate weights tables (classes with no points were removed, 37 from 500 training points, 27 from 1000 training points, and 31 from 20% training points).

Boulder ranked 500 training points							
CLASS	AREA_SQ_KM	NO_POINTS	WPLUS	S_WPLUS	WMINUS	S_WMINUS	CONTRAST
2	30.5297	5	-0.5867	0.4891	0.0081	0.0524	-0.5948
3	145.2908	52	0.4593	0.1731	-0.0419	0.0547	0.5012
4	33.7033	1	-2.4437	1.0152	0.0213	0.0523	-2.4651
5	52.4949	4	-1.4514	0.5202	0.0268	0.0524	-1.4782
6	29.065	2	-1.5614	0.7328	0.0153	0.0523	-1.5766
9	64.3154	10	-0.6485	0.3441	0.0188	0.0527	-0.6673
10	47.5663	32	1.7644	0.309	-0.0552	0.0534	1.8196
11	43.4584	23	1.1608	0.3039	-0.0326	0.0531	1.1935
12	100.3582	29	0.1433	0.2202	-0.0082	0.0536	0.1515
13	25.7305	7	0.0595	0.443	-0.0008	0.0524	0.0603
14	66.8541	21	0.2628	0.2635	-0.0101	0.0531	0.2729
15	44.6438	2	-2.016	0.7235	0.0265	0.0523	-2.0425
17	124.5493	38	0.2206	0.1946	-0.0162	0.054	0.2368
18	123.3885	36	0.1569	0.198	-0.0112	0.054	0.1681
19	64.7429	4	-1.6766	0.5162	0.0358	0.0525	-1.7124
20	32.4227	1	-2.4038	1.0158	0.0204	0.0522	-2.4242
21	23.8309	7	0.1664	0.4497	-0.0022	0.0524	0.1686
22	33.8321	6	-0.4907	0.4501	0.0077	0.0524	-0.4984
23	40.9165	34	2.6362	0.4171	-0.0657	0.0535	2.7019

24	11.8036	7	1.4203	0.5925	-0.0107	0.0524	1.431
25	70.955	15	-0.2728	0.2908	0.0098	0.0529	-0.2825
26	22.2242	18	2.4933	0.5406	-0.0338	0.0528	2.527
27	14.3883	8	1.2687	0.5306	-0.0116	0.0524	1.2804
32	20.8237	7	0.3633	0.4639	-0.0043	0.0524	0.3676
33	29.2253	9	0.234	0.4007	-0.0038	0.0525	0.2379
34	38.2115	11	0.138	0.3573	-0.0029	0.0526	0.1409
35	9.4623	6	1.5936	0.6749	-0.0097	0.0523	1.6032
36	31.8745	24	2.1582	0.4107	-0.0437	0.0531	2.2019
37	53.9642	13	-0.104	0.3183	0.0029	0.0528	-0.1069
38	60.6182	2	-2.3342	0.7191	0.0382	0.0524	-2.3724
40	48.3555	10	-0.3006	0.3551	0.0072	0.0526	-0.3078
41	29.4269	7	-0.1206	0.433	0.0018	0.0524	-0.1224
42	27.7348	8	0.1408	0.4191	-0.0021	0.0525	0.1429
43	20.1238	9	0.8319	0.4483	-0.0103	0.0525	0.8422
44	4.1336	3	2.017	1.1025	-0.0052	0.0522	2.0222
45	5.734	6	2.8355	1.0801	-0.0114	0.0523	2.8469
46	4.764	5	2.6532	1.0954	-0.0094	0.0523	2.6625
47	6.8413	5	2.0427	0.862	-0.0088	0.0523	2.0515
48	1.595	1	1.5629	1.6373	-0.0016	0.0521	1.5645
49	2.086	2	4.1903	3.4825	-0.004	0.0521	4.1943
51	6.3984	8	3.1232	1.0607	-0.0155	0.0524	3.1386
52	7.161	1	-0.7745	1.0781	0.0024	0.0521	-0.7768

CLASS	AREA_SQ_KM	NO_POINTS	S_CONTRAST	STUD_CNT	GEN_CLASS	WEIGHT	W_STD
2	30.5297	5	0.4918	-1.2093	99	0.400134	0.079067
3	145.2908	52	0.1815	2.7615	3	0.4593	0.1731
4	33.7033	1	1.0165	-2.425	4	-2.4437	1.0152
5	52.4949	4	0.5228	-2.8272	5	-1.4514	0.5202
6	29.065	2	0.7346	-2.1461	6	-1.5614	0.7328
9	64.3154	10	0.3481	-1.9169	99	0.400134	0.079067
10	47.5663	32	0.3136	5.8023	10	1.7644	0.309
11	43.4584	23	0.3085	3.8686	11	1.1608	0.3039
12	100.3582	29	0.2266	0.6686	99	0.400134	0.079067
13	25.7305	7	0.4461	0.1352	99	0.400134	0.079067
14	66.8541	21	0.2688	1.0153	99	0.400134	0.079067
15	44.6438	2	0.7254	-2.8158	15	-2.016	0.7235
17	124.5493	38	0.202	1.1725	99	0.400134	0.079067
18	123.3885	36	0.2053	0.8191	99	0.400134	0.079067
19	64.7429	4	0.5189	-3.3002	19	-1.6766	0.5162
20	32.4227	1	1.0171	-2.3834	20	-2.4038	1.0158
21	23.8309	7	0.4528	0.3724	99	0.400134	0.079067

22	33.8321	6	0.4531	-1.0999	99	0.400134	0.079067
23	40.9165	34	0.4205	6.4248	23	2.6362	0.4171
24	11.8036	7	0.5948	2.4059	24	1.4203	0.5925
25	70.955	15	0.2955	-0.956	99	0.400134	0.079067
26	22.2242	18	0.5432	4.6521	26	2.4933	0.5406
27	14.3883	8	0.5332	2.4014	27	1.2687	0.5306
32	20.8237	7	0.4668	0.7874	99	0.400134	0.079067
33	29.2253	9	0.4041	0.5886	99	0.400134	0.079067
34	38.2115	11	0.3611	0.3901	99	0.400134	0.079067
35	9.4623	6	0.6769	2.3684	35	1.5936	0.6749
36	31.8745	24	0.4141	5.3174	36	2.1582	0.4107
37	53.9642	13	0.3227	-0.3314	99	0.400134	0.079067
38	60.6182	2	0.721	-3.2905	38	-2.3342	0.7191
40	48.3555	10	0.3589	-0.8574	99	0.400134	0.079067
41	29.4269	7	0.4361	-0.2807	99	0.400134	0.079067
42	27.7348	8	0.4224	0.3384	99	0.400134	0.079067
43	20.1238	9	0.4514	1.8658	99	0.400134	0.079067
44	4.1336	3	1.1037	1.8322	99	0.400134	0.079067
45	5.734	6	1.0814	2.6326	45	2.8355	1.0801
46	4.764	5	1.0967	2.4278	46	2.6532	1.0954
47	6.8413	5	0.8636	2.3755	47	2.0427	0.862
48	1.595	1	1.6381	0.9551	99	0.400134	0.079067
49	2.086	2	3.4829	1.2042	99	0.400134	0.079067
51	6.3984	8	1.062	2.9555	51	3.1232	1.0607
52	7.161	1	1.0794	-0.7197	99	0.400134	0.079067

Boulder ranked 1000 training points

CLASS	AREA_SQ_KM	NO_POINTS	WPLUS	S_WPLUS	WMINUS	S_WMINUS	CONTRAST
2	30.5297	16	0.0129	0.3624	-0.0002	0.0461	0.0131
3	145.2908	113	1.1691	0.1995	-0.0844	0.0475	1.2535
4	33.7033	1	-3.571	1.0152	0.0353	0.0462	-3.6062
5	52.4949	9	-1.6589	0.3662	0.0395	0.0464	-1.6984
6	29.065	2	-2.6886	0.7328	0.0279	0.0461	-2.7165
7	9.0867	2	-1.3486	0.8007	0.0057	0.0458	-1.3543
8	5.4639	1	-1.5795	1.1064	0.0039	0.0458	-1.5834
9	64.3154	13	-1.4565	0.3105	0.0444	0.0466	-1.5009
10	47.5663	63	4.0597	1.0079	-0.0641	0.0465	4.1238
11	43.4584	52	3.8678	1.0096	-0.0524	0.0463	3.9202
12	100.3582	47	-0.2104	0.2	0.0116	0.047	-0.222
13	25.7305	8	-0.8793	0.4259	0.0115	0.0461	-0.8908
14	66.8541	34	-0.0492	0.2446	0.0018	0.0466	-0.051
15	44.6438	7	-1.7657	0.4116	0.0348	0.0463	-1.8006

16	31.0141	1	-3.4851	1.0165	0.0322	0.0461	-3.5174
17	124.5493	81	0.5371	0.1879	-0.036	0.0473	0.5731
18	123.3885	57	-0.236	0.1806	0.0163	0.0473	-0.2522
19	64.7429	3	-3.1078	0.5912	0.0666	0.0466	-3.1745
20	32.4227	6	-1.5659	0.4522	0.0232	0.0461	-1.5891
21	23.8309	14	0.27	0.4161	-0.0034	0.046	0.2734
22	33.8321	36	3.5	1.0138	-0.0356	0.0462	3.5357
23	40.9165	51	3.8483	1.0098	-0.0514	0.0463	3.8997
24	11.8036	23	3.052	1.0215	-0.0222	0.046	3.0742
25	70.955	49	0.7193	0.2568	-0.0261	0.0466	0.7455
26	22.2242	35	3.4719	1.0142	-0.0346	0.0461	3.5065
27	14.3883	20	2.9123	1.0247	-0.0192	0.046	2.9314
28	15.9358	1	-2.7872	1.0329	0.0154	0.0459	-2.8026
29	72.4609	3	-3.2256	0.5897	0.0757	0.0467	-3.3013
30	11.6796	1	-2.4518	1.0458	0.0107	0.0459	-2.4625
31	30.9737	1	-3.4838	1.0165	0.0322	0.0461	-3.516
32	20.8237	12	0.224	0.4435	-0.0024	0.046	0.2264
33	29.2253	13	-0.3051	0.3722	0.0047	0.0461	-0.3098
34	38.2115	22	0.2218	0.3273	-0.0045	0.0462	0.2263
35	9.4623	18	2.8069	1.0274	-0.0171	0.0459	2.824
36	31.8745	44	3.7007	1.0113	-0.044	0.0462	3.7447
37	53.9642	37	0.6963	0.2932	-0.0191	0.0464	0.7155
38	60.6182	4	-2.7335	0.5174	0.0596	0.0465	-2.7932
39	57.5225	1	-4.1181	1.0088	0.0625	0.0465	-4.1807
40	48.3555	16	-0.7877	0.3056	0.0197	0.0463	-0.8074
41	29.4269	8	-1.0687	0.4143	0.0156	0.0461	-1.0843
42	27.7348	12	-0.3544	0.3833	0.0052	0.0461	-0.3596
43	20.1238	17	1.6107	0.6156	-0.0138	0.046	1.6245
44	4.1336	5	1.526	1.0954	-0.0039	0.0458	1.5299
45	5.734	4	0.7524	0.9092	-0.0021	0.0458	0.7545
46	4.764	8	1.996	1.0607	-0.007	0.0458	2.0029
47	6.8413	9	2.1137	1.0541	-0.008	0.0458	2.1217
48	1.595	1	0.4357	1.6373	-0.0004	0.0457	0.4361
49	2.086	3	1.0151	1.1547	-0.0019	0.0458	1.0171
51	6.3984	11	2.3144	1.0445	-0.01	0.0459	2.3244
59	0.4613	1	-0.0835	1.4142	0.0001	0.0458	-0.0836
65	0.6322	1	-0.0835	1.4142	0.0001	0.0458	-0.0836
71	0.1388	1	-0.0835	1.4142	0.0001	0.0458	-0.0836
CLASS	AREA_SQ_KM	NO_POINTS	S_CONTRAST	STUD_CNT	GEN_CLASS	WEIGHT	W_STD
2	30.5297	16	0.3653	0.0359	99	0.059691	0.053806
3	145.2908	113	0.2051	6.1108	3	1.1691	0.1995

4	33.7033	1	1.0162	-3.5487	4	-3.571	1.0152
5	52.4949	9	0.3691	-4.601	5	-1.6589	0.3662
6	29.065	2	0.7342	-3.6998	6	-2.6886	0.7328
7	9.0867	2	0.802	-1.6886	99	0.059691	0.053806
8	5.4639	1	1.1073	-1.4299	99	0.059691	0.053806
9	64.3154	13	0.314	-4.7804	9	-1.4565	0.3105
10	47.5663	63	1.009	4.0871	10	4.0597	1.0079
11	43.4584	52	1.0106	3.8789	11	3.8678	1.0096
12	100.3582	47	0.2055	-1.0803	99	0.059691	0.053806
13	25.7305	8	0.4284	-2.0793	13	-0.8793	0.4259
14	66.8541	34	0.249	-0.2047	99	0.059691	0.053806
15	44.6438	7	0.4142	-4.347	15	-1.7657	0.4116
16	31.0141	1	1.0176	-3.4567	16	-3.4851	1.0165
17	124.5493	81	0.1938	2.9579	17	0.5371	0.1879
18	123.3885	57	0.1867	-1.3511	99	0.059691	0.053806
19	64.7429	3	0.593	-5.3528	19	-3.1078	0.5912
20	32.4227	6	0.4546	-3.4958	20	-1.5659	0.4522
21	23.8309	14	0.4186	0.6531	99	0.059691	0.053806
22	33.8321	36	1.0148	3.484	22	3.5	1.0138
23	40.9165	51	1.0108	3.858	23	3.8483	1.0098
24	11.8036	23	1.0225	3.0065	24	3.052	1.0215
25	70.955	49	0.261	2.8562	25	0.7193	0.2568
26	22.2242	35	1.0152	3.4539	26	3.4719	1.0142
27	14.3883	20	1.0257	2.8579	27	2.9123	1.0247
28	15.9358	1	1.034	-2.7106	28	-2.7872	1.0329
29	72.4609	3	0.5915	-5.5809	29	-3.2256	0.5897
30	11.6796	1	1.0468	-2.3525	30	-2.4518	1.0458
31	30.9737	1	1.0176	-3.4552	31	-3.4838	1.0165
32	20.8237	12	0.4458	0.5079	99	0.059691	0.053806
33	29.2253	13	0.3751	-0.826	99	0.059691	0.053806
34	38.2115	22	0.3306	0.6846	99	0.059691	0.053806
35	9.4623	18	1.0284	2.7459	35	2.8069	1.0274
36	31.8745	44	1.0124	3.699	36	3.7007	1.0113
37	53.9642	37	0.2969	2.4101	37	0.6963	0.2932
38	60.6182	4	0.5195	-5.3771	38	-2.7335	0.5174
39	57.5225	1	1.0099	-4.1398	39	-4.1181	1.0088
40	48.3555	16	0.3091	-2.6119	40	-0.7877	0.3056
41	29.4269	8	0.4169	-2.6008	41	-1.0687	0.4143
42	27.7348	12	0.386	-0.9317	99	0.059691	0.053806
43	20.1238	17	0.6173	2.6316	43	1.6107	0.6156
44	4.1336	5	1.0964	1.3954	99	0.059691	0.053806
45	5.734	4	0.9104	0.8288	99	0.059691	0.053806

46	4.764	8	1.0616	1.8866	99	0.059691	0.053806
47	6.8413	9	1.0551	2.0109	47	2.1137	1.0541
48	1.595	1	1.6379	0.2662	99	0.059691	0.053806
49	2.086	3	1.1556	0.8801	99	0.059691	0.053806
51	6.3984	11	1.0455	2.2233	51	2.3144	1.0445
59	0.4613	1	1.415	-0.0591	99	0.059691	0.053806
65	0.6322	1	1.415	-0.0591	99	0.059691	0.053806
71	0.1388	1	1.415	-0.0591	99	0.059691	0.053806
Boulder ranked 20% training points							
CLASS	AREA_SQ_KM	NO_POINTS	WPLUS	S_WPLUS	WMINUS	S_WMINUS	CONTRAST
2	30.5297	16	0.7841	0.3624	-0.0138	0.0489	0.7979
3	145.2908	35	-0.46	0.194	0.0343	0.0501	-0.4944
4	33.7033	2	-2.0755	0.7291	0.0221	0.0487	-2.0976
5	52.4949	4	-1.8074	0.5202	0.0325	0.0488	-1.84
6	29.065	3	-1.4743	0.6097	0.016	0.0487	-1.4902
9	64.3154	8	-1.2638	0.3778	0.0326	0.049	-1.2964
10	47.5663	43	2.9302	0.4922	-0.0659	0.0496	2.9961
11	43.4584	43	5.2289	1.4848	-0.0691	0.0496	5.298
12	100.3582	24	-0.4697	0.234	0.0236	0.0495	-0.4932
13	25.7305	4	-1.0047	0.5441	0.0109	0.0487	-1.0156
14	66.8541	12	-0.832	0.3187	0.0251	0.0491	-0.8571
15	44.6438	2	-2.372	0.7235	0.0309	0.0487	-2.4029
17	124.5493	35	-0.2517	0.1993	0.0167	0.0499	-0.2684
18	123.3885	22	-0.8402	0.2352	0.0479	0.0497	-0.8881
19	64.7429	3	-2.3366	0.5912	0.0449	0.0489	-2.3816
20	32.4227	2	-2.0343	0.73	0.021	0.0487	-2.0553
21	23.8309	7	-0.1896	0.4497	0.0023	0.0487	-0.1919
22	33.8321	16	0.5793	0.3444	-0.0112	0.0489	0.5905
23	40.9165	54	4.6767	1.0092	-0.0872	0.0499	4.7639
24	11.8036	9	1.854	0.684	-0.0119	0.0487	1.866
25	70.955	28	0.2598	0.2429	-0.0104	0.0494	0.2702
26	22.2242	43	4.4489	1.0116	-0.0687	0.0496	4.5176
27	14.3883	10	1.5114	0.5726	-0.0123	0.0487	1.5236
29	72.4609	3	-2.4544	0.5897	0.0513	0.049	-2.5057
30	11.6796	2	-0.8891	0.7767	0.0045	0.0485	-0.8936
31	30.9737	1	-2.7126	1.0165	0.0222	0.0486	-2.7348
32	20.8237	9	0.4148	0.4424	-0.0048	0.0487	0.4197
33	29.2253	9	-0.122	0.4007	0.0018	0.0488	-0.1238
34	38.2115	12	-0.0936	0.3485	0.0019	0.0489	-0.0954
35	9.4623	20	3.6835	1.0247	-0.0309	0.0489	3.7144
36	31.8745	46	4.5164	1.0108	-0.0737	0.0497	4.5901

37	53.9642	16	-0.1763	0.2981	0.0049	0.0491	-0.1813
38	60.6182	5	-1.7213	0.4669	0.0368	0.0489	-1.7581
39	57.5225	7	-1.2888	0.4033	0.0294	0.0489	-1.3182
40	48.3555	5	-1.4723	0.4723	0.0268	0.0488	-1.499
41	29.4269	5	-0.8985	0.4909	0.0115	0.0487	-0.91
42	27.7348	14	0.7069	0.3798	-0.0113	0.0489	0.7181
43	20.1238	7	0.0592	0.468	-0.0006	0.0487	0.0598
44	4.1336	9	2.885	1.0541	-0.0134	0.0487	2.8983
45	5.734	5	2.6064	1.25	-0.0073	0.0485	2.6137
46	4.764	6	2.4795	1.0801	-0.0086	0.0486	2.4881
47	6.8413	14	3.3268	1.0351	-0.0213	0.0488	3.3481
48	1.595	4	2.074	1.118	-0.0055	0.0485	2.0795
49	2.086	4	2.074	1.118	-0.0055	0.0485	2.0795
51	6.3984	9	2.885	1.0541	-0.0134	0.0487	2.8983
52	7.161	1	-1.1305	1.0781	0.0033	0.0485	-1.1338
59	0.4613	1	0.6877	1.4142	-0.0008	0.0484	0.6885
65	0.6322	2	1.3809	1.2247	-0.0023	0.0485	1.3832
CLASS	AREA_SQ_KM	NO_POINTS	S_CONTRAST	STUD_CNT	GEN_CLASS	WEIGHT	W_STD
2	30.5297	16	0.3657	2.1821	2	0.7841	0.3624
3	145.2908	35	0.2004	-2.4673	3	-0.46	0.194
4	33.7033	2	0.7307	-2.8707	4	-2.0755	0.7291
5	52.4949	4	0.5225	-3.5214	5	-1.8074	0.5202
6	29.065	3	0.6116	-2.4365	6	-1.4743	0.6097
9	64.3154	8	0.381	-3.4027	9	-1.2638	0.3778
10	47.5663	43	0.4947	6.0566	10	2.9302	0.4922
11	43.4584	43	1.4857	3.5661	11	5.2289	1.4848
12	100.3582	24	0.2392	-2.0621	12	-0.4697	0.234
13	25.7305	4	0.5462	-1.8593	99	0.093622	0.057773
14	66.8541	12	0.3224	-2.6582	14	-0.832	0.3187
15	44.6438	2	0.7251	-3.3137	15	-2.372	0.7235
17	124.5493	35	0.2055	-1.306	99	0.093622	0.057773
18	123.3885	22	0.2404	-3.6946	18	-0.8402	0.2352
19	64.7429	3	0.5932	-4.0146	19	-2.3366	0.5912
20	32.4227	2	0.7316	-2.8094	20	-2.0343	0.73
21	23.8309	7	0.4524	-0.4242	99	0.093622	0.057773
22	33.8321	16	0.3478	1.6978	99	0.093622	0.057773
23	40.9165	54	1.0104	4.7147	23	4.6767	1.0092
24	11.8036	9	0.6857	2.7213	24	1.854	0.684
25	70.955	28	0.2479	1.09	99	0.093622	0.057773
26	22.2242	43	1.0128	4.4606	26	4.4489	1.0116
27	14.3883	10	0.5747	2.6513	27	1.5114	0.5726

29	72.4609	3	0.5917	-4.2347	29	-2.4544	0.5897
30	11.6796	2	0.7782	-1.1483	99	0.093622	0.057773
31	30.9737	1	1.0177	-2.6872	31	-2.7126	1.0165
32	20.8237	9	0.445	0.943	99	0.093622	0.057773
33	29.2253	9	0.4037	-0.3068	99	0.093622	0.057773
34	38.2115	12	0.352	-0.2712	99	0.093622	0.057773
35	9.4623	20	1.0259	3.6207	35	3.6835	1.0247
36	31.8745	46	1.012	4.5355	36	4.5164	1.0108
37	53.9642	16	0.3021	-0.6001	99	0.093622	0.057773
38	60.6182	5	0.4694	-3.7451	38	-1.7213	0.4669
39	57.5225	7	0.4063	-3.2448	39	-1.2888	0.4033
40	48.3555	5	0.4748	-3.1571	40	-1.4723	0.4723
41	29.4269	5	0.4933	-1.8449	99	0.093622	0.057773
42	27.7348	14	0.3829	1.8754	99	0.093622	0.057773
43	20.1238	7	0.4706	0.1272	99	0.093622	0.057773
44	4.1336	9	1.0552	2.7467	44	2.885	1.0541
45	5.734	5	1.2509	2.0894	45	2.6064	1.25
46	4.764	6	1.0812	2.3012	46	2.4795	1.0801
47	6.8413	14	1.0362	3.231	47	3.3268	1.0351
48	1.595	4	1.1191	1.8582	99	0.093622	0.057773
49	2.086	4	1.1191	1.8582	99	0.093622	0.057773
51	6.3984	9	1.0552	2.7467	51	2.885	1.0541
52	7.161	1	1.0792	-1.0506	99	0.093622	0.057773
59	0.4613	1	1.415	0.4866	99	0.093622	0.057773
65	0.6322	2	1.2257	1.1285	99	0.093622	0.057773

Table H.3. Boulder County, human factor riskscapes, all classes, calculate weights tables (classes with no points were removed, 45 from 500 training points, 40 from 1000 training points, and 30 from 20% training points).

Boulder human factor 500 training points							
CLASS	AREA_SQ_KM	NO_POINTS	WPLUS	S_WPLUS	WMINUS	S_WMINUS	CONTRAST
22	31.0317	1	-2.3585	1.0165	0.0194	0.0522	-2.3779
23	19.5961	1	-1.8792	1.0265	0.0112	0.0522	-1.8904
27	31.393	5	-0.6199	0.4877	0.0087	0.0524	-0.6287
29	9.4254	1	-1.0875	1.0577	0.004	0.0521	-1.0915
30	21.2732	3	-0.7631	0.6229	0.0069	0.0523	-0.77
31	49.6119	15	0.2076	0.3091	-0.0058	0.0528	0.2134
32	36.6456	2	-1.8083	0.7272	0.0207	0.0523	-1.829
33	17.9764	1	-1.7881	1.029	0.01	0.0522	-1.7981
34	23.7782	2	-1.344	0.7389	0.0115	0.0522	-1.3555
35	89.9292	22	-0.0837	0.2453	0.004	0.0533	-0.0877

36	76.2937	11	-0.7373	0.3259	0.0249	0.0528	-0.7621
37	23.0968	10	0.774	0.4199	-0.011	0.0525	0.7849
38	29.576	4	-0.8116	0.5377	0.0102	0.0523	-0.8218
39	133.0942	38	0.1265	0.1919	-0.0097	0.0541	0.1362
40	54.9892	15	0.0632	0.3028	-0.0019	0.0528	0.0651
41	28.9223	6	-0.2966	0.4586	0.0042	0.0524	-0.3008
42	34.1628	9	0.0156	0.3884	-0.0003	0.0525	0.0159
43	156.6141	56	0.4578	0.1667	-0.0454	0.0549	0.5032
44	50.8766	14	0.0752	0.3139	-0.0021	0.0528	0.0773
45	49.796	13	0.0033	0.3226	-0.0001	0.0527	0.0034
46	50.7288	11	-0.2404	0.3407	0.0061	0.0527	-0.2466
47	135.9897	34	-0.0548	0.198	0.0041	0.054	-0.0589
48	53.8106	5	-1.2348	0.4696	0.025	0.0525	-1.2598
49	49.0783	26	1.1629	0.286	-0.0371	0.0532	1.2
50	21.9925	6	0.0634	0.4787	-0.0007	0.0524	0.0641
51	111.9836	25	-0.2031	0.2269	0.0119	0.0535	-0.2151
52	17.8365	9	1.0621	0.4736	-0.0119	0.0524	1.074
53	50.7753	28	1.2503	0.2822	-0.0415	0.0533	1.2918
54	12.1624	6	1.017	0.5735	-0.0077	0.0523	1.0248
55	40.6143	12	0.1747	0.3439	-0.0039	0.0527	0.1787
56	8.8497	1	-1.0167	1.0618	0.0035	0.0521	-1.0203
57	41.3829	37	3.1769	0.5052	-0.0739	0.0536	3.2509
58	10.9125	6	1.2437	0.6085	-0.0086	0.0523	1.2523
59	10.8699	4	0.5029	0.6289	-0.0032	0.0522	0.5061
60	5.1182	1	-0.3717	1.1148	0.0009	0.0521	-0.3726
61	56.9469	33	1.3644	0.2684	-0.0514	0.0535	1.4158
62	4.7167	1	-0.2691	1.1265	0.0006	0.0521	-0.2697
63	13.0973	4	0.2221	0.5999	-0.0016	0.0523	0.2237
65	16.5055	12	2.0233	0.5525	-0.0212	0.0525	2.0445
67	7.3125	1	-0.7988	1.0763	0.0025	0.0521	-0.8012
68	1.7856	1	1.285	1.5076	-0.0015	0.0521	1.2865
70	1.0209	1	4.9117	6.9891	-0.002	0.0521	4.9137
71	12.3892	6	0.9809	0.5685	-0.0076	0.0523	0.9885
CLASS	AREA_SQ_KM	NO_POINTS	S_CONTRAST	STUD_CNT	GEN_CLASS	WEIGHT	W_STD
22	31.0317	1	1.0179	-2.3362	22	-2.3585	1.0165
23	19.5961	1	1.0279	-1.8392	99	0.545829	0.084345
27	31.393	5	0.4905	-1.2815	99	0.545829	0.084345
29	9.4254	1	1.059	-1.0307	99	0.545829	0.084345
30	21.2732	3	0.6251	-1.2318	99	0.545829	0.084345
31	49.6119	15	0.3136	0.6804	99	0.545829	0.084345
32	36.6456	2	0.7291	-2.5086	32	-1.8083	0.7272

33	17.9764	1	1.0304	-1.7452	99	0.545829	0.084345
34	23.7782	2	0.7407	-1.83	99	0.545829	0.084345
35	89.9292	22	0.251	-0.3494	99	0.545829	0.084345
36	76.2937	11	0.3302	-2.3083	36	-0.7373	0.3259
37	23.0968	10	0.4232	1.8546	99	0.545829	0.084345
38	29.576	4	0.5402	-1.5212	99	0.545829	0.084345
39	133.0942	38	0.1994	0.6831	99	0.545829	0.084345
40	54.9892	15	0.3074	0.2117	99	0.545829	0.084345
41	28.9223	6	0.4616	-0.6517	99	0.545829	0.084345
42	34.1628	9	0.3919	0.0405	99	0.545829	0.084345
43	156.6141	56	0.1755	2.8666	43	0.4578	0.1667
44	50.8766	14	0.3183	0.2429	99	0.545829	0.084345
45	49.796	13	0.3269	0.0104	99	0.545829	0.084345
46	50.7288	11	0.3448	-0.7153	99	0.545829	0.084345
47	135.9897	34	0.2053	-0.2869	99	0.545829	0.084345
48	53.8106	5	0.4725	-2.6662	48	-1.2348	0.4696
49	49.0783	26	0.2909	4.1252	49	1.1629	0.286
50	21.9925	6	0.4816	0.1332	99	0.545829	0.084345
51	111.9836	25	0.2331	-0.9224	99	0.545829	0.084345
52	17.8365	9	0.4765	2.2541	52	1.0621	0.4736
53	50.7753	28	0.2872	4.4986	53	1.2503	0.2822
54	12.1624	6	0.5759	1.7794	99	0.545829	0.084345
55	40.6143	12	0.3479	0.5136	99	0.545829	0.084345
56	8.8497	1	1.0631	-0.9598	99	0.545829	0.084345
57	41.3829	37	0.508	6.3995	57	3.1769	0.5052
58	10.9125	6	0.6107	2.0506	58	1.2437	0.6085
59	10.8699	4	0.6311	0.8019	99	0.545829	0.084345
60	5.1182	1	1.116	-0.3338	99	0.545829	0.084345
61	56.9469	33	0.2737	5.1723	61	1.3644	0.2684
62	4.7167	1	1.1277	-0.2392	99	0.545829	0.084345
63	13.0973	4	0.6022	0.3714	99	0.545829	0.084345
65	16.5055	12	0.555	3.6837	65	2.0233	0.5525
67	7.3125	1	1.0776	-0.7436	99	0.545829	0.084345
68	1.7856	1	1.5085	0.8528	99	0.545829	0.084345
70	1.0209	1	6.9892	0.703	99	0.545829	0.084345
71	12.3892	6	0.5709	1.7314	99	0.545829	0.084345
Boulder human factor 1000 training points							
CLASS	AREA_SQ_KM	NO_POINTS	WPLUS	S_WPLUS	WMINUS	S_WMINUS	CONTRAST
17	3.7808	1	-1.1062	1.166	0.002	0.0458	-1.1082
23	19.5961	4	-1.4442	0.5605	0.0131	0.046	-1.4573
24	14.6473	1	-2.697	1.036	0.014	0.0459	-2.711

26	67.1308	1	-4.2751	1.0075	0.0738	0.0467	-4.3489
27	31.393	8	-1.1565	0.4096	0.0178	0.0461	-1.1742
30	21.2732	3	-1.8903	0.6229	0.0171	0.046	-1.9074
31	49.6119	16	-0.8258	0.3037	0.0211	0.0464	-0.8469
32	36.6456	3	-2.5007	0.6025	0.0343	0.0462	-2.5351
33	17.9764	8	-0.3043	0.4746	0.0029	0.0459	-0.3071
34	23.7782	5	-1.4067	0.5032	0.0156	0.046	-1.4224
35	89.9292	37	-0.4415	0.2143	0.0216	0.0469	-0.4631
36	76.2937	20	-1.1183	0.2603	0.043	0.0467	-1.1614
37	23.0968	13	0.1693	0.4195	-0.0021	0.046	0.1713
38	29.576	11	-0.6075	0.3804	0.0094	0.0461	-0.6168
39	133.0942	71	0.0505	0.1738	-0.0038	0.0474	0.0543
40	54.9892	37	0.6377	0.2874	-0.018	0.0464	0.6557
41	28.9223	20	0.7237	0.4026	-0.0105	0.0461	0.7342
42	34.1628	14	-0.4483	0.3479	0.0081	0.0462	-0.4563
43	156.6141	119	1.0683	0.1871	-0.0851	0.0477	1.1534
44	50.8766	23	-0.2758	0.2817	0.0075	0.0464	-0.2833
45	49.796	48	3.2022	0.76	-0.0473	0.0463	3.2495
46	50.7288	11	-1.3677	0.3407	0.0332	0.0464	-1.4008
47	135.9897	64	-0.2011	0.1718	0.0154	0.0475	-0.2165
48	53.8106	15	-1.0341	0.304	0.028	0.0464	-1.0622
49	49.0783	49	6.3555	3.5766	-0.0503	0.0463	6.4058
50	21.9925	22	3.0076	1.0225	-0.0212	0.046	3.0288
51	111.9836	64	0.2045	0.191	-0.0126	0.0471	0.2171
52	17.8365	16	2.0812	0.7791	-0.0142	0.0459	2.0954
53	50.7753	58	3.977	1.0086	-0.0588	0.0464	4.0357
54	12.1624	19	2.861	1.026	-0.0181	0.046	2.8791
55	40.6143	19	-0.2124	0.3145	0.0046	0.0462	-0.217
57	41.3829	57	3.9596	1.0087	-0.0577	0.0464	4.0173
58	10.9125	7	0.4983	0.6312	-0.0028	0.0459	0.501
59	10.8699	2	-1.573	0.7828	0.0077	0.0459	-1.5807
60	5.1182	6	1.7083	1.0801	-0.0049	0.0458	1.7132
61	56.9469	56	3.9964	1.0363	-0.0567	0.0464	4.0531
63	13.0973	14	2.5556	1.0351	-0.013	0.0459	2.5686
64	2.5322	5	1.526	1.0954	-0.0039	0.0458	1.5299
65	16.5055	24	3.0946	1.0206	-0.0233	0.046	3.1178
66	1.6353	1	0.3702	1.6044	-0.0003	0.0457	0.3705
67	7.3125	8	1.996	1.0607	-0.007	0.0458	2.0029
68	1.7856	2	0.6097	1.2247	-0.0009	0.0458	0.6106
69	2.8189	2	0.8095	1.3119	-0.0011	0.0458	0.8106
71	12.3892	6	-0.1463	0.5685	0.001	0.0459	-0.1473
73	5.8494	4	0.688	0.8892	-0.002	0.0458	0.69

75	3.4558	2	0.2341	1.0895	-0.0004	0.0458	0.2345
77	2.0263	1	-0.1094	1.4051	0.0001	0.0458	-0.1096
83	0.9063	1	-0.0835	1.4142	0.0001	0.0458	-0.0836
CLASS	AREA_SQ_KM	NO_POINTS	S_CONTRAST	STUD_CNT	GEN_CLASS	WEIGHT	W_STD
17	3.7808	1	1.1669	-0.9497	99	0.215888	0.06278
23	19.5961	4	0.5623	-2.5915	23	-1.4442	0.5605
24	14.6473	1	1.037	-2.6143	24	-2.697	1.036
26	67.1308	1	1.0086	-4.3117	26	-4.2751	1.0075
27	31.393	8	0.4122	-2.849	27	-1.1565	0.4096
30	21.2732	3	0.6246	-3.0536	30	-1.8903	0.6229
31	49.6119	16	0.3072	-2.7564	31	-0.8258	0.3037
32	36.6456	3	0.6043	-4.195	32	-2.5007	0.6025
33	17.9764	8	0.4768	-0.6442	99	0.215888	0.06278
34	23.7782	5	0.5053	-2.8147	34	-1.4067	0.5032
35	89.9292	37	0.2194	-2.1113	35	-0.4415	0.2143
36	76.2937	20	0.2645	-4.3912	36	-1.1183	0.2603
37	23.0968	13	0.422	0.4059	99	0.215888	0.06278
38	29.576	11	0.3832	-1.6095	99	0.215888	0.06278
39	133.0942	71	0.1801	0.3016	99	0.215888	0.06278
40	54.9892	37	0.2911	2.252	40	0.6377	0.2874
41	28.9223	20	0.4052	1.8118	99	0.215888	0.06278
42	34.1628	14	0.3509	-1.3004	99	0.215888	0.06278
43	156.6141	119	0.193	5.9751	43	1.0683	0.1871
44	50.8766	23	0.2855	-0.9923	99	0.215888	0.06278
45	49.796	48	0.7614	4.2676	45	3.2022	0.76
46	50.7288	11	0.3438	-4.0739	46	-1.3677	0.3407
47	135.9897	64	0.1782	-1.2147	99	0.215888	0.06278
48	53.8106	15	0.3076	-3.4536	48	-1.0341	0.304
49	49.0783	49	3.5769	1.7909	99	0.215888	0.06278
50	21.9925	22	1.0235	2.9592	50	3.0076	1.0225
51	111.9836	64	0.1967	1.104	99	0.215888	0.06278
52	17.8365	16	0.7805	2.6848	52	2.0812	0.7791
53	50.7753	58	1.0097	3.9972	53	3.977	1.0086
54	12.1624	19	1.027	2.8034	54	2.861	1.026
55	40.6143	19	0.3179	-0.6827	99	0.215888	0.06278
57	41.3829	57	1.0098	3.9783	57	3.9596	1.0087
58	10.9125	7	0.6329	0.7916	99	0.215888	0.06278
59	10.8699	2	0.7841	-2.0159	59	-1.573	0.7828
60	5.1182	6	1.0811	1.5847	99	0.215888	0.06278
61	56.9469	56	1.0373	3.9072	61	3.9964	1.0363
63	13.0973	14	1.0361	2.4791	63	2.5556	1.0351

64	2.5322	5	1.0964	1.3954	99	0.215888	0.06278
65	16.5055	24	1.0217	3.0517	65	3.0946	1.0206
66	1.6353	1	1.605	0.2308	99	0.215888	0.06278
67	7.3125	8	1.0616	1.8866	99	0.215888	0.06278
68	1.7856	2	1.2256	0.4982	99	0.215888	0.06278
69	2.8189	2	1.3127	0.6175	99	0.215888	0.06278
71	12.3892	6	0.5703	-0.2582	99	0.215888	0.06278
73	5.8494	4	0.8904	0.7749	99	0.215888	0.06278
75	3.4558	2	1.0904	0.2151	99	0.215888	0.06278
77	2.0263	1	1.4059	-0.0779	99	0.215888	0.06278
83	0.9063	1	1.415	-0.0591	99	0.215888	0.06278
Boulder human factor 20% training points							
CLASS	AREA_SQ_KM	NO_POINTS	WPLUS	S_WPLUS	WMINUS	S_WMINUS	CONTRAST
22	31.0317	1	-2.7145	1.0165	0.0223	0.0486	-2.7368
23	19.5961	1	-2.2352	1.0265	0.0131	0.0486	-2.2484
24	14.6473	1	-1.9258	1.036	0.0092	0.0485	-1.935
25	32.9107	1	-2.7752	1.0155	0.0238	0.0487	-2.799
26	67.1308	1	-3.5039	1.0075	0.0517	0.0489	-3.5556
27	31.393	6	-0.755	0.4539	0.0107	0.0487	-0.7657
28	14.8399	3	-0.6851	0.6464	0.0046	0.0486	-0.6898
29	9.4254	1	-1.4435	1.0577	0.0051	0.0485	-1.4486
31	49.6119	9	-0.8191	0.3684	0.0182	0.0489	-0.8373
32	36.6456	1	-2.8859	1.0139	0.0268	0.0487	-2.9127
33	17.9764	4	-0.5633	0.5671	0.0048	0.0486	-0.5681
34	23.7782	2	-1.7	0.7389	0.0141	0.0486	-1.7141
35	89.9292	10	-1.3908	0.3354	0.049	0.0492	-1.4398
36	76.2937	10	-1.2038	0.3392	0.0377	0.0491	-1.2415
37	23.0968	6	-0.3594	0.4745	0.0041	0.0487	-0.3635
38	29.576	9	-0.1392	0.3996	0.0021	0.0488	-0.1413
39	133.0942	26	-0.7279	0.2186	0.0463	0.0498	-0.7742
40	54.9892	21	0.2062	0.2776	-0.0063	0.0492	0.2125
41	28.9223	20	1.4949	0.4026	-0.0247	0.049	1.5196
42	34.1628	9	-0.3404	0.3884	0.0058	0.0488	-0.3462
43	156.6141	35	-0.5578	0.1918	0.0441	0.0502	-0.6019
44	50.8766	12	-0.4878	0.3302	0.0121	0.049	-0.4998
45	49.796	19	0.2048	0.2917	-0.0056	0.0491	0.2104
46	50.7288	8	-0.9877	0.3852	0.0215	0.0489	-1.0092
47	135.9897	26	-0.7546	0.2181	0.0488	0.0498	-0.8034
48	53.8106	6	-1.3878	0.4331	0.0288	0.0489	-1.4166
49	49.0783	34	1.5008	0.3094	-0.0426	0.0494	1.5434
50	21.9925	10	0.506	0.4282	-0.0063	0.0487	0.5123

51	111.9836	38	0.0215	0.1996	-0.0013	0.0499	0.0228
52	17.8365	2	-1.3814	0.7504	0.0094	0.0486	-1.3908
53	50.7753	48	3.5382	0.6174	-0.0757	0.0497	3.6138
54	12.1624	17	3.5209	1.029	-0.0261	0.0489	3.547
55	40.6143	12	-0.1813	0.3439	0.0038	0.0489	-0.1851
56	8.8497	3	0.0199	0.7101	-0.0001	0.0485	0.02
57	41.3829	44	4.4719	1.0113	-0.0703	0.0496	4.5422
58	10.9125	7	1.2695	0.6312	-0.0079	0.0486	1.2774
59	10.8699	5	0.5273	0.6086	-0.0032	0.0486	0.5305
60	5.1182	4	1.9623	1.0697	-0.0054	0.0485	1.9677
61	56.9469	77	5.0315	1.0065	-0.1272	0.0506	5.1587
62	4.7167	3	1.2459	0.957	-0.0033	0.0485	1.2493
63	13.0973	15	3.3958	1.0328	-0.0229	0.0488	3.4187
64	2.5322	5	2.2972	1.0954	-0.007	0.0486	2.3042
65	16.5055	20	3.6835	1.0247	-0.0309	0.0489	3.7144
66	1.6353	3	1.7863	1.1547	-0.0039	0.0485	1.7902
67	7.3125	6	2.2076	0.9636	-0.0084	0.0486	2.2159
68	1.7856	1	0.929	1.5076	-0.0009	0.0484	0.93
69	2.8189	2	1.5807	1.3119	-0.0025	0.0485	1.5831
70	1.0209	1	4.5557	6.9891	-0.0015	0.0484	4.5573
71	12.3892	15	3.3958	1.0328	-0.0229	0.0488	3.4187
72	0.8467	1	0.6877	1.4142	-0.0008	0.0484	0.6885
73	5.8494	6	2.4795	1.0801	-0.0086	0.0486	2.4881
75	3.4558	2	1.0053	1.0895	-0.002	0.0485	1.0073
77	2.0263	2	5.0191	6.2067	-0.0031	0.0485	5.0222
79	0.4239	3	1.7863	1.1547	-0.0039	0.0485	1.7902
80	0.09	1	0.6877	1.4142	-0.0008	0.0484	0.6885
81	1.623	3	1.7863	1.1547	-0.0039	0.0485	1.7902
83	0.9063	2	1.3809	1.2247	-0.0023	0.0485	1.3832
85	0.4066	1	0.6877	1.4142	-0.0008	0.0484	0.6885
CLASS	AREA_SQ_KM	NO_POINTS	S_CONTRAST	STUD_CNT	GEN_CLASS	WEIGHT	W_STD
22	31.0317	1	1.0177	-2.6893	22	-2.7145	1.0165
23	19.5961	1	1.0277	-2.1878	23	-2.2352	1.0265
24	14.6473	1	1.0371	-1.8657	99	0.097195	0.0587
25	32.9107	1	1.0167	-2.753	25	-2.7752	1.0155
26	67.1308	1	1.0087	-3.5249	26	-3.5039	1.0075
27	31.393	6	0.4565	-1.6772	99	0.097195	0.0587
28	14.8399	3	0.6482	-1.0642	99	0.097195	0.0587
29	9.4254	1	1.0588	-1.3682	99	0.097195	0.0587
31	49.6119	9	0.3717	-2.253	31	-0.8191	0.3684
32	36.6456	1	1.0151	-2.8694	32	-2.8859	1.0139

33	17.9764	4	0.5691	-0.9982	99	0.097195	0.0587
34	23.7782	2	0.7405	-2.315	34	-1.7	0.7389
35	89.9292	10	0.339	-4.2471	35	-1.3908	0.3354
36	76.2937	10	0.3428	-3.6217	36	-1.2038	0.3392
37	23.0968	6	0.477	-0.7621	99	0.097195	0.0587
38	29.576	9	0.4026	-0.351	99	0.097195	0.0587
39	133.0942	26	0.2242	-3.4527	39	-0.7279	0.2186
40	54.9892	21	0.2819	0.7538	99	0.097195	0.0587
41	28.9223	20	0.4056	3.7469	41	1.4949	0.4026
42	34.1628	9	0.3915	-0.8844	99	0.097195	0.0587
43	156.6141	35	0.1983	-3.0356	43	-0.5578	0.1918
44	50.8766	12	0.3338	-1.4972	99	0.097195	0.0587
45	49.796	19	0.2958	0.7113	99	0.097195	0.0587
46	50.7288	8	0.3883	-2.5989	46	-0.9877	0.3852
47	135.9897	26	0.2237	-3.5914	47	-0.7546	0.2181
48	53.8106	6	0.4359	-3.2501	48	-1.3878	0.4331
49	49.0783	34	0.3133	4.926	49	1.5008	0.3094
50	21.9925	10	0.431	1.1886	99	0.097195	0.0587
51	111.9836	38	0.2057	0.1109	99	0.097195	0.0587
52	17.8365	2	0.752	-1.8495	99	0.097195	0.0587
53	50.7753	48	0.6194	5.8346	53	3.5382	0.6174
54	12.1624	17	1.0302	3.4432	54	3.5209	1.029
55	40.6143	12	0.3474	-0.5328	99	0.097195	0.0587
56	8.8497	3	0.7118	0.0282	99	0.097195	0.0587
57	41.3829	44	1.0125	4.4861	57	4.4719	1.0113
58	10.9125	7	0.6331	2.0176	58	1.2695	0.6312
59	10.8699	5	0.6105	0.869	99	0.097195	0.0587
60	5.1182	4	1.0708	1.8376	99	0.097195	0.0587
61	56.9469	77	1.0077	5.1191	61	5.0315	1.0065
62	4.7167	3	0.9582	1.3037	99	0.097195	0.0587
63	13.0973	15	1.0339	3.3064	63	3.3958	1.0328
64	2.5322	5	1.0965	2.1014	64	2.2972	1.0954
65	16.5055	20	1.0259	3.6207	65	3.6835	1.0247
66	1.6353	3	1.1557	1.549	99	0.097195	0.0587
67	7.3125	6	0.9648	2.2967	67	2.2076	0.9636
68	1.7856	1	1.5084	0.6165	99	0.097195	0.0587
69	2.8189	2	1.3128	1.2059	99	0.097195	0.0587
70	1.0209	1	6.9892	0.652	99	0.097195	0.0587
71	12.3892	15	1.0339	3.3064	71	3.3958	1.0328
72	0.8467	1	1.415	0.4866	99	0.097195	0.0587
73	5.8494	6	1.0812	2.3012	73	2.4795	1.0801
75	3.4558	2	1.0905	0.9237	99	0.097195	0.0587

77	2.0263	2	6.2069	0.8091	99	0.097195	0.0587
79	0.4239	3	1.1557	1.549	99	0.097195	0.0587
80	0.09	1	1.415	0.4866	99	0.097195	0.0587
81	1.623	3	1.1557	1.549	99	0.097195	0.0587
83	0.9063	2	1.2257	1.1285	99	0.097195	0.0587
85	0.4066	1	1.415	0.4866	99	0.097195	0.0587

Table H.4. Larimer County, binary riskscapes, all classes, calculate weights tables (classes with no points were removed, 7 from 500 training points, 7 from 1000 training points, and 6 from 20% training points).

Larimer binary 500 training points							
CLASS	AREA_SQ_KM	NO_POINTS	WPLUS	S_WPLUS	WMINUS	S_WMINUS	CONTRAST
6	66.2343	1	-1.6416	1.0076	0.0084	0.0465	-1.65
7	4293.154	285	-0.1072	0.0613	0.1626	0.0713	-0.2698
8	1825.175	187	0.3661	0.0772	-0.1682	0.0584	0.5343
9	374.936	20	-0.3399	0.2298	0.017	0.0474	-0.3569
10	166.9407	7	-0.5925	0.3861	0.0115	0.0468	-0.6041
CLASS	AREA_SQ_KM	NO_POINTS	S_CONTRAST	STUD_CNT	GEN_CLASS	WEIGHT	W_STD
6	66.2343	1	1.0087	-1.6358	99	0.054572	0.047914
7	4293.154	285	0.094	-2.8695	7	-0.1072	0.0613
8	1825.175	187	0.0968	5.5209	8	0.3661	0.0772
9	374.936	20	0.2347	-1.5207	99	0.054572	0.047914
10	166.9407	7	0.389	-1.553	99	0.054572	0.047914
Larimer binary 1000 training points							
CLASS	AREA_SQ_KM	NO_POINTS	WPLUS	S_WPLUS	WMINUS	S_WMINUS	CONTRAST
7	4293.154	580	-0.0959	0.0446	0.1496	0.0534	-0.2455
8	1825.175	381	0.4282	0.0576	-0.1943	0.0429	0.6225
9	374.936	32	-0.6111	0.1848	0.0282	0.0349	-0.6393
10	166.9407	6	-1.5285	0.4158	0.022	0.0344	-1.5506
11	19.0804	1	-1.1341	1.0273	0.0021	0.0343	-1.1362
CLASS	AREA_SQ_KM	NO_POINTS	S_CONTRAST	STUD_CNT	GEN_CLASS	WEIGHT	W_STD
7	4293.154	580	0.0696	-3.5246	7	-0.0959	0.0446
8	1825.175	381	0.0718	8.665	8	0.4282	0.0576
9	374.936	32	0.1881	-3.3988	9	-0.6111	0.1848
10	166.9407	6	0.4172	-3.7165	10	-1.5285	0.4158
11	19.0804	1	1.0279	-1.1054	99	0.026106	0.034317

Larimer binary 20% training points							
CLASS	AREA_SQ_KM	NO_POINTS	WPLUS	S_WPLUS	WMINUS	S_WMINUS	CONTRAST
6	66.2343	3	-2.6807	0.5909	0.0147	0.0247	-2.6955
7	4293.154	996	-0.8295	0.0362	1.2653	0.0439	-2.0948
8	1825.175	1577	2.2167	0.0683	-0.7698	0.033	2.9865
9	374.936	191	0.4052	0.1033	-0.0242	0.0254	0.4294
10	166.9407	21	-1.5712	0.2334	0.0293	0.0249	-1.6005
11	19.0804	1	-2.5273	1.0273	0.0041	0.0247	-2.5314
CLASS	AREA_SQ_KM	NO_POINTS	S_CONTRAST	STUD_CNT	GEN_CLASS	WEIGHT	W_STD
6	66.2343	3	0.5914	-4.5577	6	-2.6807	0.5909
7	4293.154	996	0.0569	-36.8381	7	-0.8295	0.0362
8	1825.175	1577	0.0758	39.3737	8	2.2167	0.0683
9	374.936	191	0.1064	4.0365	9	0.4052	0.1033
10	166.9407	21	0.2347	-6.819	10	-1.5712	0.2334
11	19.0804	1	1.0276	-2.4635	11	-2.5273	1.0273

Table H.5. Larimer County, ranked riskscapes, all classes, calculate weights tables (classes with no points were removed, 41 from 500 training points, 38 from 1000 training points, and 34 from 20% training points).

Larimer ranked 500 training points							
CLASS	AREA_SQ_KM	NO_POINTS	WPLUS	S_WPLUS	WMINUS	S_WMINUS	CONTRAST
1	97.7953	4	-0.6185	0.5106	0.0069	0.0467	-0.6254
2	226.3861	14	-0.183	0.2759	0.0058	0.0471	-0.1888
3	110.2138	12	0.4341	0.3058	-0.0086	0.047	0.4427
4	184.7382	18	0.3103	0.2481	-0.0099	0.0473	0.3202
5	433.3508	34	0.0729	0.1787	-0.0051	0.0481	0.078
6	761.3872	65	0.1648	0.1297	-0.0225	0.0498	0.1873
7	848.4271	51	-0.2132	0.1444	0.0274	0.0491	-0.2406
8	212.6253	30	0.7301	0.197	-0.0325	0.0479	0.7627
9	274.1969	36	0.6468	0.1788	-0.0363	0.0482	0.6831
10	237.4545	44	1.0555	0.167	-0.061	0.0485	1.1165
11	114.9416	8	-0.0565	0.3665	0.0009	0.0468	-0.0574
12	195.0585	14	-0.0234	0.2774	0.0007	0.0471	-0.0241
13	183.5318	22	0.5427	0.2273	-0.0191	0.0475	0.5618
14	158.1779	29	1.0425	0.2055	-0.0391	0.0478	1.0815
15	52.9822	11	1.197	0.3387	-0.0156	0.047	1.2126
16	30.1758	1	-0.837	1.017	0.0026	0.0465	-0.8396

17	453.2443	40	0.2012	0.1656	-0.0157	0.0484	0.2169
18	124.4156	5	-0.6368	0.4565	0.009	0.0467	-0.6459
19	176.5249	10	-0.2762	0.3256	0.0065	0.0469	-0.2827
20	24.8646	3	0.5501	0.6157	-0.0026	0.0466	0.5526
21	48.3108	7	0.7611	0.4087	-0.0075	0.0468	0.7687
22	127.5572	11	0.1759	0.3154	-0.0036	0.047	0.1795
24	25.4611	4	0.8564	0.5446	-0.0046	0.0466	0.861
25	71.1853	3	-0.5873	0.5899	0.0048	0.0466	-0.5921
26	96.1063	7	-0.0076	0.3925	0.0001	0.0468	-0.0077
27	71.133	1	-1.714	1.0071	0.0092	0.0465	-1.7232
29	44.0026	1	-1.2249	1.0116	0.0048	0.0465	-1.2297
30	80.5802	1	-1.8404	1.0063	0.0107	0.0465	-1.8511
31	56.9372	1	-1.4879	1.0089	0.0069	0.0465	-1.4948
32	116.9601	2	-1.5151	0.7132	0.0144	0.0466	-1.5294
34	127.8379	1	-2.3066	1.0039	0.0183	0.0465	-2.3248
37	37.5096	1	-1.0612	1.0136	0.0038	0.0465	-1.065
38	163.2613	3	-1.4418	0.5827	0.0197	0.0466	-1.4615
39	55.7302	1	-1.4661	1.0091	0.0067	0.0465	-1.4728
41	60.4175	2	-0.8381	0.7191	0.0053	0.0466	-0.8434
48	14.1845	2	0.7293	0.7629	-0.0021	0.0465	0.7314
50	3.3675	1	1.6745	1.1926	-0.0016	0.0465	1.6761
CLASS	AREA_SQ_KM	NO_POINTS	S_CONTRAST	STUD_CNT	GEN_CLASS	WEIGHT	W_STD
1	97.7953	4	0.5127	-1.2199	99	0.510998	0.079745
2	226.3861	14	0.2799	-0.6745	99	0.510998	0.079745
3	110.2138	12	0.3094	1.431	99	0.510998	0.079745
4	184.7382	18	0.2526	1.2678	99	0.510998	0.079745
5	433.3508	34	0.185	0.4215	99	0.510998	0.079745
6	761.3872	65	0.1389	1.3482	99	0.510998	0.079745
7	848.4271	51	0.1525	-1.5771	99	0.510998	0.079745
8	212.6253	30	0.2027	3.7619	8	0.7301	0.197
9	274.1969	36	0.1852	3.6884	9	0.6468	0.1788
10	237.4545	44	0.1739	6.4192	10	1.0555	0.167
11	114.9416	8	0.3695	-0.1554	99	0.510998	0.079745
12	195.0585	14	0.2814	-0.0856	99	0.510998	0.079745
13	183.5318	22	0.2322	2.4198	13	0.5427	0.2273
14	158.1779	29	0.211	5.1265	14	1.0425	0.2055
15	52.9822	11	0.342	3.546	15	1.197	0.3387
16	30.1758	1	1.0181	-0.8247	99	0.510998	0.079745
17	453.2443	40	0.1725	1.2573	99	0.510998	0.079745
18	124.4156	5	0.4589	-1.4075	99	0.510998	0.079745
19	176.5249	10	0.329	-0.8595	99	0.510998	0.079745

20	24.8646	3	0.6174	0.8951	99	0.510998	0.079745
21	48.3108	7	0.4114	1.8684	99	0.510998	0.079745
22	127.5572	11	0.3189	0.5628	99	0.510998	0.079745
24	25.4611	4	0.5466	1.5753	99	0.510998	0.079745
25	71.1853	3	0.5918	-1.0006	99	0.510998	0.079745
26	96.1063	7	0.3953	-0.0194	99	0.510998	0.079745
27	71.133	1	1.0082	-1.7092	99	0.510998	0.079745
29	44.0026	1	1.0126	-1.2144	99	0.510998	0.079745
30	80.5802	1	1.0073	-1.8376	99	0.510998	0.079745
31	56.9372	1	1.01	-1.48	99	0.510998	0.079745
32	116.9601	2	0.7148	-2.1398	32	-1.5151	0.7132
34	127.8379	1	1.005	-2.3132	34	-2.3066	1.0039
37	37.5096	1	1.0147	-1.0496	99	0.510998	0.079745
38	163.2613	3	0.5846	-2.5001	38	-1.4418	0.5827
39	55.7302	1	1.0102	-1.4579	99	0.510998	0.079745
41	60.4175	2	0.7206	-1.1704	99	0.510998	0.079745
48	14.1845	2	0.7644	0.9569	99	0.510998	0.079745
50	3.3675	1	1.1935	1.4043	99	0.510998	0.079745
Larimer ranked 1000 training points							
CLASS	AREA_SQ_KM	NO_POINTS	WPLUS	S_WPLUS	WMINUS	S_WMINUS	CONTRAST
1	97.7953	1	-2.8119	1.0052	0.0158	0.0343	-2.8276
2	226.3861	35	0.0618	0.1838	-0.0022	0.0348	0.064
3	110.2138	19	0.192	0.2522	-0.0034	0.0346	0.1954
4	184.7382	32	0.1978	0.1944	-0.0059	0.0348	0.2037
5	433.3508	71	0.1308	0.1298	-0.0093	0.0355	0.1401
6	761.3872	117	0.0546	0.1005	-0.007	0.0364	0.0616
7	848.4271	117	-0.0721	0.0996	0.01	0.0365	-0.082
8	212.6253	36	0.1702	0.1829	-0.0058	0.0349	0.1761
9	274.1969	83	0.9263	0.1314	-0.0532	0.0356	0.9795
10	237.4545	73	0.9486	0.1406	-0.0471	0.0354	0.9957
11	114.9416	14	-0.2147	0.2852	0.0034	0.0345	-0.2181
12	195.0585	29	0.0157	0.2013	-0.0005	0.0347	0.0162
13	183.5318	44	0.6066	0.1729	-0.0207	0.035	0.6274
14	158.1779	47	0.8998	0.174	-0.0288	0.035	0.9286
15	52.9822	20	1.2605	0.2834	-0.0145	0.0345	1.275
16	30.1758	11	1.205	0.3782	-0.0078	0.0344	1.2127
17	453.2443	84	0.2801	0.1209	-0.0222	0.0357	0.3023
18	124.4156	23	0.277	0.231	-0.0057	0.0346	0.2827
19	176.5249	21	-0.2415	0.2325	0.0059	0.0346	-0.2474
20	24.8646	3	-0.2255	0.6157	0.0008	0.0343	-0.2263
21	48.3108	17	1.15	0.3013	-0.0117	0.0345	1.1617

22	127.5572	22	0.1925	0.2344	-0.0039	0.0346	0.1965
23	1.8739	1	1.8955	1.4643	-0.0009	0.0342	1.8964
24	25.4611	3	-0.2524	0.6147	0.0009	0.0343	-0.2533
25	71.1853	5	-0.8223	0.4638	0.0064	0.0343	-0.8287
26	96.1063	10	-0.3923	0.3341	0.0049	0.0344	-0.3971
27	71.133	11	0.0621	0.3279	-0.0007	0.0344	0.0627
28	108.6949	1	-2.9186	1.0046	0.0177	0.0343	-2.9362
29	44.0026	9	0.4025	0.3737	-0.003	0.0344	0.4056
30	80.5802	1	-2.616	1.0063	0.0128	0.0343	-2.6288
31	56.9372	5	-0.5799	0.4682	0.004	0.0343	-0.5838
32	116.9601	6	-1.1567	0.4191	0.0132	0.0344	-1.1699
33	80.9314	1	-2.6204	1.0062	0.0128	0.0343	-2.6333
34	127.8379	1	-3.0822	1.0039	0.021	0.0343	-3.1032
36	62.0113	1	-2.3503	1.0082	0.0095	0.0343	-2.3599
37	37.5096	7	0.2886	0.4191	-0.0018	0.0343	0.2904
38	163.2613	10	-0.9688	0.3264	0.0167	0.0344	-0.9855
39	55.7302	1	-2.2417	1.0091	0.0085	0.0343	-2.2501
41	60.4175	4	-0.8857	0.5174	0.0057	0.0343	-0.8915
48	14.1845	4	0.8262	0.5901	-0.0023	0.0343	0.8284

CLASS	AREA_SQ_KM	NO_POINTS	S_CONTRAST	STUD_CNT	GEN_CLASS	WEIGHT	W_STD
1	97.7953	1	1.0057	-2.8115	1	-2.8119	1.0052
2	226.3861	35	0.1871	0.3419	99	0.191984	0.054825
3	110.2138	19	0.2545	0.7675	99	0.191984	0.054825
4	184.7382	32	0.1975	1.0312	99	0.191984	0.054825
5	433.3508	71	0.1346	1.0415	99	0.191984	0.054825
6	761.3872	117	0.1069	0.5766	99	0.191984	0.054825
7	848.4271	117	0.106	-0.7736	99	0.191984	0.054825
8	212.6253	36	0.1862	0.9458	99	0.191984	0.054825
9	274.1969	83	0.1362	7.1924	9	0.9263	0.1314
10	237.4545	73	0.145	6.8652	10	0.9486	0.1406
11	114.9416	14	0.2873	-0.7594	99	0.191984	0.054825
12	195.0585	29	0.2042	0.0791	99	0.191984	0.054825
13	183.5318	44	0.1764	3.5565	13	0.6066	0.1729
14	158.1779	47	0.1775	5.2324	14	0.8998	0.174
15	52.9822	20	0.2855	4.4659	15	1.2605	0.2834
16	30.1758	11	0.3798	3.1932	16	1.205	0.3782
17	453.2443	84	0.126	2.3979	17	0.2801	0.1209
18	124.4156	23	0.2335	1.2105	99	0.191984	0.054825
19	176.5249	21	0.235	-1.0526	99	0.191984	0.054825
20	24.8646	3	0.6166	-0.3669	99	0.191984	0.054825
21	48.3108	17	0.3032	3.8312	21	1.15	0.3013

22	127.5572	22	0.2369	0.8293	99	0.191984	0.054825
23	1.8739	1	1.4647	1.2947	99	0.191984	0.054825
24	25.4611	3	0.6157	-0.4114	99	0.191984	0.054825
25	71.1853	5	0.4651	-1.7819	99	0.191984	0.054825
26	96.1063	10	0.3359	-1.1824	99	0.191984	0.054825
27	71.133	11	0.3297	0.1903	99	0.191984	0.054825
28	108.6949	1	1.0052	-2.921	28	-2.9186	1.0046
29	44.0026	9	0.3753	1.0806	99	0.191984	0.054825
30	80.5802	1	1.0068	-2.6109	30	-2.616	1.0063
31	56.9372	5	0.4695	-1.2435	99	0.191984	0.054825
32	116.9601	6	0.4205	-2.7819	32	-1.1567	0.4191
33	80.9314	1	1.0068	-2.6154	33	-2.6204	1.0062
34	127.8379	1	1.0045	-3.0892	34	-3.0822	1.0039
36	62.0113	1	1.0087	-2.3394	36	-2.3503	1.0082
37	37.5096	7	0.4205	0.6906	99	0.191984	0.054825
38	163.2613	10	0.3282	-3.0027	38	-0.9688	0.3264
39	55.7302	1	1.0097	-2.2286	39	-2.2417	1.0091
41	60.4175	4	0.5186	-1.7192	99	0.191984	0.054825
48	14.1845	4	0.5911	1.4016	99	0.191984	0.054825
Larimer ranked 20% training points							
CLASS	AREA_SQ_KM	NO_POINTS	WPLUS	S_WPLUS	WMINUS	S_WMINUS	CONTRAST
1	97.7953	7	-2.1952	0.3923	0.0203	0.0248	-2.2155
2	226.3861	72	-0.3953	0.1427	0.0129	0.025	-0.4082
3	110.2138	90	1.861	0.2461	-0.0278	0.0249	1.8887
4	184.7382	41	-0.8869	0.1771	0.0215	0.0249	-0.9084
5	433.3508	123	-0.558	0.1065	0.0351	0.0254	-0.5931
6	761.3872	175	-0.8417	0.0861	0.0925	0.0259	-0.9342
7	848.4271	248	-0.5167	0.0755	0.0683	0.0262	-0.585
8	212.6253	56	-0.661	0.1557	0.0194	0.025	-0.6804
9	274.1969	364	6.2647	1.0014	-0.1396	0.0257	6.4043
10	237.4545	290	6.0374	1.0017	-0.1095	0.0255	6.147
11	114.9416	25	-0.9128	0.2261	0.0136	0.0248	-0.9263
12	195.0585	54	-0.5927	0.16	0.0161	0.025	-0.6088
13	183.5318	188	5.604	1.0027	-0.0695	0.0252	5.6735
14	158.1779	217	5.7474	1.0023	-0.0808	0.0252	5.8282
15	52.9822	64	4.5264	1.0078	-0.023	0.0248	4.5494
16	30.1758	31	3.8015	1.016	-0.0109	0.0247	3.8124
17	453.2443	137	-0.469	0.1023	0.0314	0.0254	-0.5004
18	124.4156	39	-0.4164	0.1933	0.0074	0.0248	-0.4238
19	176.5249	41	-0.8281	0.1782	0.0194	0.0249	-0.8475
20	24.8646	28	3.6997	1.0177	-0.0098	0.0247	3.7096

21	48.3108	58	4.428	1.0086	-0.0208	0.0248	4.4487
22	127.5572	72	0.6268	0.1786	-0.0123	0.0249	0.639
23	1.8739	6	2.1593	1.0801	-0.0019	0.0247	2.1612
24	25.4611	37	3.9784	1.0134	-0.0131	0.0247	3.9916
25	71.1853	8	-1.6991	0.3753	0.0129	0.0247	-1.712
26	96.1063	56	0.7013	0.2069	-0.0103	0.0248	0.7116
27	71.133	38	0.5046	0.2377	-0.0055	0.0248	0.51
28	108.6949	2	-3.6093	0.7137	0.0261	0.0248	-3.6354
29	44.0026	41	2.9816	0.5979	-0.0141	0.0247	2.9957
30	80.5802	6	-2.1526	0.4244	0.0165	0.0247	-2.1691
31	56.9372	22	-0.095	0.2722	0.0008	0.0247	-0.0958
32	116.9601	34	-0.5245	0.2036	0.0085	0.0248	-0.533
33	80.9314	5	-2.3529	0.4617	0.0172	0.0247	-2.3701
34	127.8379	12	-1.8998	0.3033	0.0249	0.0248	-1.9246
36	62.0113	2	-3.0339	0.7188	0.0143	0.0247	-3.0482
37	37.5096	36	3.5392	0.8308	-0.0126	0.0247	3.5518
38	163.2613	17	-1.7847	0.2562	0.0309	0.0249	-1.8155
39	55.7302	4	-2.1922	0.519	0.0115	0.0247	-2.2037
41	60.4175	10	-1.2502	0.3462	0.009	0.0247	-1.2592
43	27.4719	1	-2.9086	1.0187	0.0062	0.0247	-2.9148
45	35.0384	1	-3.16	1.0146	0.0081	0.0247	-3.1681
48	14.1845	20	3.3633	1.0247	-0.0069	0.0247	3.3702
50	3.3675	9	2.5648	1.0541	-0.003	0.0247	2.5677
55	1.4555	2	1.0607	1.2247	-0.0005	0.0246	1.0611
CLASS	AREA_SQ_KM	NO_POINTS	S_CONTRAST	STUD_CNT	GEN_CLASS	WEIGHT	W_STD
1	97.7953	7	0.393	-5.6367	1	-2.1952	0.3923
2	226.3861	72	0.1449	-2.8173	2	-0.3953	0.1427
3	110.2138	90	0.2474	7.6346	3	1.861	0.2461
4	184.7382	41	0.1788	-5.0807	4	-0.8869	0.1771
5	433.3508	123	0.1095	-5.4148	5	-0.558	0.1065
6	761.3872	175	0.09	-10.3847	6	-0.8417	0.0861
7	848.4271	248	0.0799	-7.322	7	-0.5167	0.0755
8	212.6253	56	0.1577	-4.3145	8	-0.661	0.1557
9	274.1969	364	1.0017	6.3934	9	6.2647	1.0014
10	237.4545	290	1.002	6.1344	10	6.0374	1.0017
11	114.9416	25	0.2275	-4.0727	11	-0.9128	0.2261
12	195.0585	54	0.162	-3.7587	12	-0.5927	0.16
13	183.5318	188	1.003	5.6567	13	5.604	1.0027
14	158.1779	217	1.0026	5.8129	14	5.7474	1.0023
15	52.9822	64	1.0081	4.5129	15	4.5264	1.0078
16	30.1758	31	1.0163	3.7513	16	3.8015	1.016

17	453.2443	137	0.1054	-4.748	17	-0.469	0.1023
18	124.4156	39	0.1948	-2.175	18	-0.4164	0.1933
19	176.5249	41	0.18	-4.7089	19	-0.8281	0.1782
20	24.8646	28	1.018	3.644	20	3.6997	1.0177
21	48.3108	58	1.0089	4.4095	21	4.428	1.0086
22	127.5572	72	0.1803	3.5443	22	0.6268	0.1786
23	1.8739	6	1.0804	2.0004	23	2.1593	1.0801
24	25.4611	37	1.0137	3.9375	24	3.9784	1.0134
25	71.1853	8	0.3761	-4.5523	25	-1.6991	0.3753
26	96.1063	56	0.2083	3.4156	26	0.7013	0.2069
27	71.133	38	0.239	2.1343	27	0.5046	0.2377
28	108.6949	2	0.7141	-5.0907	28	-3.6093	0.7137
29	44.0026	41	0.5984	5.0064	29	2.9816	0.5979
30	80.5802	6	0.4251	-5.1029	30	-2.1526	0.4244
31	56.9372	22	0.2733	-0.3504	99	0.104991	0.025295
32	116.9601	34	0.2051	-2.5983	32	-0.5245	0.2036
33	80.9314	5	0.4624	-5.126	33	-2.3529	0.4617
34	127.8379	12	0.3043	-6.3253	34	-1.8998	0.3033
36	62.0113	2	0.7192	-4.2381	36	-3.0339	0.7188
37	37.5096	36	0.8312	4.2734	37	3.5392	0.8308
38	163.2613	17	0.2574	-7.052	38	-1.7847	0.2562
39	55.7302	4	0.5196	-4.2415	39	-2.1922	0.519
41	60.4175	10	0.3471	-3.6284	41	-1.2502	0.3462
43	27.4719	1	1.019	-2.8604	43	-2.9086	1.0187
45	35.0384	1	1.0149	-3.1216	45	-3.16	1.0146
48	14.1845	20	1.025	3.288	48	3.3633	1.0247
50	3.3675	9	1.0544	2.4353	50	2.5648	1.0541
55	1.4555	2	1.225	0.8662	99	0.104991	0.025295

Table H.6. Larimer County, human factor riskscapes, all classes, calculate weights tables (classes with no points were removed, 46 from 500 training points, 44 from 1000 training points, and 37 from 20% training points).

Larimer human factor 500 training points							
CLASS	AREA_SQ_KM	NO_POINTS	WPLUS	S_WPLUS	WMINUS	S_WMINUS	CONTRAST
25	34.1093	1	-0.9635	1.015	0.0033	0.0465	-0.9667
28	21.3932	2	0.2646	0.7427	-0.0009	0.0465	0.2655
29	37.1179	2	-0.3292	0.727	0.0016	0.0466	-0.3308
31	114.0816	2	-1.4897	0.7134	0.0139	0.0466	-1.5036
32	121.7675	15	0.5738	0.2757	-0.0134	0.0471	0.5872
33	46.9365	1	-1.2909	1.0108	0.0053	0.0465	-1.2962

34	56.3791	1	-1.4778	1.009	0.0068	0.0465	-1.4847
35	167.5198	1	-2.5788	1.003	0.0247	0.0465	-2.6035
36	202.4578	10	-0.4209	0.3243	0.0107	0.0469	-0.4317
37	93.8947	7	0.0176	0.3929	-0.0002	0.0468	0.0178
39	174.8619	10	-0.2662	0.3257	0.0062	0.0469	-0.2724
40	433.9934	27	-0.1766	0.1987	0.0111	0.0478	-0.1877
41	203.0477	11	-0.3235	0.31	0.0086	0.047	-0.3321
42	62.2836	1	-1.5792	1.0081	0.0077	0.0465	-1.5869
43	134.9354	6	-0.5312	0.4176	0.0086	0.0468	-0.5397
44	672.2936	60	0.2135	0.1353	-0.0259	0.0495	0.2394
45	244.6585	26	0.4069	0.2074	-0.0182	0.0477	0.4251
46	90.7534	6	-0.1116	0.4225	0.0014	0.0467	-0.1131
47	109.6419	6	-0.3128	0.4199	0.0045	0.0467	-0.3173
48	965.4948	57	-0.2324	0.1365	0.0342	0.0494	-0.2666
49	156.8386	14	0.2137	0.2801	-0.0055	0.0471	0.2192
50	167.7401	17	0.354	0.2558	-0.0104	0.0473	0.3644
51	69.745	4	-0.2631	0.515	0.0024	0.0466	-0.2656
52	642.3273	53	0.1277	0.1434	-0.0141	0.0491	0.1418
53	57.2685	1	-1.4938	1.0088	0.0069	0.0465	-1.5007
54	213.4337	37	0.9743	0.1808	-0.0486	0.0482	1.0229
55	71.8917	13	1.0256	0.3064	-0.017	0.047	1.0426
56	21.0073	1	-0.4597	1.0247	0.0012	0.0465	-0.4609
57	51.5146	2	-0.6728	0.7212	0.0039	0.0466	-0.6766
58	358.3549	42	0.5172	0.1642	-0.0364	0.0485	0.5535
59	44.8587	2	-0.5284	0.7234	0.0028	0.0466	-0.5312
60	30.5939	4	0.642	0.5363	-0.0038	0.0466	0.6458
61	7.7349	1	0.6291	1.0717	-0.0009	0.0465	0.63
62	252.1137	43	0.9547	0.1674	-0.0563	0.0485	1.0109
63	7.1268	1	0.7237	1.0785	-0.001	0.0465	0.7247
64	26.7518	4	0.798	0.5422	-0.0044	0.0466	0.8024
68	20.5906	2	0.3068	0.7442	-0.0011	0.0465	0.3079
69	5.275	1	1.0836	1.1108	-0.0013	0.0465	1.0849
70	7.228	4	2.7508	0.7482	-0.0075	0.0466	2.7583
72	14.0065	1	-0.0291	1.0377	0.0001	0.0465	-0.0292
74	4.4912	1	1.2861	1.1342	-0.0014	0.0465	1.2876
CLASS	AREA_SQ_KM	NO_POINTS	S_CONTRAST	STUD_CNT	GEN_CLASS	WEIGHT	W_STD
25	34.1093	1	1.0161	-0.9514	99	0.524699	0.078711
28	21.3932	2	0.7441	0.3568	99	0.524699	0.078711
29	37.1179	2	0.7285	-0.4541	99	0.524699	0.078711
31	114.0816	2	0.7149	-2.1032	31	-1.4897	0.7134
32	121.7675	15	0.2797	2.0989	32	0.5738	0.2757

33	46.9365	1	1.0119	-1.281	99	0.524699	0.078711
34	56.3791	1	1.0101	-1.4699	99	0.524699	0.078711
35	167.5198	1	1.0041	-2.5929	35	-2.5788	1.003
36	202.4578	10	0.3277	-1.3172	99	0.524699	0.078711
37	93.8947	7	0.3957	0.045	99	0.524699	0.078711
39	174.8619	10	0.329	-0.8279	99	0.524699	0.078711
40	433.9934	27	0.2044	-0.9183	99	0.524699	0.078711
41	203.0477	11	0.3136	-1.0592	99	0.524699	0.078711
42	62.2836	1	1.0092	-1.5724	99	0.524699	0.078711
43	134.9354	6	0.4202	-1.2844	99	0.524699	0.078711
44	672.2936	60	0.144	1.6618	99	0.524699	0.078711
45	244.6585	26	0.2129	1.9972	45	0.4069	0.2074
46	90.7534	6	0.425	-0.266	99	0.524699	0.078711
47	109.6419	6	0.4225	-0.751	99	0.524699	0.078711
48	965.4948	57	0.1452	-1.8361	99	0.524699	0.078711
49	156.8386	14	0.284	0.7719	99	0.524699	0.078711
50	167.7401	17	0.2602	1.4008	99	0.524699	0.078711
51	69.745	4	0.5171	-0.5136	99	0.524699	0.078711
52	642.3273	53	0.1516	0.9353	99	0.524699	0.078711
53	57.2685	1	1.0099	-1.486	99	0.524699	0.078711
54	213.4337	37	0.1871	5.4661	54	0.9743	0.1808
55	71.8917	13	0.31	3.3629	55	1.0256	0.3064
56	21.0073	1	1.0257	-0.4493	99	0.524699	0.078711
57	51.5146	2	0.7227	-0.9362	99	0.524699	0.078711
58	358.3549	42	0.1712	3.2326	58	0.5172	0.1642
59	44.8587	2	0.7249	-0.7328	99	0.524699	0.078711
60	30.5939	4	0.5383	1.1996	99	0.524699	0.078711
61	7.7349	1	1.0727	0.5873	99	0.524699	0.078711
62	252.1137	43	0.1743	5.7991	62	0.9547	0.1674
63	7.1268	1	1.0795	0.6713	99	0.524699	0.078711
64	26.7518	4	0.5442	1.4746	99	0.524699	0.078711
68	20.5906	2	0.7456	0.4129	99	0.524699	0.078711
69	5.275	1	1.1118	0.9758	99	0.524699	0.078711
70	7.228	4	0.7496	3.6795	70	2.7508	0.7482
72	14.0065	1	1.0388	-0.0281	99	0.524699	0.078711
74	4.4912	1	1.1352	1.1342	99	0.524699	0.078711
Larimer human factor 1000 training points							
CLASS	AREA_SQ_KM	NO_POINTS	WPLUS	S_WPLUS	WMINUS	S_WMINUS	CONTRAST
26	85.0345	1	-2.6705	1.0059	0.0136	0.0343	-2.684
27	39.8363	1	-1.8986	1.0128	0.0057	0.0343	-1.9043
29	37.1179	2	-1.1048	0.727	0.0041	0.0343	-1.1089

31	114.0816	6	-1.1304	0.4194	0.0127	0.0344	-1.1431
32	121.7675	29	0.5979	0.2127	-0.0134	0.0347	0.6113
33	46.9365	4	-0.6127	0.5228	0.0034	0.0343	-0.6161
34	56.3791	1	-2.2535	1.009	0.0086	0.0343	-2.262
35	167.5198	6	-1.5321	0.4158	0.0221	0.0344	-1.5543
36	202.4578	28	-0.0687	0.2036	0.0021	0.0347	-0.0708
37	93.8947	10	-0.3662	0.3345	0.0045	0.0344	-0.3707
38	40.2171	2	-1.1894	0.7254	0.0046	0.0343	-1.194
39	174.8619	16	-0.5347	0.2623	0.0116	0.0345	-0.5463
40	433.9934	58	-0.1084	0.1411	0.0071	0.0353	-0.1155
41	203.0477	23	-0.297	0.2214	0.0082	0.0347	-0.3052
42	62.2836	7	-0.3058	0.4012	0.0025	0.0344	-0.3083
43	134.9354	20	0.0121	0.2423	-0.0002	0.0346	0.0124
44	672.2936	102	0.0396	0.1075	-0.0044	0.0361	0.044
45	244.6585	40	0.1283	0.1729	-0.005	0.0349	0.1333
46	90.7534	11	-0.2203	0.3216	0.0027	0.0344	-0.223
47	109.6419	11	-0.4329	0.3179	0.006	0.0344	-0.4389
48	965.4948	131	-0.0909	0.094	0.0144	0.0368	-0.1053
49	156.8386	23	-0.0004	0.2257	0	0.0346	-0.0004
50	167.7401	34	0.3912	0.1921	-0.0113	0.0348	0.4025
51	69.745	15	0.4661	0.2914	-0.0057	0.0345	0.4718
52	642.3273	107	0.1507	0.1059	-0.0166	0.0362	0.1673
53	57.2685	11	0.3242	0.3354	-0.0031	0.0344	0.3273
54	213.4337	50	0.5764	0.1616	-0.0228	0.0351	0.5992
55	71.8917	23	1.0066	0.2528	-0.0148	0.0346	1.0215
56	21.0073	3	-0.0314	0.6236	0.0001	0.0343	-0.0315
57	51.5146	10	0.3373	0.3523	-0.0029	0.0344	0.3402
58	358.3549	102	0.8392	0.1171	-0.0625	0.036	0.9017
59	44.8587	15	1.0723	0.3165	-0.01	0.0345	1.0823
60	30.5939	5	0.1278	0.4889	-0.0006	0.0343	0.1284
62	252.1137	77	0.9391	0.1367	-0.0496	0.0355	0.9887
63	7.1268	2	0.8194	0.8337	-0.0011	0.0343	0.8205
64	26.7518	2	-0.755	0.7351	0.0023	0.0343	-0.7573
65	6.3784	1	0.0784	1.089	-0.0001	0.0343	0.0784
66	4.8265	1	0.4188	1.1231	-0.0003	0.0342	0.4191
67	4.8114	3	2.2653	0.941	-0.0027	0.0343	2.2679
70	7.228	1	-0.0683	1.0773	0.0001	0.0343	-0.0684
72	14.0065	4	0.8438	0.5916	-0.0023	0.0343	0.8461
78	0.4905	1	1.7607	1.4142	-0.0008	0.0342	1.7616
80	0.5463	1	1.7607	1.4142	-0.0008	0.0342	1.7616

CLASS	AREA_SQ_KM	NO_POINTS	S_CONTRAST	STUD_CNT	GEN_CLASS	WEIGHT	W_STD

26	85.0345	1	1.0065	-2.6667	26	-2.6705	1.0059
27	39.8363	1	1.0134	-1.8792	99	0.362232	0.05861
29	37.1179	2	0.7278	-1.5237	99	0.362232	0.05861
31	114.0816	6	0.4208	-2.7163	31	-1.1304	0.4194
32	121.7675	29	0.2156	2.8358	32	0.5979	0.2127
33	46.9365	4	0.5239	-1.176	99	0.362232	0.05861
34	56.3791	1	1.0096	-2.2406	34	-2.2535	1.009
35	167.5198	6	0.4172	-3.7256	35	-1.5321	0.4158
36	202.4578	28	0.2065	-0.3428	99	0.362232	0.05861
37	93.8947	10	0.3363	-1.1023	99	0.362232	0.05861
38	40.2171	2	0.7262	-1.6442	99	0.362232	0.05861
39	174.8619	16	0.2646	-2.0649	39	-0.5347	0.2623
40	433.9934	58	0.1454	-0.794	99	0.362232	0.05861
41	203.0477	23	0.2241	-1.3615	99	0.362232	0.05861
42	62.2836	7	0.4026	-0.7658	99	0.362232	0.05861
43	134.9354	20	0.2447	0.0505	99	0.362232	0.05861
44	672.2936	102	0.1134	0.3876	99	0.362232	0.05861
45	244.6585	40	0.1764	0.7557	99	0.362232	0.05861
46	90.7534	11	0.3235	-0.6895	99	0.362232	0.05861
47	109.6419	11	0.3197	-1.3727	99	0.362232	0.05861
48	965.4948	131	0.1009	-1.0438	99	0.362232	0.05861
49	156.8386	23	0.2284	-0.0018	99	0.362232	0.05861
50	167.7401	34	0.1952	2.0623	50	0.3912	0.1921
51	69.745	15	0.2935	1.6076	99	0.362232	0.05861
52	642.3273	107	0.1119	1.4952	99	0.362232	0.05861
53	57.2685	11	0.3372	0.9705	99	0.362232	0.05861
54	213.4337	50	0.1654	3.623	54	0.5764	0.1616
55	71.8917	23	0.2552	4.0025	55	1.0066	0.2528
56	21.0073	3	0.6245	-0.0505	99	0.362232	0.05861
57	51.5146	10	0.3539	0.9611	99	0.362232	0.05861
58	358.3549	102	0.1225	7.3625	58	0.8392	0.1171
59	44.8587	15	0.3183	3.3997	59	1.0723	0.3165
60	30.5939	5	0.4902	0.262	99	0.362232	0.05861
62	252.1137	77	0.1413	6.9983	62	0.9391	0.1367
63	7.1268	2	0.8344	0.9834	99	0.362232	0.05861
64	26.7518	2	0.7359	-1.029	99	0.362232	0.05861
65	6.3784	1	1.0895	0.072	99	0.362232	0.05861
66	4.8265	1	1.1236	0.373	99	0.362232	0.05861
67	4.8114	3	0.9416	2.4087	67	2.2653	0.941
70	7.228	1	1.0778	-0.0634	99	0.362232	0.05861
72	14.0065	4	0.5925	1.4279	99	0.362232	0.05861
78	0.4905	1	1.4146	1.2453	99	0.362232	0.05861

80	0.5463	1	1.4146	1.2453	99	0.362232	0.05861
Larimer human factor 20% training points							
CLASS	AREA_SQ_KM	NO_POINTS	WPLUS	S_WPLUS	WMINUS	S_WMINUS	CONTRAST
24	14.2509	1	-2.2165	1.037	0.0029	0.0247	-2.2195
25	34.1093	2	-2.4085	0.7288	0.0073	0.0247	-2.4158
26	85.0345	2	-3.3586	0.7156	0.0201	0.0247	-3.3787
28	21.3932	3	-1.4458	0.6227	0.0035	0.0247	-1.4493
29	37.1179	3	-2.0637	0.6022	0.0074	0.0247	-2.0711
30	155.2265	9	-2.4204	0.3434	0.0337	0.0248	-2.4542
31	114.0816	22	-1.0641	0.2373	0.0152	0.0248	-1.0793
32	121.7675	26	-0.9363	0.2211	0.0147	0.0248	-0.951
33	46.9365	6	-1.5527	0.4371	0.0081	0.0247	-1.5608
34	56.3791	4	-2.2047	0.5187	0.0117	0.0247	-2.2163
35	167.5198	23	-1.4704	0.2245	0.0283	0.0249	-1.4987
36	202.4578	43	-0.9431	0.1718	0.0249	0.025	-0.9679
37	93.8947	21	-0.877	0.2477	0.0107	0.0248	-0.8877
38	40.2171	4	-1.8357	0.5269	0.0076	0.0247	-1.8433
39	174.8619	34	-1.0539	0.1911	0.0233	0.0249	-1.0772
40	433.9934	111	-0.7006	0.11	0.043	0.0254	-0.7436
41	203.0477	44	-0.9175	0.1703	0.0244	0.025	-0.9419
42	62.2836	16	-0.6947	0.29	0.0058	0.0247	-0.7005
43	134.9354	25	-1.1135	0.2216	0.0187	0.0248	-1.1322
44	672.2936	166	-0.7476	0.0894	0.073	0.0258	-0.8206
45	244.6585	59	-0.7788	0.1495	0.0258	0.025	-0.8047
46	90.7534	52	0.6616	0.2122	-0.0092	0.0248	0.6707
47	109.6419	46	0.0429	0.1935	-0.0007	0.0248	0.0436
48	965.4948	266	-0.5993	0.072	0.0905	0.0264	-0.6899
49	156.8386	70	0.152	0.1606	-0.0036	0.0249	0.1556
50	167.7401	146	2.272	0.2299	-0.0484	0.0251	2.3203
51	69.745	43	0.8424	0.2463	-0.0089	0.0248	0.8513
52	642.3273	169	-0.6624	0.0896	0.0625	0.0257	-0.7249
53	57.2685	39	1.1259	0.2835	-0.0095	0.0248	1.1354
54	213.4337	226	5.7881	1.0022	-0.0843	0.0253	5.8723
55	71.8917	88	4.8449	1.0057	-0.0318	0.0249	4.8767
56	21.0073	12	0.6544	0.4409	-0.0021	0.0247	0.6565
57	51.5146	46	2.4888	0.4506	-0.0153	0.0248	2.504
58	358.3549	455	6.4878	1.0011	-0.1779	0.026	6.6657
59	44.8587	49	4.2593	1.0102	-0.0175	0.0248	4.2768
60	30.5939	37	3.9784	1.0134	-0.0131	0.0247	3.9916
61	7.7349	8	2.447	1.0607	-0.0026	0.0247	2.4496
62	252.1137	318	6.1296	1.0016	-0.1208	0.0256	6.2504

63	7.1268	7	4.3786	2.8336	-0.0025	0.0247	4.3811
64	26.7518	26	3.9109	1.1699	-0.0092	0.0247	3.9201
65	6.3784	2	-0.416	0.8535	0.0004	0.0246	-0.4164
66	4.8265	2	0.0216	0.924	0	0.0246	0.0217
67	4.8114	2	0.027	0.925	0	0.0246	0.027
68	20.5906	17	1.9224	0.5808	-0.0052	0.0247	1.9276
69	5.275	5	3.2679	1.9587	-0.0017	0.0246	3.2697
70	7.228	3	0.0244	0.7549	0	0.0246	0.0244
71	0.9323	1	0.3675	1.4142	-0.0001	0.0246	0.3676
72	14.0065	24	3.5456	1.0206	-0.0084	0.0247	3.554
74	4.4912	5	1.977	1.0954	-0.0015	0.0246	1.9785
82	0.2859	1	0.3675	1.4142	-0.0001	0.0246	0.3676
CLASS	AREA_SQ_KM	NO_POINTS	S_CONTRAST	STUD_CNT	GEN_CLASS	WEIGHT	W_STD
24	14.2509	1	1.0373	-2.1396	24	-2.2165	1.037
25	34.1093	2	0.7292	-3.3128	25	-2.4085	0.7288
26	85.0345	2	0.716	-4.7189	26	-3.3586	0.7156
28	21.3932	3	0.6231	-2.3259	28	-1.4458	0.6227
29	37.1179	3	0.6027	-3.4364	29	-2.0637	0.6022
30	155.2265	9	0.3443	-7.1272	30	-2.4204	0.3434
31	114.0816	22	0.2386	-4.5235	31	-1.0641	0.2373
32	121.7675	26	0.2225	-4.2736	32	-0.9363	0.2211
33	46.9365	6	0.4378	-3.5648	33	-1.5527	0.4371
34	56.3791	4	0.5193	-4.2677	34	-2.2047	0.5187
35	167.5198	23	0.2259	-6.6351	35	-1.4704	0.2245
36	202.4578	43	0.1736	-5.5743	36	-0.9431	0.1718
37	93.8947	21	0.2489	-3.5664	37	-0.877	0.2477
38	40.2171	4	0.5275	-3.4946	38	-1.8357	0.5269
39	174.8619	34	0.1927	-5.5903	39	-1.0539	0.1911
40	433.9934	111	0.1129	-6.5854	40	-0.7006	0.11
41	203.0477	44	0.1722	-5.4711	41	-0.9175	0.1703
42	62.2836	16	0.2911	-2.4066	42	-0.6947	0.29
43	134.9354	25	0.223	-5.0778	43	-1.1135	0.2216
44	672.2936	166	0.0931	-8.8155	44	-0.7476	0.0894
45	244.6585	59	0.1515	-5.3101	45	-0.7788	0.1495
46	90.7534	52	0.2137	3.1391	46	0.6616	0.2122
47	109.6419	46	0.1951	0.2235	99	0.063468	0.025691
48	965.4948	266	0.0767	-8.992	48	-0.5993	0.072
49	156.8386	70	0.1626	0.9572	99	0.063468	0.025691
50	167.7401	146	0.2312	10.034	50	2.272	0.2299
51	69.745	43	0.2475	3.4393	51	0.8424	0.2463
52	642.3273	169	0.0932	-7.7746	52	-0.6624	0.0896

53	57.2685	39	0.2846	3.9897	53	1.1259	0.2835
54	213.4337	226	1.0025	5.8575	54	5.7881	1.0022
55	71.8917	88	1.006	4.8477	55	4.8449	1.0057
56	21.0073	12	0.4415	1.4868	99	0.063468	0.025691
57	51.5146	46	0.4513	5.5482	57	2.4888	0.4506
58	358.3549	455	1.0014	6.6561	58	6.4878	1.0011
59	44.8587	49	1.0105	4.2326	59	4.2593	1.0102
60	30.5939	37	1.0137	3.9375	60	3.9784	1.0134
61	7.7349	8	1.0609	2.3089	61	2.447	1.0607
62	252.1137	318	1.0019	6.2386	62	6.1296	1.0016
63	7.1268	7	2.8337	1.5461	99	0.063468	0.025691
64	26.7518	26	1.1701	3.3501	64	3.9109	1.1699
65	6.3784	2	0.8538	-0.4877	99	0.063468	0.025691
66	4.8265	2	0.9243	0.0234	99	0.063468	0.025691
67	4.8114	2	0.9254	0.0292	99	0.063468	0.025691
68	20.5906	17	0.5813	3.316	68	1.9224	0.5808
69	5.275	5	1.9588	1.6692	99	0.063468	0.025691
70	7.228	3	0.7553	0.0324	99	0.063468	0.025691
71	0.9323	1	1.4144	0.2599	99	0.063468	0.025691
72	14.0065	24	1.0209	3.4812	72	3.5456	1.0206
74	4.4912	5	1.0957	1.8057	99	0.063468	0.025691
82	0.2859	1	1.4144	0.2599	99	0.063468	0.025691